An Experimental Study of the State of Equilibrium in an Inductively-Coupled Plasma Torch

A thesis
submitted in fulfilment
of the requirements for the Degree
of
Doctor of Philosophy
at the
University of Waikato
by
GEORGE PAUL MILLER

University of Waikato
1987

Abstract

An experimental study of the state of equilibrium existing in an atmospheric pressure argon inductively-coupled plasma torch (ICPT) has been undertaken using several diagnostic methods. In particular, a relaxation technique was used which involved pulsing off the RF field rapidly ($<3\mu s$) and monitoring the subsequent intensity changes in the optically-thin excited argon I spectral lines. The removal of the RF field is accompanied by a sharp intensity increase persisting for about $18\mu s$ before falling monotonically. This effect is explained in terms of the theory of collision-radiation decay of a plasma.

The increase in spectral line intensity is used to ascertain whether the optically-thin excited Ar I states conform to a Boltzmann distribution for various operating conditions of the ICPT. For those cases where the excited states are close to a Boltzmann distribution, this method is used to determine the difference in temperature between the electrons (T_e) and the heavy particles (T_g) as well as the electron temperature. In addition, the same technique applied to a near saturated (optically thick) Ar I spectral line (811.5nm) is used to observe changes in radiative losses from the plasma.

The results obtained show that a single flow (coolant only) ICPT plasma is in a state of pLTE in the central regions ($r < 7mm$). Not only do the optically-thin excited Ar I states conform to a Boltzmann distribution but centrally $T_e = T_g$ to closer than 3% and $T_e \approx$ 10,000 K.

The introduction of a second (aerosol) flow axially through the plasma is shown to cause a deviation from excitational equilibrium across the entire plasma radius. Increasing this flow from 1 l/min to 2 l/min appeared to return the plasma to a state of excitational equilibrium, but the temperatures obtained became inconsistent with the validity of Saha's equation, i.e. indicating a non-Boltzmann distribution of the Ar I states. The radiative losses are increased significantly. The introduction of certain aerosols viz, 4%H_2, 4%Air, H_2O and KCl, into the plasma are shown to have negligible effect on the state of equilibrium.

Four different methods used to obtain the electron density, (Stark broadening, interferometry, absolute intensity of the continuum, and Saha's equation calculations) were compared for various cases. With a single flow plasma the results were consistent, and are typically in the range $10^{21} - 10^{22}$ m^{-3}. With the introduction of the second flow, the method based on Saha's equation yields results inconsistent with the other methods, confirming the significant deviation from equilibrium for this system.

Calculations show that the deviation from excitational equilibrium is consistent with convective losses resulting from the forced flow of argon through the torch.

Acknowledgements

To complete this thesis required the assistance of many people to whom I now wish to express my gratitude, especially to the following

Professor Bruce Liley, for the many helpful discussions along the way and for his patience in reading and commenting on the various sections of this thesis.

Dr Evan Bydder, for his advice and expertise and for being available when needed.

Norman Wood, for the technical expertise that helped fill that large gap which exists between proposed experiment and final results.

Robin Holdsworth, for his knowledge of RF transmitters and all their foibles.

M.Deutsch and I.Beniaminy, for the use of their computer program.

Graham Radford, for his assistance in the formatting of this thesis.

Richard Sutherland, for his assistance with the circuit diagrams.

June 1987 G.P.Miller

Contents

List of Figures

List of Photographs

List of Tables

Chapter 1

Introduction

1.1. Research Aim

An inductively-coupled atmospheric pressure argon plasma torch, commonly (and hereafter) called an ICPT is an arrangement in which a high intensity RF field is coupled by an air cored transformer into a single turn gas flow, constrained by a quartz tube system in which at least two different gas flows of argon at atmospheric pressure are directed. This is shown in Figure 1.1. The RF field causes ionisation of the flowing gas, producing a plasma in the vicinity of the work-coil which is typically 1% ionised. The gas temperature reached is of the order of five to ten thousand degrees, and so the device is a useful optical emission source for spectrochemical analysis, particularly suitable due to the high temperatures for refractory compounds. The coolant flow supplies argon to the plasma and maintains the tube wall temperature below the softening point of SiO_2 while the aerosol flows through the center of the torch and is used to bring the sample to be heated into the plasma.

While a full description of the apparatus and ignition procedure is given later (Chapter 5) it may be useful to provide an illustration of a typical ICPT. Although the details of torch design, input power and gas flow vary with different research workers, the annular plasma formed as a result of the introduction of the aerosol flow is characteristic of the ICPT. Figure 1.1 gives a schematic diagram of a typical ICPT detailing the torch assembly and resulting plasma.

The first successful attempt to use an inductively-coupled argon plasma as an optical emission source was that by Read in 1961. This was followed by intensive development and by 1974 commercial versions were available for operation as optical emission sources for chemical analysis, although the detailed behaviour of the system was by no means fully understood. A survey of the literature describing the development in torch design, operating conditions, results of temperature and electron

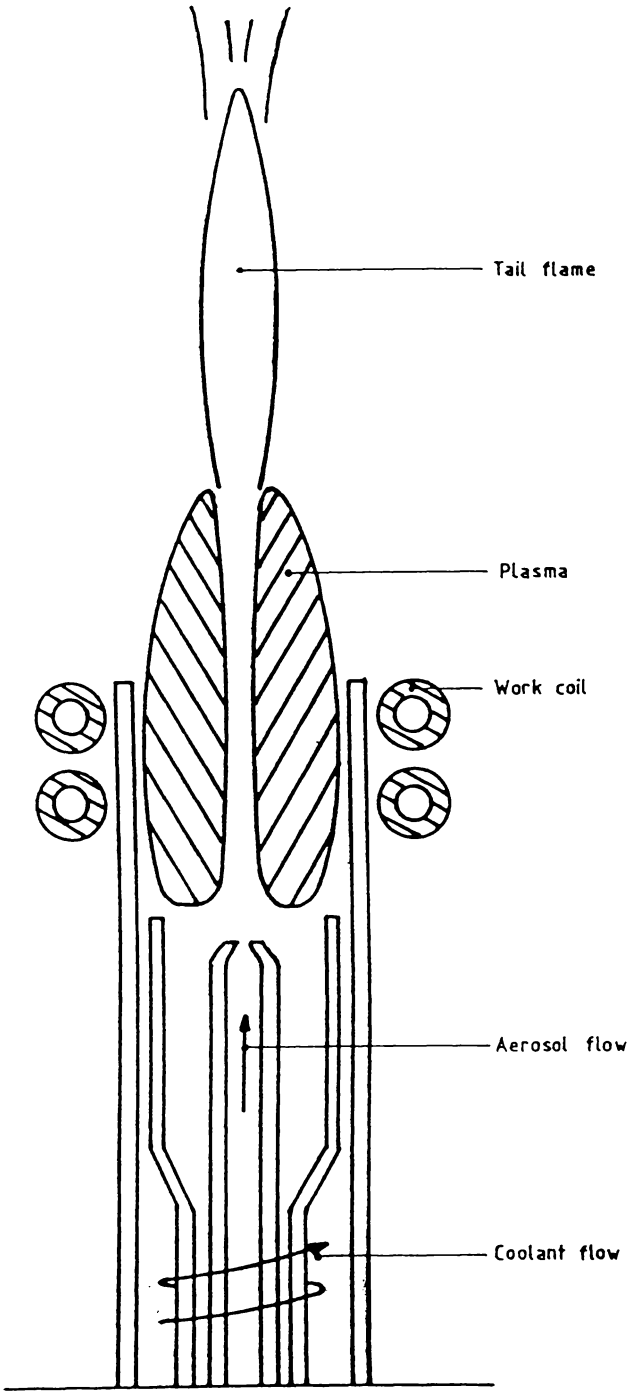

Figure 1.1: A Schematic Diagram of the Plasma Torch.

density measurements, and the various theoretical models used to explain the plasma behaviour is given in Chapter 2. An ICPT system cannot normally be 'ignited' by the simple application of the RF field to the flowing gas. Initially, it is necessary to introduce a load into the circuit so that energy can be taken up from the RF field. This is achieved by the introduction of a source of electrons, in this case by means of a carbon rod, into the zone of the work coil.

Once ignition has occurred a steady state is reached in which there is efficient energy transfer from the RF field to the thermal energy of the electrons in the resulting plasma. The electrons produce continuous ionisations to sustain the plasma, but at the temperature range present in the ICPT, energy is transferred to the gas particles (neutral atoms and ions) by elastic collisions. Thus the gas temperature must be less than the electron temperature. However no consensus has been arrived at in the literature of the magnitude of the difference in temperatures or in the detailed energy balance mechanism that produces it, or the excitation mechanism that give rise to the analytical characteristics of the ICPT. This has been due in the main because standard diagnostic methods available for use in determining the temperatures of the different components of the plasma (see Chapter 2) are either too insensitive or the margin of error too great for an accurate determination. The one parameter upon which satisfactory agreement has been reached, the electron density, indicates that Griem's criteria for the presence of partial local thermodynamic equilibrium (pLTE) is only marginally satisfied (Chapter 3), however, because of the inherent simplifications possible the plasma is commonly regarded as being in state of at least pLTE. It is assumed that although the plasma is effectively optically-thin, the electron density is sufficiently high that the plasma is collision dominated, that is, contributions from photo-processes are essentially negligible and excitational equilibrium is reached by the establishment of a detailed balance between the excitation due to the electrons and de-excitation by means of collisions of the second kind.

The aim of this thesis is to determine the degree to which the assumption of pLTE is valid in the steady-state plasma produced by an ICPT using a technique sensitive enough to evaluate the cause of any deviation. The nature and magnitude of the deviation from equilibrium and kinetic temperature difference between the electrons and argon atoms is evaluated and compared with possible mechanisms that can produce these values.

1.2. Experimental Technique.

In Chapter 4 a relaxation method which provides a sensitive method of

evaluating the state of equilibrium present in the plasma plus which allows a relatively accurate determination of this temperature difference is discussed. It is shown that if the RF field is removed, the electrons thermally relax to the temperature of the argon gas (99% of the plasma) in $\approx 10^{-5}$ seconds, and that since the recombination time is of the order of 10^{-3} seconds, the electron density will remain essentially constant during this time. While in general, energy is transferred by elastic collision, with the removal of the RF field another mechanism becomes available. In plasmas formed from elements such as argon the excited states are coupled to the continuum. Thus the free-bound radiationless transition

$$Ar_k^+ + e \rightarrow Ar_i$$

(where Ar_i, the excited state associated with ionisation energy E_j, lies within the continuum of the series associated with energy E_k ($E_k < E_j$)) provides a means by which the state of thermal equilibrium of the plasma can be investigated. The resulting density increase in the optically-thin excited states will be accompanied by an increase in measurable line radiation from these states. Therefore when the RF field is removed, provided the electron temperature is higher than the gas temperature, these optically-thin excited argon I spectral line intensities will exhibit a sharp increase in intensity before slowly decreasing. Using Saha's equation, a method is described which determines whether the excited argon states conform to a Boltzmann distribution and if so establish the difference in temperature ($T_e - T_g$) between electrons and gas in the steady-state plasma as well as giving the electron temperature. This method is not only sensitive to differences in temperature but also to any deviation from excitation equilibrium.

While the plasma produced in the ICPT is collision-dominanted, increases in radiative losses can still contribute to any deviation from equilibrium. The relaxation of the electrons with the removal of the RF field is shown to also provide a sensitive method of observing an increase in the radiative losses. This follows from the fact that as a saturated or near-saturated spectral line is radiating as a (near) blackbody, relaxation of the electrons can cause an increase in observed spectral intensity only up to the blackbody intensity. Therefore the effect changes in operating conditions have on the radiative losses can be observed and an increase in radiative loss from the plasma would result in a near-saturated spectral line becoming more optically-thin and thus showing an increase in the intensity jump with the removal of the RF field.

To utilise this relaxation method it is necessary to

i) to switch off the RF field in less than the relaxation time of the electrons,

ii) have suitable diagnostic equipment to measure the various parameters of the plasma.

iii) preferably switch on the RF field within a sufficiently short time period so that enough electrons remain within the region to re-ignite the plasma, to allow many measurements to be made under the same conditions.

Chapter 5 describes the basic apparatus and diagnostic equipment used to investigate the physical characteristics of the plasma and details the method used to remove the RF field. Briefly, this is achieved by the positioning of a gating tube between the oscillator and buffer stages in the RF generator. By applying a short voltage pulse it is possible to repetitively pulse off the ICPT in $\approx 3\mu s$.

1.3. Experimental Results.

In Chapter 6 the expected increase in spectral line intensity upon the removal of the RF field is confirmed and the assumptions made in Chapter 4 substantiated (e.g. that n_e remains constant). Optically thin spectral lines are found, and the 811.5nm Ar I spectral line is shown to be optically saturated or nearly so over a large area of a plasma formed using the coolant flow only.

In Chapter 7 the assumption that a ICPT plasma can be consider to be axisymmetric if a lateral scan of the intensity of a spectral line is axisymmetric is shown to be invalid. Experimental results indicate that the degree of axisymmetry is dependent on coolant flow and observation height.

The state of equilibrium of the plasma is investigated in Chapter 8 under a variety of operating conditions. Starting first with a plasma formed using coolant flow only (10 l/min), it is shown that the excited Ar I states not only conform to a Boltzmann distribution (for plasma radii r $<$ 7.5mm) but that in the central region (r $<$ 3mm) the temperatures are equal ($T_e = T_g$). Outside this region the temperature difference, $T_e - T_g$ varied, increasing to a maximum at a radius of $\approx$6mm. The magnitude of the temperature difference $T_e - T_g$ varied from $\approx 30\% T_e$ 15mm below the top of the work-coil to $\approx 6\% T_e$ 5mm above the work-coil at a radius of 6mm. The 811.5nm Ar I spectral line is shown to remain saturated up to height of 5mm above the work-coil.

That is, the central region of the plasma is in excitational and kinetic equilibrium which indicates that a coolant-only plasma formed in the ICPT is at least in partial LTE.

The introduction of the aerosol flow (argon only 1l/min) is shown to cause a deviation from excitational equilibrium. Increasing this flow to 2l/min gives the appearance of restoring the equilibrium but a calculation of the temperature from the slope of the graph yields values exceeding 60,000 K as compared to approximately 10,000 K obtained from a Boltzmann plot using measurements obtained under steady-state conditions. This indicates that the use of Saha's equation is no longer valid. While correct values for the temperature difference $T_e - T_g$ could no longer be obtained the results appear to indicate an increase in the temperature difference to $\approx 9\% T_e$. Reducing the input power from 1200 Watts appears to cause the plasma to approach nearer to a Boltzmann distribution but the temperature difference is consistent with an increase to $\approx 14\% T_e$ for an input power of 800 Watts. Observations of the 811.5 nm Ar I spectral line showed that the introduction of the aerosol flow reduced the optical depth to such an extent that the line radiation was no longer trapped, the increase in aerosol flow-rate from 1 to 2 litres/minute further enhanced this effect.

As the operation of this particular torch as an emission light source requires an aerosol flow-rate of 2 litres/minute, experiments were performed with the introduction of Ar + 4%H_2, Ar + 4%air and aerosols of H_2O and H_2O + 1%KCL at this flow-rate. These experiments showed that while hydrogen and air has certain effects, most noticeably an increase in the width of the aerosol channel, the aerosols of H_2O and KCL have little or no effect. These effects are, in all cases, small compared with those caused by the introduction of the argon aerosol flow. Similarly the introduction of air has the most effect on the temperature difference, increasing it to $\approx 14\% T_e$ while the aqueous aerosols appear to have no noticeable effect.

These results suggest that the deviation from excitational equilibrium is due to the loss of energy from the plasma arising from the introduction of the gas flow through the center of the plasma. To confirm this the electron density is determined by four different methods (Chapter 9), three of which, Stark broadening, interferometry and absolute intensity of the continuum are largely independent of the state of equilibrium. The fourth method, which is based on Saha's equation is, however, strongly dependent on the state of equilibrium of the plasma. The results in this chapter agree with other studies in that the electron density in the ICPT is of the order of 10^{21} to 10^{22} m^{-3}. For the plasma formed using coolant flow only, that is, when the plasma is very close to equilibrium all four methods produce consistent results. With the introduction of the aerosol flow the results obtained from using Saha,s equation (especially when using the temperatures obtained from the intensities

of Fe I spectral lines introduced as an aerosol) differ substantially from those obtained using methods independent of the state of equilibrium. A comparison of the electron density present in a plasma with and without aerosol and the variation in electron density with height permitted an estimate of the aerosol flow velocity (24 m/s) which is in excellent agreement with both the expected value and the experimental results obtained elsewhere (Chapter 2) and indicates that the deviation from excitational equilibrium arises from convective losses.

As the electron density remains relatively unchanged immediately after the electrons have relaxed to the temperature of the heavy particles this implied that the degree of ionisation exceeded its equilibrium value. This permitted an estimation of the recombination rate ($\alpha \approx 2.5 \times 10^{-17}$ m $^3s^{-1}$).

The experimental results are discussed in Chapter 10 and it is concluded that while the re-absorption of the 4p - 4s line radiation plays a role in the establishment of excitational equilibrium in the ICPT it is the loss of electrons by convection and ambipolar diffusion is the dominant cause of the deviation from excitational equilibrium present in the ICPT. This effectively decreases the collision rate which together with the increase in radiative losses is shown to give rise to an overpopulation of the 4s energy level which is consistent with that which has been reported in the literature.

Appendix A gives the results of experiments which relate to the formation of the plasma but which are not directly related to the steady-state conditions of the plasma. As the RF field is repetitively pulsed off and on it is possible to investigate the formation of the plasma in the $\approx$8 milliseconds it takes for the plasma to re-establish itself with the resumption of the RF field (provided the off period is sufficiently short). The off period used depended on the operating conditions and varied between 150μs and 1800μs. The oscillations in the spectral line and continuum intensities were investigated and shown to be due to bulk motion of the plasma, this conclusion was supported by the variation in the excitation temperature. As physical changes in the plasma volume are governed by the mean thermal velocity it was possible from the periodic behaviour of the plasma to estimate this velocity for a coolant-only plasma ($\approx$ 12.5 m/s).

Chapter 2

Literature Review

2.1. Introduction

While the first reference to a high frequency inductively-coupled plasma is encountered in the work of Hittorf (1884), it was not until 1942 that an atmospheric pressure argon inductively-coupled discharge was obtained. The development of powerful vacuum tube oscillators enabled Babat (1942) to generate such a plasma. Operating the RF supply at a frequency of 3 MHz he obtained plasmas in quartz tubes of 100 - 400 mm diameter. The power of the discharges was such that the 100 mm quartz tube melted in several seconds.

While there were various attempts to utilise inductively-coupled plasmas as a light source for emission spectroscopy (Birkoff, 1958; Straub, 1958) it was not until 1961 with Reed's description of such a torch, operating at atmospheric pressure on argon and powered by a 10kW RF generator at a frequency of 4MHz, that there was any degree of success. However it is the torch designed by Greenfield *et al* (1963) specifically as a spectroscopic light source and similar designs (Wendt and Fassel, 1966; Boumans and De Boer, 1976; Scott *et al*, 1974 Miller, 1978;) to which the term inductively-coupled plasma torch and its abbreviation (ICPT) is now generally held to refer to. This torch design (Figure 2.1a) consists of three concentric quartz tubes, the two outer tubes being used to direct the gas flow to the plasma, with the inner tube being used to inject an aerosol through the center, once the plasma has formed. The tube assembly is held concentric with the work-coil of the RF generator.

This torch design may be compared with the design (Figure 2.1b) used for purposes other than emission spectroscopy, such as plasma etching or as a heat source. Although, inductively-coupled plasmas have and can be used for many purposes, and while the types of plasmas of interest in this thesis are those for or related to emission spectroscopy, a comparison of results is useful. Following Kornblum and De Galan

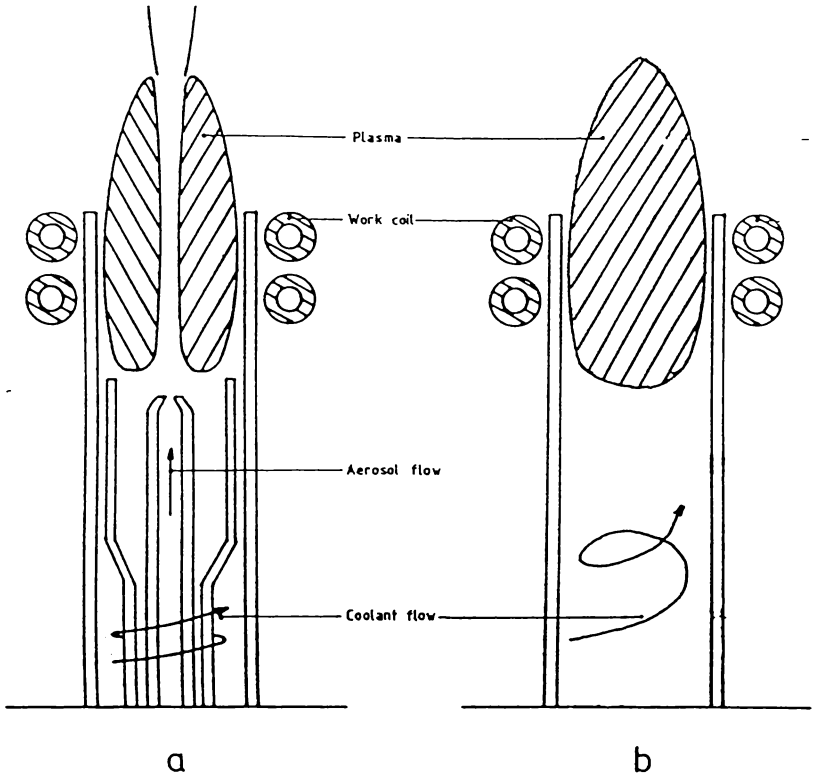

Figure 2.1: Tube assembly a) analytical b) physical

(1977), the plasma formed using the ICPT torch assembly (Figure 2.1a) is called an 'analytical' plasma while that produced with a single quartz tube being (Figure 2.1b) denoted as a 'physical' plasma.

Due to the lack of spectral interferences and high efficiency in exciting analyte species together with its remarkable stability and versatility (Fassel, 1979) the development of the ICPT as a spectro-chemical light source has proceeded rapidly until today it is an important and useful device appropriate to any analytical laboratory. The history of this development and the present state of the art is described in recent reviews by Ward, (1978); Barnes, (1982); Thompson, (1985); Boulos, (1985); and Ebdon *et al*, (1986).

Almost as soon as the analytical potential of the ICPT was recognised, experiments were undertaken to characterise the plasma in terms of its physical parameters (mainly by spectroscopic methods). Comparisons between the different experiments is complicated by the wide variety of operating conditions. These include

the means of plasma generation, such as a variation of frequency from 0.3 MHz to 144 MHz (Dymshits and Koretskii, 1964; Walters *et al*, 1977), and input powers ranging from 0.3 to 100 kW. Other variations occur in such parameters as the work coil configuration (perpendicular to the plasma tube, cylindrical or polygonal in shape (Babat, 1947)), length and number of turns, plasma tube and coil diameter (15 - 460 mm), gas flow-rate (0 to 180 l/min) and type of tube cooling (argon, water, air) (Boulos, 1985). It also becomes necessary to differentiate between physical and analytical plasmas, with analytical plasmas having additional variables attached such as multiple gas flows (coolant flow-rate 0.8 - 40 l/min)), support flow-rate (0 - 15 l/min) and aerosol flow (0.07 - 5.4 l/min)), aperture diameter (1 - 6mm). A further difficulty in comparing experimental results arises from the use of different experimental techniques, for example, different methods of measuring the temperature (in the same torch and under identical operating conditions) may yield different results. These difficulties are shown clearly by the following review.

2.2. Review of the literature

2.2.1. Temperature measurements

2.2.1.1. Electron Temperature

While normally employed to establish the electron density, the measurement of the absolute intensity of continuum resulting from the free-bound (ϵ_λ^{fb}) and free-free (ϵ_λ^{ff}) electron transitions has been used to determine the electron temperature. That is, the continuum intensity is given by

$$\epsilon_\lambda^{cont} = \epsilon_\lambda^{fb} + \epsilon_\lambda^{ff} \tag{2.1}$$

where

$$\epsilon_\lambda^{fb} = C\,\xi(\lambda, T_e)\frac{n_e^2}{T_e^{\frac{1}{2}}}\left(1 - e^{-hc/\lambda k T_e}\right) \tag{2.2}$$

and

$$\epsilon_\lambda^{ff} = C\,\xi(\lambda, T_e)\frac{n_e^2}{T_e^{\frac{1}{2}}}e^{-hc/\lambda k T_e} \tag{2.3}$$

where

$$C = \frac{16\pi}{3\sqrt{3}}\frac{1}{mc^3(2\pi mk)^{\frac{1}{2}}}\left(\frac{e^2}{4\pi\epsilon_0}\right)^3 \tag{2.4}$$

and

ϵ_λ^{cont} is the absolute intensity of the continuum

m is the mass

c is the speed of light

k is Boltzmann's constant

h is Planck's constant

T_e is the electron temperature

n_e is the electron density

λ the wavelength

ϵ_0 is the permittivity

ξ the radiative recombination factor which is only weakly temperature and wavelength dependent (Griem, 1964). Over the spectral range 400 - 700 nm and with a electron temperature of 10,000 K ξ has a value of $\approx$ 1.8.

For sufficiently long wavelengths ($\frac{hc}{\lambda} << kT_e$) the last term in equation 2.2 tends to $\frac{hc}{\lambda T_e}$ while the last term in equation 2.3 tends to 1. Thus equation 2.1 can be written as

$$\epsilon_\lambda^{cont} = C\,\xi(\lambda, T_e)\frac{n_e^2}{T_e^{\frac{1}{2}}}. \qquad (2.5)$$

However it must be noted that ϵ_λ cannot remain constant to indefinitely long wavelengths as it will eventually hit the blackbody curve and will then decrease as $\frac{1}{\lambda^2}$.

Errors can arise from the presence of self-absorption, possible contributions to the continuum intensity from negative-ion and molecular continua, and the inclusion of unresolved spectral lines in the wavelength region observed by the monochromator. Even when these are accounted for it is obvious that the electron temperature is critically dependent on the accuracy to which the electron density n_e has been determined. Assuming that the electron and ion temperatures are equal allows the use of Saha's equation to establish a value for the electron density. Results have been obtained using absolute intensities for physical plasmas by Gold'farb *et al* (1965), Rovenskii *et al* (1967) and Stokes (1971) with electron temperatures ranging from 8700 to 9500 K. Dresvin and El'-Mikati (1978) obtained a temperature of 10,000 K utilising absolute continuum intensities taken at the 450 nm region. Using relative continuum intensities, Kleinmann (1969) obtained an electron temperature of 11,400

K, Barnes and Schleicher (1980) in a 0.46 kW ICPT with coolant flow only, showed that the electron temperature obtained from the absolute intensity of the continuum (533 nm) was equal to the excitation temperature only at the center of the plasma, the temperature difference increasing with increasing radius. Batal *et al* (1981) using the ratio of an argon line to the adjacent continuum found the electron temperature to be about 10,000 K which they noted to be significantly different from excitation temperatures obtained.

2.2.1.2. Excitation temperature

Assuming that the excitation is thermal and that the plasma is optically thin (in the region of the spectral line), the emission intensity of a spectral line can be expressed, in terms of an excitation temperature T_{exc}, as

$$I_i = 2\pi n_a l f_i \frac{g_i}{g_a} \frac{he^2}{m\lambda_i^3} \exp\left(\frac{-E_i}{kT_{exc}}\right) \qquad (2.6)$$

Where

n_a is the ground state density of the relevant atom or ion

l is the source depth

f_i is the oscillator strength

g_a and g_i are the statistical weight of the ground state and the ith level respectively

e and m the charge and mass of the electron

λ the wavelength of the relevant spectral transition

E_i the excitation energy

k Boltzmanns constant

and

T_{exc} the excitation temperature.

Thus the measurement of the absolute intensity I_i allows the determination of the excitation temperature provided the ground state density is known. This is usually determined from the ideal gas law, which for argon can be written as

$$n_a T_g = 7.34 \times 10^{27}\ \mathrm{m}^{-3}\ \mathrm{K} \qquad (2.7)$$

Where T_g is the gas kinetic temperature.

Uncertainty in the excitation temperature measurements arise mainly from the

degree of accuracy to which the absolute oscillator strengths f_i are known ($\approx 15\%$) and the degree to which the excitation and the gas kinetic temperature differ. Excitation temperatures have been determined from absolute argon spectral line intensities for both physical and analytical plasmas (Gold'farb and Dresvin, 1965; Scholz and Anderson, 1968; Leonard, 1972; Barnes and Schleicher, 1980; Barnes and Genna, 1981; Meubus, 1982) with observed maximum values between 7000 and 12,000 K.

The excitation temperature can be also be determined using relative spectral line intensities. Following from equation 2.6, the ratio of two spectral line intensities I_i and I_j yields

$$\ln\frac{I_i}{I_j} = \ln\left(\frac{g_i f_i \lambda_j{}^3}{g_j f_j \lambda_i{}^3}\right) + \frac{(E_j - E_i)}{kT_{exc}} \tag{2.8}$$

Provided the transition probability relative to each other is known, a common excitation temperature is easily determined. Extending the ratio measurement to many lines, the linearity of a (Boltzmann) plot of

$$\ln\left(\frac{I_i \lambda_i{}^3}{g_i f_i}\right) \text{ versus } E \tag{2.9}$$

not only determines a value for T_{exc} but also verifies the assumption of a common excitation temperature, if only for the energy levels plotted. For a completely thermal plasma a common excitation temperature will prevail for all energy levels. In plasmas deviating from equilibrium, energy levels lying close together may exhibit a common excitation temperature but it is doubtful that this temperature will be applicable to energy levels outside of this range. Errors may also arise due to the small difference in the energy of these levels. Overall, however, the many-line method is more accurate than that obtainable using equation 2.6 due to the relative transition probabilities being more accurately known than the absolute values. It should, nevertheless, be noted that the use of different sets of transition probabilities can lead to differences of up to 1100 K in the excitation temperature of argon (Mermet, 1975).

The Boltzmann plot method has been applied to argon spectral lines for both physical plasmas (Scholz and Andersson, 1968; Desai and Corcoran, 1968, 1969; Johnson, 1966; Shamin and Wooding, 1971) and analytical plasmas (Alder and Mermet, 1973; Mermet, 1975; Kornblum and De Galan, 1974, 1977; Uchida *et al*, 1981). It has also been applied to hydrogen spectral lines in the argon plasma (Visser *et al* 1976). Argon excitation temperatures obtained using this method have ranged from 3000 to 11,000 K.

The two-line ratio method (equation 2.8) has also been applied to the spectral lines emitted by the elements introduced by the aerosol flow through the center of the plasma. This technique not only increases the energy differences ($E_i - E_j$) available but allows the use of more accurately known transition probabilities. Excitation temperatures obtained with the introduction of zinc (Boumans and De Boer, 1976; Kornblum and De Galan, 1977), titanium (Mermet, 1975; Jarosz, Mermet and Robin, 1978), vanadium (Jarosz, Mermet and Robin, 1978) and iron (Mermet, 1975; Kalnicky, Kniseley and Fassel, 1975; Alder, Bombelka and Kirkbright, 1980; Furata and Horlick, 1981; Uchida *et al*, 1981; Blades and Caughlin, 1985) have shown that the excitation temperature increases from 5000 to 6500 K for the lower excitation energies (5.3 eV, Fe, Ti) to 6000 - 8000 K for higher excitation energies (7.7 eV, Zn).

2.2.1.3. Gas Kinetic Temperature

One of the central problems in determining the state of equilibrium of the plasma in the ICPT is the separate determination of the electron and gas (heavy-particle) temperatures. However, an accurate method of establishing the gas kinetic temperature in a low temperature plasma remains a major diagnostic problem. Table 2.1 lists some of the available methods together with their parameter temperature dependence and significant experimental problems. Of the methods available that are not completely dependent on the the plasma being in LTE, only two have been applied to analytical plasmas, namely Doppler-broadening and molecular rotation lines. Of these two, the molecular rotation has taken precedence due to the high dispersion monochromators required and the difficulty of isolating the Doppler-broadening from the high pressure broadening present in the ICPT. The rotational temperature is in the majority of cases very close to the gas kinetic temperature as the interaction between the heavy particles forming the plasma is effective at the low energys that exist between rotation levels and equilibrium is generally established within a few collisions. Determination of the rotation temperature is established by measuring the relative intensities of rotational lines within the same vibrational band.

The gas kinetic temperatures obtained by various authors using these two methods have varied considerably. Using OH-rotation lines, Kornblum and De Galan (1974) measured a temperature of 3100 K in a 50 MHz 0.4 kW ICPT whereas Kleinmann *et al* (1969) in a similar ICPT (50 MHz, 0.27 kW) obtained a temperature around 2100 K using CN-rotation lines and argon line widths. Human and Scott (1976) using Doppler line-widths reported temperatures ranging from 5000 K obtained utilising Ca and Sr spectral lines to 6700 K from argon spectral lines. Kawaguchi, Ito

Experimentally measured Quantity	Temperature Dependence	Conditions of applicability Difficulties, References
Absolute intensity of atomic spectral lines	T_G^{-1}	Depends on state of equilibrium, excitation temperature must be known accurately
Rotational temperature	$\exp\left(\frac{-A}{T_G}\right)$	low temperatures molecular gases
Doppler broadening	$T_G^{-\frac{1}{2}}$	Noise from other broadening
Heat flux	T_G	Depends on state of boundary layer, transport coefficient
Shock-wave velocity	$T_G^{-\frac{1}{2}}$	depends on thermo-dynamic quantities complex measurements
Flow enthalpy	T_G	Depends on composition, state of equilibrium
Rayleigh scattering	T_G^{-1}	low intensity, noise from other types of scattering
Interferometry (phase difference)	T_G^{-1}	weak temperature dependence
Deflection of light	T_G^{-1}	weak temperature dependence
α , γ and x-ray absorption coefficients	T_G^{-1}	noise from surrounding cold gas

Table 2.1: Methods of Measuring Gas Temperature in ICPT

and Mizuike (1981) determined the gas and excitation temperatures from OH and Fe I lines respectively in a 2.5 kW 27.12 MHz ICPT. They found a difference between the temperatures exceeding 2000 K up to a height of 20 mm above the work-coil. Analysis by high resolution Fourier transform spectroscopy of the line-widths from 81 Fe I spectral lines by Faires, Palmer and Brault (1985) yielded a temperature of 6310 K. Higher powered ICPT's reported, as would be expected, higher gas kinetic temperatures. Talayrach *et al* (1972) using a 6.3 MHz, 12 kW generator reported a gas temperature of 5000 K from BO-spectral lines in an argon plasma, while C_2 spectral lines yielded a temperature of 6100 K from an argon-methane plasma produced by a 5.4 MHz, 6 kW R.F generator (Alder and Mermet, 1973).

2.2.1.4. Conclusions.

The wide range of gas, ionisation, excitation and electron temperatures reported for ICPT's (2000 to 12,000 K) can in part be traced back to variations in operating conditions and experimental techniques. However it is evident that the differences between the electron, excitational and gas kinetic temperatures can not be totally explained in these terms and that the general form of the results obtained to date indicate that

$$T_{gas} < T_{excitation} < T_{electron}$$

and that the excitation temperature T_{exc} determined increases with the excitation energy of the spectrometric species used (Kornblum and De Galan, 1977; Boumans and De Boer, 1978 and De Galan, 1984).

2.2.2. Electron Density

2.2.2.1. Measurement by Stark Broadening

Stark broadening of spectral lines emitted by argon and hydrogen (H_β) provides a method that allows the determination of the electron density, in the ICPT, free of any assumptions regarding the composition or state of equilibrium of the plasma and which is largely independent of the temperature (Griem, 1964). However only in the case of H_β is the accuracy of the calculated Stark-broadening parameters better than 5% while for argon the error is approximately 10%. Other causes of uncertainty arise from other causes of line broadening. Of these only instrumental broadening and thermal Doppler broadening are important. Errors can also arise if self-absorption is important and from the presence of density gradients.

Results derived from the addition of a small amount of hydrogen into the plasma to enable the use of H_β broadening gives a range of electron densities from 3×10^{21}

to 2.7 x 10^{22} m^{-3} for typical ICPT plasmas. Jarosz *et al* (1974) found that the argon I 549.95 nm spectral line yielded density measurements 10 - 25% less than the value derived from H_β (1.2 x 10^{22} m^{-3}). Also using argon, Mermet (1975) found that the axial density decreased (1.1 x 10^{22} to 3.0 x 10^{21} m^{-3}) with increasing height above the work coil (10 - 20 mm) and also with increasing aerosol flow-rate (0 - 2.5 l/min). Uchida *et al* (1981) obtained an electron density of 5 x 10^{21} m^{-3} with an input power of 1.5 kW and an aerosol flow-rate of 0.65 l/min. Results using H_β by Caughlin and Blades (1981) obtained with various input powers and observation heights indicated that increasing the input power increased the electron density at all observation heights. The electron density at 0.75 kW (0.3 – 1.5 x 10^{21} m^{-3}) differed by almost an order of magnitude from that at 1.75 kW (2.0 – 5.0 x 10^{21} m^{-3}). Blades and Caughlin (1984) found that the electron density fell from 4 x 10^{21} m^{-3} for plasma with an aqueous solution being introduced through the center to 2 x 10^{21} m^{-3} upon the introduction of an organic solution. Furuta, Nojiri and Fuwa (1985) utilised a SIT detector together with a photomultiplier tube to build a complete contour map of the electron density of a plasma produced in a 1.1 kW 27 MHz ICPT. They found that the maximum electron density (4 x 10^{21} m^{-3}) occurred at a height of $\approx$ 2mm above work-coil and at a radius of 5mm.

Montaser and Fassel (1981, 1982) using a technique based on the fact that as the principal quantum number increases, the wings of Stark broadened spectral lines start to overlap each other, and will, before reaching the series limit, merge completely to form a continuum. They obtained electron densities ranging from 4 x 10^{20} to 3 x 10^{21} m^{-3} depending on the observation height and gas flow-rate for an argon ICPT. They also compared the electron densities between an argon and a argon-nitrogen ICPT and found the values for the argon-nitrogen torch, at the same input power to be consistently less (8.5 x 10^{19} to 4 x 10^{20} m^{-3}).

2.2.2.2. Measurement of the Electron Density from the Continuum Intensity

As the dependence of equation (2.5) on the electron temperature is very weak ($n_e \propto T_e^{\frac{1}{4}}$) the electron density is readily derived from the continuum intensity. Kornblum *et al* (1974) reported values for the electron density ranging between 5 x 10^{20} and 2 x 10^{21} m^{-3}. Batal, Jaroz and Mermet (1981) determined the electron density from the continuum to be (5 x 10^{20} m^{-3}) in good agreement with the value obtained from the Stark broadening of the Ar I 549.5 nm spectral line in their 40 MHz plasma.

2.2.2.3. Electron Density Calculated from Saha's Equation

Assuming local thermal equilibrium, Saha's equation for ionisation equilibrium is given by

$$\frac{n_{ion}\, n_e}{n_i} = \left(\frac{2g_{ion}}{g_i}\right)\left(\frac{(2\pi m_e k T_{ion})^{\frac{3}{2}}}{h^3}\right)\exp\left(\frac{-E_{ion}}{kT_{ion}}\right) \qquad (2.10)$$

where

n_{ion}, n_e and n_i are the number densities of the ions, electrons and argon neutral level i respectively.

g_{ion} and g_i the respective statistical weights.

and

E_{ion} is the ionisation energy.

Provided the ionisation temperature (T_{ion}) is known then this equation can be used to derive the electron density where

$$n_e = n_{ion} = n_{total} - n_i \qquad (2.11)$$

where n_{total} and n_i are the total and excited neutral number densities respectively.

Assuming the ionisation temperature is equal to the excitation temperature as determined from argon spectral lines, Gold'farb and Dresvin (1965) and Desai and Corcoran (1968) obtained electron densities ranging from 1×10^{21} to 4×10^{21} m^{-3}.

With the introduction of suitable elements into the plasma via the aerosol flow, equation (2.8) can again be utilised, this time with n_i and n_{ion} determined from the relevant neutral and ionic spectral line. Electron densities determined by this method cover a wide range (Boumans *et al*, (1973)) 2×10^{20} m^{-3}, (Kornblum *et al*, (1974)) 10^{23} m^{-3}, (Mermet, (1975)) 2×10^{19} m^{-3}). This spread of values cannot be totally explained by the different operating conditions and must in part be due to differences in the ion temperatures used and thus raises serious doubts as to whether the ratio of neutral/ion spectral line intensities relates directly to the neutral/ion density ratio.

2.2.2.4. Conclusion

Apart from the results obtained using Saha's equation, the electron density is found to be in the range of 10^{21} to 10^{22} m^{-3}.

The electron densities determined with the use of Saha's equation are highly dependent on the value of the ionisation temperature employed. Therefore the variation in the electron densities obtained using methods less sensitive to the state of

equilibrium is a further indication of a deviation from thermal equilibrium in the ICPT plasma. Furthermore it appears that the measured electron densities are irreconcilable with the excitation and ionisation temperatures which have been shown to vary with the diagnostic element used.

A comparison of the measured electron densities, other than those obtained by Saha's equation, with Eckert's (1968) empirical relation

$$n_e R \approx 10^{20}\ \mathrm{m}^{-2} \qquad (2.12)$$

(where R, the radius of the torch, is 1 to 2 centimetres) yields results that are in good agreement.

2.2.3. Gas Flow Dynamics

In the development of the ICPT as a suitable source in emission spectroscopy the gas flow-rate was optimised, together with the input power and observation height, empirically. Since one of the factors causing a possible deviation from equilibrium is the loss of energy due to the loss of charged particles from the system by the forced flow along the torch it has become necessary to obtain a better understanding of the flow dynamics in the ICPT. However, determination of the velocity distribution in the ICPT is both difficult and complex. Three methods have been used to obtain results. These are

i) water-cooled pitot or total impact tubes (Gold'farb *et al*, 1967; Dresvin and Kubnikin, 1971; Chase, 1971; Klubnikin, 1977; Dresvin and Kh.El'-Mikati, 1977; Barnes and Schleicher, 1981; Barnes and Genna, 1981);

ii) Tracer-photographic techniques (Desai, Daniel and Corcoran, 1968; Meubus, 1974; Gold, 1977);

iii) Laser-Doppler anemometry (Gouesbet, 1975; Gouesbet and Trinite, 1977; Lesinski, Gagne and Boulos, 1981).

Chase (1971), using tracer techniques and high speed photography, was the first to detect the presence of recirculatory motion in the plasma. Klubnikin (1975) using a water-cooled pitot tube obtained velocity distribution measurements from a 40mm plasma torch operating with a frequency of 6 MHz and an input power of $\approx$7 kW. His results are shown in Figure 2.2. The stationary recirculation patterns arise from electromagnetic pumping and were found to move downstream as the flow increases. It was also noted that at low flow-rates surrounding air was entrapped in the plasma.

Gouesbet *et al* (1975, 1977) using laser Doppler anemometry obtained velocity

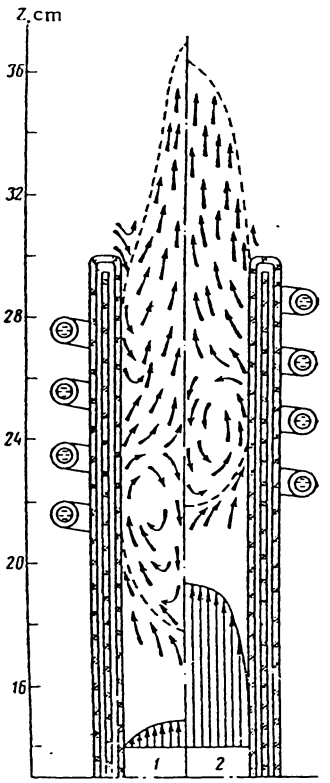

Figure 2.2: Schematic of the Flow Pattern of a Atmospheric Pressure Argon Plasma;
1) Flow-rate = 5l/min, 2) Flow-rate = 40l/min
(after Klubnikin (1975)).

profiles at the exit of the torch of a 5 kW atmospheric pressure inductively-coupled plasma for a gas flow of 21 l/min. They found a near parabolic profile with a maximum of 15 m/s along the centerline.

Of these results only those of Barnes and Lesinski refer to an analytical plasma, for which the introduction of an aerosol flow through the center of the plasma greatly increases the complexity of the flow. Lesinski, Gagne and Boulos (1981) using laser Doppler anemometry reported gas and particle velocity measurements for a high flow-rate ICPT. An argon coolant flow-rate of 63 l/min, support flow-rate of approximately

12 l/min were used together with an aerosol flow that varied from 4.8 to 7.4 l/min. Figure 2.3 gives the velocity profiles obtained over the central region of the plasma.

Barnes and Genna (1981) using a low-powered ICPT operating at a frequency of 26.5 MHz with a coolant flow of 10 to 19 l/min and aerosol flow from 0 to 1.2 l/min, the aerosol nozzle diameter being 0.9 to 2.1 millimetres, found that while the central channel gas velocity and temperatures varied with the aerosol flow-rate and the aerosol tube nozzle diameter there appeared to be little bulk gas mixing of the aerosol flow with the plasma below the top of the work coil. Increasing the coolant flow-rate increased the linear velocities near the walls but decreased them within the rest of the plasma. Little change was noted in the temperature distribution with the increase in coolant flow-rate.

Attempts have been made to mathematically model the temperature, gas flow, density distributions in the ICPT (see review, Boulos, 1985). However, the necessary simplifications and assumptions taken to make the computations tractable make the relevance of the conclusions to the actual ICPT rather dubious.

2.3. Excitation mechanism: Proposed Models

There is clear evidence as outlined above that the plasma in the ICPT is not in a state of local thermal equilibrium (LTE). Together with the reported variations in the temperature measurements were the reports of apparent high analyte ionic sensitivities and the absence of significant matrix effects (Boumans and De Boer, 1975, 1977; Scott *et al*, 1974). As these later two are advantageous analytically and yet sensitive to the operating conditions (input power, flow-rate, sample uptake, observation height) and can not be understood in terms of the model of partial local equilibrium (pLTE), various attempts have been made to establish a model of the plasma that will describe the dominant processes.

Over approximately the last ten years various models have been postulated which have suggested that one or other of a number of possible mechanisms available to the plasma is the dominant cause of the experimental observations made in the ICPT. These mechanisms will be discussed in detail in Chapter Three, but first the various models are summarised.

Mermet's idea (1975) of an overpopulation of argon metastable populations was developed by Boumans and De Boer (1977) in an attempt to explain the observed analyte atom/ion spectral line intensity ratios. They calculated the metastable population through Saha's equation using an assumed electron density of 10^{22} m^{-3} and a temperature of 6000 K which under the constraints of the LTE is clearly not valid

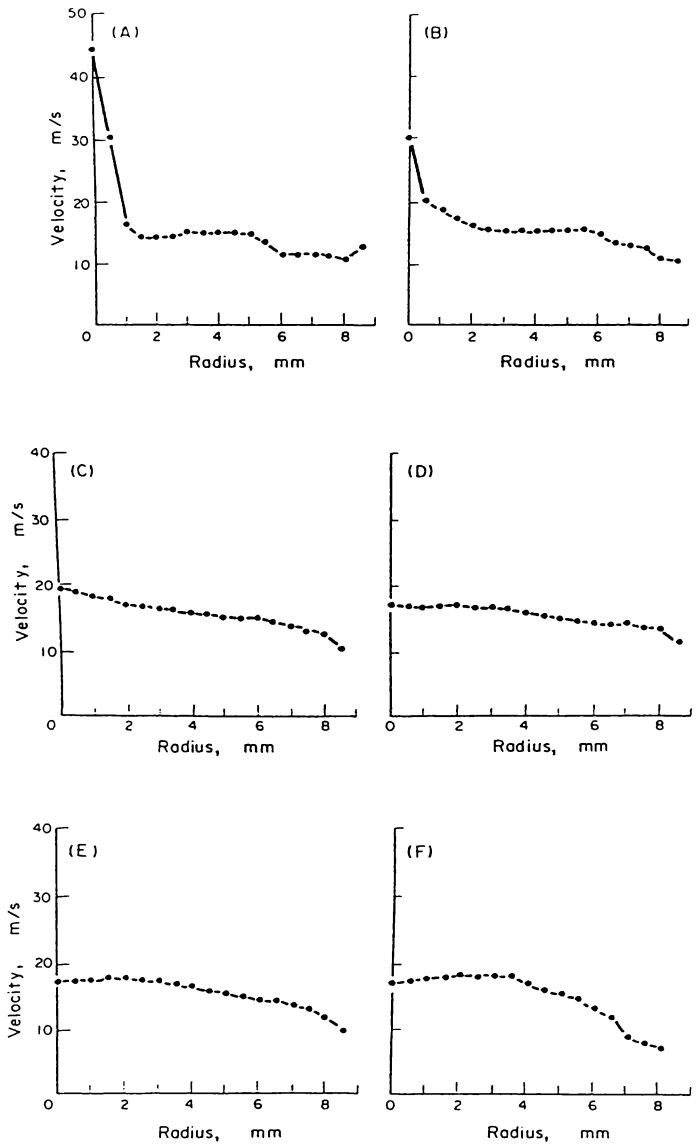

Figure 2.3: Plasma Velocity Profiles for a ICPT
A = middle of coil, B = top of coil, C = 4mm above, D = 6mm, E = 10mm, F = 12mm, nozzle diameter = 1.45mm.
(after Barnes and Genna, 1981)

(see Chapter 3). As the plasma is collision-dominated, according to Blades and Hieftje (1982) both the radiative and metastable 4s levels (11.54 to 11.82 eV, Figure (3.1)) will have similar lifetimes and thus similar populations therefore there would not appear to be anything special with regard to the argon metastables. The measurement of the metastable population has been attempted by Uchida *et al* (1981) by atomic absorption techniques and, just recently, by Houk, Fassel and LaFreniere (1986) by direct detection of the vacuum ultraviolet radiation using an optical sampling orifice. Houk *et al* estimated the number density of the upper state of the Ar I 106.67 nm spectral line to be of the order of 10^{17} m^{-3}. This is similar in magnitude to the population of the metastable argon levels measured by Uchida *et al.* Evidence was also presented indicating that the argon resonant radiation can be trapped in the ICPT. Blades and Hieftje (1982) in an attempt to explain the high concentration of metastables (it should be noted that the concentration is only higher than expected if the plasma is in LTE, that is, the excitation temperature obtained is indeed the appropriate temperature to describe the system) proposed that while transitions between the metastable and ground state are forbidden, the presence of nearby levels capable of radiating to the ground level rapidly equilibrate the metastable levels by collision. It was still possible to maintain a superthermal population of metastables due to radiation trapping of the vacuum ultraviolet emitted by these levels (see Figure (3.1)). Calculations by Mills and Hieftje (1984) deduced a metastable lifetime of only 1.6 μs from which they conceded that it is impossible for this mechanism to sustain the plasma up to 15-30 mm above the work coil.

In 1982 Aeschbach published a model where the temperature and electron densities are calculated using the input power transferred from the work coil of the R.F generator to the plasma. This results in a two-temperature plasma, where the gas temperature, that is, the kinetic temperature of the neutral atoms and ions is significantly lower than the electron (kinetic) temperature. Ionisation occurs inside the work coil to a depth limited by the skin effect to the outer edges of the plasma. The electrons produced then move into the cooler regions of the plasma by axial convection and ambipolar diffusion. Calculations using the experimental parameters (the spatial distribution of the two temperatures and electron density) obtained from two ICPT's (Kornblum and De Galan, 1977; Kalnicky, Fassel and Kniseley, 1977) gave (with minor modifications of the input data) good agreement with published experimental results.

Aeschbach's model suggested that the electron density was uniformly high across the plasma (10^{21} to 10^{22} m^{-3}) and exceeded the LTE value calculated from the 'gas'

temperature by several orders of magnitude. These electron densities persisted up to 30mm above the work coil. The 'gas' temperature equaled the electron temperature in the hot annular plasma but dropped to 5000 K in the central channel and to 3000 K in the outer edges of the plasma, while the electron temperature remained at 8000 K up to at least 8mm above the work coil.

While this model is very simple and cannot, for example, explain the relative populations of energy levels of any one species or the observed increase in excitation temperature with increasing excitation energy, it does offer an explanation of the origin of the high electron densities observed in the ICPT and it also provided, through the indicated temperature difference, the initial stimulation that led to the application of the relaxation method and hence the experimental results presented in this thesis.

In a recent paper, De Galan (1984) proposed an excitation model which attempts to utilise features of the above models together with the idea that the plasma in the ICPT is a plasma which is decaying from, to use his words, "conditions of heterogeneous disequilibrium to a situation of a homogeneous thermal plasma". That is, the properties of the analytical zone (10-30mm above the work coil) would be more that of an afterglow as distinct from some other plasma sources such as arcs and microwave discharges where the observations are made in the region of excitation. Raaijmakers *et al* (1983) and Schram *et al* (1983) proposed that although the plasma is not in equilibrium it is sufficiently close to LTE so that the system can be described using the measured electron density to deduce the electron temperature. From energy and mass balance considerations they argued that the deviation from equilibrium is 'sufficiently' small and that the argon ground state is underpopulated with respect to LTE, whereas the excited state densities of argon neutrals and analyte neutrals and ions are in reasonable agreement with this slightly non-LTE plasma. The overpopulation of the excited analyte ions with respect to LTE was explained by means of a charge transfer process. They concluded by stating that it appeared to be reasonably accurate to describe the plasma as an expanding hot gas, that is, the dynamics of the plasma could be evaluated using a gas dynamic approach in which the charged particles play only a minor role.

Theoretical calculations taking into account thermal conduction, ambipolar diffusion, collisional and radiative recombination, ionisation, axial convection, compression and expansion processes have been made by Huang and Liu (1986). These showed that above the work-coil (0-20mm) both thermal conduction and ambipolar diffusion processes are important in the decay of the plasma. It was also

indicated that compression heating of the plasma region caused by the decrease in temperature with increasing height has a significant influence in sustaining the plasma. The possibility of there being a temperature difference between the electrons and the other particles forming the plasma was ignored in this study.

2.3.0.1. Conclusions

The above models of the dominant excitation mechanism in the ICPT are only briefly sketched, with some of the problems inherent in each being mentioned. The major problem common to them all is that they are speculative, which emphasizes that there is a great need for quantitative experimental and theoretical data. The principal problem of obtaining sufficiently accurate data is that the deviation from equilibrium present in the ICPT is less than the error inherent in most of the available experimental techniques. However Aeschbach's two temperature model suggested an experimental technique which is not only very sensitive to any deviation from equilibrium but which would yield a direct measure of the difference between the electron and 'gas' temperatures. This is described in chapter 4.

Chapter 3

Equilibrium Conditions Relating to the ICPT

3.1. Introduction

A powerful concept in plasma spectroscopy is that of local thermal equilibrium (LTE). In plasmas where LTE prevails, the densities in specific quantum states are those pertaining to a system in complete thermodynamic equilibrium which has the same properties (density, temperature, chemical composition) as the actual plasma. In a stationary and spatially homogeneous optically-thin plasma, LTE can be expected to hold if collisional processes with the electrons dominate the radiative processes, namely, radiative decay and recombination. This condition is especially stringent for the lower-lying levels (see Figure 3.1) because their radiative lifetimes tend to be short and their collisional cross-sections small. When this condition does not hold down to the ground level but only to some higher state the plasma is said to be in a state of partial LTE (pLTE).

The normal operation of the ICPT produces a steady state plasma, which cannot be in a complete LTE since there is a net energy input into some regions of the plasma and a net energy output from others. However, because of the high thermal and electrical conductivity of many plasmas, such as the ICPT, the plasma will remain close to LTE, that is, having relatively small gradients of temperature and density (Griem, 1964). To fully understand the physical processes governing the behaviour of such a plasma it is necessary to establish the steady state properties present in the plasma under normal operating conditions. To explain any observed non-equilibrium phenomena it is necessary to not only establish the degree of this deviation from equilibrium but also its cause or causes.

Various dominant mechanisms have been proposed in an attempt to explain the characteristics of the plasma produced in the ICPT (Chapter 2). However, not withstanding these attempts, the reasons for the observed deviations from equilibrium

have not been conclusively established and the relationship between the electron temperature, the electron density and the argon level populations has not been satisfactorily explained. This may be partly due to the smallness of the deviation from equilibrium and partly to a lack of accurate radially resolved experimental results together with the lack of accurate and reliable atomic constants (transition probabilities, continuous absorption coefficients, etc). It has also been frustrated by attempts to explain the emission characteristics of analytes excited by the torch without regard to the state of equilibrium pertaining to the argon plasma.

As the degree of deviation from equilibrium is small it is feasible to use the equilibrium relations themselves to investigate the plasma. A method to do this is detailed in the next chapter, but first these relations require further discussion.

3.2. Equilibrium conditions

Attempts to determine measured excitation temperatures and densities have generally assumed local thermal equilibrium (LTE). Calculations, again assuming LTE, yielding the atom-ion distributions have given values one or two orders of magnitude greater than is obtained by experiment. The postulates of LTE demand that defining a certain number density (at a constant pressure) automatically defines the temperature (and vice versa) of the plasma. This can be seen from the following discussion.

3.2.1. Local Thermal Equilibrium

In the ICPT it is realistic to assume that only atoms and singly charged ions exist since $T_e \approx$ 1eV and that the total pressure is constant (atmospheric). Then for such a plasma in LTE the following relations hold.

i) Charge neutrality:

$$n_e = n_{ion} \tag{3.1}$$

ii) Boltzmann's Relation:

$$\frac{n_i}{n_j} = \left(\frac{g_i}{g_j}\right) \exp\left(\frac{-(E_i - E_j)}{kT_e}\right) \tag{3.2}$$

iii) Saha's Equation: see Equation (2.10)

and

iv) Dalton's law

$$P = kT_e(n_g + n_e + \sum_j n_j) \tag{3.3}$$

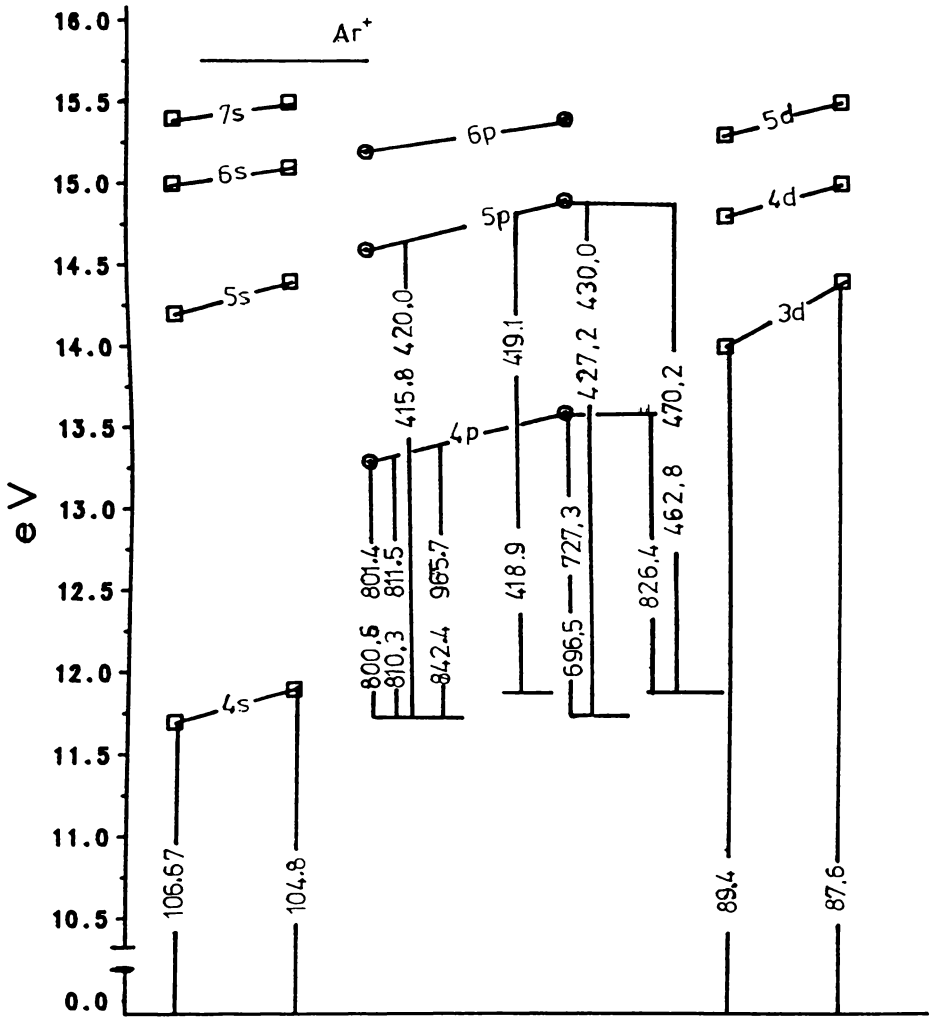

Figure 3.1: A Simplified Energy Level Diagram for Argon I

where

n_i , n_j are the number densities of the levels i,j belonging to the same species

n_g the neutral ground state density

g_i, g_j the statistical weights of the levels i, j

$E_{i,j}$ the energy of level i, j

$\sum_j$ is the summation over the excited states

k is Boltzmann's constant

It is evident that (given n_g) when one of n_i , n_e or T is determined with sufficient accuracy, these four equations are all that is necessary to determine the remaining parameters and thus fully describe an equilibrium ICPT plasma.

3.2.2. Criteria for the Establishment of Local Thermal Equilibrium

In an optically-thin homogeneous plasma, LTE can exist only if collisional processes dominate radiative processes. As electrons are the dominant excitation mechanism in the ICPT the electron density will be the deciding factor. Griem (1964) established the following criteria for the existence of complete thermal equilibrium in such a plasma

$$n_e \geq 9 \times 10^{23} \left(\frac{E_{21}}{E_{ion}}\right)^3 \left(\frac{kT}{E_{ion}}\right)^{\frac{1}{2}} \text{m}^{-3} \qquad (3.4)$$

where E_{21} is the energy gap between the ground state and the first excited state (11.52 eV for argon), and E_{ion} is the ionisation energy (15.72 eV for argon).

Thus for the ICPT, temperature $\approx$ 10,000 K, operating in argon, Griem's condition for LTE requires

$$n_e \geq 3.1 \times 10^{22} \text{ m}^{-3} \qquad (3.5)$$

This is approximately a magnitude greater than the electron density present in the plasma produced by an ICPT ($\approx 4 \times 10^{21}$ m^{-3}).

However if the resonance lines are optically trapped then the critical value for the electron density can be reduced by an order of magnitude (Griem, 1964) which would brings the measured electron densities within range of Griem's criteria. This result means that the excited states above the resonance levels will conform to a Boltzmann distribution. This is discussed further in the next section.

3.2.3. Partial LTE

A more probable state of equilibrium pertaining to the ICPT is that described as partial LTE (pLTE). If a plasma is in pLTE, Saha's equation is now valid only between the excited energy levels and the *ion* ground state. Saha equilibrium no longer exists between the *neutral* ground state and its excited states or the ion ground state. This deviation, generally, is due to losses caused by radiation and/or significant contributions to the balance equation (equations 3.6 and 3.7) arising from transport losses involving the neutral and ion ground levels (due to the higher collision transition rates the excited levels can generally be ignored (Griem, 1964)).

A comprehensive review of the validity conditions for LTE and pLTE is given by Griem (1964) and by Drawin (1976).

3.3. Deviations from Equilibrium

The degree to which a plasma complies with the concept of LTE is determined by

i) The number of elastic and inelastic collisions in any time period
ii) The density of the plasma
iii) The transfer co-efficients which equilibrate the temperature
iv) The magnitude of the heat exchange between the plasma and its surroundings
v) The co-efficient of optical absorption
vi) The rate of loss of charged particles from the plasma
vii) The power supplied to a plasma from the external RF source.

For a plasma to be in complete LTE there must be a detailed balance of each collision process or radiative transfer with its reverse process. Figure 3.2 is an energy exchange diagram for the first and second order collisions in a steady-state argon ICPT. The absence of detailed balance, indicated by the different thicknesses of the arrows, denotes a deviation from equilibrium, and therefore since the concept of temperature for the electrons (T_e), excitation (T_{exc}), neutral argon atoms (T_g) and ionisation (T_{ion}) requires the presence of a Maxwellian velocity distribution, and a Boltzmann distribution of the excited states, and ionisation equilibrium, it is no longer strictly correct to use the term 'temperature'. A disturbance in the detailed balance implies the non-fulfillment of these conditions and while it is not expected that a small laboratory plasma, such as the ICPT, would be in perfect balance, the survey of the literature shows that the deviation is not large and therefore we shall continue to use the term temperature. The aim of this thesis is to identify the extent of this disturbance and its cause; but first it is appropriate to give a discussion of some of the possible causes.

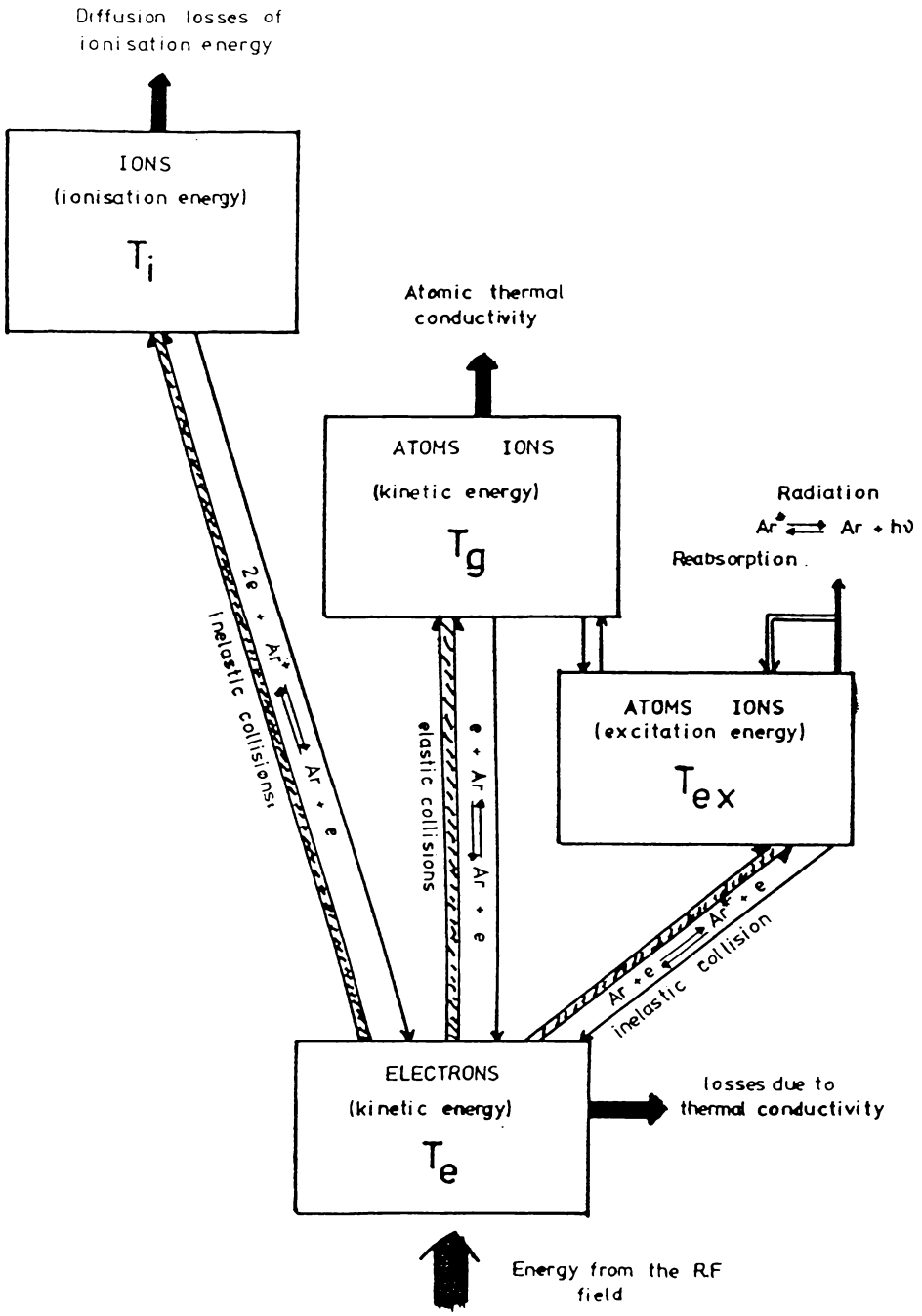

Figure 3.2: Energy-exchange diagram for a argon ICPT

3.3.1. Deviation from a Maxwellian Velocity Distribution

It is generally assumed that each species (electrons, ions, and neutral argon atoms) present in the ICPT can be approximated to a very high degree of accuracy as having a Maxwellian velocity distribution everywhere except very close to the walls. Any deviation from a Maxwellian distribution would involve a decrease in the number of high energy electrons in comparison with that expected (Griem, 1964; Alexandrov, Gurevich and Podmoshenskii 1967) and as the diagnostic methods used (see Chapter 4) depend on electrons of average energy any such deviation can be neglected.

3.3.2. Kinetic Equilibrium

If the assumption of a Maxwellian velocity distribution for each species present is valid. Then a temperature may be defined for each component distribution. These temperatures are not necessarily the same and may vary from species to species. The electron temperature is the highest because the energy supplied by the RF field is taken up by the lightest and most mobile component in the plasma, the electrons. These collide with the argon atoms and ions, transferring some of their energy. These collisions also knock the electrons out of phase with the electric field and thus the electrons rapidly regain the lost energy from the RF field and the cycle continues. It follows therefore that the electron temperature must always exceed that of the other species constituting the plasma while external energy is being pumped into the system by the RF field.

The rate of heating of the argon neutrals and ions together with the state of kinetic equilibrium are determined by the balance between the energy transferred from the electrons and the energy lost from the system. This is given by the following balance equations. The electrons by

$$\overline{\sigma E^2} = \frac{3}{2}\delta \nu_e n_e k (T_e - T_g) - \nabla \lambda_e \nabla T_e + U_r \tag{3.6}$$

and the heavy particles by

$$n_a v c_p \nabla T = \frac{3}{2}\delta \nu_e n_e k (T_e - T_g) + \nabla \lambda_a \nabla T \tag{3.7}$$

where

$\overline{\sigma E^2}$ is the average value of the power supplied by the RF field.

δ is the portion of electron energy lost per collision.

ν_e is the electron collision frequency.

σ is the electrical conductivity

λ_e, λ_a the electronic and atomic thermal conductivities

U_r is the radiation losses

Now if the temperature dependence of the thermal conductivity is ignored then from equation 3.6

$$T_e - T_g = \frac{(\overline{\sigma E^2} + \lambda_e \nabla^2 T_e - U_r)}{\frac{3}{2}\delta \nu_e n_e k} \tag{3.8}$$

However, in the case of the ICPT, it is more useful to use the the heavy particle balance equation (3.7) which becomes

$$T_e - T_g = \frac{(n_a v c_p \nabla T - \lambda_a \nabla^2 T_g)}{\frac{3}{2}\delta \nu_e n_e k} \tag{3.9}$$

This reduces, in the case of a forced gas flow, to

$$T_e - T_g = \left(\frac{n_a v c_p}{\frac{3}{2}\delta \nu_e n_e k}\right)\left(\frac{dT_g}{dz}\right) \tag{3.10}$$

Below 12,000-13,000 K, the transferable fraction of energy per electron/argon atom collision, δ, can be regarded as the portion transferred by elastic collisions, that is

$$\delta = \delta_{el} = \frac{2m_e}{M} \tag{3.11}$$

where m_e and M are the mass of the electron and argon atom respectively. With each collision an electron will transfer only $2m_e/M$ of its energy, while the collision frequency (the number of collisions per second) is of the order of 10^{10} (at 10,000 K).

3.3.3. Excitation Equilibrium

Excitation equilibrium requires a Boltzmann distribution for the excited states in the plasma. As can be seen from Figure 3.2 the only processes which may significantly affect the state of the excitation equilibrium in the argon ICPT plasma are,

(i) excitation by electron

(ii) photoabsorption

(iii)de-excitation by collisions of the second kind

and

(iv) photoemission.

If the plasma is collision-dominated, contributions of photo-processes are essentially negligible, and the excitation equilibrium can be established provided a detailed balance exists between the excitation by electrons and the de-excitation by

collisions of the second kind. This results in the population of the argon I excited states assuming a Boltzmann's distribution. Deviations from excitation equilibrium arise as a result of the loss of particles (neutral, ions and electrons) from the plasma. However as the plasma in the ICPT is (mostly) optically-thin, the radiation emitted from the plasma is lost from the system. This indicates a disturbance of the Boltzmann distribution of the excited states. But since the collisional cross-sections increase and the probability of radiation transitions decreases with the higher the excited state and provided the electron density is sufficiently high the excited states will still conform to a Boltzmann distribution.

Any deviation (from a Boltzmann distribution) first presents evidence of itself with the excited states closest to the neutral ground state (4s levels) and then progressively affects higher states as the deviation increases. The various processes which have a bearing on the population density of the 4s level are

$$Ar(4s) + e \rightleftarrows Ar(4p) + e \tag{3.12}$$

$$Ar(4p) \rightarrow Ar(4s) + h\nu \tag{3.13}$$

$$Ar(3p) + e \rightleftarrows Ar(4s) + e \tag{3.14}$$

$$Ar^{+} + e + e \rightleftarrows Ar(4s) + e \tag{3.15}$$

$$Ar(4s) + e \rightleftarrows Ar(5p) + e \tag{3.16}$$

$$Ar(5p) \rightleftarrows Ar(4s) + h\nu \tag{3.17}$$

Giannaric and Incropera (1973) in a theoretical study of an atmospheric pressure argon arc, having similar properties to that of the ICPT, calculated the transition probabilities of the above processes (see Figure 3.3). The results of this study applied to the ICPT indicates that the collisional exchange between the 4s and 4p level (equation 3.12) has the dominant effect on the 4s population. However, it must be noted that while the radiative decay (equation 3.13) is only of moderate importance it is these two processes that are the major contributors to the 4s population. This together with with an electron density less than that required to satisfy Griem's criteria for the establishment of LTE implies a reduction in the capacity of the electrons to dominate, that is, the 4p - 4s collisional exchange rate will approach the 4p - 4s radiative decay rate which means that if the 4s - 4p line radiation is not re-absorbed in the plasma it will give rise to the over-population of the 4s state. In turn to maintain an over-all

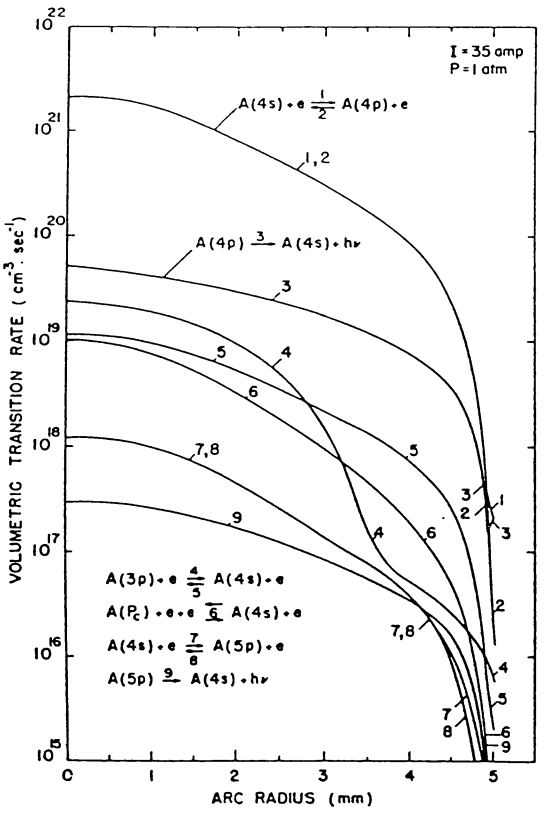

Figure 3.3: Transition Rates for Processes which Establish the 4s Level Population in a Argon Arc.
After Giannaris and Incropera, 1973.

rate balance the 4s - 4p excitation rate must be greater than the 4p - 4s de-excitation rate which requires a further increase in the 4s population.

Thus in a plasma where the electron density has decreased due to convective losses to the extent that the plasma is no longer collision dominated down to the 4s state and where the 4s - 4p spectral lines are optically-thin a state of excitational equilibrium will not extend to include the 4s energy levels.

3.3.4. Ionisation Equilibrium

Ionisation in the ICPT is caused by electron collisions and photo-absorption, and

recombination occurs predominately from three-body collisions and photo-combination. As the plasma is optically thin for most of the spectral range, the effect of photo-ionisation can be regarded as insignificant.

When the temperature of the electrons and the neutral/ion gas are different or when there is a preferential loss of particles of one type from the system, the steady state no longer corresponds to that described by Saha's equation. In this case the concentration of charged particles in ionisation-recombination type reactions is determined from the balance equation for the density of the particles.

$$\frac{\partial n_e}{\partial t} = \beta n_a n_e - \alpha n_e n_{ion} - \nabla \cdot I \tag{3.18}$$

During the operation of the torch the system is in a steady state, therefore

$$\frac{\partial n_e}{\partial t} = 0 \tag{3.19}$$

and taking $n_{ion} = n_e$

$$\alpha n_e^2 = \beta n_a n_e - \nabla \cdot I \tag{3.20}$$

If the system is in complete LTE, $\nabla \cdot I = 0$ and this equation becomes

$$n_a n_e \beta = \alpha n_e^2 \tag{3.21}$$

That is,

$$\beta n_a = \alpha (n_e)_{equi}. \tag{3.22}$$

Now if the plasma is close to LTE, $\nabla \cdot I$ is small and assuming α and β are unchanged equation 3.20 becomes

$$\alpha (n_e)_{equi} n_e = \alpha n_e^2 + \nabla \cdot I. \tag{3.23}$$

Noting that the recombination time is given by

$$\tau = \frac{1}{\alpha n_e} \tag{3.24}$$

then

$$(n_e)_{equi} - n_e = \tau \nabla \cdot I \tag{3.25}$$

α and β are the co-efficients of recombination and ionisation respectively and $\nabla \cdot I$ the divergence of the flow of particles I out of the plasma. For the ICPT the flux of electrons from the system occurs by two methods, ambipolar diffusion and convection due to the gas flow. To simplify the problem further only those convective losses in the vertical direction will be considered. Thus equation 3.25 becomes

$$(n_e)_{equi} - n_e = -\tau \left[\nabla \cdot (D_a \nabla \cdot n_e) - v_z \frac{\partial n_e}{\partial z} \right] \tag{3.26}$$

Assuming the plasma is axisymmetric and close to LTE this equation becomes

$$(n_e)_{equi} - n_e = -\tau \left[-v_z \frac{\partial n_e}{\partial z} + \frac{\partial D_a}{\partial T_e} \frac{\partial T_e}{\partial n_e} \left[\left(\frac{\partial n_e}{\partial r} \right)^2 + \left(\frac{\partial n_e}{\partial z} \right)^2 \right] \right. \tag{3.27}$$

$$\left. + D_a \left(\frac{\partial^2 n_e}{\partial r^2} + \frac{1}{r} \frac{\partial n_e}{\partial r} + \frac{\partial^2 n_e}{\partial z^2} \right) \right]$$

where the substitution of typical values expected over the range of operating conditions used indicated that the term $\frac{\partial D_a}{\partial T_e}$ could be neglected. Thus

$$(n_e)_{equi} - n_e = -\tau \left[v_z \frac{\partial n_e}{\partial z} - D_a \left(\frac{\partial^2 n_e}{\partial r^2} + \frac{1}{r} \frac{\partial n_e}{\partial r} + \frac{\partial^2 n_e}{\partial z^2} \right) \right] \tag{3.28}$$

Apart from ambipolar diffusion, recombination and convective losses another possible cause of deviation is losses arising from atomic diffusion. Griem (1964) has indicated that provided the following criteria is satisfied

$$\frac{1}{T} \frac{\partial T}{\partial r} d = \epsilon << 1 \tag{3.29}$$

where d is the mean atom excitation distance, any deviation due to atomic diffusion is insignificant. However according to Stokes (1971) this criteria is over restrictive for steady-state plasmas as excitation is due almost entirely to electron impact and provided an LTE population of unexcited atoms is present it is unimportant how far they have travelled since they were last excited. That is, unless the diffusion is such as to prevent the atoms from following the temperature gradient it can be safely neglected. Calculations show that for the ICPT atomic diffusion is relatively insignificant.

3.3.5. Effect of Molecular Additives on the State of Equilibrium

Up to this point the discussion has been concerned only with a pure argon plasma. The introduction of molecular additives into the plasma will assist the approach to thermal equilibrium, due to the presence of molecular ionisation and recombination, energy exchange via rotational and vibrational states and the exchange of excitation energy.

Measurements on arcs operating at atmospheric pressure in pure argon with the addition of small controlled quantities of molecular gases (hydrogen, nitrogen, oxygen and air) have shown that the introduction of these molecular traces changes not only

the parameters of the arc plasma but also the degree of deviation from equilibrium (Polak and Slovetskii, 1975a, 1975b; Kasakov and Gol'dfarb, 1980). It was found that when the molecular gas concentration was increased the electron density decreased, and when the concentration of the trace gas exceeded one per cent the component temperatures became equilibrated.

In the ICPT, the additives are introduced through the center of the plasma which is effectively screened from the RF field, and as shown in Chapter seven, the effect on the plasma is reduced.

3.4. Conclusion

The results of this study of equilibrium conditions as they pertain to the ICPT high-lights the fact that all the processes in a plasma are inter-related, changes in one process necessarily changes the entire system. The radiative losses in the ICPT are generally regarded as negligible, however, observations of the radiative losses provide another piece of the picture leading to an understanding of the processes governing the plasma. In Chapter 4 a method is described that is sufficiently sensitive to enable the determination of the state of equilibrium in the ICPT plasma and the cause of any deviation present.

Chapter 4

Methodology

4.1. Introduction

Arising from the experimental evidence (Chapter 2) and the means of energy exchange (Chapter 3) it is reasonable to accept that for the argon plasma in the ICPT the kinetic temperatures are such that

$$T_{electron} > T_{gas} \tag{4.1}$$

although the degree of difference in the temperatures is unknown.

This deviation from kinetic equilibrium allows the utilisation of a relaxation method. Generally, experiments involving relaxation phenomena perturb an equilibrium situation by rapidly changing an external parameter such as temperature, pressure or electric field strengths. By measuring the associated relaxation times, kinetic information is obtained. In the case of an ICPT plasma the approach may be reversed. Since the steady state plasma is not in equilibrium, rather than perturbing the plasma it is appropriate to remove the energy source holding the plasma in its state of non-equilibrium (the RF field).

4.2. Thermal Relaxation

When the external heating (RF field) of the plasma is removed the plasma starts to relax to the energy level of its surroundings. From the relaxation processes available to an argon plasma (see equation 3.6) it can be shown that the various components of the plasma (electrons, atoms) possess different relaxation times. That is, in particular,

$$\tau_e \neq \tau_g \tag{4.2}$$

where τ is the respective relaxation time.

For an atmospheric pressure inductively-coupled argon plasma, the electron

relaxation time can be estimated from

$$\tau_e = H/P \tag{4.3}$$

where H is the amount of heat liberated by the electrons cooling, P is the input power, ΔT is the expected drop in temperature (assumed to be ≈ 1000 K) and Ω is the plasma volume. This can be written as

$$= \frac{\frac{3}{2} n_e k \Delta T \Omega}{P}$$

which under normal operating conditions in the ICPT is of the order of

$$\approx 10^{-5} \text{seconds}$$

On the other hand significant changes in the plasma can be estimated using the recombination time

$$\tau_a = \frac{1}{\alpha n_e} \tag{4.4}$$

$$\approx 10^{-3} \text{seconds}$$

so that for this plasma

$$\tau_e << \tau_a . \tag{4.5}$$

Thus the electrons will first relax to the temperature of the neutral/ion gas and then the entire system relaxes uniformly to the temperature of its surroundings, that is, room temperature. Therefore removal of the R.F field results in the excess energy possessed by the electrons over that of the argon gas being transferred, in $\approx 10^{-5}$ seconds, into the argon gas.

Since the excitation, ionisation and recombination in an argon plasma of the form produced in the ICPT is collision dominated and of a step-wise nature it follows from the theory of collision-radiation decay of plasmas (Bates *et al*, 1962) that the excited states will be coupled by electron collision to the continuum. That is, quoting Condon and Shortly (1935), a system is coupled to the continuum when "terms lying higher than the ionisation potential of the atom are in a position to interact strongly with states in the continuous spectrum corresponding to unclosed electron orbits of one electron relative to the ion."

In terms of the argon plasma present in the ICPT this can be expressed more clearly along the lines used by Bates and Dalgarno (1962). The argon atom contains a

series of energy levels that converge to the ionisation energies that correspond to the various levels of the argon ion (see Figure 4.1). If an energy level i of the series

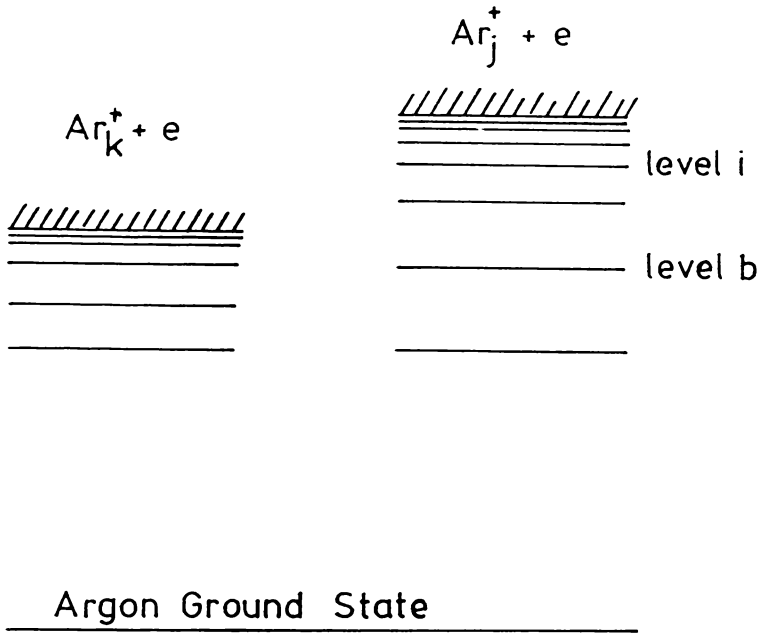

Figure 4.1: Schematic of an Energy Level Diagram.

associated with the ionisation energy E_j lies within the continuum of the series associated with energy E_k ($E_k < E_j$) and if the required selection rules (Condon and Shortley, 1935) are satisfied, when a free electron is present the free-bound radiationless transition

$$Ar_k^+ + e \rightarrow Ar_i \tag{4.6}$$

can occur. In general this is a transient recombination, with the reverse process (autoionisation)

$$Ar_i \rightarrow Ar_k^+ + e \tag{4.7}$$

maintaining a quasi-equilibrium where the population density $n(Ar_i)$ is very small. Under circumstances where the reverse process is inhibited it becomes possible for

true recombination to occur. Stabilisation can occur via three pathways

i) dielectronic recombination

$$Ar_k^+ + e \underset{\leftarrow}{\rightarrow} Ar_i \rightarrow Ar_b + h\nu \tag{4.8}$$

that is, the stabilisation is effected by a radiative transition from level i to some level b which is not subject to auto-ionisation.

ii) collisional stabilisation

$$Ar_k^+ + e \underset{\leftarrow}{\rightarrow} Ar_i + e \rightarrow Ar_b + e \tag{4.9}$$

and

iii) molecular stabilisation

$$ArX^+ + e \underset{\leftarrow}{\rightarrow} ArX' \rightarrow Ar' + X' \tag{4.10}$$

where X is another atom and $'$ is an exited state. Collisional stabilisation is more effective than radiative stabilisation at electron densities greater than $10^{19}\ m^{-3}$ but both processes are much slower than molecular stabilisation which is limited only by the radiation-less transition rate (Bates *et al* 1962). However, under the conditions prevailing in the ICPT collisional stabilisation will be the dominant process.

If P_1 is the probability of process 4.6 being true recombination and P_2 is the probability of auto-ionisation occurring then the recombination rate is given by $n(Ar_i)P_1$ and the population density by

$$n(Ar_i) = \left(\frac{P_2}{P_1 + P_2}\right) n_{equi}(Ar_i) \tag{4.11}$$

where $n_{equi}(Ar_i)$ is the population density of level i for the system in Saha equilibrium. Thus

$$\frac{n(Ar_k^+)n_e}{n_{equi}(Ar_i)} = \frac{2g_k}{g_i}\left(\frac{2\pi m_e kT_e}{h^2}\right)^{\frac{3}{2}} e^{-\left(\frac{\eta_{ik}}{kT_e}\right)} \tag{4.12}$$

where η_{ik} is the difference in energy between the Ar_i and the ionisation energy level of Ar_k^+. That is, for the ICPT the population of the ith state is given by the equation

$$\frac{n_e^2}{n_i} = \frac{2g_{ion}}{g_i}\left(\frac{2\pi m_e kT_e}{h^2}\right)^{\frac{3}{2}} e^{-\left(\frac{E_{ion}-E_i}{kT_e}\right)} \tag{4.13}$$

where

n_e is the electron density

n_i refers to the density of an excited state i above the resonance level

g_i, g_{ion} the statistical weights of level i and the ionisation level

m_e is the mass of the electron

T_e the electron temperature

and

E_i, E_{ion} the energy of the ith level and the ionisation energy respectively.

With the removal of the RF field and the relaxation of the electrons to the gas temperature and since the electron relaxation time is so much shorter than the recombination time that the electron density (n_e) will remain relatively unchanged as the electron temperature drops; and as

$$T_e \rightarrow T_g \tag{4.14}$$

equation 4.13 becomes

$$\frac{n_e^2}{n_i^*} = \left(\frac{2g_{ion}}{g_i}\right)\left(\frac{2\pi m_e k T_g}{h^2}\right)^{\frac{3}{2}} e^{-\left(\frac{E_{ion} - E_i}{kT_g}\right)} \tag{4.15}$$

where now n_i^* is the density of level i. Thus the population of the excited argon states will increase as the electron temperature drops to that of the gas temperature. That is,

$$n_i^* > n_i \tag{4.16}$$

This, in turn, will cause a sharp increase in the intensity of the respective spectral lines. This will then be followed by a monotonic drop in intensity as the system as a whole relaxes. If the RF field is switched on again (provided the break in the R.F field is sufficiently short), there will be an equally sharp decrease in intensity, as T_e increases to its steady non-equilibrium value, and this is then followed by a monotonic rise in intensity to the undisturbed steady state ICPT level. This behaviour is displayed in Photograph 6.1.

In the opposite case, where the excited states are coupled to the ground state, as in the case with metals, it can be seen from the Boltzmann relation

$$\frac{n_i}{N} = \frac{g_i}{Z(T)} e^{\frac{-E_i}{kT_e}} \tag{4.17}$$

where

N is the number of neutral atoms

and

$Z(T)$ is the partition function,

that the spectral line intensity in this case will drop suddenly with the removal of the RF field. Apart from any equilibrium considerations, this method reveals whether the system is coupled to the ground state or continuum.

4.3. Previous Applications of this Technique

Using the different relaxation times of the different particles in a plasma was first applied as a diagnostic method to plasmas, by Gurevich and Podmoshenskii (1964) to a mercury arc. By cutting the current flow to the arc they noted a sharp decrease in intensity of the mercury I 491.6 nm spectral line. Using the line intensities before and after cutting the current together with Boltzmann's relation yielded the temperature difference:

$$\Delta T = \left(\frac{kT_{exc}}{E_i}\right) \ln \left(\frac{I_o}{I_1}\right) \tag{4.18}$$

where I_o and I_1 are the initial and final intensity of the spectral line. They obtained temperature differences ranging from 0.5% for a discharge in air to 14% in mercury.

In a further study using an arc burning in an argon atmosphere, Alexandrov, Gurevich and Podmoshenskii (1967) clamped the arc current to zero in $\approx 2 \times 10^{-8}$ seconds, instead of decreasing in intensity the excited argon spectral line intensities increased sharply. As stated before this was due to the excited argon states being coupled to the continuum whereas the mercury line is coupled to the ground state. Using measurements of the absolute intensities of fifteen argon I spectral lines they established that the average difference between the electron temperature and the gas temperature was 2800 K, that is, the electron temperature decreased from 9400 K to 6600 K once the current was switched off. The authors noted the observed deviation from equilibrium was due to the loss of ionisation energy outside the discharge zone arising from ambipolar diffusion and convection. Since then this method has been used to investigate the state of equilibrium in other arcs (Aleksandrov, Gruzdeva and Podmoshenskii, 1974; Gruzdeva, Nikolaevskii and Podmoshenskii, 1974; Nick, Richter and Helbig, 1984)

In what appears to be the only application of this method to an inductively-coupled plasma, apart from the present thesis, Apsit (1971) investigated the behaviour of a 'physical' argon plasma by triggering the grid-leak circuit of the RF generator. He

noted the sharp increase in intensity of the excited argon spectral lines and by plotting the logarithm of the intensity ratio (before and after switching) against the energy difference ($E_{ion} - E_i$) where E_{ion} is the ionisation energy, he demonstrated that the excited argon states were in equilibrium with the free electrons. Then, using the relative spectral line/continuum method (Ar I 451.0nm, 450.0nm continuum) he showed that the plasma electron temperature was substantially higher than the gas temperature, the difference ranging from 2500-1500 K for input powers of 1-10 kW. The temperature difference decreased slightly with increased power. The greatest difference in temperature was located within the work coil being largest at the edge of the plasma and reducing rapidly towards the center. It was also noted that the temperature difference was radially asymmetric due to the introduction of cold argon gas. Figures 4.2 and 4.3 shows the distribution of the temperature difference with respect to the radius and height as determined by Apsit.

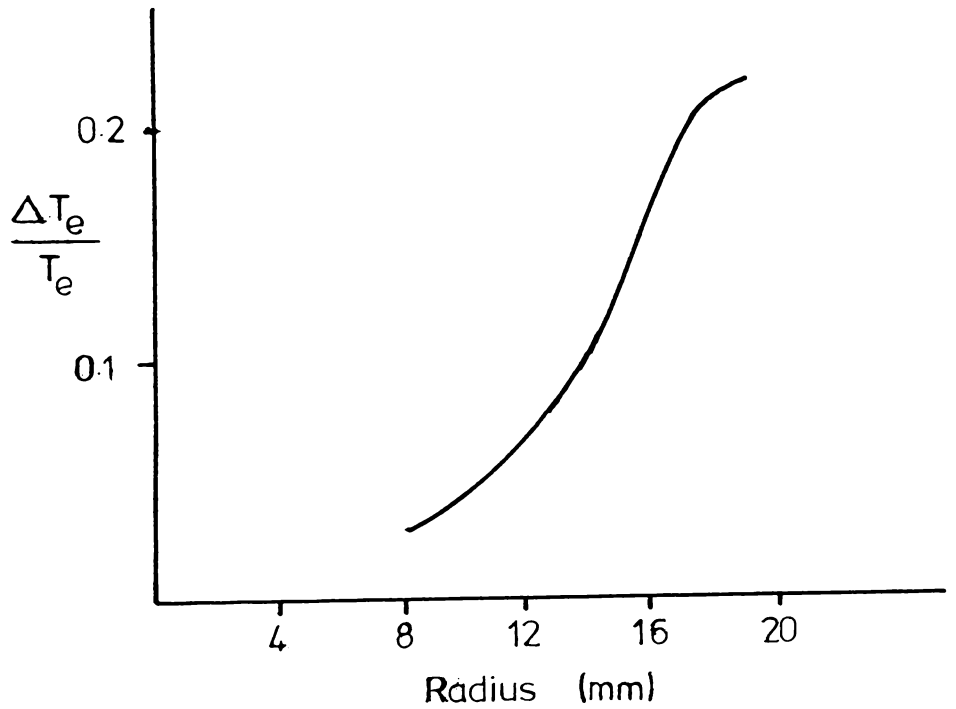

Figure 4.2: Radial distribution of the change in temperature $\frac{\Delta T_e}{T_e}$.

Input power = 3 kW.

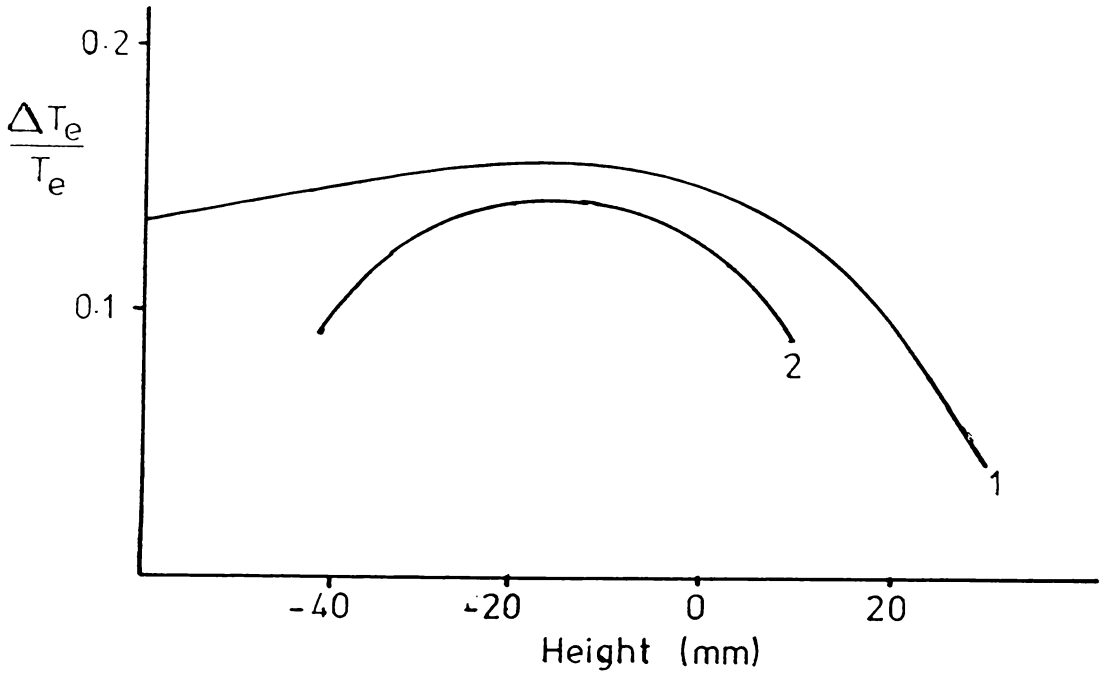

Figure 4.3: Variation of the temperature difference with Height.
Flow-rate 1) 40 l/min, 2) 0.

To enlarge on and extend the initial work of Alexandrov, Gurevich, Podmoshenskii and Aspit to the analytical plasma produced in the ICPT, a rapid switch off method for the removal of the RF field was developed. This allowed the study of the state of equilibrium under normal operating conditions. The following section describes how the removal of the RF field and its effect on the behaviour of the excited argon I spectral lines was used to determine and explain any deviations from equilibrium. The mechanics of achieving the actual RF field switching are described in Chapter 5.

4.4. Diagnostic Methods

4.4.1. Optically Thin Spectral Lines: Boltzmann Distribution and Saha's Equation

An essential requirement for both LTE and pLTE is that the excited argon I energy levels are in equilibrium with the free electrons. If the deviation from pLTE is small then the Saha equation (equation 4.13) remains valid. Then assuming that the

electron density (n_e) remains constant during the time taken for the electrons to cool to the gas temperature (this assumption is validated in chapter 6) and letting T_e be the electron temperature before the R.F field is switched off, and T_g the gas temperature to which the electron temperature relaxes to after the field is switched off, it follows from equations 4.13 and 4.15 that

$$\frac{n_i^*}{n_i} = \left(\frac{T_e}{T_g}\right)^{\frac{3}{2}} e^{\left(\frac{E_{ion}-E_i}{kT_g} - \frac{E_{ion}-E_i}{kT_e}\right)} \tag{4.19}$$

where n_i and n_i^* = the density of the i th energy level immediately before and after the electronic relaxation following switching. Letting

$$\frac{T_e}{T_g} = \gamma \tag{4.20}$$

then

$$\ln\left(\frac{I^*}{I}\right) = \frac{3}{2}\ln\gamma + (E_{ion}-E_i)\left(\frac{\gamma-1}{kT_e}\right) \tag{4.21}$$

where I and I^* are the relative intensities of the relevant excited argon I spectral line before and after switching.

Thus by measuring the relative change in intensity of optically thin excited argon I spectral lines before and after switch off it is possible to measure whether there is a Boltzmann distribution of the excited argon population levels. The establishment of a Boltzmann distribution, as shown graphically in Figure 4.4, allows an accurate determination of the difference between the electron and gas temperatures as well as a providing a measure of the electron temperature. The absence of a linear relationship in Figure 4.4 implies the lack of a Boltzmann distribution and/or a Maxwellian electron distribution.

Being a differential method this technique provides a very sensitive method of evaluating the state of equilibrium present in the plasma under varying operating conditions such as input power, gas flow-rates, introduction of molecules etc.

4.5. Radiative Losses

The effect of a rapid change in intensity of the spectral lines also presents the opportunity of investigating whether changes in radiative losses, arising from variations in the operating conditions, are significant and whether evidence of a change in radiation losses is indicative of a change in the state of equilibrium in the plasma. How this is achieved is discussed below.

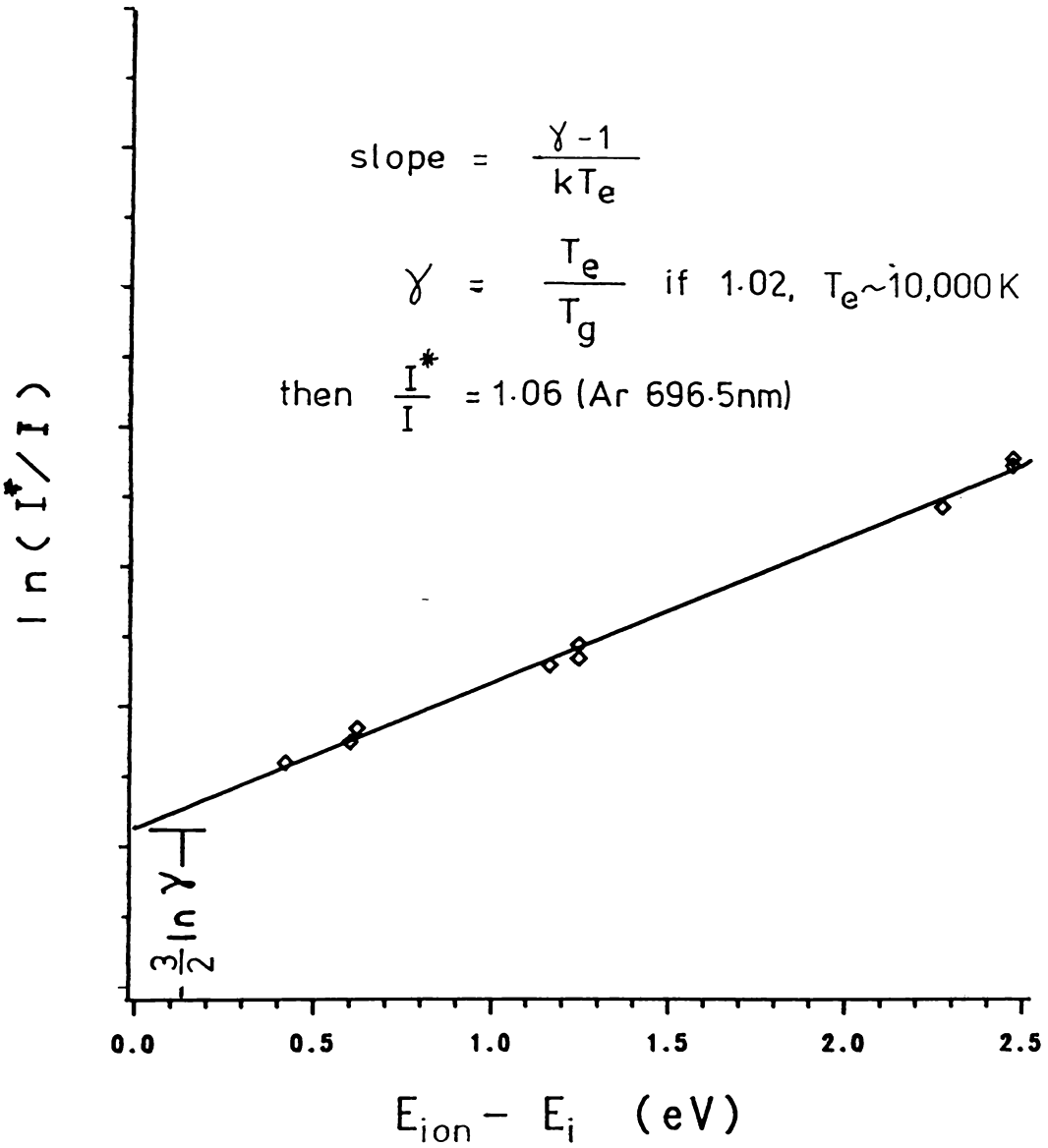

Figure 4.4 :Logarithm of the relative change in intensity as a function of energy difference.

4.5.1. Optically Saturated Spectral Lines: Blackbody temperature

For any plasma to be in complete thermal equilibrium the radiation field must be such that it can be described by the Planck function

$$B_\nu = \frac{2h\nu^3}{c^2}\left(\frac{1}{e^{\frac{h\nu}{kT_B}} - 1}\right) \tag{4.22}$$

where

B_ν is the blackbody intensity

ν is the frequency

h is Planck's constant

c is the speed of light

and

T_B is the Blackbody temperature.

That is, the plasma either has to be contained in a vessel whose walls are maintained at the plasma temperature or the plasma must occupy a sufficiently large volume so that the central part of the plasma is unaffected by the boundary conditions. In the later case, the plasma is optically thick and radiates with a blackbody temperature equal to the plasma temperature. The plasma produced in an inductively-coupled plasma torch with dimensions in centimetres is optically thin over a wide wavelength range and thus Plancks function does not describe the plasma radiation emission.

However, optical depth varies greatly with frequency and so the plasma may be optically thin for one spectral line and yet optically thick for another. Griem's criteria giving the minimum electron density for the existence of LTE in an optically thin homogeneous plasma can be reduced by an order of magnitude provided the argon resonance spectral lines are optically thick. Unfortunately, the transitions involved in a argon plasma are in the far ultraviolet (104.8nm and 106.7nm respectively) and can not be examined simply.

It has been noted (Nick, Richter and Helbig, 1984) that many of the near infrared argon lines of the 4s - 4p transition array (see table 6.1) are emitted optically saturated when observed end-on in atmospheric pressure argon arcs. The data presented in this thesis appears to be the first to observe this effect for plasmas produced in ICPT's. To understand how this can be used to investigate changes in the state of equilibrium a description of optical saturation is necessary.

4.5.2. Saturation

Each photon emitted at a sufficiently large optical depth in the plasma must be absorbed and re-emitted many times on its way out of the plasma, and this is exactly what occurs to radiation in equilibrium. The surface brightness of the plasma reaches a saturation value equal to that of a blackbody (Figure 4.5). Saturation is reached first at the center of the line and then spreads outwards to the wings as optical depth increases. As the plasma present in the ICPT is somewhat less than ideal (due to radial and vertical density and temperature gradients etc.) it is necessary to distinguish saturation from self-absorption and self-reversal. These effects occur when the edges are cooler than the middle due to the lower density of excited atoms at the edges, resulting in more absorption than emission occurring.

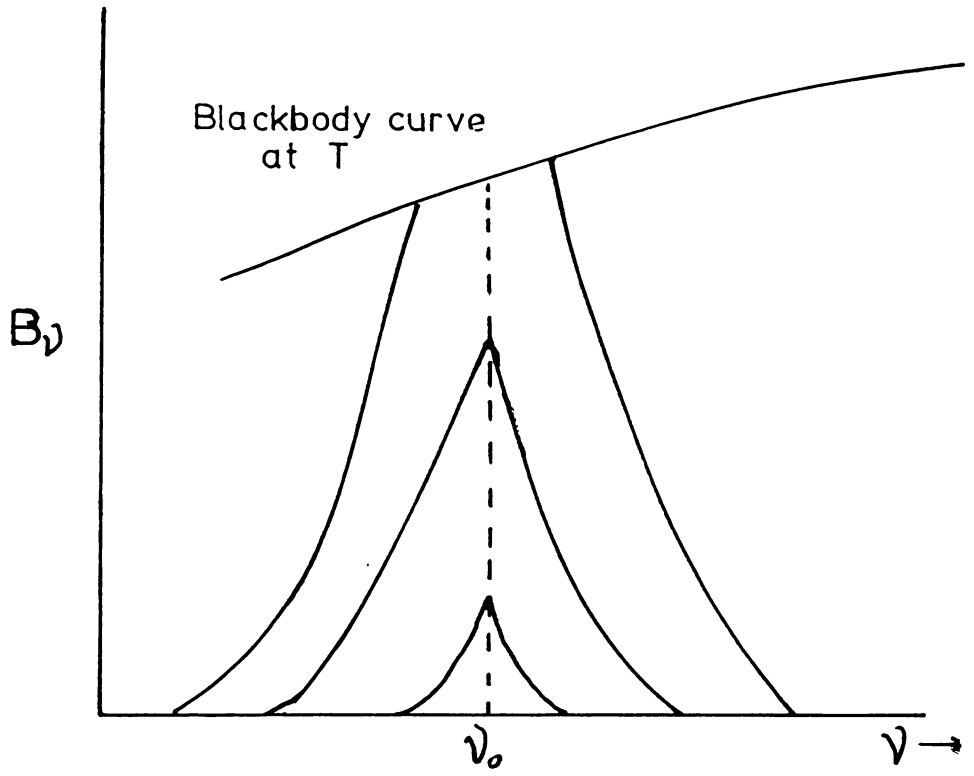

Figure 4.5: Effect of increasing optical depth on the surface brightness for spectral line radiation.

When the R.F field is removed, the recombinative process described earlier can not cause a sharp increase in the intensity of an optically saturated spectral line as it is already radiating at the blackbody temperature. Similarly, spectral lines close to optical

saturation can only increase in intensity until they too are radiating at the relevant blackbody temperature. This provides a qualitative method of determining how radiative losses vary with the operating conditions and allows an investigation of the importance of the reabsorption of the 4p - 4s radiation within the plasma on the establishment of equilibrium in the ICPT.

With the identification of a saturated spectral line, provided a suitable calibration source is available, the blackbody temperature is calculated from equation 4.22.

4.6. Recombination Rate

When there is a rapid, significant drop in the electron temperature on switching off the RF field, there is a possibility that the degree of ionisation in the plasma will exceed its equilibrium value for the relaxed electron temperature. Therefore, provided the loss of charged particles by means other than recombination is small, the decrease in the continuum radiation intensity shortly after switching the RF field off allows the determination of recombination coefficients (see Chapter 9).

4.7. Ionisation Rates

If the RF field is pulsed off for a short period only, there is the possibility of investigating the reverse processes of those mentioned earlier (section 4.2) and hence enable the determination of the ionisation rate from the decrease in the intensity of the excited argon I spectral lines as the electron temperature increases with the resumption of the RF field. However, as will be explained in Chapter 6, accurate results of the ionisation rate were impossible to obtain.

4.8. Electron Density

To complete the characterisation of the plasma, standard diagnostic techniques were employed to determine the electron density. Four methods were used, three of which are independent of the prevailing state of equilibrium, viz Stark broadening of the H_β spectral line and CO_2 laser interferometry, absolute intensity measurements of the continuum and calculations from Saha's equation. These methods are discussed fully in Chapter 9.

4.9. Summary

Repetitive short period pulsing off of the RF field provides, with suitable variation of parameters, a method of investigating not only the state of non-equilibrium, independent of atomic constants, but also the causes of any deviation from equilibrium. The use of the intensity ratios before and after switching not only

yields the temperature differences but is also very sensitive to any departure from equilibrium. Observations of the behaviour of a saturated spectral line under differing conditions gives an indication of the changes in the radiative losses from the plasma under various operating conditions.

These results together with those concerning the electron density and recombination rate will indicate the physical pattern to which any model of the excitation mechanism must conform.

Chapter 5

Instrumentation

5.1. Introduction

In chapter 4 the techniques that may be used in conjunction with the rapid pulsing off of the RF field to investigate the state of equilibrium were discussed. This chapter details, first, the apparatus necessary to operate (and pulse) an atmospheric pressure inductively-coupled argon plasma torch (ICPT) with parameters similar to those ICPT's developed as light sources for emission spectroscopy, and secondly, the available diagnostic equipment that was used to investigate the plasma.

Although as described in Chapter 2 there is a wide variation in operating conditions such as, frequency, power input and gas flow-rate used to obtain plasmas in ICPTs, commercially available ICPT's have tended to concentrate on certain power and frequency ranges (2 kW, 27 MHz) and gas flow-rates (coolant 8 - 14 l/min, aerosol 0.7 - 2 l/min) for economic and legal reasons. While the torch described here is not a commercial model it uses similar parameters.

5.2. Plasma Generation

Apart from the modifications necessary to rapidly pulse the RF field (Section 5.3) the system is similar to that described by Ong (1977) and Miller (1978). The RF power is supplied by a 2 kW RCA A.V.T-22A communications transmitter which was modified (Ong, 1977) to give c.w. operation at a fixed frequency of 27.12 MHz. A 50Ω U.R.67 coaxial cable feeds the RF power to a matching unit which matches the 50Ω impedance of the coaxial cable to the impedance ($\approx 2\Omega$) of the water-cooled work coil (Figure 5.1). To eliminate problems arising from arcing between plates of the variable capacitors the matching unit was further modified (Figure 5.2). The two turn copper work-coil (radius 11mm) couples the RF power into the plasma, variations in the load impedance being compensated by adjustments to the variable capacitors in the matching unit. The input and reflected power are monitored by an in-line RF

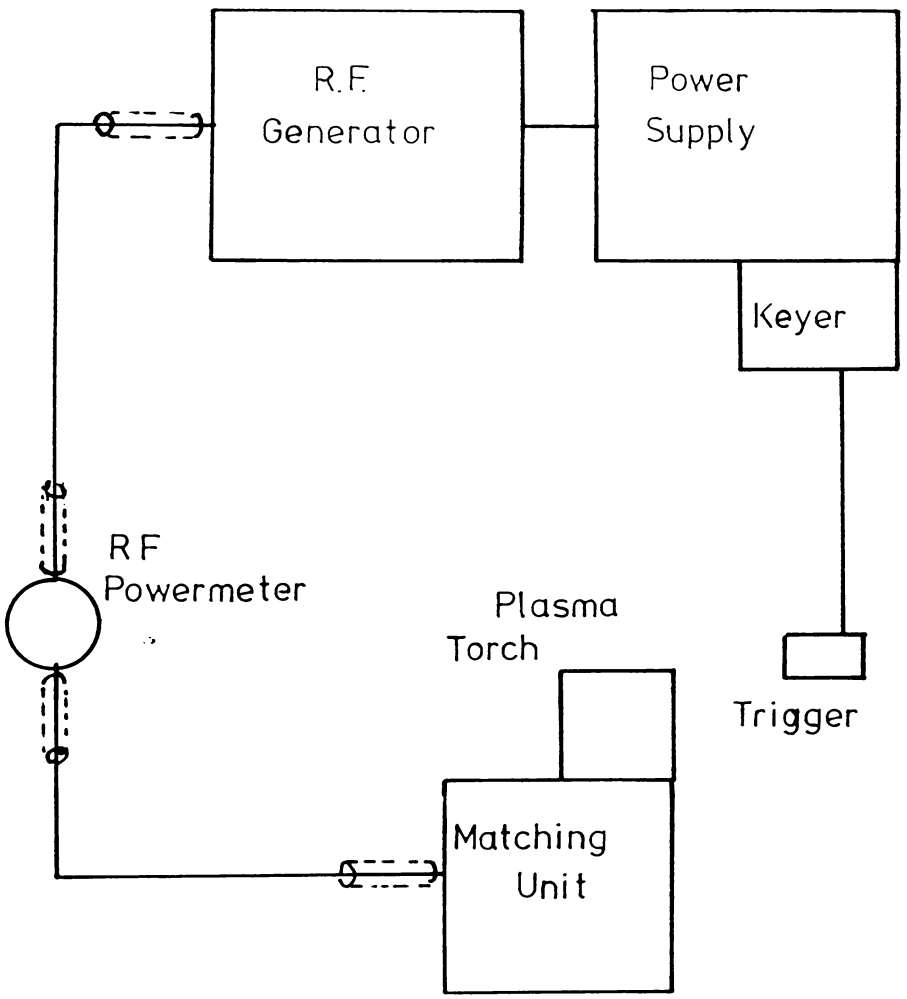

Figure 5.1: Block Diagram of the ICPT.

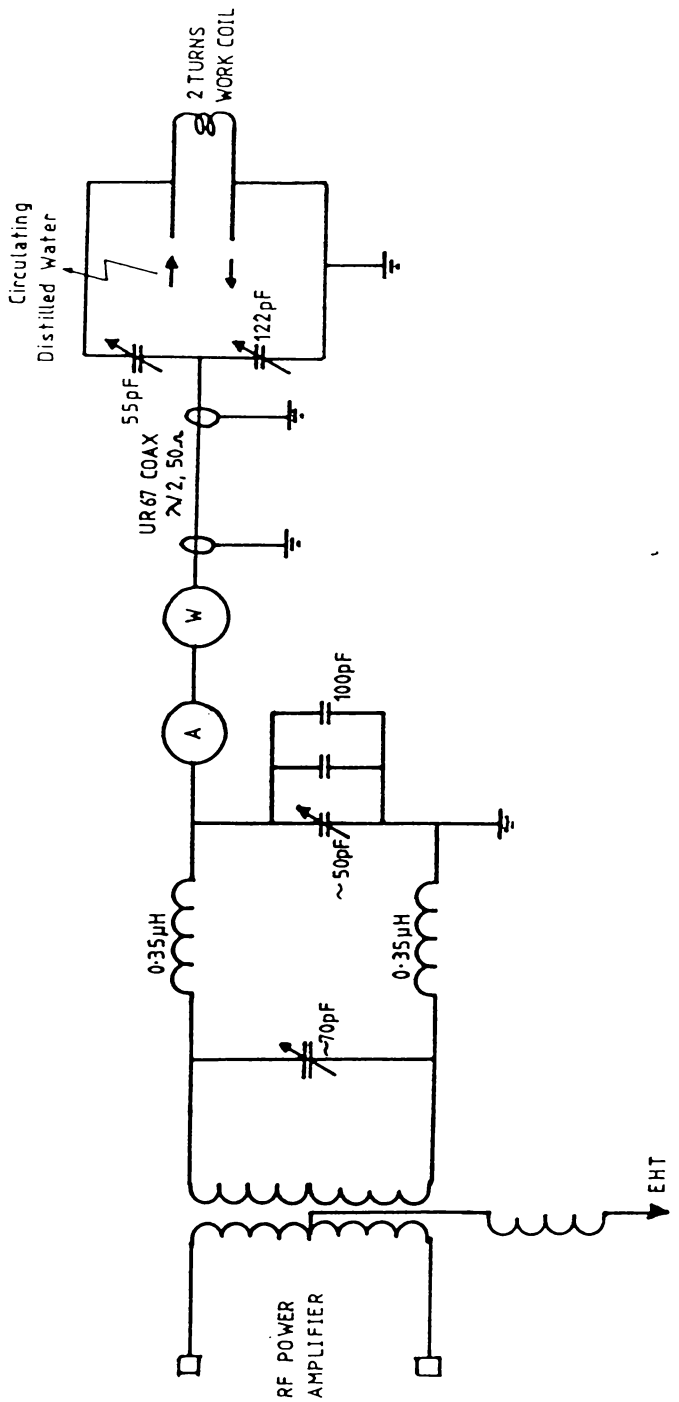

Figure 5.2: Coupling circuit.

power Watt-meter (Drake RF power Watt-meter model W4). The matching is achieved in practice by adjusting for a minimum reflected power (typically $\leq$ 2 Watts). The plasma is generated and maintained in a modified version of the plasma torch described by Boumans and De Boer (1976).

The plasma torch assembly is identical to that used by Miller (1978) and consists of three clear fused quartz tubes, the edges of which are flame-polished so as to reduce disturbances to the gas flow to a minimum. Each tube is mounted into an individual aluminium cylinder and these are assembled to allow for adjustments of the relative positions of the three tubes. This system allows for the simple replacement of damaged or worn parts and for the precise centering of the three quartz tubes, an essential pre-requisite for the successful operation of the torch and the establishment of axisymmetry in the generated plasma. Diagrams of the torch assembly are given in Appendix B.

The torch is operated on argon (Industrial Welding grade) which is introduced tangentially into the outer tube in the case of the coolant flow, to provide vortex stabilisation. It was found to be unnecessary to provide support flow through the second tube. Sample introduction was provided by the central tube through a 1.5mm orifice, with argon as the carrier gas.

The plasma is most easily and conveniently initiated by suspending a small block of graphite ($\approx$ 5mm x 5mm x 5mm) into the torch, at the height of the middle of the work-coil. The graphite rapidly becomes red hot and emits sufficient electrons to cause the RF breakdown of the argon gas to occur. When this begins to happen the matching unit is re-tuned and the graphite is withdrawn thereby giving rise (usually) to the formation of a stable plasma within the tube. Once formed the matching unit again requires re-tuning for minimum reflected power. When the RF field is pulsed off, the off period is sufficiently short that enough electrons remain in the torch to allow it to re-ignite. This off period is dependent on the operating conditions and is always less than 2 milliseconds.

Table 5.1 lists the specifications of the basic apparatus used to produce a steady-state plasma suitable for use as a light source in emission spectroscopy.

5.3. Pulsed Operation

The measuring techniques described in Chapter 4 require that the RF field be cut-off within approximately 5 microseconds. Initial experiments with keying the screens of the power output tubes (RCA 813) using the original transmitter keying circuits (Figure 5.3) produced cut-off times of approximately 30 microseconds. These

Table 5.1:
Specifications of the Operating Equipment.

RF Generator:

A A.V.T-22B communication transmitter with impedance matching unit built into the output circuit. This is frequency controlled at 27.12MHz by a crystal oscillator, and modified for either c.w. or pulsed off/on operation.
Input power: 0-1.2 kW Reflected power: < 2 W.
Pulse rate: single or once every two seconds.
Off pulse length: 150-1800 microseconds.
Rise-time off: ≈3 microseconds.
on: ≈50 " " " " .

Work coil:

Two turn water-cooled copper tubing.
tubing 6mm OD, 4mm ID.
radius 11 mm.
length 10 mm.
Coolant: double distilled H_2O recycled through a heat exchanger.

Plasma Torch Assembly:

Three concentric fused quartz tubes (diagrams see Appendix B) a modified version of Boumans and De Boer's design (1975).
Plasma (outer) tube: 18mm ID, 20mm OD.
Auxiliary (inner) tube: 13mm ID, 15mm OD.
Aerosol (middle) tube: 3mm OD, orifice: 1.5mm.

Gas supply:

Types:
Argon, Industrial Welding Grade.
Argon plus 4% hydrogen.

Flow-rate:
coolant flow-rate : 10 - 40 litres/min.
aerosol flow-rate : 0 - 2 litres/min.

Aerosol Nebuliser:

Pneumatic nebuliser of the Varian Techtron Standard Type.
Efficiency: 3%.

RF Power Meter:

Drake RF power Watt-meter model W4.

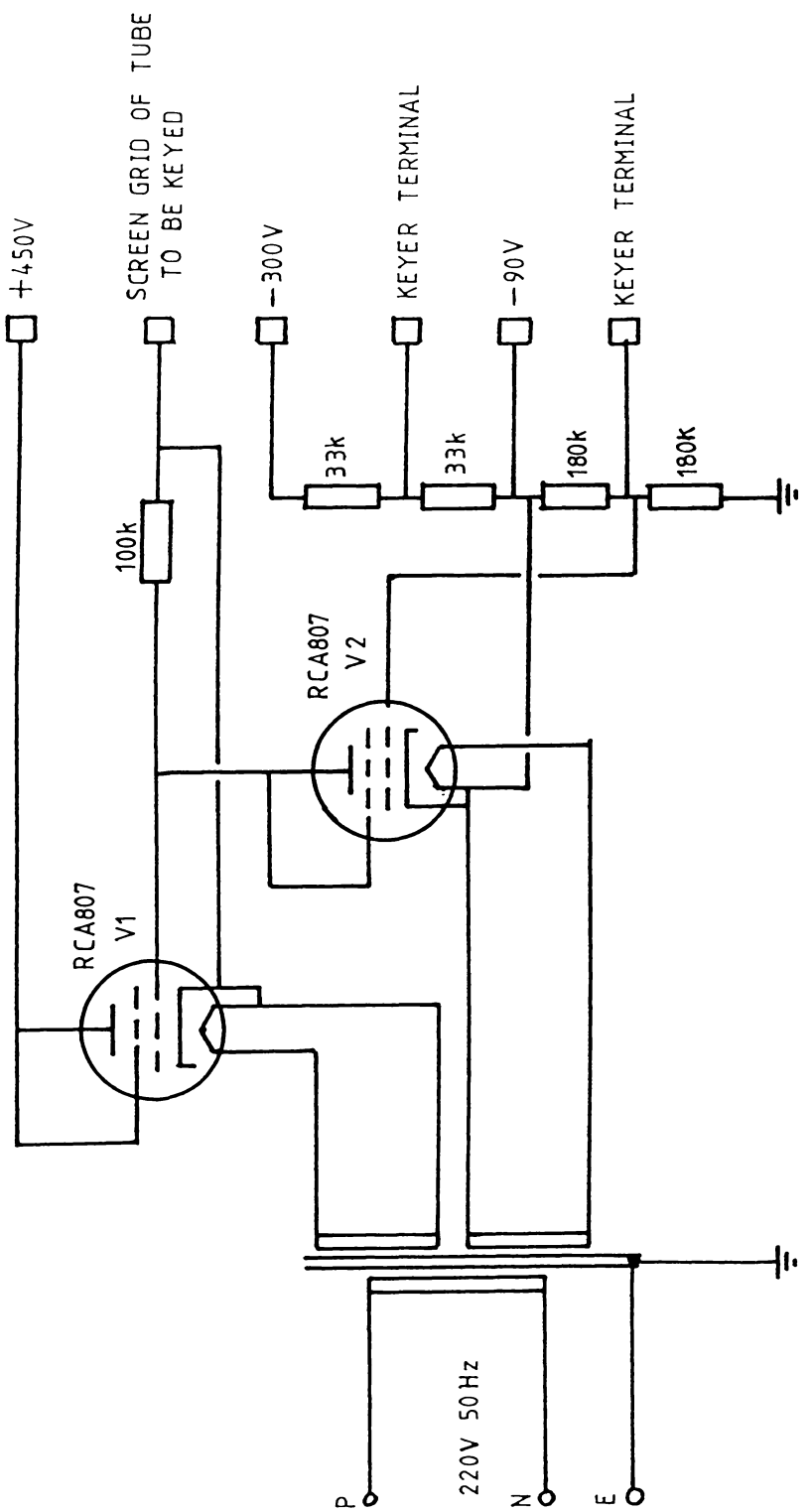

Figure 5.3: Original Keying Circuit.

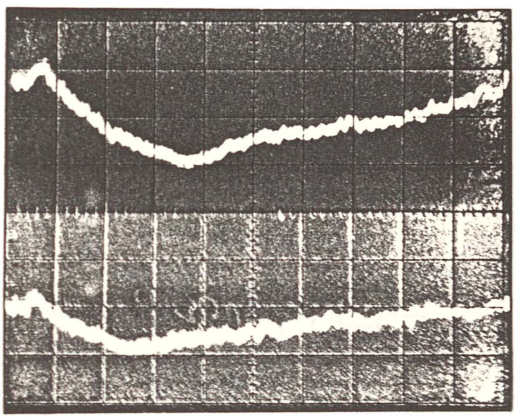

Photograph 5.1: Change in intensity of Ar I spectral line, cut-off time = 30 μs.
Top Ar I 420nm, bottom Ar I 430nm spectral line.

were too long to be of use for investigating the state of equilibrium in the plasma but were sufficiently short to provide encouragement, in the form of an increase in spectral line intensity (see photograph 5.1), to reduce the cut-off time further. However to achieve the cut-off time required of less than the necessary 5 microseconds, more substantial modifications were required.

5.3.1. High-speed Pulsing

To reduce the cut-off time to the required level ($< 5\mu s$) it proved necessary to introduce a gating valve (12BY7) between the oscillator and buffer valves in the RF generator (Figure 5.4). This valve, together with the screens of the 813 power tubes, were driven by the modified keying circuit shown in Figure 5.5. Apart from the short periods the RF field is off the operation mode is c.w. To trigger the keying unit a voltage pulse of variable length ($150-1800\mu s$) was applied by a trigger circuit (Figure 5.6) to the keying unit causing it to apply a voltage to the screen of the gate valve and

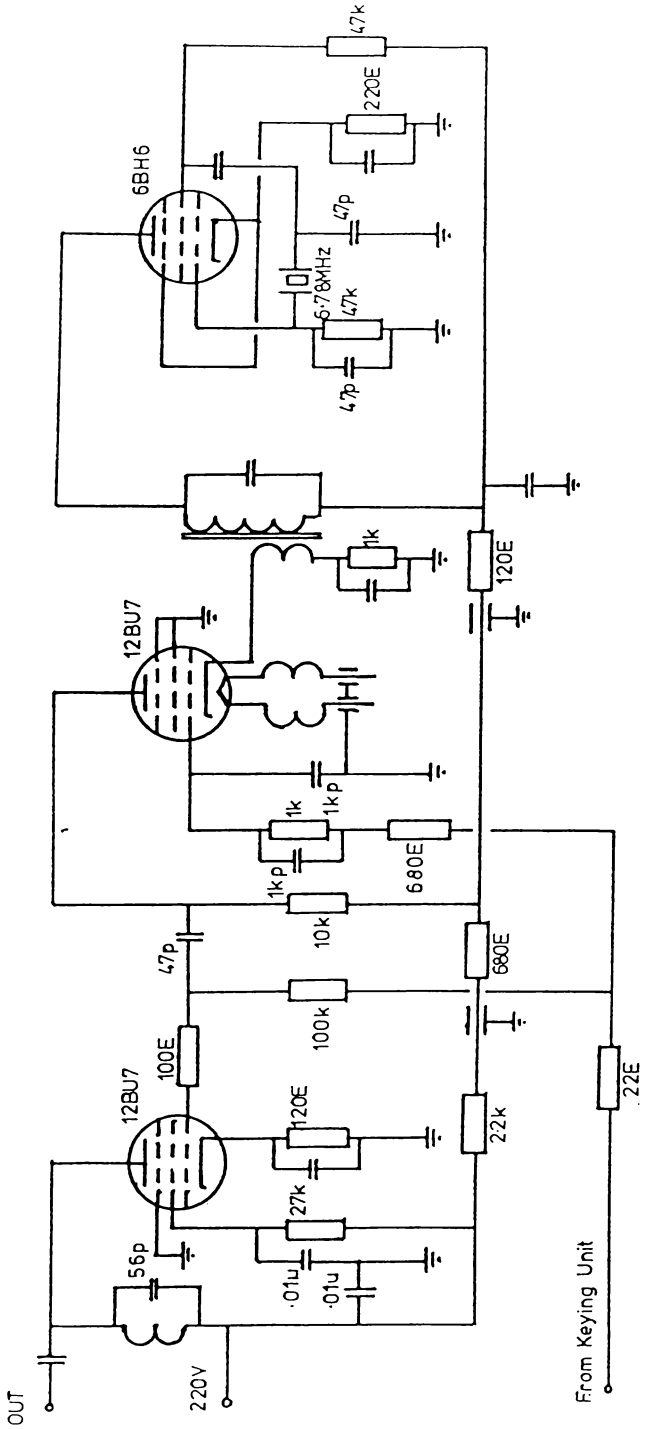

Figure 5.4: Schematic of the Gate valve Circuitry

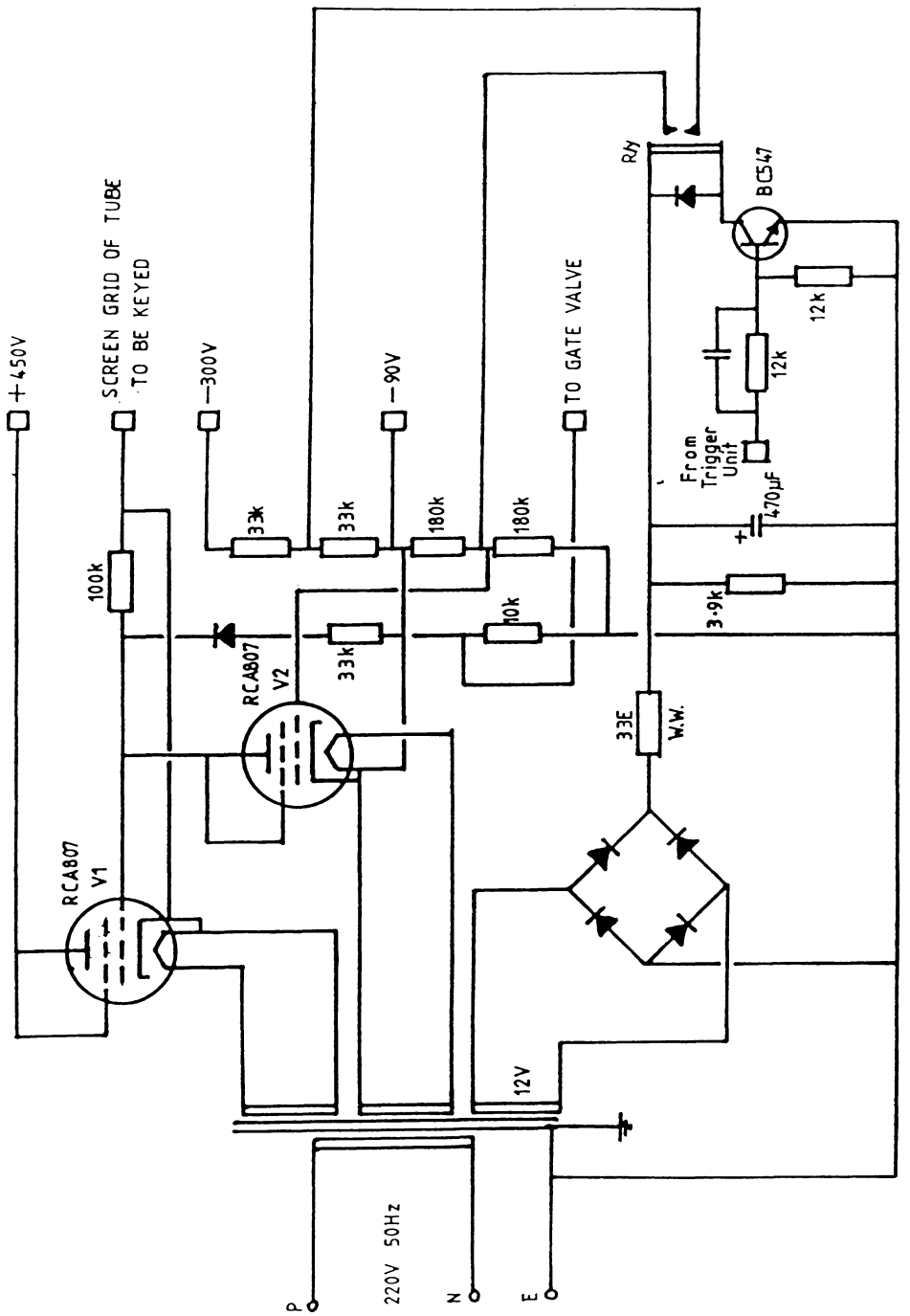

Figure 5.5: Schematic of Modified Keying Unit

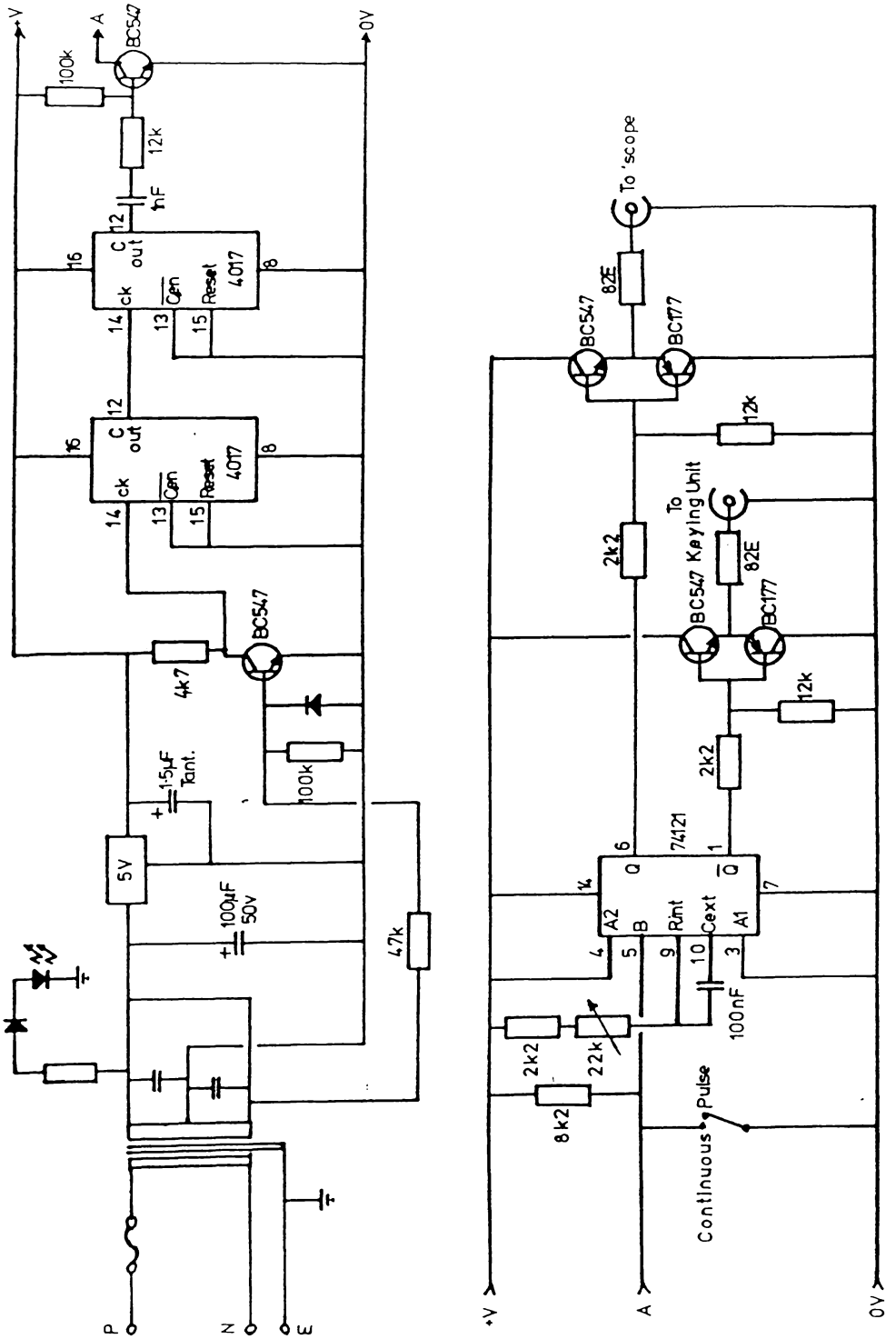

Figure 5.6: Schematic of Trigger Unit.

the 813 tubes reducing the RF field to zero in approximately 3 microseconds. This circuit also triggers storage oscilloscopes used for recording the output from the monochromator.

The trigger circuit could be operated manually in a single shot mode or automatically, so that it triggers the keying circuit once every two seconds. As pointed out above, repetitive cut-off operation of the torch was possible provided the pulse length was sufficiently short. This off time period is dependent on the input power and gas flow and was determined empirically. As an added precaution, to remove the effect of any residual mains hum on the RF field and therefore on the plasma characteristics, the trigger unit was itself triggered on the same part of the mains voltage wave function each time.

The effect of the switching circuits on the output of the RF generator is shown in Photographs 5.2 and 5.3. The RF field is cut completely within 3 microseconds and returns to full strength in approximately 50 microseconds.

5.4. Diagnostic Apparatus

Apart from those electron density measurements, obtained by interferometric methods, all other results given in this thesis were obtained using the emitted light from the plasma, that is, by emission spectroscopy. The experimental arrangement to detect and record the light output is shown in the block diagram given in Figure 5.7.

The torch and matching unit are mounted on a cast-iron base that can be moved both laterally and vertically. The torch position was monitored by a He-Ne laser. All the diagnostic equipment was mounted on a one metre by two metre granite optical table.

The light emitted by the plasma is focused by a 10 centimetre focal length quartz lens to form a x1 image on the entrance slit of a GCA/McPherson EU700 series scanning monochromator. This uses a 1180 line/millimetre grating blazed at 250.0 nanometres, having a reciprocal dispersion of approximately 2 nanometres per millimetre. A Hamumatsu R955 photomultipler tube (spectral range 160 - 900 nanometres) was positioned at the exit slit. The photomultipler output was taken, via an amplifier, to either a Hitachi digital storage oscilloscope (model V.C.6041) or a Tektronix 434 storage oscilloscope. The output displayed by the oscilloscopes was either photographed or (in the case of the VC6041) plotted onto graph paper by a Heathkit chart-recorder (model EU20VE).

The response time of the optical detection system was measured to be

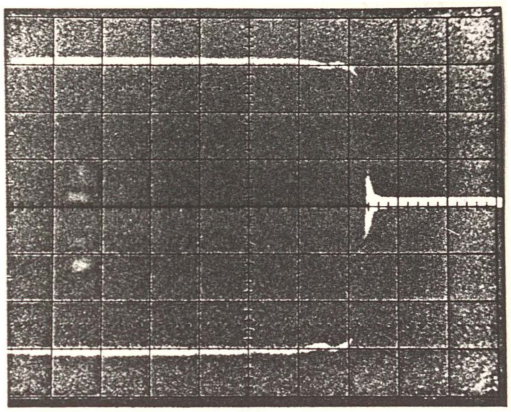

Photograph 5.2: Cut-off of RF Field
Time base 10 μs / div

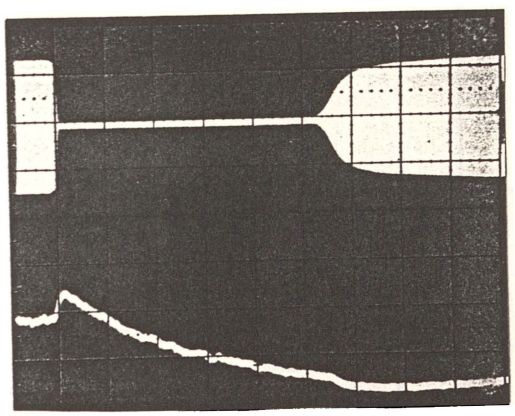

Photograph 5.3: RF Field Off Pulse
Time Base 50 μs / div

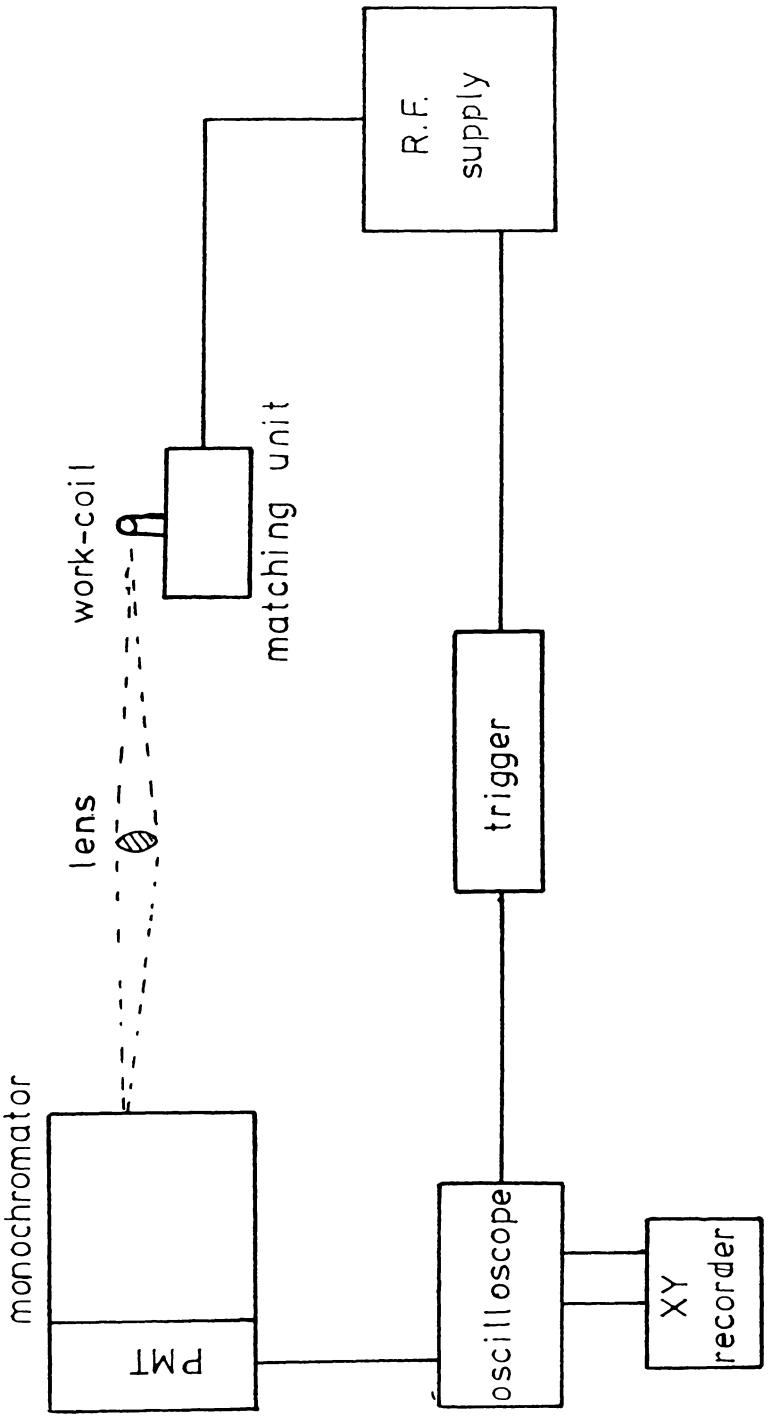

Figure 5.7
Block diagram of the Experimental Lay-out.

Table 5.2

Specifications of the Diagnostic Apparatus for Emission Spectroscopy Measurements.

Spectrometer: GCA/McPherson Scanning Monochromator.
- Model: EUE-700.
- Grating: 1180 lines/mm, blazed at 250nm.
- Resolution: < 0.1 nm.
- Dispersion: 2 nm/mm.
- Filters: Eight filters giving broad-band isolation of given spectral regions between 250 nm and the near-infrared.
- Slit Width: Adjustable 0 - 2000 microns.
- Slit Height: Set at 3mm.

Photomultipler Tube: Hamamatsu.
- Model: R959.
- Spectral Range: 160 - 900 nm.
- Power Supply: GCA/McPherson Model EU-701-30, 300 to 1500 Volts.

Optics:
- Type: Quartz.
- Focal length: 10 cm.

Data Collection: The output from the photomultiplier was displayed on either
- Tektronix Model 434 storage Oscilloscope,

or
- Hitachi Model VC6041 storage Oscilloscope.

Chart-recorder:
- Heathkit Model EU 20VE.

Microwave Generated Light Source.
- EMI Microwave power generator Type T.1002.
- Frequency 2450 MHz.
- Modulation frequency 1 kHz.
- Discharge tube EMI type 9776.

Lock-in Amplifier.
- PAR model 126.
- Pre-amplifier PAR model 184.

approximately 2 microseconds.

The specifications of the diagnostic apparatus are given in Table 5.2

5.4.1. Slit-Width and Slit-Height

As the entrance and exit slits are coupled on the GCA/McPherson monochromator this places restrictions on the available exit slit-width. When the plasma was being investigated in the steady-state mode, satisfactory results were obtained with a slit-width of 10 microns, with an appropriate integration time. In the pulse mode, it was determined empirically that a slit-width of 100 microns was necessary to provide sufficient illumination to the photomultiplier to obtain satisfactory results while retaining sufficient resolution for the study of spectral lines.

For measurement of the continuum it was necessary to increase the slit-width to 200 microns. To ensure the absence of any weak spectral lines in the spectral range concerned, the relevant wavelengths were first scanned using a narrow slit width (10 microns) when the plasma was operating in the steady state.

The slit-height remained fixed at 3 millimetres throughout the series of experiments contained in this thesis.

5.4.2. Intensity Calibration

Calibration of the optical system was performed with the use of a Tungsten-ribbon standard lamp.

5.4.3. Gas Supply

The argon gas used throughout the experiments was 'Standard Welding Grade'. The argon was checked for the presence of impurities by scanning for the presence of the H_β spectral line (486.1 nm). Only those cylinders where it proved impossible to discern any difference in intensity from the background continuum were utilised.

5.5. Absorption Measurements

A modulated (1kHz) light source was employed for absorption measurements in the ICPT. The light source which was generated in an electrodeless discharge tube powered by a RF field, of 2450MHz frequency, produced by a microwave generator (EMI type T.1002) was passed through the plasma of the ICPT. A lock-in amplifier (Princeton Applied Research, model 126) was used to monitor the output of the photomultiplier tube. Figure 5.8 gives a schematic diagram of the optical setup.

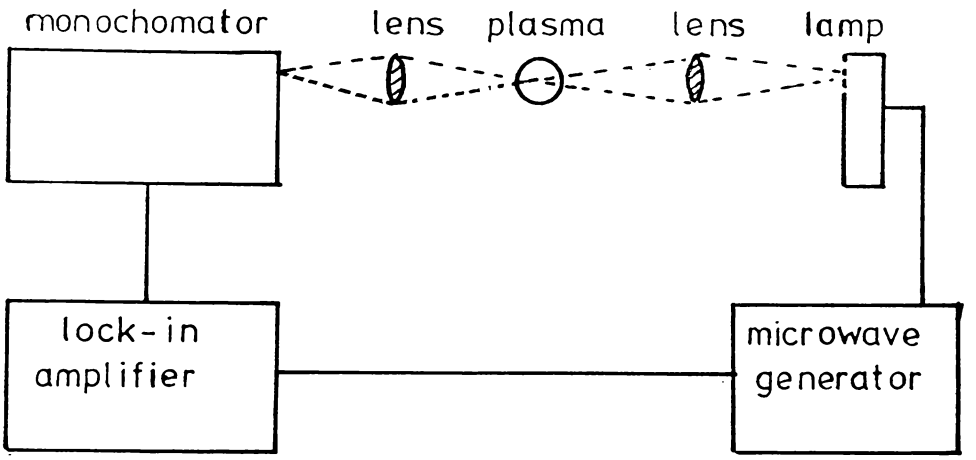

Figure 5.8: Schematic Diagram of the Optical Arrangement for Absorption Measurements in the ICPT.

5.6. Laser Interferometry

A Michelson interferometer utilising a 10.6 micron CO_2 laser as the radiation source was constructed to obtain measurements of the electron density independent of emission spectroscopy methods.

A schematic diagram of the interferometer is given in Figure 5.9. Table 5.3 lists the relevant specifications. A Germanium beam-splitter passes approximately half the CO_2 laser beam through the plasma, the beam is then chopped by a low-duty cycle chopper (60Hz). This beam is returned back along its original path by a 1m radius concave mirror which approximately focuses the exit aperture of the laser onto the detector. The other half of the laser beam is reflected off a similar 1m radius concave mirror, which is mounted on a piezoelectric speaker, back also to the detector.

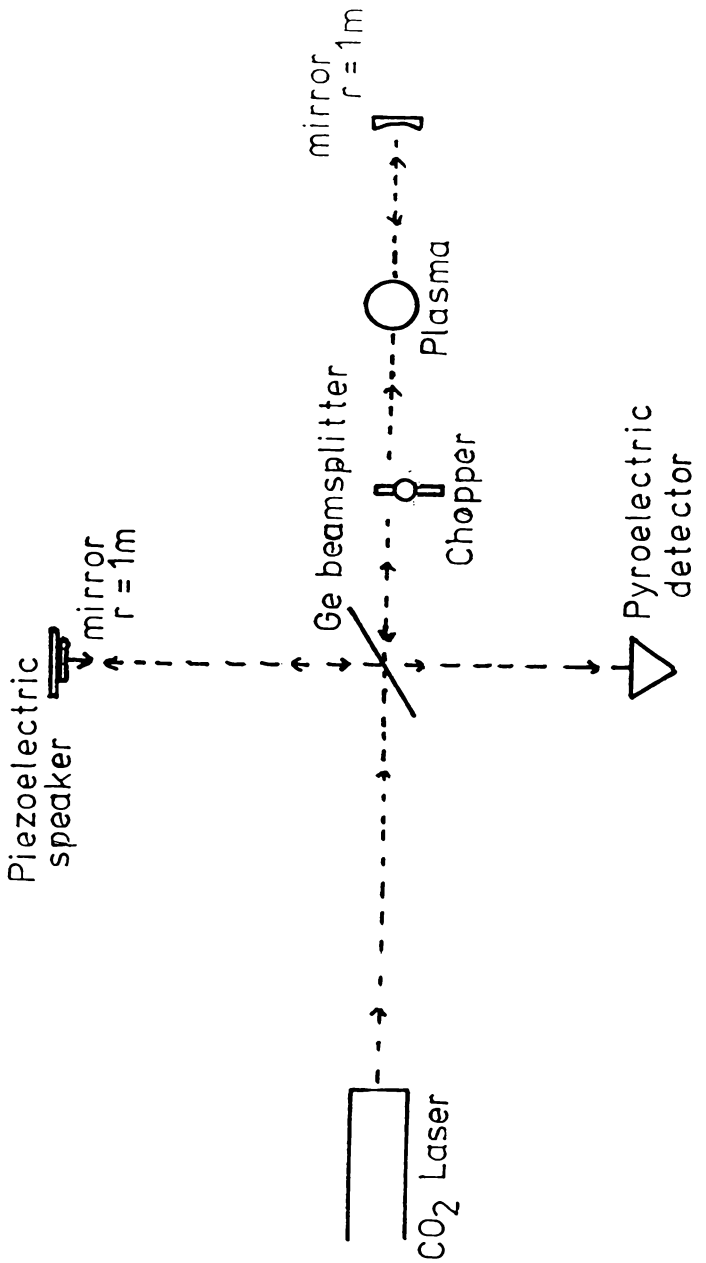

Figure 5.9: Schematic of the $C0_2$ Laser Interferometer.

Table 5.3: Specifications of Interferometer.

Light Source: A 10.6μm CO_2 laser.
Output Power: $\approx \frac{1}{2}$Watt.
Mirrors; 2.5cm plane Germanium mirror, grating blazed at 8μm.

Beam-splitter: Germanium anti-reflection coated on one side.

Pyroelectric Detector: A Lithium-tantalate crystal detector.
Model; Molectron P1-11H.
Sensitivity; 2.5μA per watt over a 1mm^2.

Translator: Piezoelectric loudspeaker.

Mirrors: 1 meter radius of curvature surface coated.

Beam-chopper: low-duty cycle chopper.
Frequency; 60Hz.

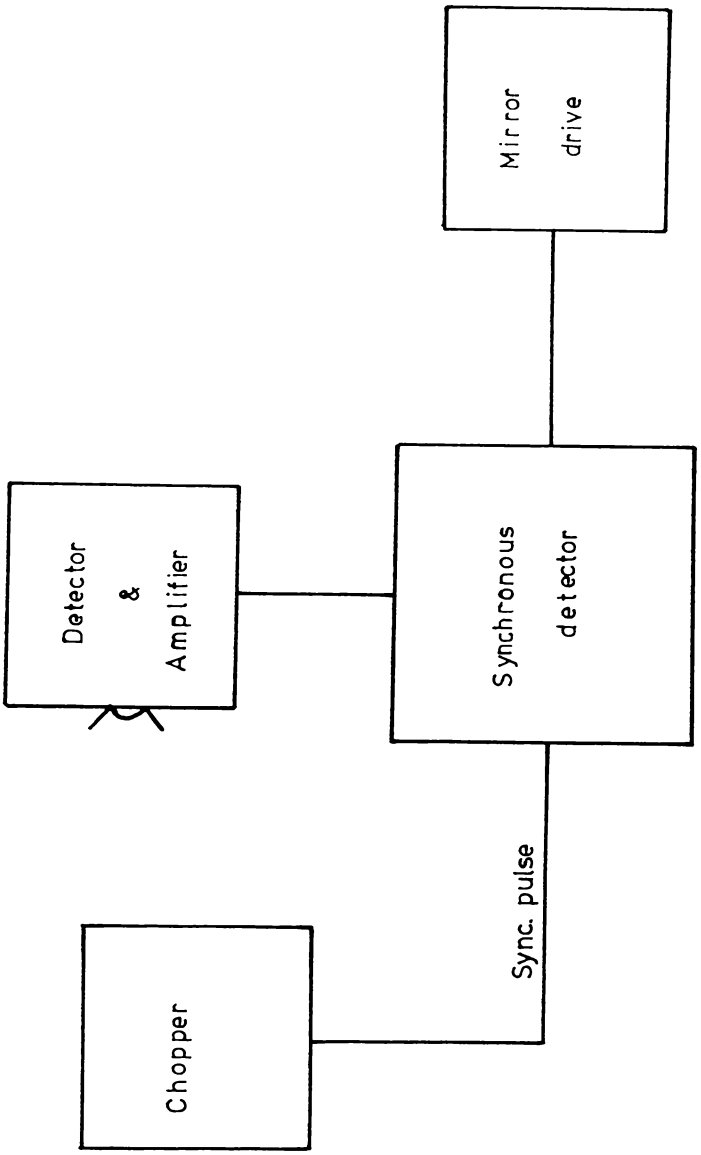

Figure 5.10: Block Diagram of the Path-length Compensator Circuitry

The pyroelectric detector is a Lithium-tantalate crystal (Molectron P1-11H) with a sensitivity of 2.5μA per Watt over a 1mm^2 area. The signal is amplified by an integrated circuit amplifier which drives a co-axial cable.

To maximise the interferometer sensitivity, the path length of the reference beam was adjustable to maintain a phase difference of 90° between the two beams. To maintain this path difference a feedback stabilisation method was used, the piezoelectric translator (loudspeaker), to which the reference beam concave mirror was mounted, maintained a phase difference of 90° by a circuit which sensed the phase difference between the two beams. This circuit then adjusted the voltage across the

translator to maintain a path difference yielding a phase difference of 90^o between the two beams. From the value of voltage required the electron density could be established (see Chapter 9). The interferometer was calibrated by driving the translator through several fringes thereby yielding the peak to peak voltage, that is, the necessary voltage to compensate for a phase shift of 90^o. The block diagram of the Path-length Compensator circuits is shown in Figure 5.10. Circuit diagrams of the various elements are given in Appendix C.

Chapter 6

Preliminary Experiments I

6.1. Introduction

As shown in Chapter 4, the rapid removal of the external RF field provides a sensitive differential method for investigating the degree of non-equilibrium in the ICPT and the dominant mechanisms giving rise to this deviation, provided the assumptions underlying the use of the relevant equations are valid. Before proceeding to investigate the state of equilibrium pertaining to the ICPT plasma it was necessary to establish the validity and limits of these various assumptions as well as those assumptions standard to the use of the emission spectroscopy techniques.

The basic assumption underlying the validity of equations 4.13 and 4.15 is that the plasma is close to equilibrium, that is

i) that the electrons possess a Maxwellian velocity distribution;

ii) that the excited argon I states conform to a Boltzmann distribution;

iii) that the temperature difference between the electrons and the neutrals is relatively small (10 - 20%);

In addition the following assumptions need to be substantiated:

iv) that the time for the electrons to relax to the gas temperature is sufficiently short, such that the electron density remains constant over this period; and

v) the spectral lines utilised to investigate the state of equilibrium in the plasma are either optically thin or near saturation.

The experimental results presented in Chapter 2 demonstrate that the plasma is close to equilibrium.

The first two assumptions, if valid, imply that the plasma is at least in pLTE and

if assumption iii) is valid in that there is a common temperature, then the plasma can be considered to be in LTE. It will be shown in Chapter 8 that these first two assumptions are adequately valid in a single flow torch and that the central region of the plasma is in kinetic equilibrium as well. However before it is possible to establish the validity or otherwise of assumptions i), ii) and iii) it is necessary to determine whether the remaining assumptions iv) and v) are correct as well as obtaining the appropriate experimental pre-conditions to provide accurate repeatable results.

6.2. Behaviour of the Spectral Emission Intensity upon removal of RF field

To utilise equation 4.21 required the rapid removal of the R.F field together with a fast response measurement of the resulting increase in the spectral line intensity. By suitable modifications to the R.F generator (Chapter 5) it was possible to pulse off the R.F field in less than the required time of $\approx 10^{-5}$ seconds.

Photographs 6.1 and 6.2 show the behaviour of an excited argon I spectral line emission and the continuum emission, respectively, with the removal and return of the R.F field. As an introduction to later work, the information obtainable from the observation of the time-dependent behaviour of the plasma emission is itemised (see the numbered regions).

Region 1): the plasma is in a steady state:

Under steady-state conditions the electron density was determined from the absolute intensity of the continuum, by laser interferometry, and Stark broadening, all of which are independent of the prevailing state of equilibrium. The excitation temperature was determined from a Boltzmann plot of the emission intensities from optically-thin excited argon I spectral lines.

Region 2) The variation in the intensity of the argon I spectral lines and the continuum at the instant of RF switching:

The sharp increase in spectral line intensity indicates a difference in temperature between the various components making up the plasma. This together with the lack of response in the continuum intensity allowed the investigation of the state of equilibrium and the cause of any deviation. Once the presence of a Boltzmann distribution between the excited argon states is established, the degree of difference in temperature between the various components (electrons, atoms) constituting the plasma may be determined. By changing the various parameters influencing the state of equilibrium (gas flow, input power etc.) an indication of the parameters to which the equilibrium deviation is most sensitive could be established, and thus an indication

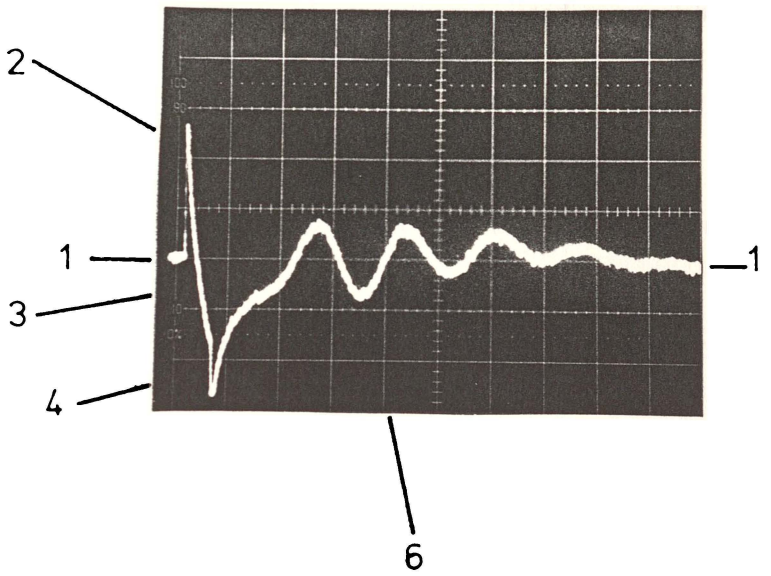

Photograph 6.1: Spectral line variation on pulsing off R.F field.
Numbered regions, see text. Time-scale: 1 ms/div.

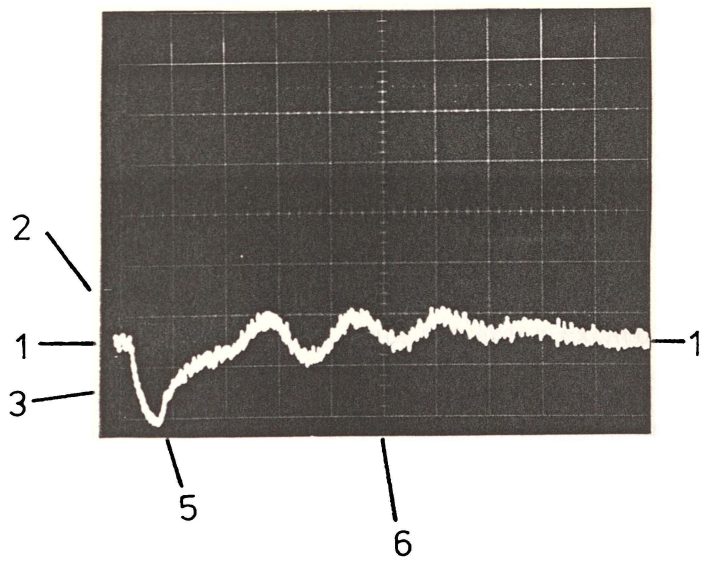

Photograph 6.2: Variation of Continuum intensity on pulsing off R.F field.

of the likely causes of the disequilibrium. The investigation of optically thick spectral lines provided further evidence in support of determining the causes of the deviation from equilibrium. In the case of optically saturated spectral lines the measurement of the blackbody temperature was attempted.

Region 3) Monotonic decrease in intensity:

Observation of the rate of change in the continuum intensity shortly after the RF field is switched off allowed an estimate of the radiative-collisional recombination rate.

Regions 4) and 5)

Due to problems with the experimental apparatus (Chapter 5) it proved impossible to obtain sufficiently accurate time-resolved results from this area so as to obtain the rate of ionisation and to enable an investigation of the reverse process of that shown in region 2)

Region 6) Oscillating intensities:

The oscillations in the line and continuum were determined to arise from the bulk motion of the plasma and as these had no effect on the steady-state plasma they were considered beyond the scope of this thesis. However some interesting results were obtained and are included in Appendix A.

The above list gives a brief outline of information that was obtainable under present operating conditions from the study of the transient behaviour of a ICPT plasma.

6.3. A Temperature Difference

In Chapter 4 it was shown that removing the R.F field results in the excess energy possessed by the electrons over that of the argon gas being dumped, in $\approx 10^{-5}$ seconds into the gas, thereby causing, since the argon excited levels are coupled to the continuum, a sharp increase in the intensity of the excited argon I lines. This is followed by a monotonic drop in intensity and an equally sharp decrease in intensity, as T_e increases, upon the resumption of the R.F field (provided the break in the R.F field is sufficiently short).

Photographs 6.3 and 6.4 demonstrates this change in the behaviour of the intensity of an excited argon I spectral lines when the R.F field is cut within $3\mu s$. Photograph 6.3 shows the sharp rise and fall in intensity of the 696.5nm Ar I spectral line over a period of 1 millisecond when the RF field is switched off and back on. Photograph 6.4 shows, on a shorter time-base, the change in spectral intensity with respect to the RF field.

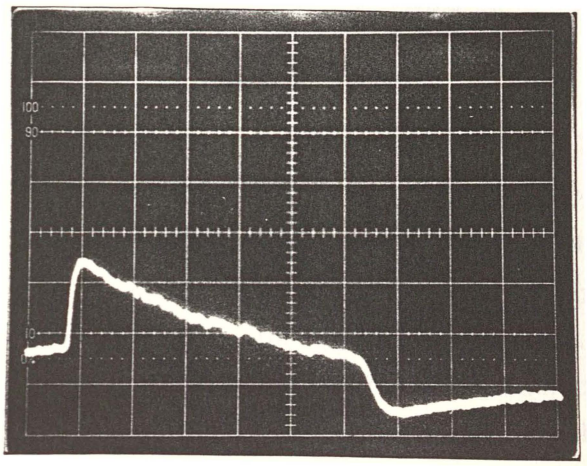

Photograph 6.3: Change in intensity of 696.5nm Ar I spectral line with the removal of the R.F field.
Time scale; 0.1ms/div.

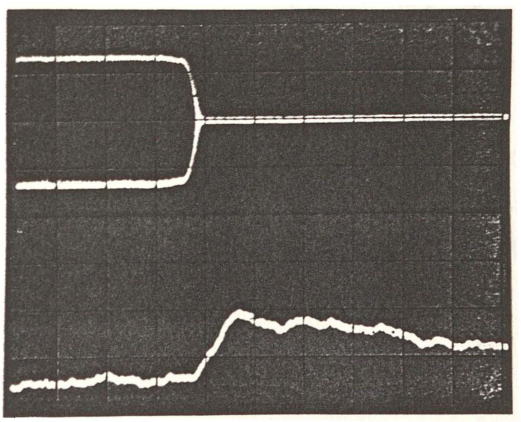

Photograph 6.4: Relaxation of the R.F field and 696.5nm Ar I spectral line.
Time scale: 20 μs/div.

From photograph 6.4 it was possible to estimate the relaxation time of the electrons since although the emitted light is from an excited state the rise time is governed by the electron relaxation time and a value of

$$\tau_e \approx 18\mu s \qquad (6.1)$$

was obtained. This is in reasonable agreement with that determined by calculation in Chapter 4 (response time of the diagnostic equipment $< 2\ \mu s$).

The evidence displayed by the photographs 6.3 and 6.4 is itself sufficient proof that in the plasma of an inductively-coupled atmospheric pressure argon torch the electron temperature is not equal to the gas (atom/ion) kinetic temperature as well as confirming that the excited states are coupled to the continuum by electron collisions. Therefore, as expected, the plasma is not in a state of thermal equilibrium. The requirements for partial LTE, being less stringent, necessitate further study as does the degree to which the electron and gas temperatures differ.

6.4. On the Assumption of a constant Electron Density during Electron Relaxation

Since the electron relaxation time in the ICPT is much shorter than the plasma recombination time it appears reasonable to assume that the electron density will remain constant during the time taken ($\approx 10^{-5}$ seconds) for the electrons to cool to the gas temperature. From equation 2.5 it can be seen that the plasma continuum intensity is highly dependent on the electron density while being only slightly dependent on the electron temperature viz $n_e \alpha T_e^{\frac{1}{4}}$. To investigate whether the electron density is indeed constant during this phase, the behaviour of the continuum (450nm) upon switching off the RF field was noted. Photographs 6.5 and 6.6 show the behaviour of the Ar I 696.5nm spectral line and the continuum at 450.nm. This demonstrates that there is no change in the continuum intensity until after the spectral line intensity has reached its maximum value, implying that the electron density remains relatively constant over the required time period.

6.5. Optical Thickness

In emission spectroscopy it is a pre-requisite that for temperature or density determination based on absolute intensity measurements, and/or Boltzmann's plots, two-line methods, etc, the plasma must be optically thin for the spectral lines used. Self-absorbed lines yielding anomalous results. On the other hand, however,if the spectral line is optically saturated then it is possible, using Planck's equation, to determine the blackbody temperature of the plasma.

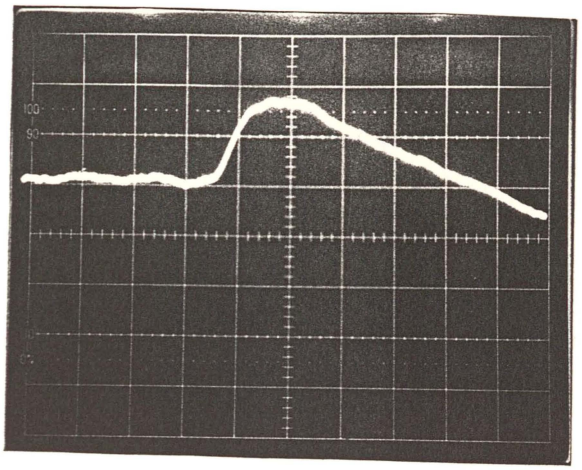

Photograph 6.5: Change in Intensity of Argon I 696.5nm spectral line with the removal of the RF field.
Time-base = 20 μseconds.

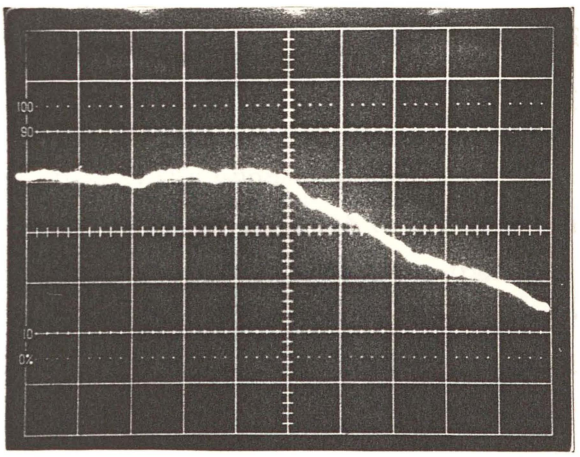

Photograph 6.6: Change in Intensity of the Argon Continuum 450nm.
Time-base = 20 μseconds.

The normal method for determining if a spectral line is optically thin is by varying the length of the light source (l) and observing the variation in line intensity. If

$$I_\phi \approx B_\phi k_\phi l \ , \tag{6.2}$$

that is, corresponding to

$$k_\phi l << 1 \tag{6.3}$$

the spectral line is optically thin. In the opposite case, if

$$I_\phi \approx B_\phi, \tag{6.4}$$

corresponding to

$$k_\phi l \geq 1, \tag{6.5}$$

the spectral line is optically thick (saturated). Where

I_ϕ is the emitted intensity,

B_ϕ Planck's function (equation 4.22)

and ϕ frequency

k_ϕ the absorption coefficient,

To increase the effective length (l) of the plasma a concave mirror was placed at twice its focal length as an extension of the optical path (Figure 6.1). Reflecting the light emitted back through the plasma effectively doubled the length of the plasma. Theoretically, with an optically thin line, this should double the light intensity received at the detector; problems arising from losses at the mirror surfaces and difficulties in optical alignment make this ideal very difficult, if not impossible, to achieve. To avoid this problem the change in intensity upon doubling of the path-length was compared between spectral lines with little likelyhood (due to the small transition probability) of being self-absorbed and those more likely (with larger transition proability) to be self-absorbed. For example, the 696.5 nm Ar I spectral line is approximately three hundred times more likely to be affected by self-absorption than the 430.0 nm Ar I spectral line.

This is a simple and easy method of determining whether a spectral line can be regarded as being optically thin, although it does not yield a measure of $k_\phi l$. Table 6.1 lists the argon spectral lines tested using this method and indicates whether they can be considered optically thin or not.

It should be noted that this method showed that the near-infrared lines of the 4s - 4p transition array could not be considered optically-thin, especially the 811.5 nm

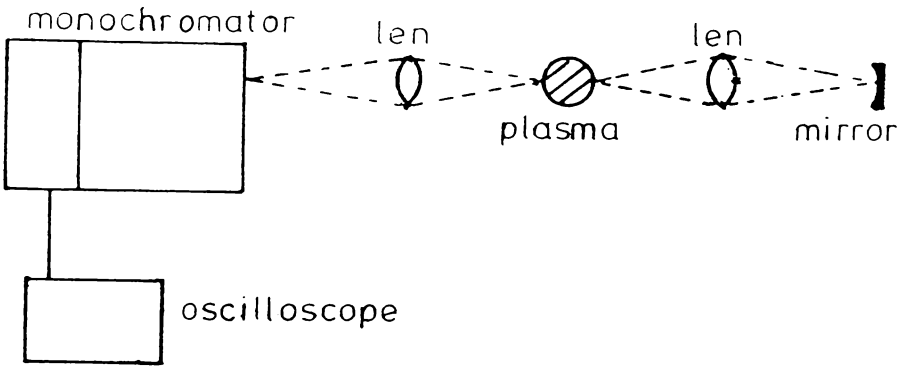

Figure 6.1: Schematic diagram of the Experimental Arrangement to test for Optical Thinness.

spectral line which is optically saturated (or nearly so).

6.5.1. Optical Saturation

When the R.F field is removed, the excess energy dumped by the electrons into neutrals can not cause a sharp increase in the intensity of an optically saturated spectral line as it is already radiating at the blackbody temperature. Spectral lines close to optical saturation will increase in intensity only until they too are radiating at the relevant blackbody temperature. This is one of the reasons for identifying spectral lines that are optically thin. However the presence of spectral lines that are saturated or nearly so provides a method of quantitatively investigating how radiative losses vary with operating conditions. This can be done by comparing the change in intensity with switching of the RF field for a nearly saturated spectral line under various operating conditions.

For example, for the infrared 4s -4p transitions the behaviour of the 811.5 Ar I

Wavelength (nm)	Transition	Energy (eV)	Optically Thin
420.0	4s - 5p	14.5	yes
427.2	4s - 5p	14.53	yes
430.0	4s - 5p	14.5	yes
451.0	4s - 5p	14.58	yes
518.7	4p - 5d	15.25	yes
555.9	4p - 5d	15.14	yes
560.7	4p - 5d	15.12	yes
696.5	4s - 4p	13.33	yes
727.3	4s - 4p	13.33	yes
750.3	4s - 4p	13.48	yes
800.6	4s - 4p	13.17	no
811.5	4s - 4p	13.07	no
842.4	4s - 4p	13.09	no

Table 6.1:
Results of test of the optical thinness of the excited Ar I spectral lines.

line ($\approx$ saturated) was compared to that of the 696.5 nm Ar I line (optically thin) when the RF field was pulsed off, for different heights and radii in the plasma. As the following photographs show, the jump in intensity decreases from a maximum below the work-coil to a minimum just above the work-coil and then increases again before starting to decrease as the observation height is increased, whereas the 696.5 nm Ar I spectral line intensity jump uniformly decreases with increasing height. To check that this variation for the 811.5nm Ar I spectral line occurs because the line is approaching saturation rather than because of any deviation from equilibrium, the intensity ratios of all the spectral lines given in Table 6.1 are plotted in Figure 6.2, and it is evident that apart from the near-infrared lines, the excited argon I states conform to a Boltzmann distribution.* While the nearby line ratios are lower than might be expected, it is the 811.5nm Ar I spectral line that is most strongly affected.

As an additional confirmation that the Ar I 811.5 nm spectral line is saturated, a modulated (1 kHz) light source was used to determine the degree of absorption present in the ICPT. The results are shown in Figure 6.3. These support the proposition that the 811.5 Ar I spectral line is either optically saturated or nearly so (depending on the operating conditions and observation height). The light source used was an electrodeless discharge tube operated at 2450 MHz, used in conjunction with a lock-in amplifier; the specifications of this apparatus are given in Chapter 5.

6.6. Experimental Considerations:

6.6.1. Plasma Stability and Pulse Repetition:

The sharp increase in intensity of the spectral lines when the RF field is removed is relatively small in relation to that experienced in arcs, (Chapter 4), and is an indication that the plasma is close to equilibrium. While adding support to the use of equilibrium relations to investigate a loss of equilibrium this increases the experimental difficulties.

As noted in Chapter 4, the light gathering instrument used was a scanning monochromator, (i.e. single line). Thus each switching cycle gave the intensity change of one spectral line at one position. To build a picture of the state of equilibrium throughout the torch, results were required for many spectral lines each viewing the plasma in many lateral positions. The smallness of the intensity increase necessitated the averaging of the output signal from the spectral lines over many pulses.

---

* Note: The relaxation of the electrons provides a novel, if somewhat restricted, method of determining whether a spectral line is optically thin.

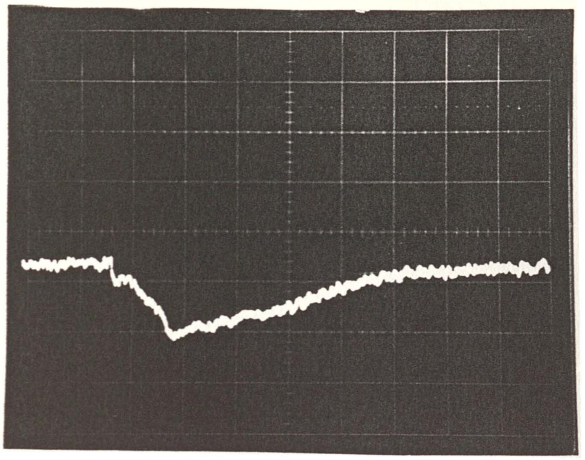

Photograph 6.7(a): Intensity Jump of the 811.5nm Argon I spectral line: 15mm below the Top of the Work-coil, center of the plasma

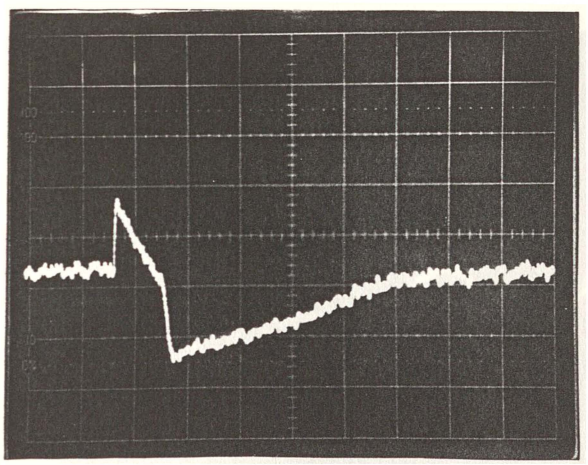

Photograph 6.7(b): Intensity Jump of the 696.5nm Argon I spectral line: 15mm below the Top of the Work-coil, center of the plasma

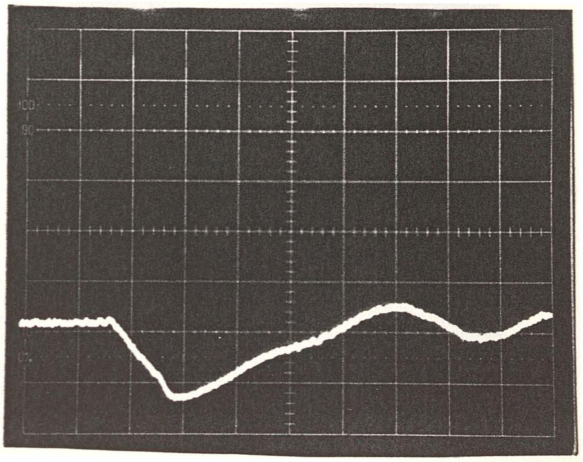

Photograph 6.8(a): Intensity Jump of the 811.5nm Argon I spectral line: 2.5mm above the Top of the Work-coil, center of the plasma

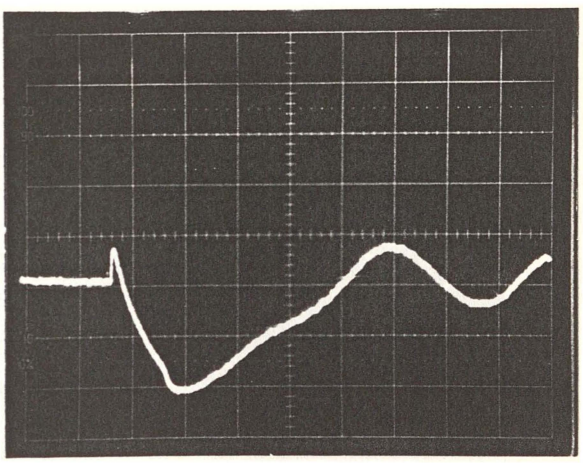

Photograph 6.8(b): Intensity Jump of the 696.5nm Argon I spectral line: 2.5mm above the Top of the Work-coil, center of the plasma

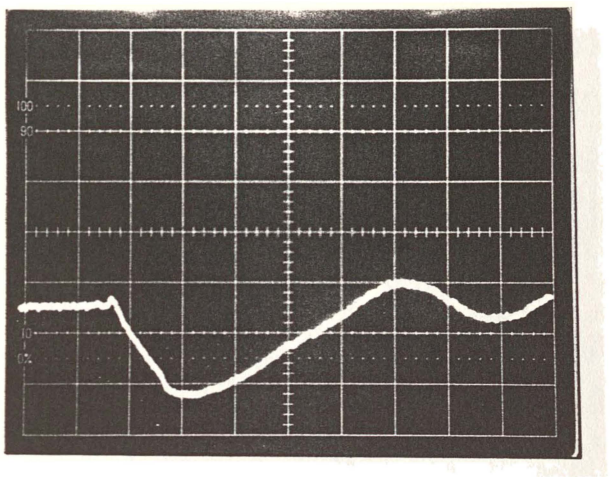

Photograph 6.9(a): Intensity Jump of the 811.5nm Argon I spectral line: 10mm above the Top of the Work-coil, center of the plasma

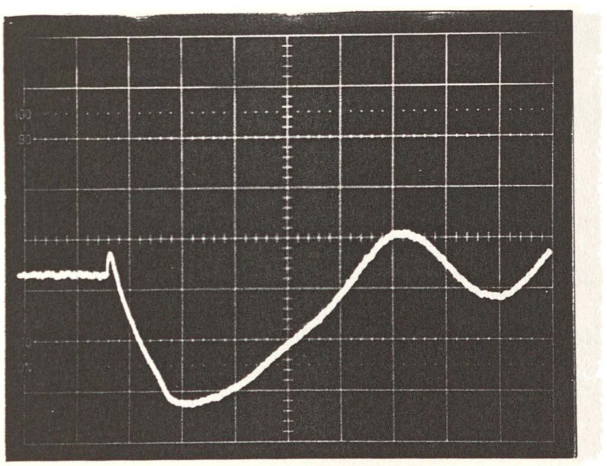

Photograph 6.9(b): Intensity Jump of the 696.5nm Argon I spectral line: 10mm above the Top of the Work-coil, center of the plasma

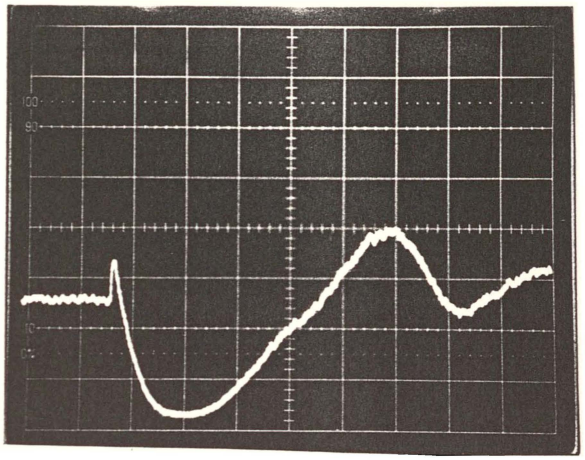

Photograph 6.10(a): Intensity Jump of the 811.5nm Argon I spectral line: 5mm above the Top of the Work-coil, edge of the plasma (r = 7.5mm)

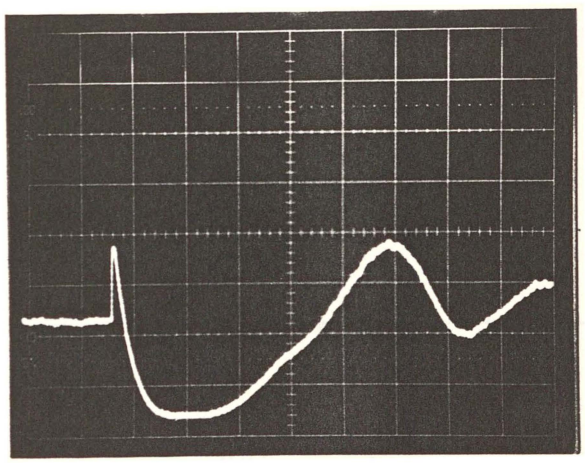

Photograph 6.10(b): Intensity Jump of the 696.5nm Argon I spectral line: 5mm above the Top of the Work-coil, edge of the plasma (r = 7.5mm)

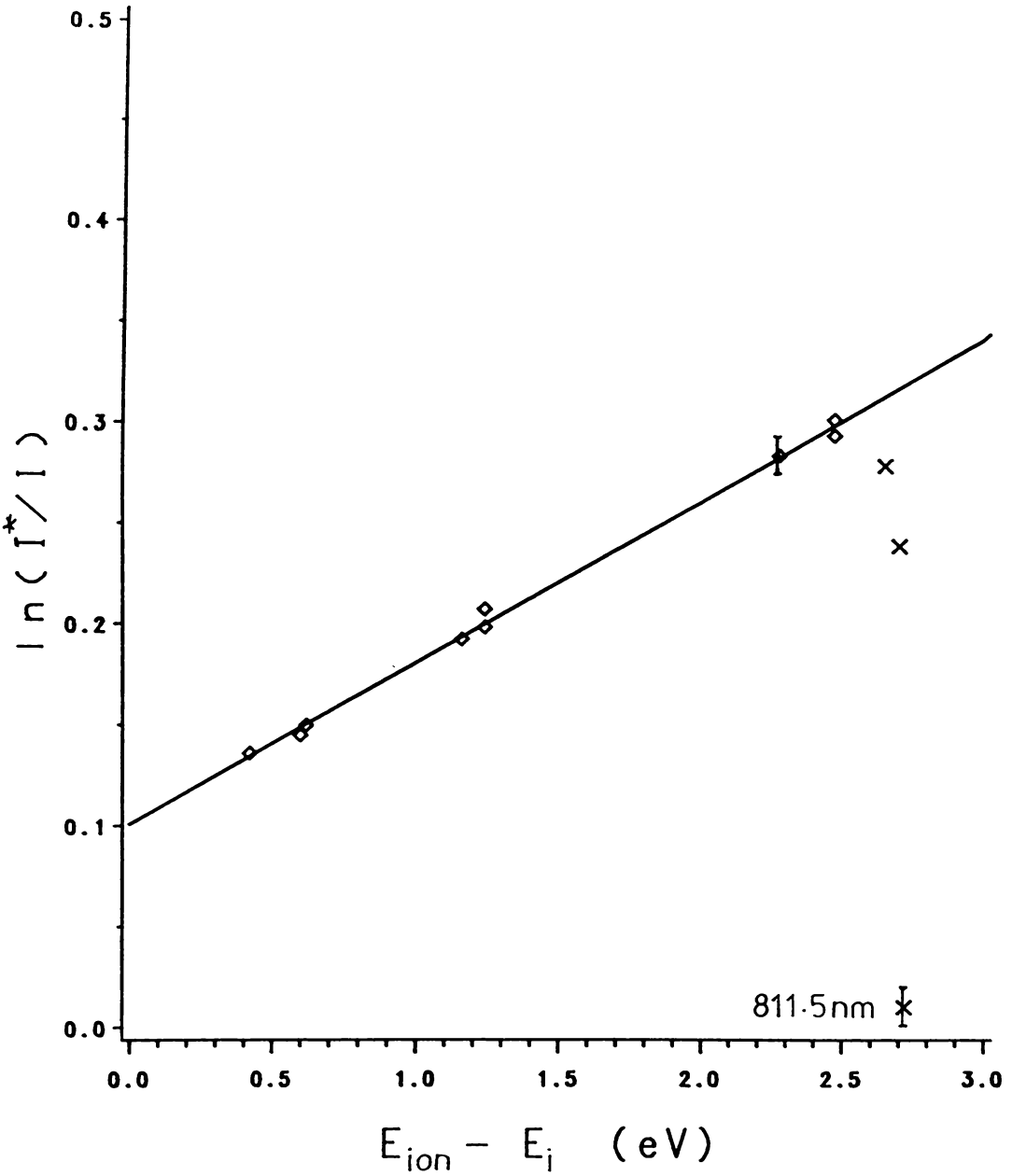

Figure 6.2: Plot of the Logarithm of the Intensity Ratio as a Function of Energy Difference.

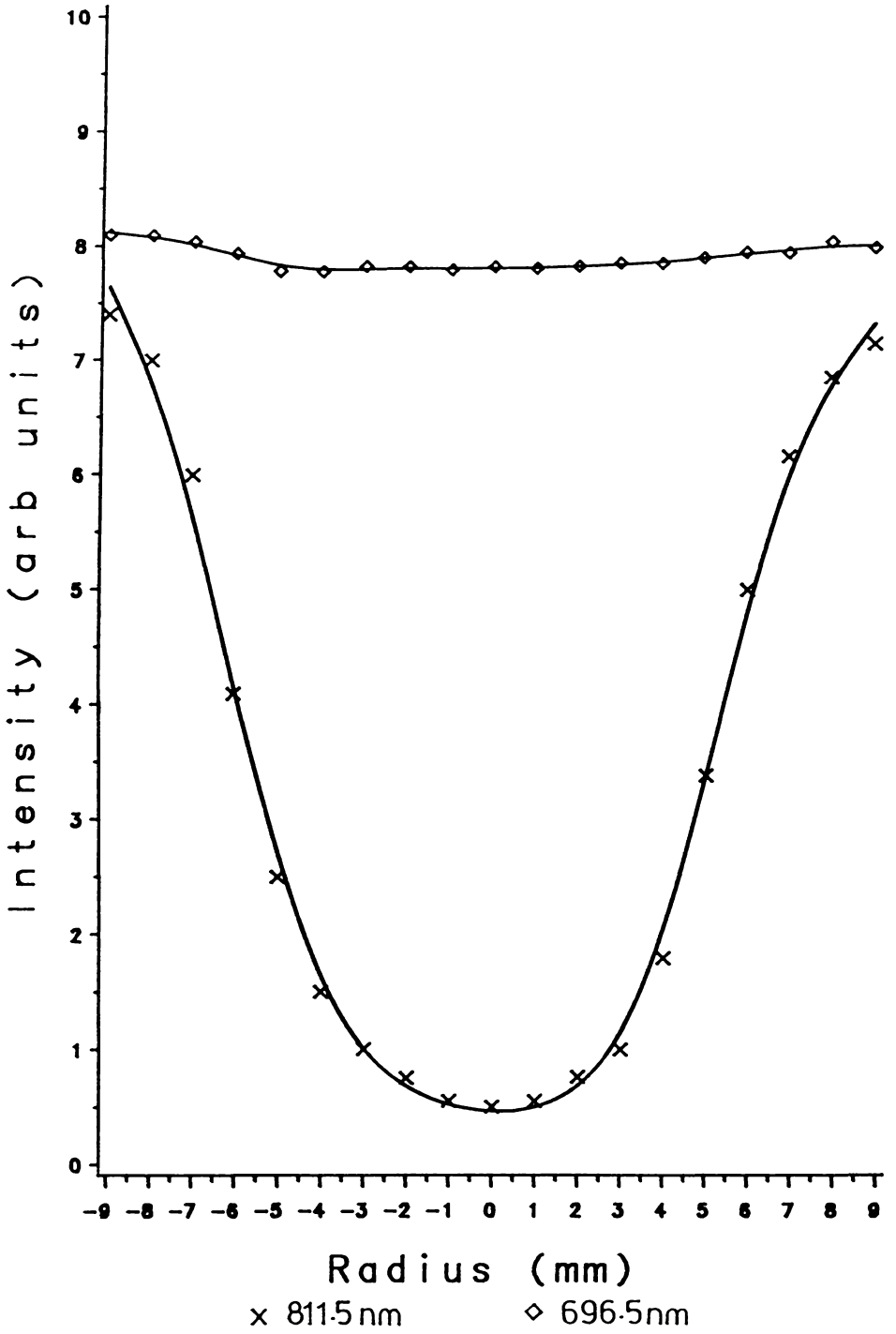

Figure 6.3: Absorption of Modulated Signal versus Radius.
Height = 5mm above work coil, Slit width = 10μm Input power = 1200 W, Flow-rate = 10 l/min coolant only.

These equipment limitations meant that good stability and reproducibility of the ICPT was needed to obtain accurate results. It is generally agreed that the long term stability of ICPTs is excellent (Boumans and De Boer, 1976; Kornblum and De Galan, 1977; Miller, 1978; etc) and this ICPT is no exception. Variations in the light emission could be maintained at less than two per cent for periods of greater than seven hours. Slight stability problems arose on very cold winter days due to variations in the line voltage arising from load shedding and switching by the local supply authority, however, these were avoided by re-scheduling the affected experiments.

The short term ($< 10^{-2}$ seconds) stability and reproducibility was also found to be excellent for certain regions of the plasma but decreased with increasing height and radius. This variation in stability with radius and height suggested turbulence as the possible cause. An attempt was made to measure the turbulence present in the ICPT, using the CO_2 laser, . The laser beam was passed through the plasma onto the pyro-electric detector. The output of which, via an A.C amplifier and a precision F.W. rectifier, yielded an indication of the turbulence in terms of plasma density fluctuations. Figure 6.4 shows the variation in signal for a cross-section of the plasma. It shows that the central region is relatively free of turbulent effects out to a radius of 7 to 8 millimetres; beyond this the turbulence increases rapidly . A similar result was obtained with increasing height above the work-coil, where the turbulence increased rapidly above a height of 10 millimetres above the work-coil.

Other possible contributors to short-term measurement instabilities such as changing optical path-lengths, vibrations etc were found to be insignificant, since all the instruments were mounted on a solid optical table, resting on an air suspension.

Measurements over repeated RF switching pulses yielded intensity variations of up to 3 to 5 per cent within certain regions of the plasma, that is, from 10 mm above the work coil to 15mm below the work coil and out to a radius of 7 to 8 millimetres as demonstrated by photographs 6.11 and 6.12. Outside this region it was impossible to produce accurate repeatable results due to the increased turbulence (Photographs 6.13, 6.14). As mentioned earlier, the closeness to equilibrium meant that the signal-to-noise ratio was poor for spectral lines with their upper energy levels close to the ionisation energy (e.g. $3p^5 - 5d$ _____ $3p^5 - 4p$ transitions). Taking advantage of the repeatability of the plasma, the signal-to-noise ratio was improved with the use of a storage oscilloscope (Hitachi VC6041) which could average the signal for up to 256 pulses. An example of the effect of the averaging is shown in Photographs 6.15 and 6.16.

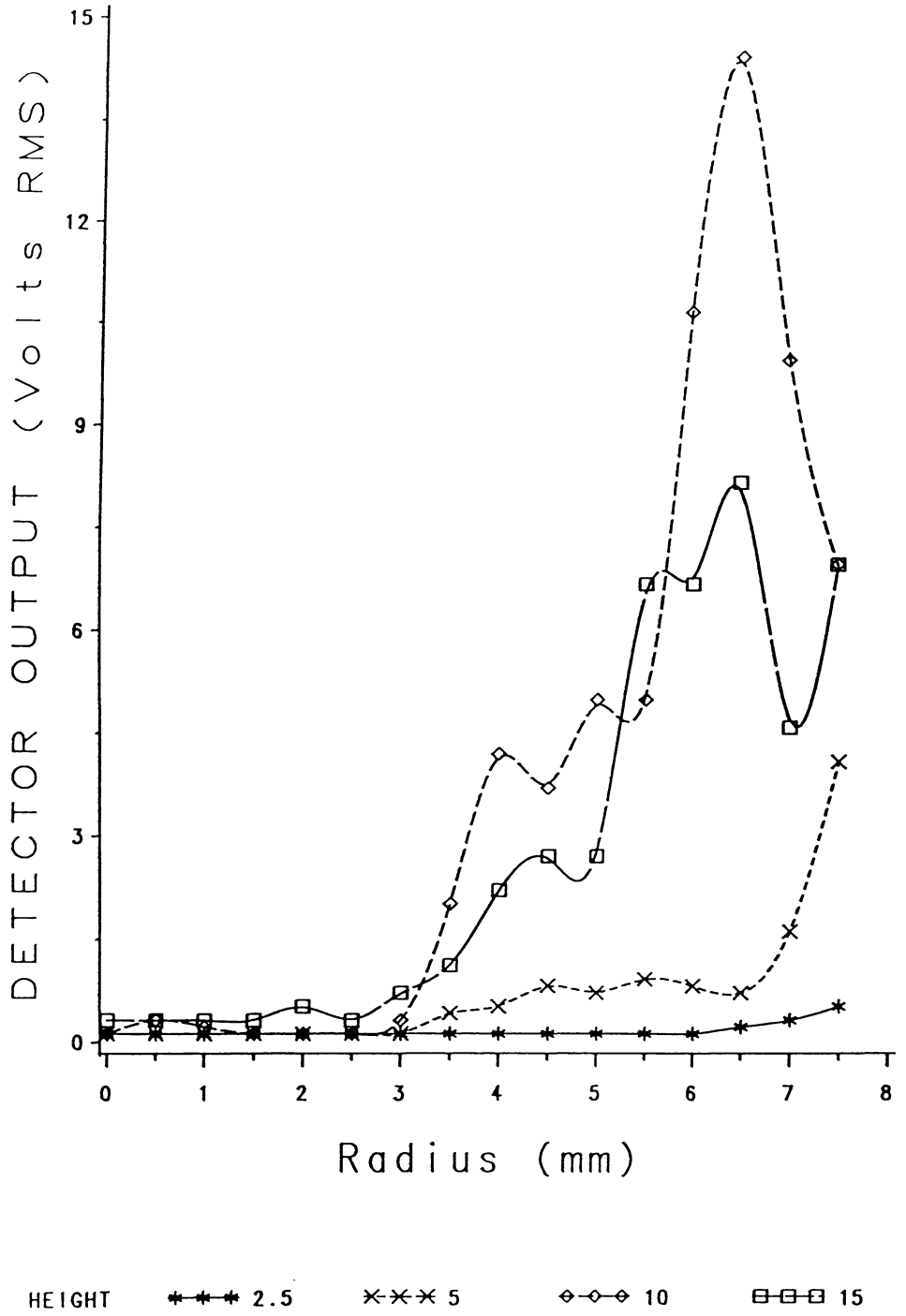

Figure 6.4: Turbulence in the ICPT as indicated by the RMS variation in the CO_2 Laser Intensity.

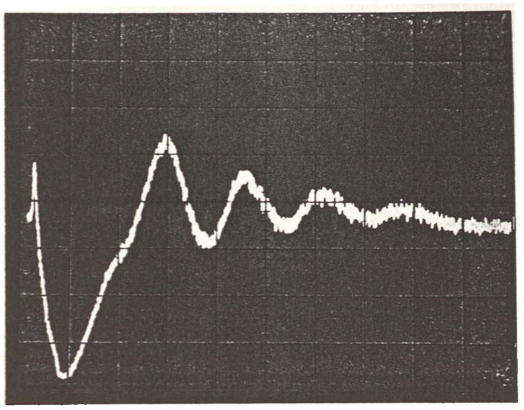

Photograph 6.11: Single Pulse of Ar I 696.5 nm Spectral Line.
Time-scale = 1ms/div, Slit-width = 100μm.

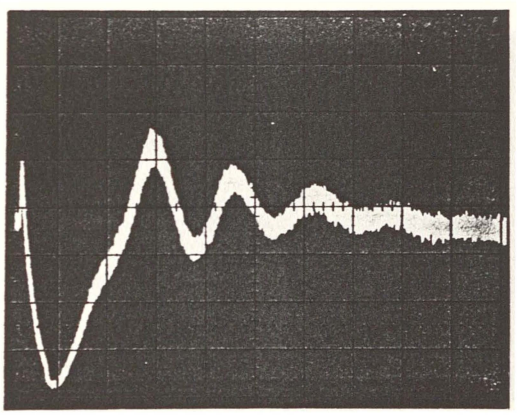

Photograph 6.12: Overlay of Ten Pulses, same parameters as Photograph 6.11.
Time-scale = 1ms/div, Slit-width = 100μm.

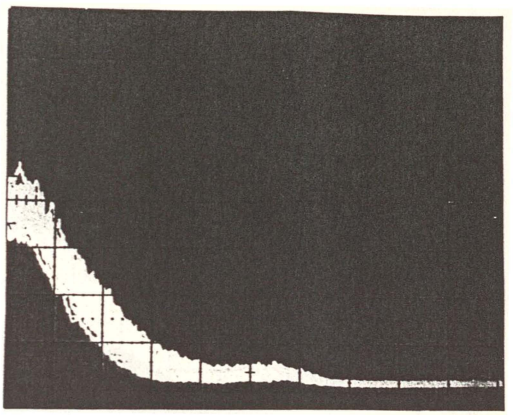

Photograph 6.13: Variation in Spectral Line Increase at 15 mm above the top of the Work-coil.
Overlay of twenty pulses, central region of the plasma.

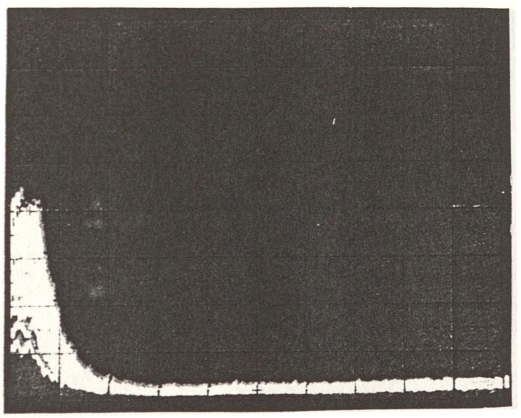

Photograph 6.14: Variation in Spectral Line Increase at a Height of 10mm and Radius of 9mm.
Overlay of twenty pulses.

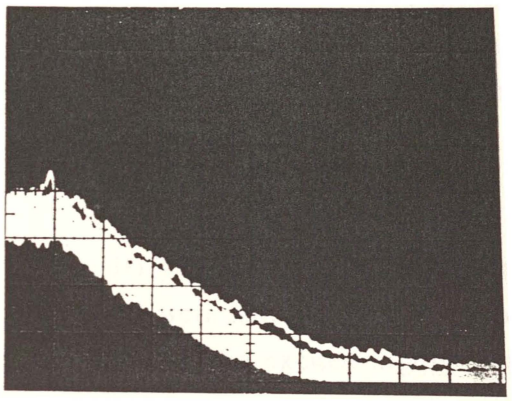

Photograph 6.15:Overlay of Thirty-two Pulses plus one.
Spectral line: 696.5nm Ar I, Height: 15mm above coil, coolant flow only 10l/min.

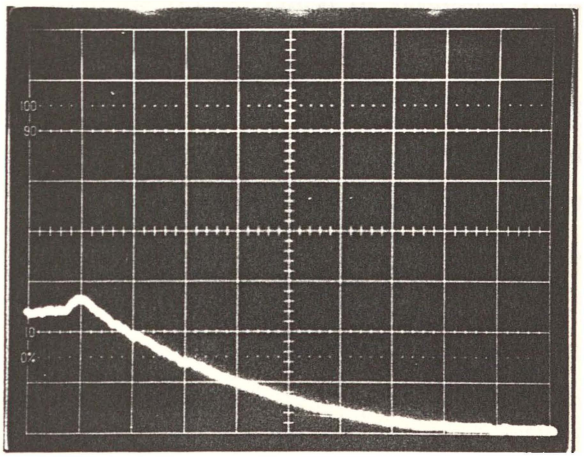

Photograph 6.16: Averaged Signal Output from Thirty-two pulses.
same parameters as Photo 6.15.

The single pulse line (indicated by the arrow) in photograph 6.15 indicates the possibility of a jump in intensity but the noise level prevents any accurate measurements. The averaged signal indicates a clear jump in intensity, the variation caused by turbulence as well as the smallness of the intensity increase ruled out any investigation of the state of equilibrium of the plasma at this height above the coil but this photograph does indicate that at 15 millimetres above the coil the electrons are still at a higher temperature than the neutrals.

6.7. Conclusions

In this chapter the underlying assumptions necessary for the use of the relaxation method outlined in Chapter 4 were listed. After first showing the information available from observing the behaviour of the excited argon spectral line intensities, when the RF field is pulsed off, each assumption and condition, where possible, was investigated.

The electron density was shown to remain effectively constant during the time required for the electrons to relax to the gas temperature.

Excited argon spectral lines were investigated to establish which were optically-thin. It was established that the infrared lines of the 4s - 4p transition were approaching saturation especially the 811.5nm line.

The stability of the plasma was established to be very good and it was demonstrated that repeatable results could be obtained from measurements associated with pulsing off the RF field.

The one remaining assumption, that of obtaining accurate local values of the various physical parameters from measurements obtained by lateral scans of the plasma, that is, the question whether the plasma is axisymmetric, is discussed in the next chapter.

Chapter 7

Preliminary Experiments II

Axisymmetry

7.1. Introduction

In most studies involving ICPT plasmas where emission spectroscopy is used as the diagnostic method of investigating the plasma properties, the means of obtaining the radial profiles necessary to understanding the behaviour of the plasma (T_e, T_g, n_e etc) is by first obtaining a lateral scan across the plasma and then with the use of Abel's transform converting these lateral results into radial values. This method is simple and avoids the experimental difficulties involved in observing the plasma end-on where a scan measures the radial intensities directly.

However in converting lateral intensities to radial via Abel's transform accurately, certain conditions are imposed. Ideally, the plasma should be optically-thin and axisymmetrical. Although the plasma in the ICPT is not optically-thin over all wavelengths it is the requirement of axisymmetry that is most critical to the accuracy of the final result. Usually a lateral scan across the plasma of the emission intensity of a spectral line that is axisymmetric is taken as a adequate proof that the plasma can be considered axisysmmetric for all the plasma parameters. As to whether this is indeed sufficient proof is however debatable and as the relaxation method provides a sensitive means of directly comparing different parameters of the plasma it was used to investigate the validity of this assumption. However, before investigating whether the plasma is indeed axisymmetric a discussion of Abel's transform is in order.

7.2. Abel's Transform

The variation of intensity with radius is more useful and relevant than the lateral intensity variation as it allows the determination of the local values of the various plasma parameters. Radially resolved results are obtained from the lateral

measurement with the solution of Abel's Transform, that is

$$\epsilon(r) = -\frac{1}{\pi}\int_{r}^{r_0} \frac{I'(y)dy}{(y^2 - r^2)^{\frac{1}{2}}} \tag{7.1}$$

$$= -\frac{1}{\pi}\int_{r}^{r_0} \frac{I'(x)dx}{(x^2 - r^2)^{\frac{1}{2}}} \tag{7.2}$$

This equation relates to a cylindrical column observed in the x direction at a distance y from the zx plane (see Figure 7.1) in which the emission depends only on the r co-ordinate.

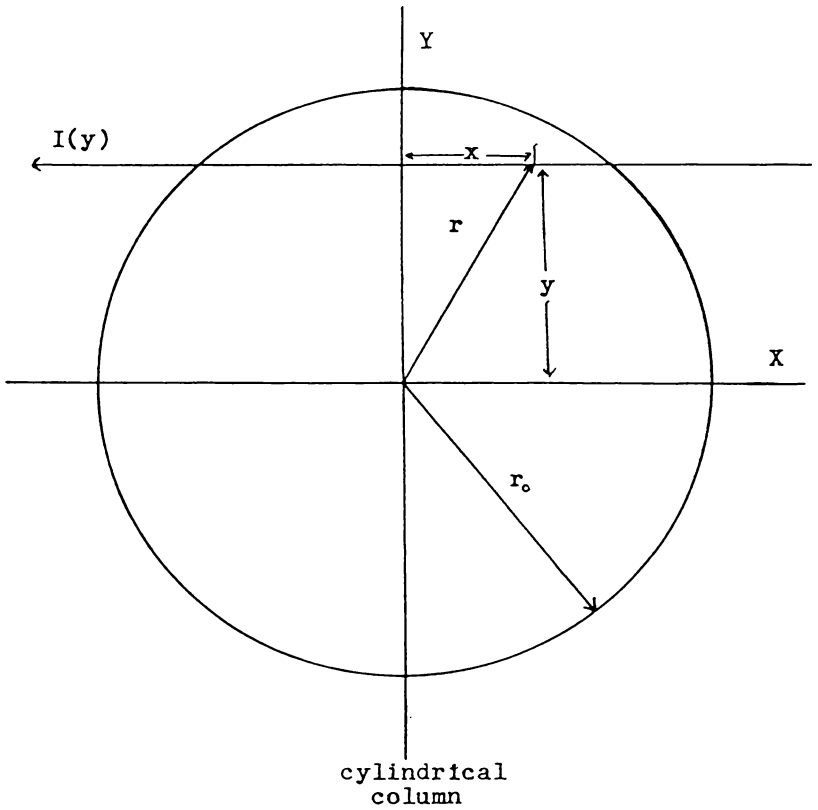

Figure 7.1: Schematic view of a Cylindrical plasma.

A variety of mathematical methods have been proposed (Nestor and Olsen, 1960; Bockasten, 1961; Cremers and Birkebak, 1966; Robinson, 1971; Glasser, Chapelle and Boettner, 1978; and Deutsch and Beniaminy, 1982, 1983), of varying accuracy, to solve this equation. One of the most accurate (Deutsch and Beniaming, 1983) is that which uses a piece-wise cubic spline function which is least-square fitted to the data to

calculate the inverse of Abel's integral equation. A computer program (supplied by Deutsch and Beniaming) using this method was used to calculate the radial intensities given later.

7.3. Experimental Results

As axisymmetry is an essential requirement to convert lateral intensities to radial intensities using Abel's Transform, it is therefore important to determine whether, or where, or when this is the case. The following experiments were performed to establish under what conditions the plasma in an ICPT this requirement is met.

7.3.1. Minimum Flow: Coolant only

To isolate possible causes of any asymmetry arising in the plasma, the initial experiments were performed under operating conditions of an input power of 1200 Watts and a coolant flow-rate of 10 litres/minute, with no aerosol flow. Lateral scans of the intensity of the 696.5nm Ar I spectral line were taken at a distance of 15 millimetres below the top of the work-coil, and at heights of 2.5, 5 and 10 millimetres. Due to the shape of the work-coil, it was impossible to obtain a full scan across the plasma in the middle of the work-coil. Figure 7.2 gives a plot of the lateral intensity versus the radius and Figure 7.3 gives the corresponding lateral intensity ratio at the removal of the RF field, that is $\frac{I^*}{I}$ versus radius where I and I^* are spectral line intensity before and after the RF field is pulsed, at various heights in the plasma for this coolant flow which is the minimum flow usable for sustained operation of the torch. These results demonstrate that the plasma is axisymmetric above the work coil in terms of both the intensity and the intensity ratio. Below the coil, neither of these parameters could be considered to be axisymmetric.

The shape of the curves in Figure 7.3 shows that the largest intensity ratios are in the outer 3 to 4 millimetres of the plasma corresponding, of course, to the maximum temperature difference between the electrons and the heavy particles constituting the plasma (see Chapter 8). This is to be expected as the central region is shielded from direct RF heating of the electrons by the outer region plasma at a thickness corresponding to the skin-depth at 27 MHz (Ong, 1977).

7.3.2. The Effect of Increased Coolant Flow

Apsit (1971) in his study of a physical plasma had found that a flow of gas along a single tube produced an axially asymmetrical distribution of the temperature difference, that is, the temperature difference was greater on the side of the plasma

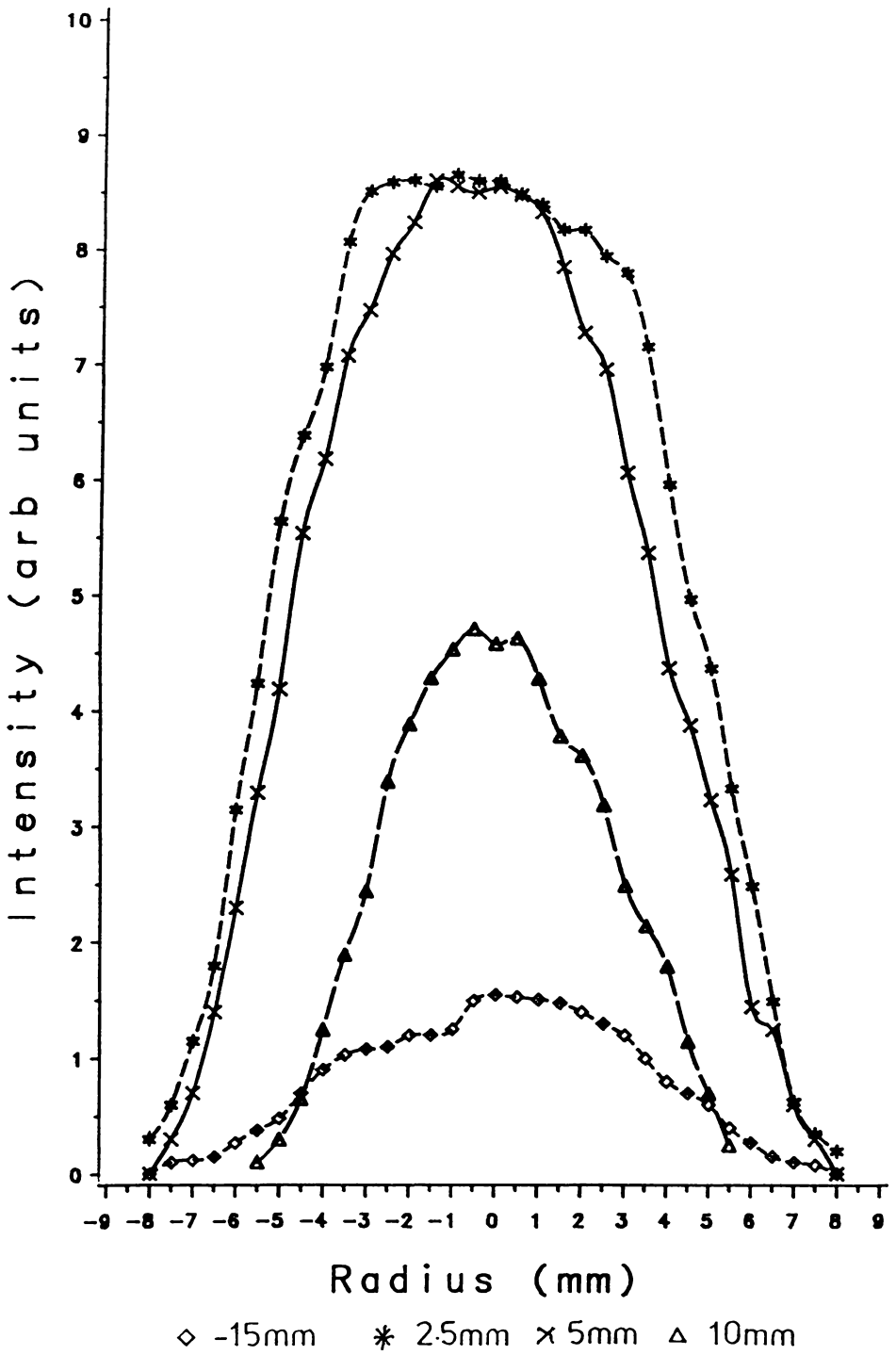

Figure 7.2 : Lateral Intensity Scan of Ar I 696.5nm for various heights.
Coolant flow: 10l/min, input power: 1200 W.

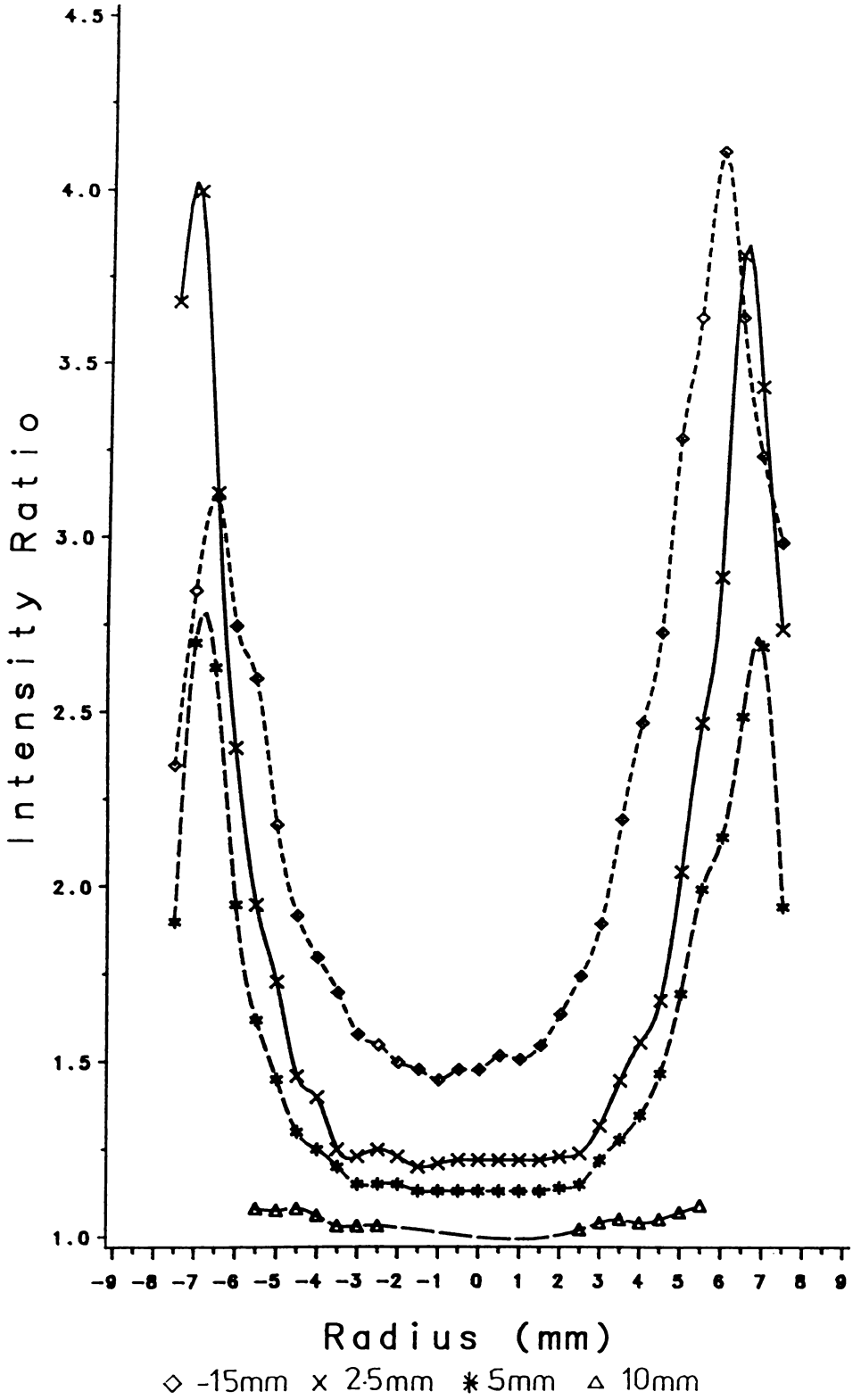

Figure 7.3: Lateral Scan of the Intensity Ratio $\frac{I^*}{I}$ of Ar I 696.5nm for various heights in the Plasma.
Same parameters as Figure 7.2.

that the cold argon was introduced. Thus to investigate the effect of increasing the coolant flow-rate on axisymmetry of the 'analytical' plasma present in the ICPT, a series of experiments were performed. First, to investigate the asymmetry found below the coil, the coolant flow was increased in steps from 10 litres a minute to 30 litres a minute. As in section 7.3.1, lateral scans of the 696.5nm argon I spectral line were made using the same parameters with the exception of flow-rate. Increasing the flow-rate visibly increased the length of the plasma both above and below the coil. Figures 7.4 and 7.5 gives a comparison of the lateral spectral intensity and intensity ratio $\frac{I^*}{I}$ with respect to the coolant flow-rate at 15 millimetres below the top of the coil. Figure 7.4 shows that the asymmetry below the work-coil in the spectral intensity, as shown in Figure 7.2, arises from the geometrical configuration of the work-coil rather than from any effect due to the gas flow as the asymmetry did not change with variations in input power or flow-rate. The intensity ratios shown in Figure 7.5 gave some interesting results. Increasing the flow-rate decreases the intensity ratio below the work-coil and there is also a decrease in the degree of asymmetry. This decrease in the intensity ratio together with the increase in the relative intensity with increasing flow-rate is probably due to the low pressure zone, generated in the central region of the plasma by the higher gas velocities at the circumference, constraining the plasma (see Figure 2.2).

The effects on the spectral intensity and intensity ratio above the work-coil are shown in Figures 7.6 and 7.7. Figure 7.6 shows that doubling the coolant flow-rate has little effect on the intensity of the 696.5 Ar I spectral line apart from the broadening of the discharge at a height of 10 millimetes. A comparison of Figure 7.5 with Figure 7.7 demonstrates two major changes; the plasma is no longer axisymmetric with regard to the intensity ratio at heights of 2.5 and 5 millimetres above the work-coil, and the intensity ratio has increased markedly at a height of 10 millimetres, especially at the periphery.

To investigate this loss of axisymmetry a series of scans of the plasma were made at a fixed height (5mm) above the work-coil with the coolant flow-rate varying from 10 litres per minute to 40 litres per minute. The results from these scans are given in Figures 7.8 and 7.9.

Figure 7.8 confirms that the intensity of the spectral line emission is relatively independent of the coolant flow-rate above the work-coil. The intensity ratio, however, as shown by Figure 7.9, is very dependent at the periphery of the plasma on the coolant flow-rate. The degree of asymmetry at first increases when the flow-rate is

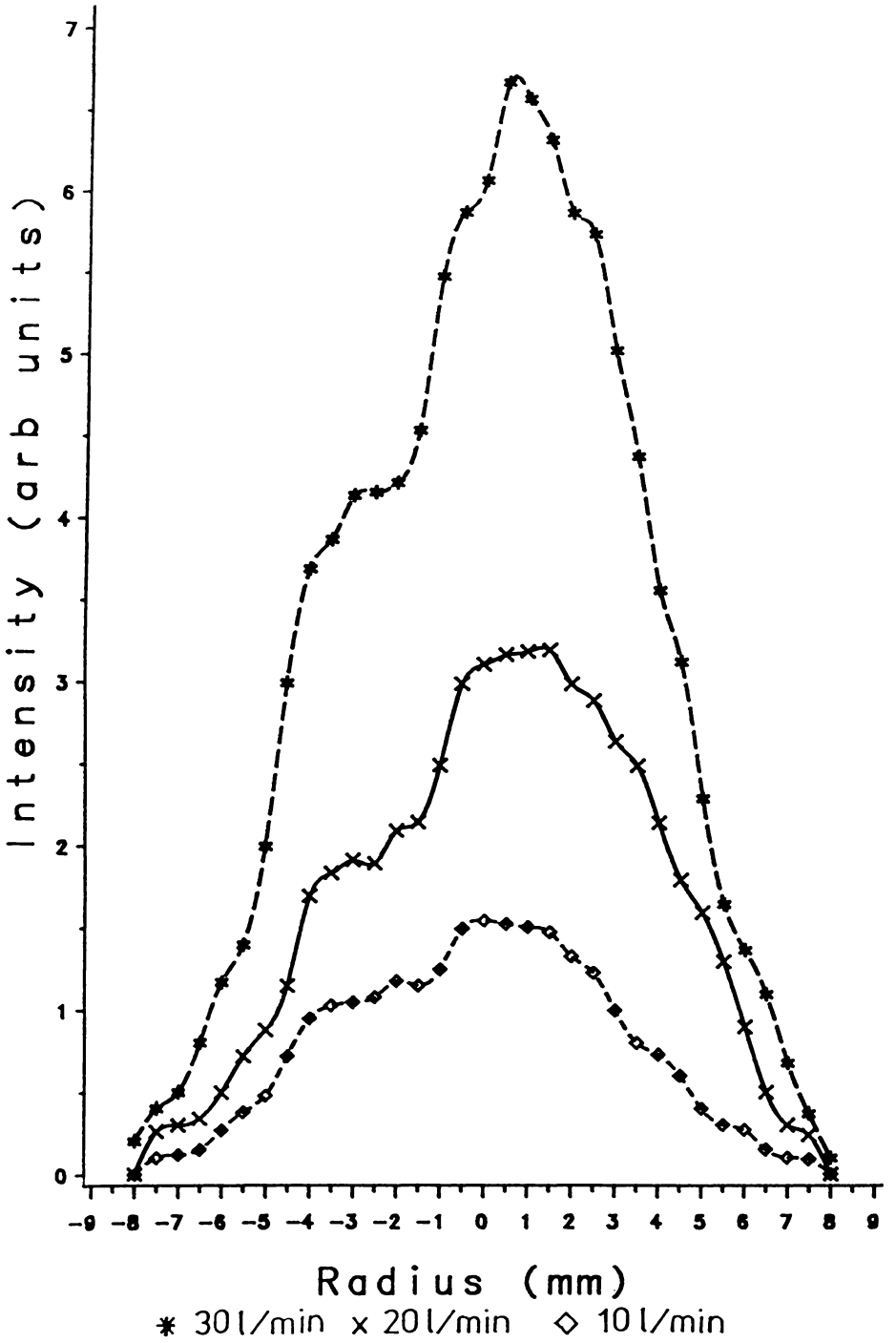

Figure 7.4: Variation in Relative Intensity with Increasing Coolant Flow-rate Below the Work-coil.
Spectral line: Ar I 696.5nm; Height: 15mm below top of coil; Input power: 1200W.

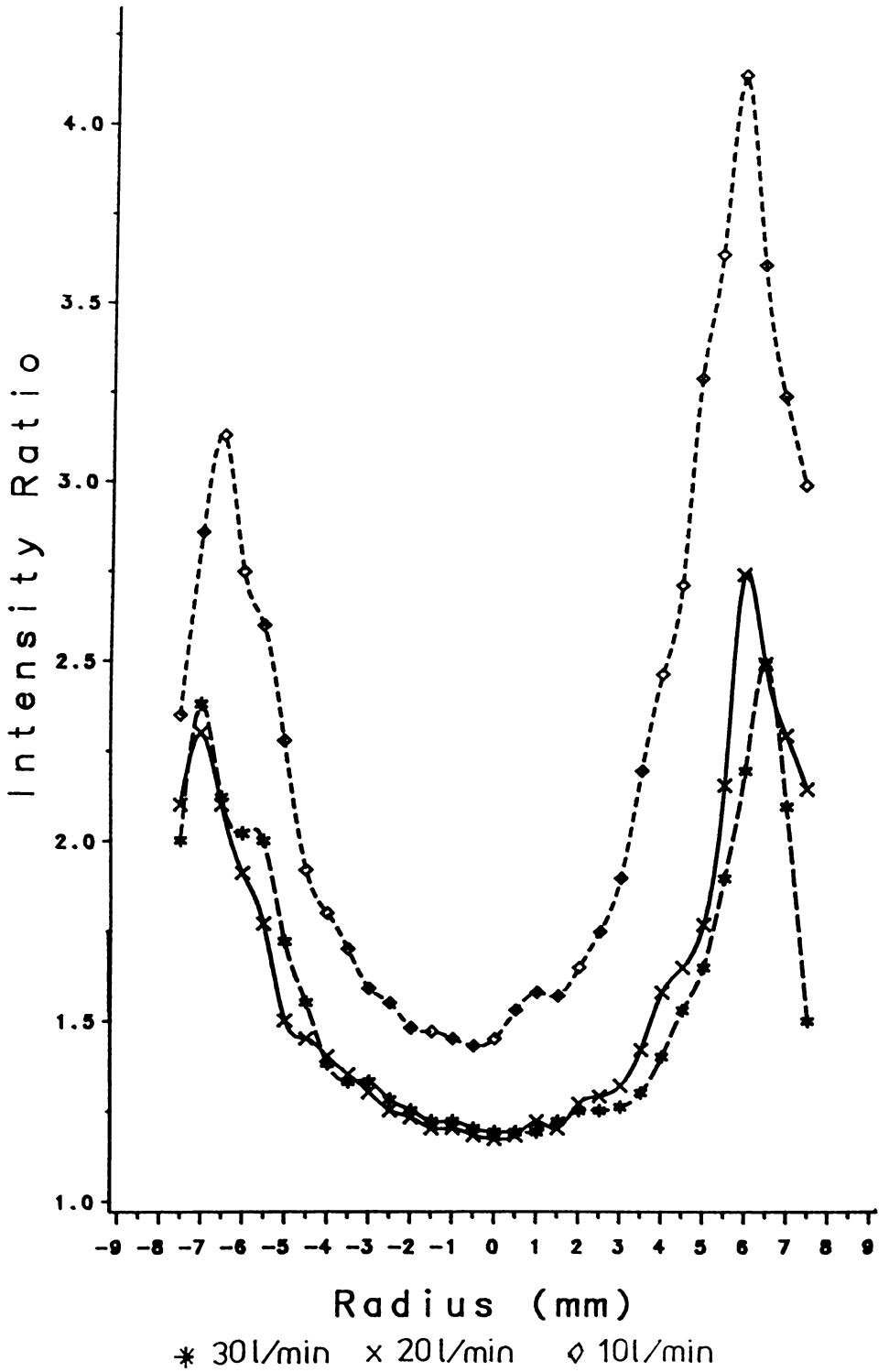

Figure 7.5: Variation in Intensity Ratio with Increasing Coolant Flow-rate Below the Work-coil.
Spectral line: Ar I 696.5nm; Height: 15mm below top of coil; Input power: 1200W.

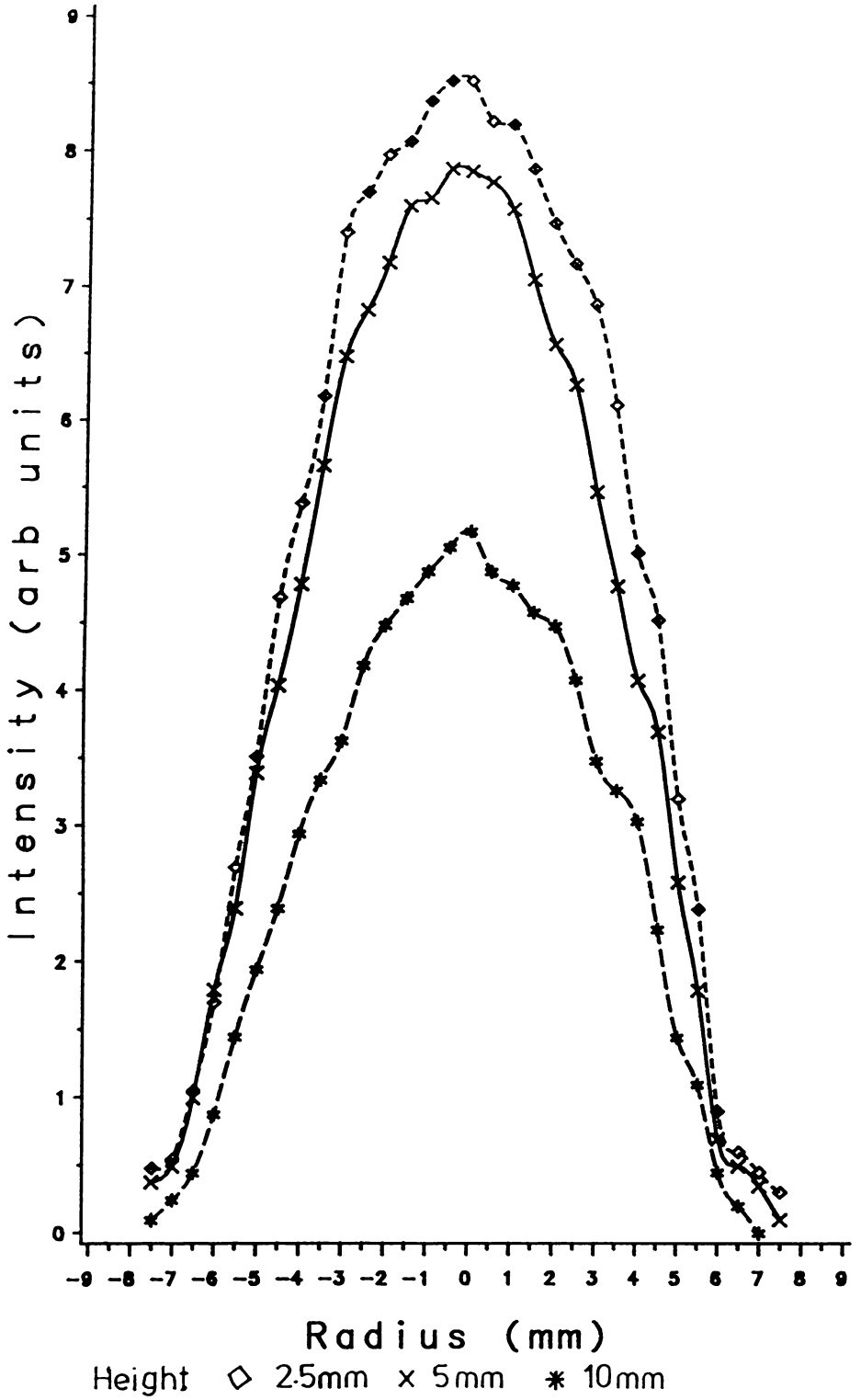

Figure 7.6: Lateral Scan of the Relative Intensity of Ar I 696.5nm with Coolant Flow of 20l/min Above the Work-coil.
Input power: 1200W.

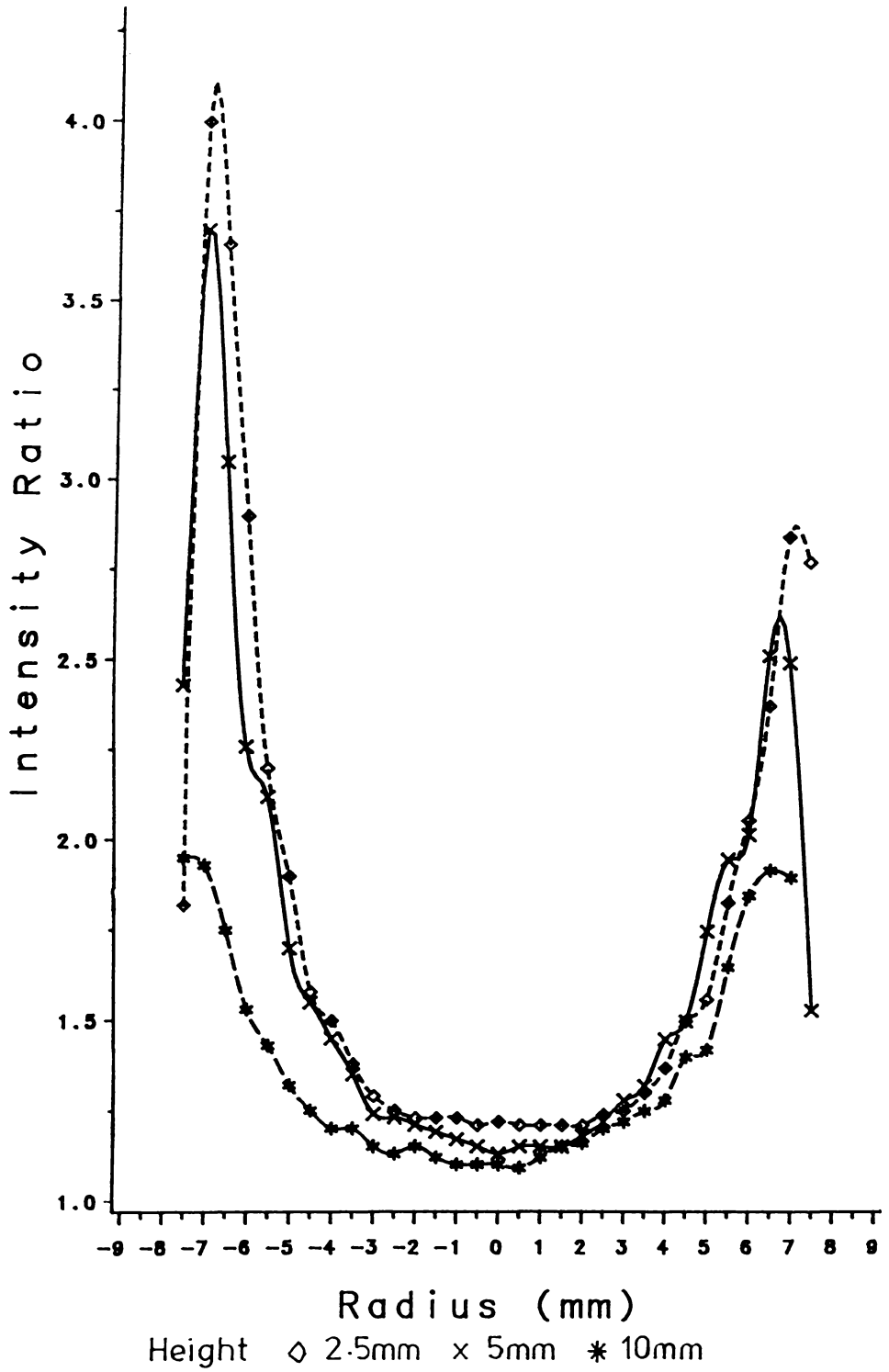

Figure 7.7: Scan of the Intensity Ratio for a Coolant Flow of 20l/min Above the Work-coil.
Spectral line: Ar I 696.5nm; Input power: 1200W.

increased from 10 litres per minute to 20 litres per minute and then decreases again as the coolant flow is increased up to 40 litres per minute. When these results are compared with those obtained below the work-coil (Figure 7.5), peak values for $\frac{I^*}{I}$ occur on opposing sides of the plasma, with opposite effects in these two positions on the intensity ratio developing with increasing flow. It appears that these asymmetries arise from changes in the flow pattern of the vortex flow, used to stabilise the plasma as well as from the effect of the increasing volume of cold argon passing through the torch.

It is also evident from the results that altering the coolant flow-rate has little effect on the central region of the plasma. Below the work-coil increasing the flow-rate initially decreased the intensity ratio after which it remained relatively steady. Above the work-coil the intensity increased slightly with an increase in coolant flow but then also remained relatively stable.

7.3.3. Introduction of the Aerosol Flow

To utilise the ICPT as a light source in emission spectroscopy it is necessary to introduce the sample to be analysed into the plasma. This is generally done in the form of an aerosol carried by a laminar flow of argon through the center of the plasma. The high frequency that is used to heat the plasma with a corresponding thin skin depth ($\approx$3mm) assists in a channel being formed by the gas flow through the center of the plasma. This flow with or without a sample is denoted hereafter as the aerosol flow. For the experiments described in this chapter the aerosol flow used consists of argon only.

The aerosol flow is introduced through a central tube having an orifice of 1.5 millimetres. At flows below 1 litre per minute the aerosol flow lifts the plasma slightly but flows around the outside of the plasma. For flow-rates of 1 litre per minute and higher a hole is forced through the center of the plasma. While aerosol flow-rates of 8 litres per minute are easily sustained by the plasma, only flow-rates of 1 and 2 litres per minute were investigated, these being in the range used in introducing samples to the plasma (see Chapter 2). The coolant flow was maintained at a constant rate of 10 litres per minute for those experiments involving aerosol flow.

The visual effects of introducing the aerosol flow were a decrease in the

Figure 7.8: Variation in Relative Intensity with Increasing Coolant Flow-rate.
Input power: 1200W; height: 5mm above work-coil; Spectral line: Ar I 696.5nm.

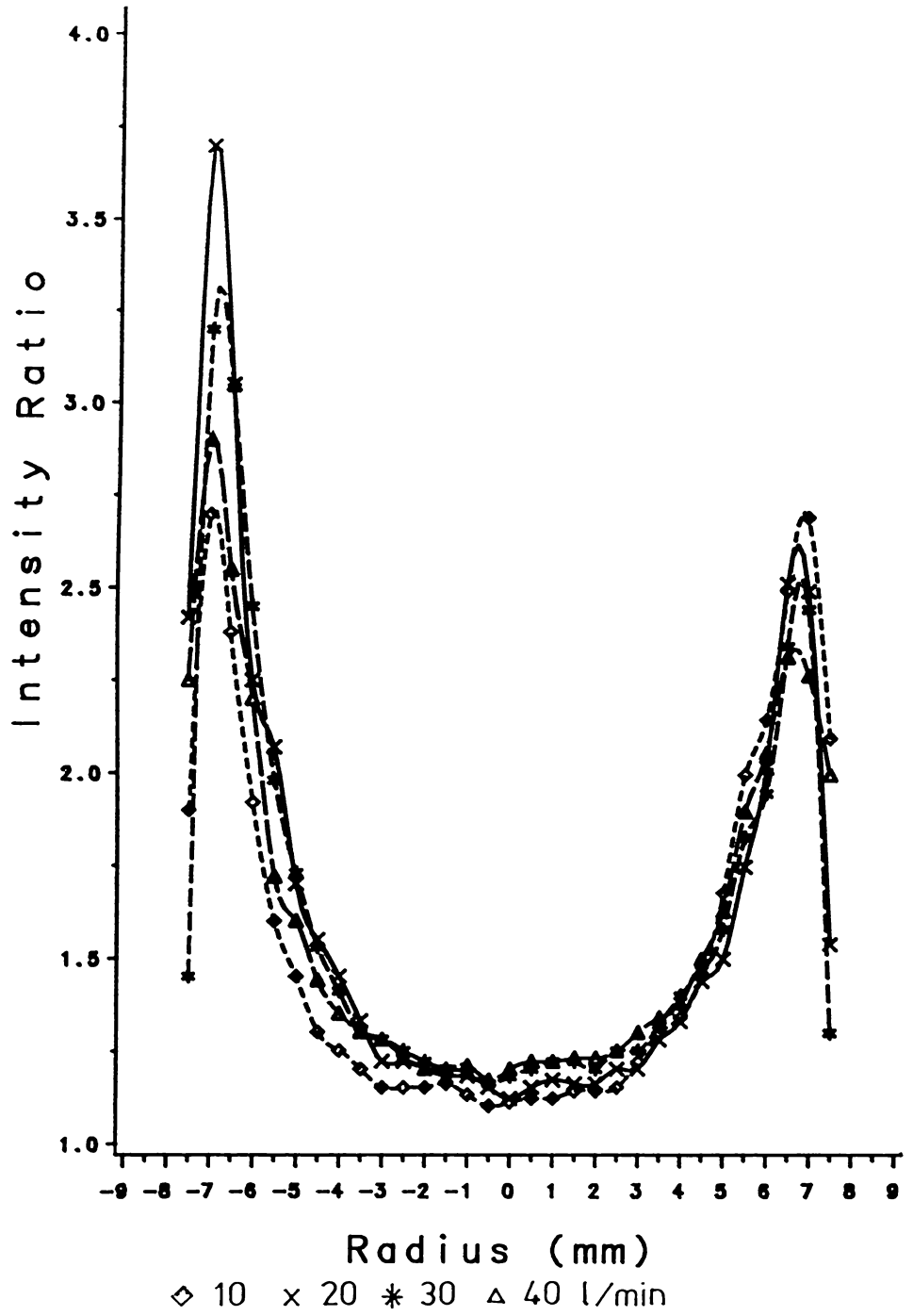

Figure 7.9: Variation in Intensity Ratio with Increasing Coolant Flow-rate.
Spectral line: Ar I 696.5nm; Input power: 1200W; Height: 5mm above coil.

brightness of the plasma, the aerosol channel being easily visible. The change in load characteristics necessitated a minor re-tune of the matching unit.

Lateral scans of the Ar I 696.5nm spectral line were repeated at the same heights as in the previous section under the same conditions with the exception of the addition of an aerosol flow consisting of argon. Figures 7.10 and 7.11 illustrates the behaviour of the spectral line intensity with the introduction of 1 and 2 litres per minute aerosol flow. When compared with Figure 7.2 the drop in intensity is evident as is the characteristic annular shape of the ICPT plasma in the analytical mode of operation.

The effect of the aerosol flow on the intensity ratio $\frac{I^*}{I}$ is shown in Figures 7.12 and 7.13. Apart from improving the symmetry below the work-coil, the introduction of the aerosol flow does not appear to affect the axisymmetry provided the aerosol tube is aligned correctly when the torch is assembled. Mis-alignment, as well as destroying axisymmetry, creates problems of pushing a channel through the plasma with a tendency to extinguish the discharge.

The doubling of the intensity ratio in the central region was the first indication of the significance of the aerosol flow on the state of equilibrium in the plasma.

7.3.4. Radial Intensities

Figure 7.9 demonstrated that the plasma is axisymmetric at height of 5 millimetres with a coolant flow of 10 litres per minute, therefore it is sensible and realistic to convert these lateral results into radial values with Abel's Transform. Figure 7.14 gives a plot of the result of this, showing the lateral and radial intensity ratios of the Argon I 696.5nm spectral line. It shows that in the central region of the plasma there is no increase in intensity upon pulsing the RF field implying that no temperature difference exists between the various components of the plasma in the central region of the plasma (this is of course with no aerosol flow). Only in the outer three millimetres is the intensity ratio significantly greater than one. This is further investigated in the following chapter.

The introduction of the aerosol flow complicates the picture considerably as Figure 7.15 shows. The spectral intensity decreases rapidly towards the central region of the plasma thereby increasing the likely errors in determining the intensity ratios and correspondingly the temperature differences. To increase the accuracy of the radial result the number of sampling points was increased, which improved the accuracy in the central region of the plasma but as will be shown later the state of equilibrium was

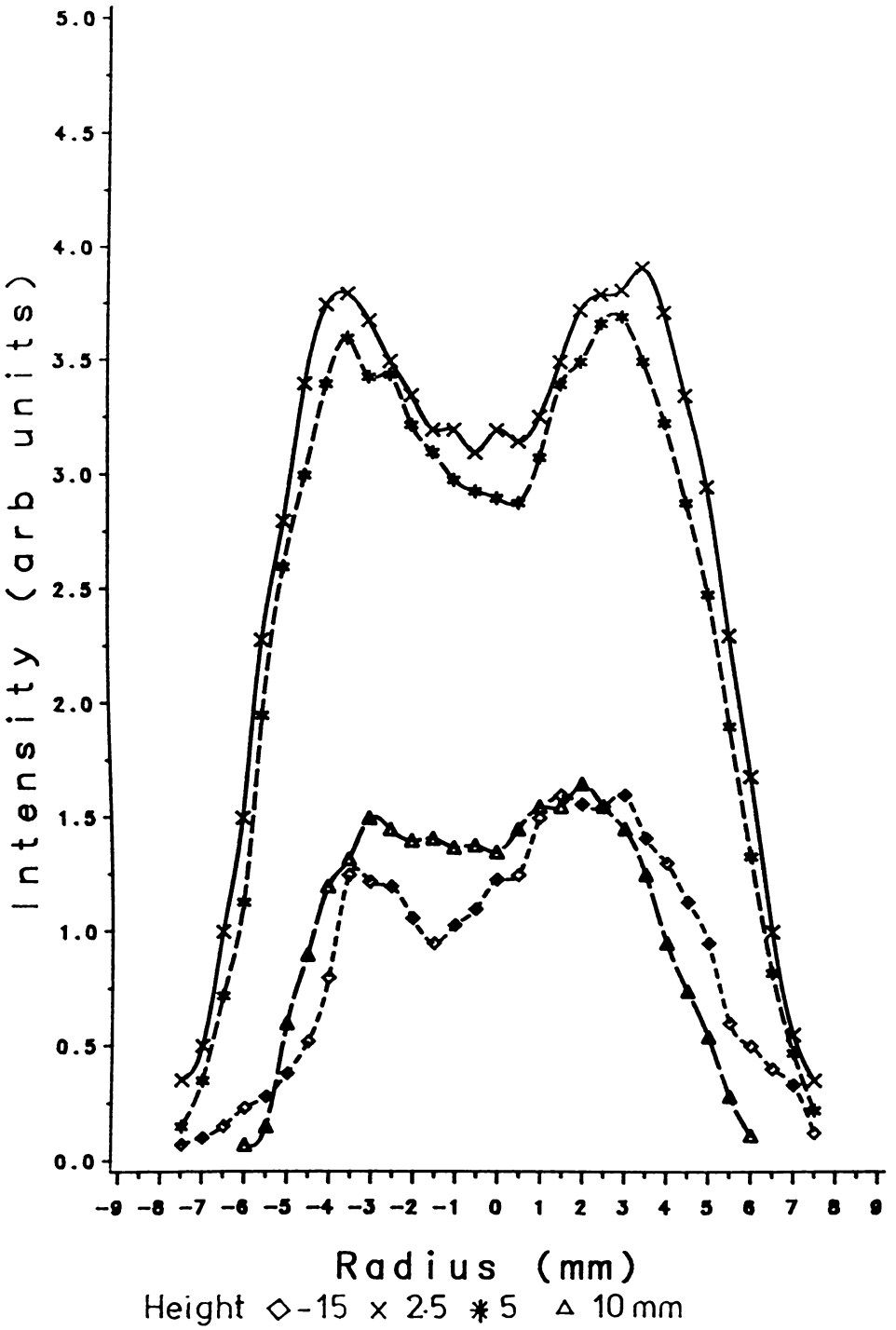

Figure 7.10: Variation in Relative Intensity with the Addition of One Litre per minute Aerosol Flow.
Gas: Argon; Coolant flow-rate: 10l/min; Input power: 1200W; Spectral line: Ar I 696.5nm.

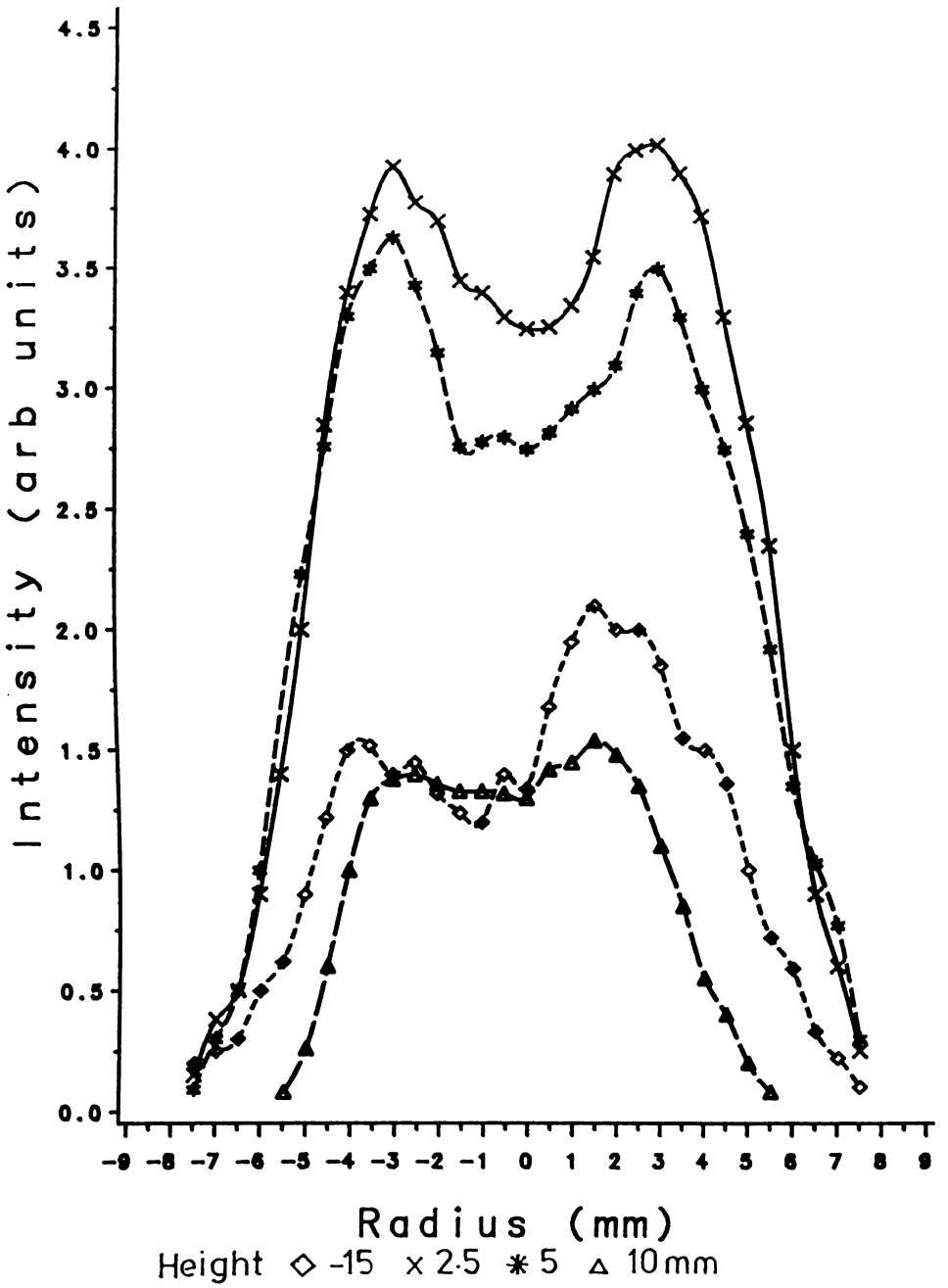

Figure 7.11: Variation in Relative Intensity with the Addition of Two Litres per Minute Aerosol Flow.
Same parameters as Figure 7.10.

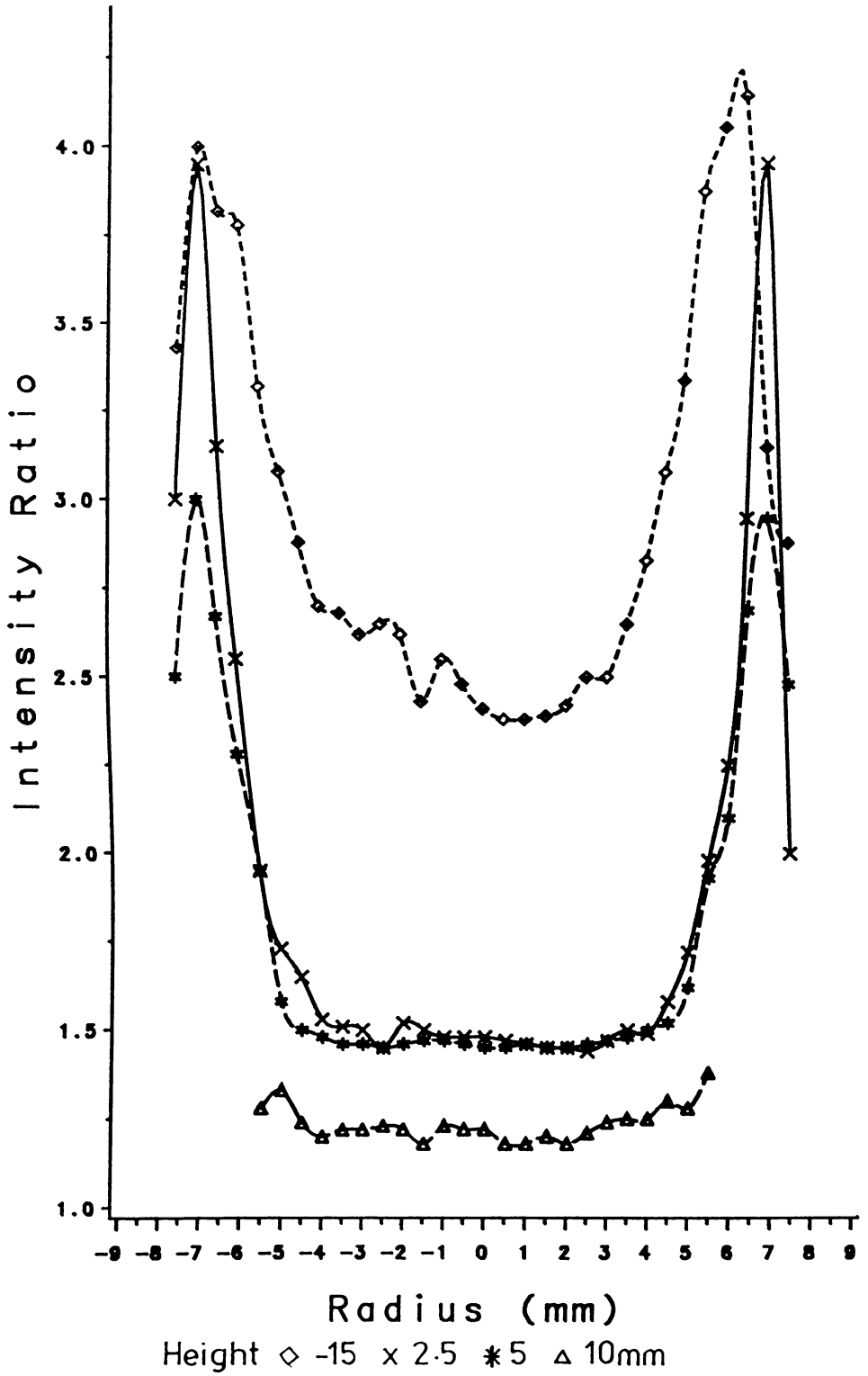

Figure 7.12: Variation in Intensity Ratio with the Introduction of Aerosol Flow, one litre/minute.
Same parameters as Figure 7.10.

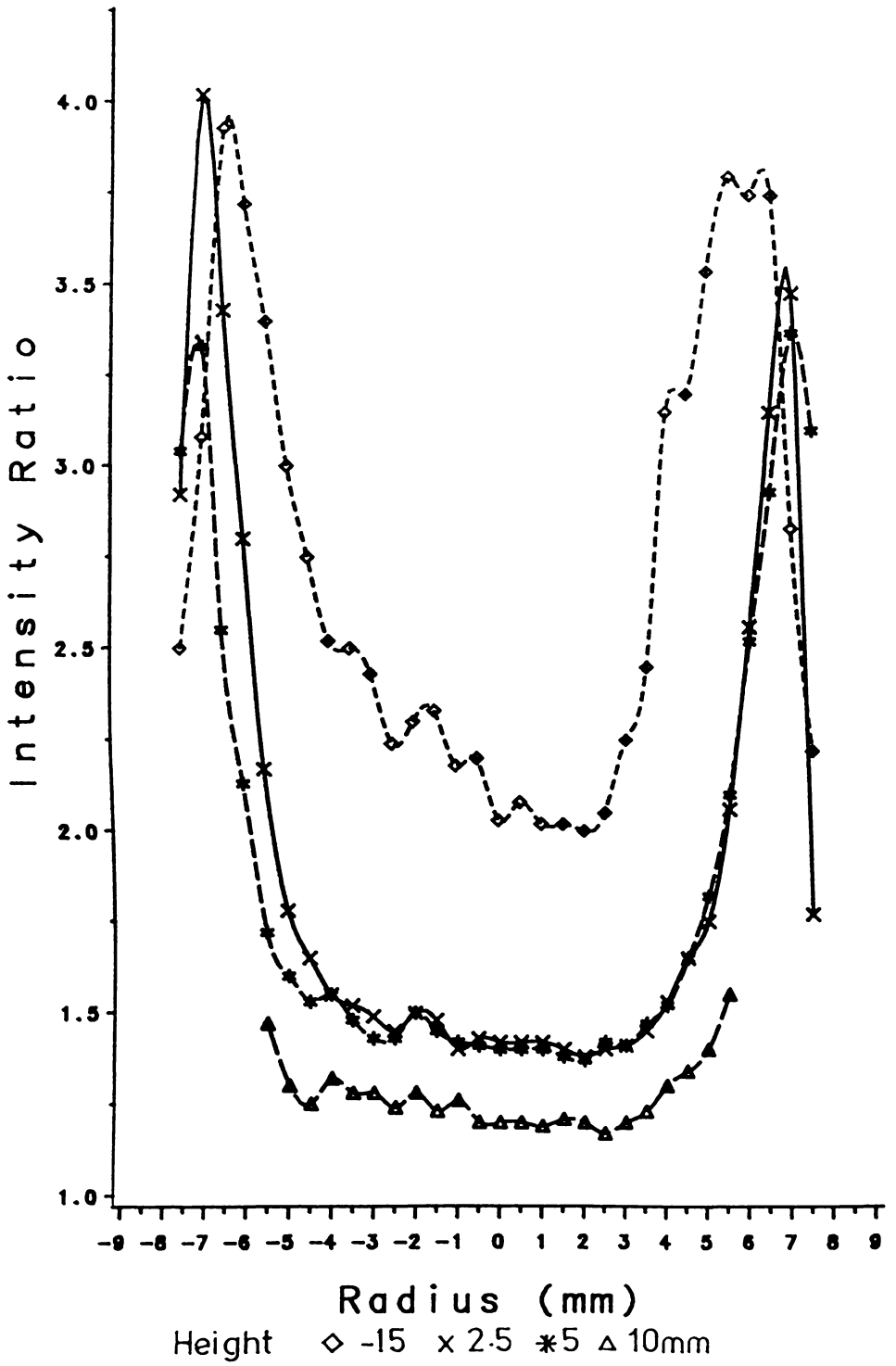

Figure 7.13: Variation in Intensity Ratio with the Introduction of Aerosol Flow, two litres/minute.
Same parameters as Figure 7.10.

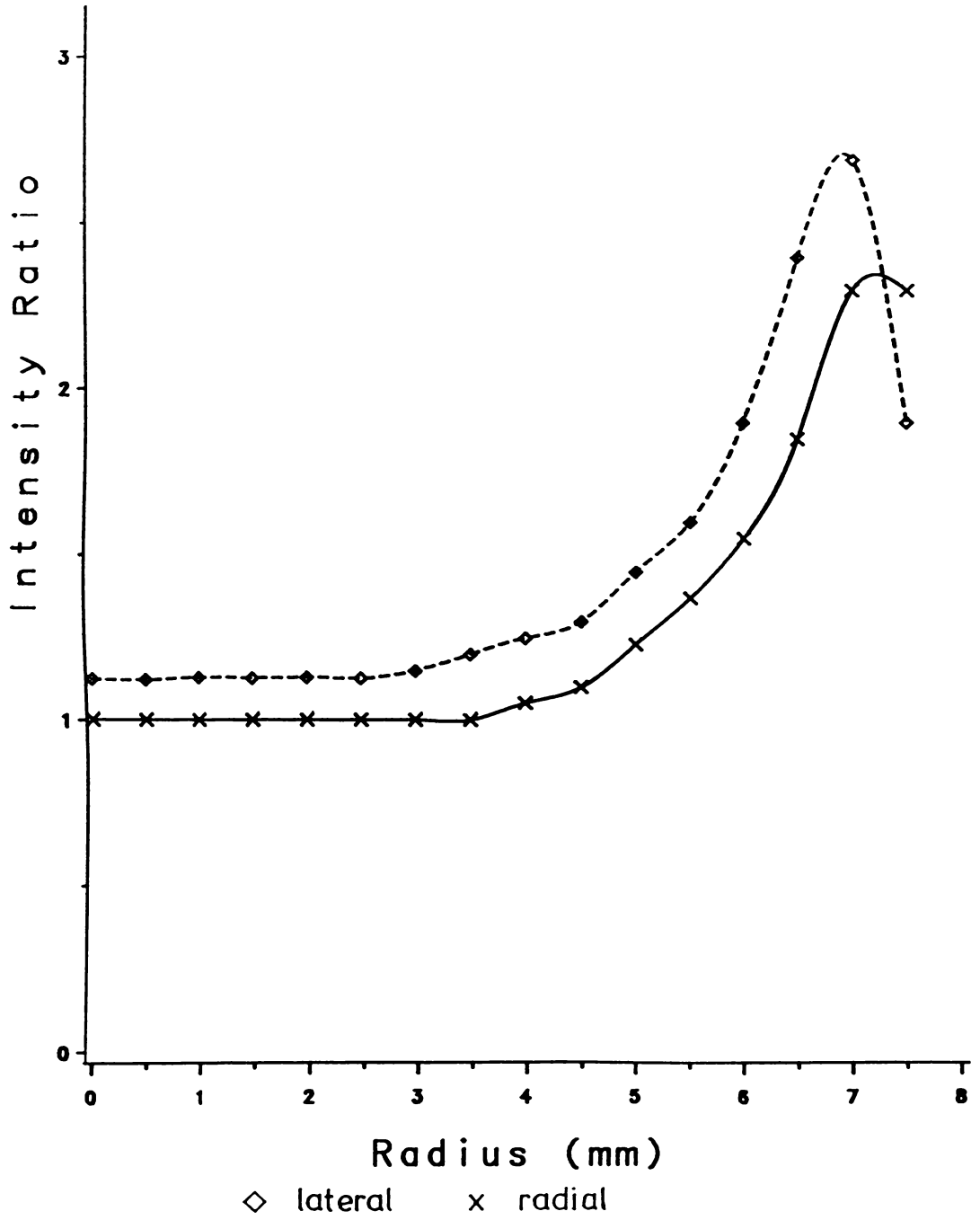

Figure 7.14: Comparison of the Lateral and Radial Intensity Ratios; Coolant Flow only.
Flow-rate; 10 l/min, height; 5mm above work-coil.

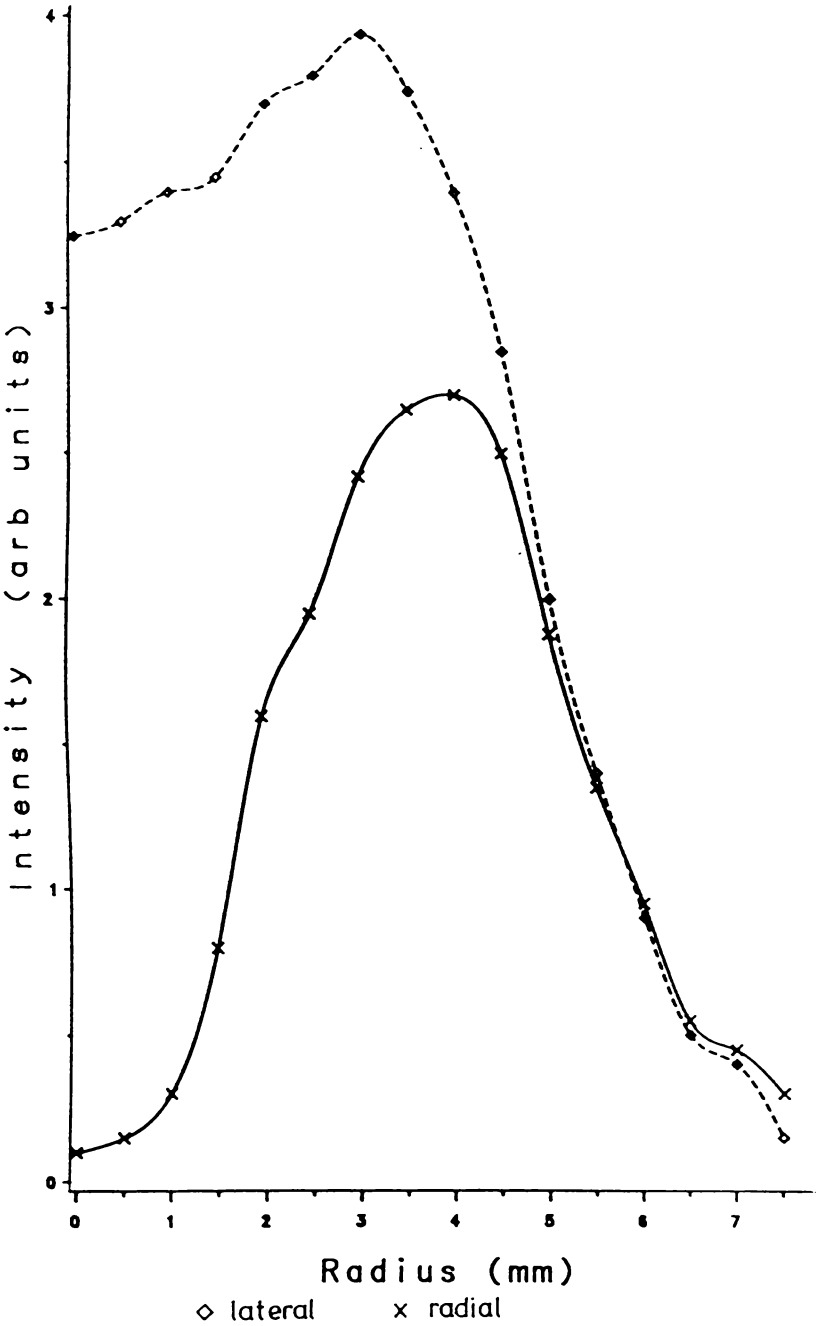

Figure 7.15: Comparison of Lateral and Radial Intensities with the Introduction of an Aerosol Flow.
Coolant Flow-rate; 10l/min, Aerosol Flow-rate; 2l/min, Height; 5mm above Work-coil.

such that the extra sampling points made little difference.

7.4. Conclusions

The assumption of axisymmetry as determine from the intensity of a spectral line was found to be valid only in certain regions of the discharge and dependent on the operating conditions. For example the intensity ratios indicated that the axisymmetry depended on the coolant gas flow-rate. The aerosol flow-rate did not appear to affect the symmetry of the plasma provided the aerosol tube was properly aligned.

Finally the effect of converting from lateral to radial intensities was demonstrated to give a more useful interpretation of the result of spectral scans of the plasma.

The results presented in this chapter casts serious doubt on the widespread assumption of axisymmetry in the ICPT when it is based only on the lateral scan of spectral line intensity. The development of asymmetry, in the case of the intensity ratio, with increasing coolant flow and its variation with height implies a temperature difference arising from the flow pattern of the coolant gas. At the lowest sustainable coolant flow (10l/min) and height of 5 millimetres above the work-coil the plasma appears to be axisymmetric for both the intensity and intensity ratio. This height is suitable to investigate the state of equilibrium of the plasma because as well as the intensity ratio being sufficiently large, it is also the beginning of the zone that is used for analytical purposes.

Chapter 8

Excitation and Kinetic Equilibrium in the ICPT

8.1. Introduction

The assumptions underlying the use of the relaxation method to investigate the excitation mechanisms of the ICPT were examined in Chapter 6 and were shown to be valid for major regions of the plasma. In Chapter 7 the assumption that the plasma is axisymmetric if the emitted intensity of a spectral line is axisymmetric was examined and was found to be invalid. However, under certain operating conditions the plasma could be considered axisymmetric at certain heights above the work-coil.

A series of experiments were then developed and performed to investigate the state of equilibrium prevailing in the ICPT. The deviation from equilibrium is relatively small and any deviation from excitation equilibrium will decrease with increasing energy (level) until equilibrium with the electrons is re-established. The presence of any deviation is most likely to be evident in the lower excited states especially the 4s level. This is due to the fact that with step-wise excitation dominant in the ICPT the lower the level the more probable it is that the level is an end point for collisional transitions to the ground state, and for radiative transfers from upper levels and the continuum. It is also less likely to undergo collisional excitation to the upper energy states or ionisation. Moreover, the 4s state in particular will be subject to the possibility of over-population as it is effectively incapable of de-populating by radiative means as the resonance lines are almost certainly trapped (Griem, 1964; Houk, Fassel and LaFreniere, 1986).

To investigate and determine the cause of any deviation from a state of equilibrium it is necessary to isolate each of the external parameters, in as far as this is possible, that could significantly influence the state of the plasma and by elimination

establish the dominant mechanisms. These parameters are

1) Input power

2) Gas flow

3) Introduction of foreign components

4) Frequency

As the RF generator operates at a fixed frequency it was, however, not possible to investigated the effect of frequency on the plasma.

The state of excitation and kinetic equilibrium in the plasma was investigated by observing the behaviour of nine optically-thin argon spectral lines across the plasma at the various heights and flow-rates given in Chapters 6 and 7. Variation in the radiative losses were noted by observing the behaviour of the 811.5nm spectral line. Table 8.1 lists these spectral lines, together with the appropriate atomic constants. The transition probabilities were obtained from Katsonis and Drawin (1980). Radial intensities were determined by using Abel's transform, where the plasma could be considered to be axisymmetric.

Using equation 4.21, repeated here for convenience,

$$\ln\left(\frac{I^*}{I}\right) = \frac{3}{2}\ln\gamma + (E_{ion} - E_i)\frac{\gamma - 1}{kT_e}$$

the presence, or otherwise, of a Boltzmann distribution among the excited argon states was experimentally established by checking the consistency of this equation over the range of spectral lines given in Table 8.1. Where a Boltzmann distribution was confirmed the temperature difference $T_e - T_g$ was determined. As a comparison the excitation temperature was determined from Boltzmann plots of the same spectral lines under steady-state conditions.

Using the intensity ratio method to observe a nearly saturated spectral line, in this case the 811.5nm line, a reduction in the optical thickness will provide evidence of an increase in radiative losses from the plasma, and thereby supply further evidence of the cause of the deviation from excitational equilibrium and of the resulting population distribution among the excited states. To simplify the problem as much as possible and to enable a comparison with the only other similar study on an inductively-coupled plasma (Aspit, 1971) the initial experiments were limited to a single flow (coolant) plasma.

8.2. Coolant Flow Only

8.2.1. Introduction

The results given in Chapter 7 showed that the intensity ratio $\frac{I^*}{I}$ was relatively unaffected in the central region of the plasma by the coolant flow-rate, and that major changes were limited to the outer edges of the plasma. To investigate whether this extended to all the spectral lines given in Table 8.1, and to the respective heights and flow-rates used in Chapters 6 and 7 a series of experiments were performed. As the experiments in Chapter 7 indicated, for an input power of 1200 Watts, for the central region ($r < 3$mm radius) the intensity ratio $\frac{I^*}{I}$ approached one. This implied that in this region the various temperatures are equal which in turn would indicate that the central region of a single flow ICPT is in local thermal equilibrium at least up to a coolant flow-rate of 40 litres/minute. For economic reasons, in line with the normal procedure for commercially operated ICPT's, the coolant flow-rate was maintained at the minimum flow necessary to sustain a reasonable tube lifetime, and hence the results from here on will relate to a constant coolant flow-rate of 10 litres/minute.

8.2.2. Full Input Power: 1200W

To permit an evaluation of the causes of any deviation from equilibrium in the plasma it is necessary to have a starting point from which to compare the effect on the state of equilibrium of varying the operating conditions. This starting point was chosen to be a single flow plasma at a specified gas flow (10 l/min) and with an input power of 1200W.

Measurements of the intensity ratios taken at various radii from the center of the plasma out to a radius of 7mm are plotted in the form $\ln(\frac{I^*}{I})$ versus $E_{ion} - E_i$ in Figures 8.1(a - f) using nine argon spectral lines at each lateral position. Each plot corresponds to a single radius, and the presence of a straight line indicates the presence of a Boltzmann distribution with the intersection of the y-axis yielding the temperature difference $T_e - T_g$ and the slope of the straight line the temperature T_e (see Figure 4.4).

As demonstrated by Figure 8.1(a), in the central region of the plasma ($r <$ 3mm) the intensity ratios of all the observed spectral lines approached one. This confirmed the earlier indications in Chapter 7 that in the central region the electron and gas temperatures are equal and that this region of the plasma can be considered to be in at least pLTE.

Transition	Wavelength (nm)	Statistical Weight (g)	Transition Probability ($x\ 10^5\ s^{-1}$)	Energy (eV)
4s - 5p	420.0	7	7.75	14.50
4s - 5p	427.2	3	5.92	14.53
4s - 5p	430.0	5	3.9	14.50
4s - 5p	451.0	1	9.44	14.58
4p - 5d	518.7	5	13.8	15.30
4p - 5d	555.9	5	11.8	15.14
4p - 5d	560.7	3	22.0	15.12
4s - 4p	696.5	3	73.4	13.33
4s - 4p	727.3	3	19.0	13.33
4s - 4p	750.3	1	425.0	13.48
4s - 4p	811.5	7	336.0	13.08

Table 8.1
List of Argon I Spectral Lines Used

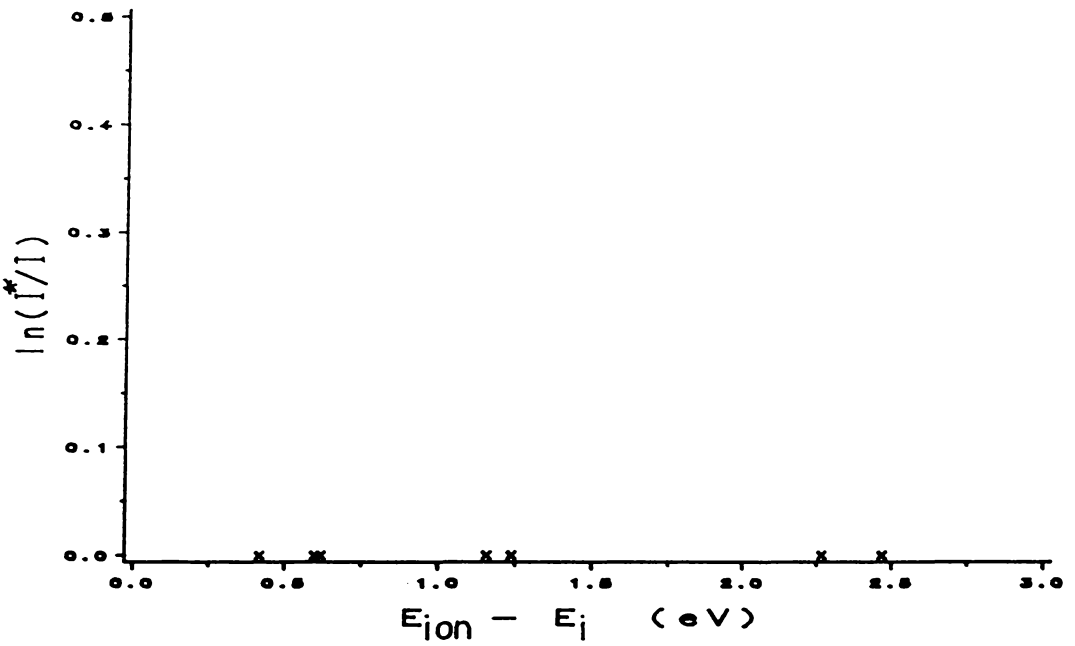

Figure 8.1(a): Intensity Ratio $\frac{I^*}{I}$ versus $E_{ion} - E_i$: Center of Plasma.
Coolant flow-rate; 10l/min, Input power; 1.2kW, Height; 5mm above work-coil.

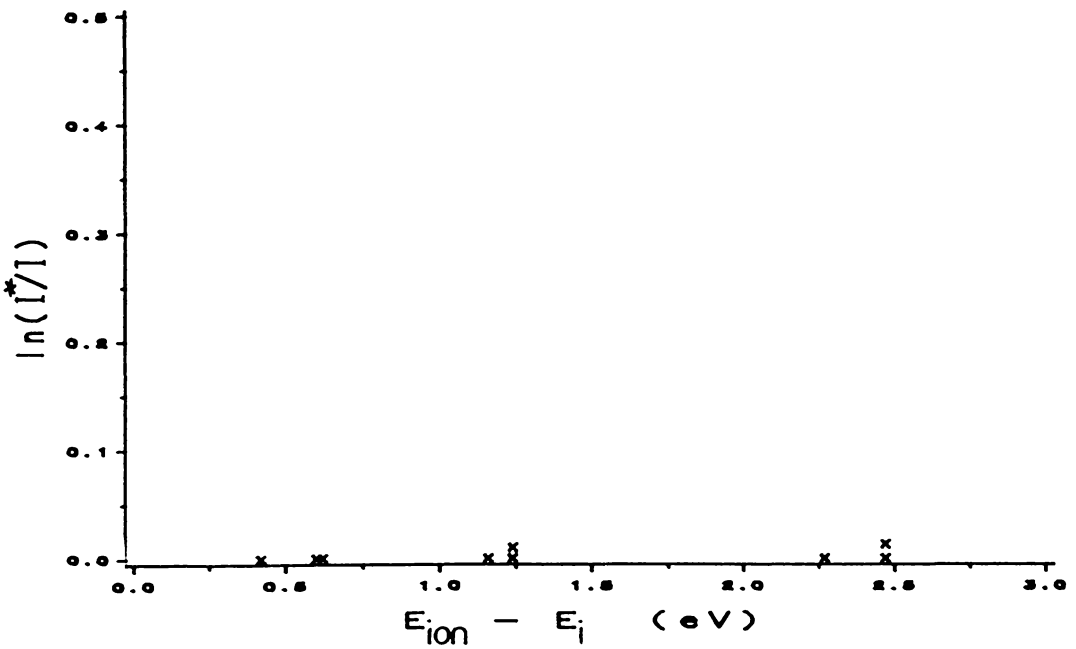

Figure 8.1(b): Intensity Ratio $\frac{I^*}{I}$ versus $E_{ion} - E_i$: 3mm radius.
Same operating parameters as Figure 8.1(a).

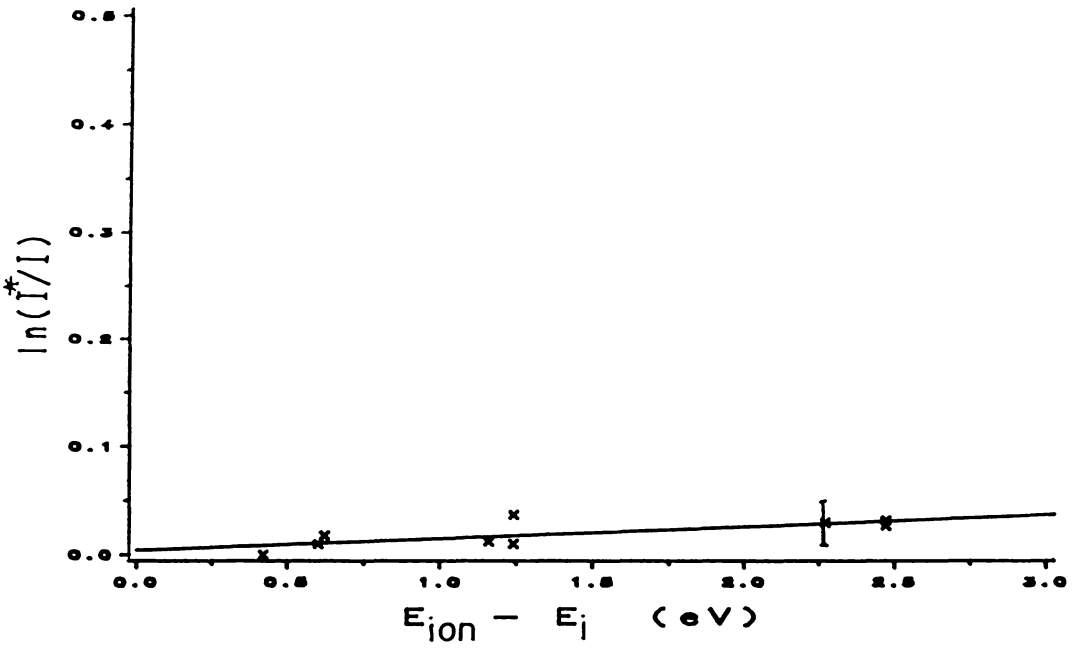

Figure 8.1(c): Intensity Ratio $\frac{I^*}{I}$ versus $E_{ion} - E_i$: 4mm radius.
Same operating parameters as Figure 8.1(a).

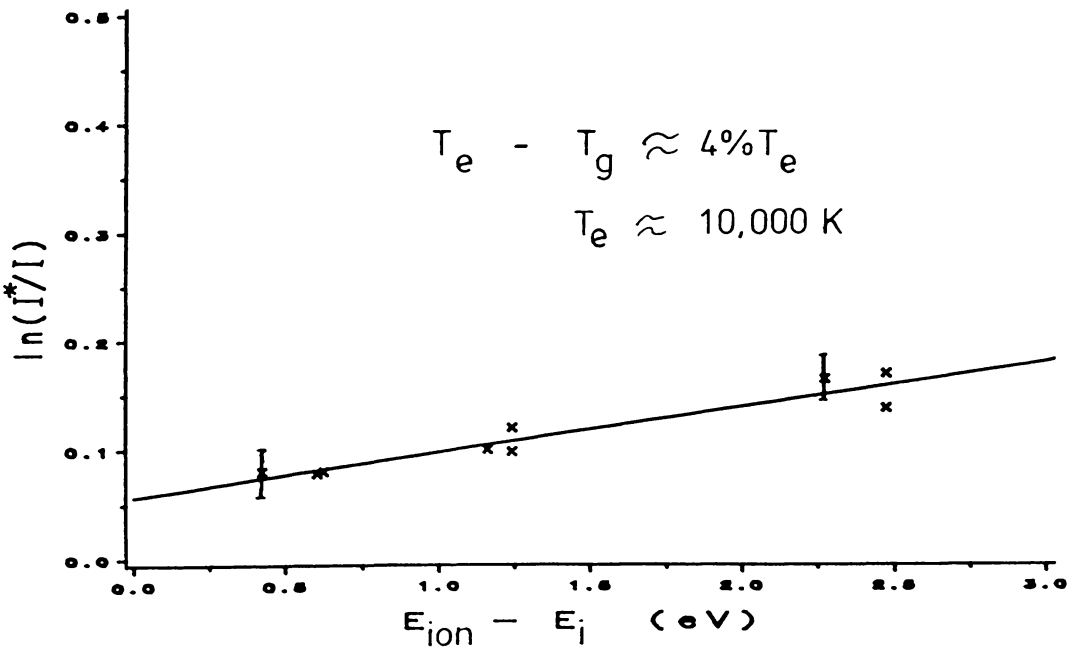

Figure 8.1(d): Intensity Ratio $\frac{I^*}{I}$ versus $E_{ion} - E_i$: 5mm radius.
Same operating parameters as Figure 8.1(a).

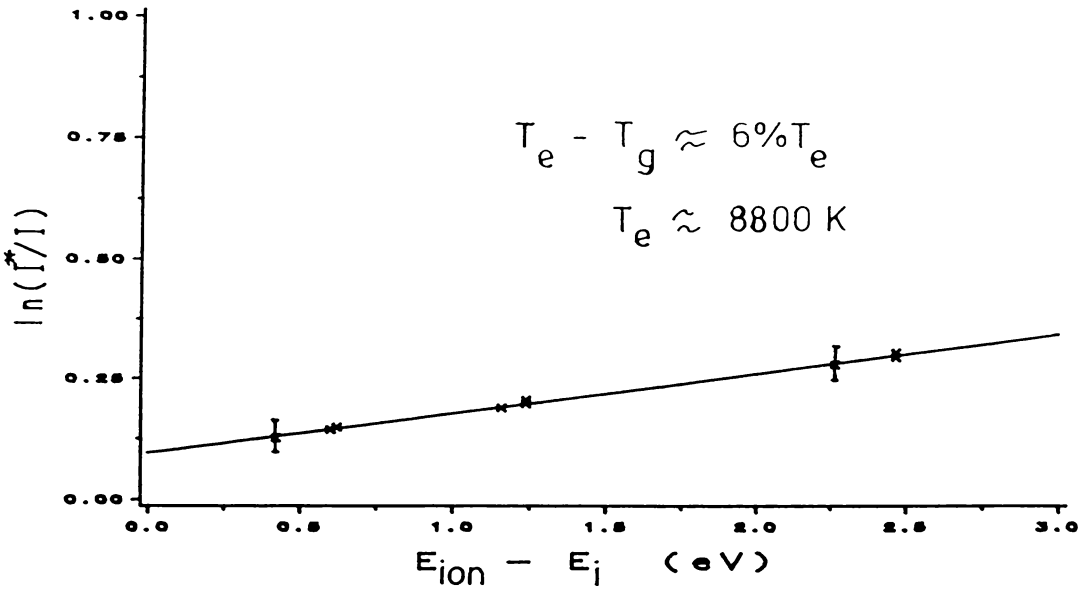

Figure 8.1(e): Intensity Ratio $\frac{I^*}{I}$ versus $E_{ion} - E_i$: 6mm radius.
Same operating parameters as Figure 8.1(a).

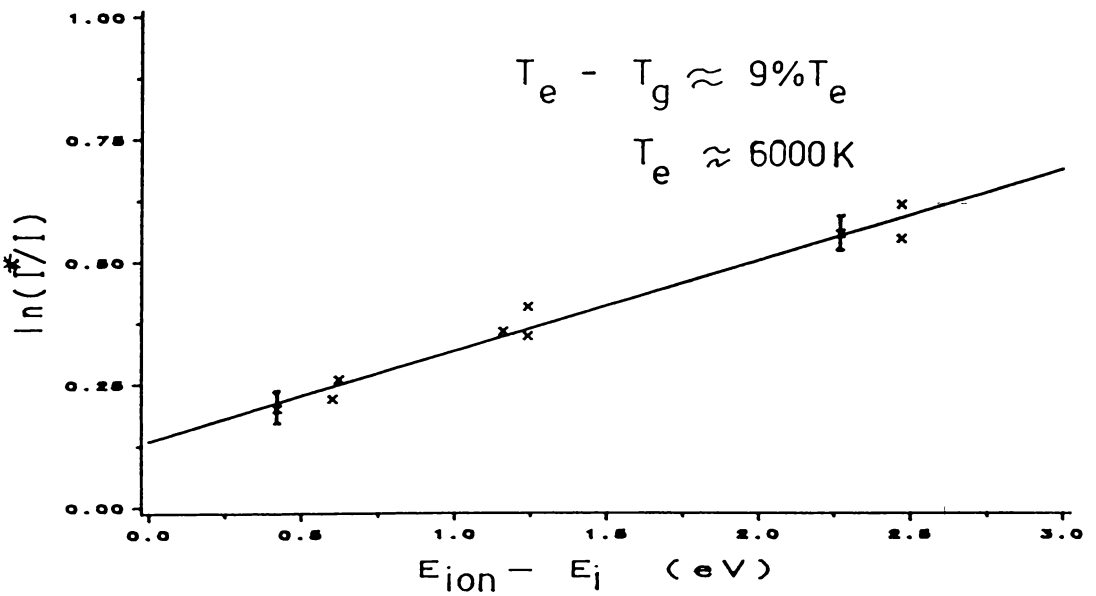

Figure 8.1(f): Intensity Ratio $\frac{I^*}{I}$ versus $E_{ion} - E_i$: 7mm radius.
Same operating parameters as Figure 8.1(a).

Plots of $\ln\frac{I^*}{I}$ versus $E_{ion} - E_i$ as the radius is increased from 3mm to 7mm (Figures 8.1(b) - 8.1(f)) show that there is a Boltzmann distribution among the excited argon states. From these, values for the temperature difference were determined which ranged (at a radius of 6mm) from approximately $30\%T_e$ 15mm below the work-coil (lateral results)[1] to approximately $6\%T_e$ 5mm above the work-coil (radial result). The distribution of the temperature difference $T_e - T_g$ is given in Figure 8.2.

Plots of the intensity ratios obtained in the outer regions of the plasma (radius > 7mm) showed a deviation from a Boltzmann distribution among the excited argon states (Figure 8.3). This is discussed further in section 8.7

Since the temperatures are equilibrated in the central region it was not possible to obtain a full radial determination of the electron temperature from equation 4.21 (i.e using the relaxation method). To circumvent this problem, measurements of the relative intensities of the spectral lines given in Table 8.1 were obtained with the ICPT operating in the steady-state mode. These results were converted to radial intensities and a Boltzmann's plot performed at half a millimetre steps through the plasma. These data points were curve-fitted using a least-square fitting computer program and from the slope of the graph the excitation temperature distribution was determined. These results together with those obtained using equation 4.21 are given in Figure 8.4. Due to the small energy differences between individual spectral lines used for the Boltzmann's plot and the small values of $E_{ion} - E_i$ in the case of equation 4.21 both sets of temperature measurements contain a large margin of error (> 1000 K). This error margin includes the additional uncertainties which arose from the need to scan the spectral lines sequentially and from the inaccuracies in the transition probabilities. The temperatures obtained by these two different methods are within error limits and are similar to those obtained elsewhere (see Chapter two). In addition the relaxation method gives the temperature difference which as a specific parameter is much less sensitive to error, than the measurement of the temperature. The variations in the temperature difference $T_e - T_g$ were less than 5% from repeated scans of the plasma.

8.2.3. Radiative Losses:Behaviour of the 811.5nm Argon Spectral Line

As shown in Chapter 6, the 811.5nm Ar I spectral line is optically saturated or nearly so in the ICPT under the current operating conditions. This provided a method

---

Due to the plasma being asymmetric it was not possible to obtain radial values at this observation height (see Chapter 7).

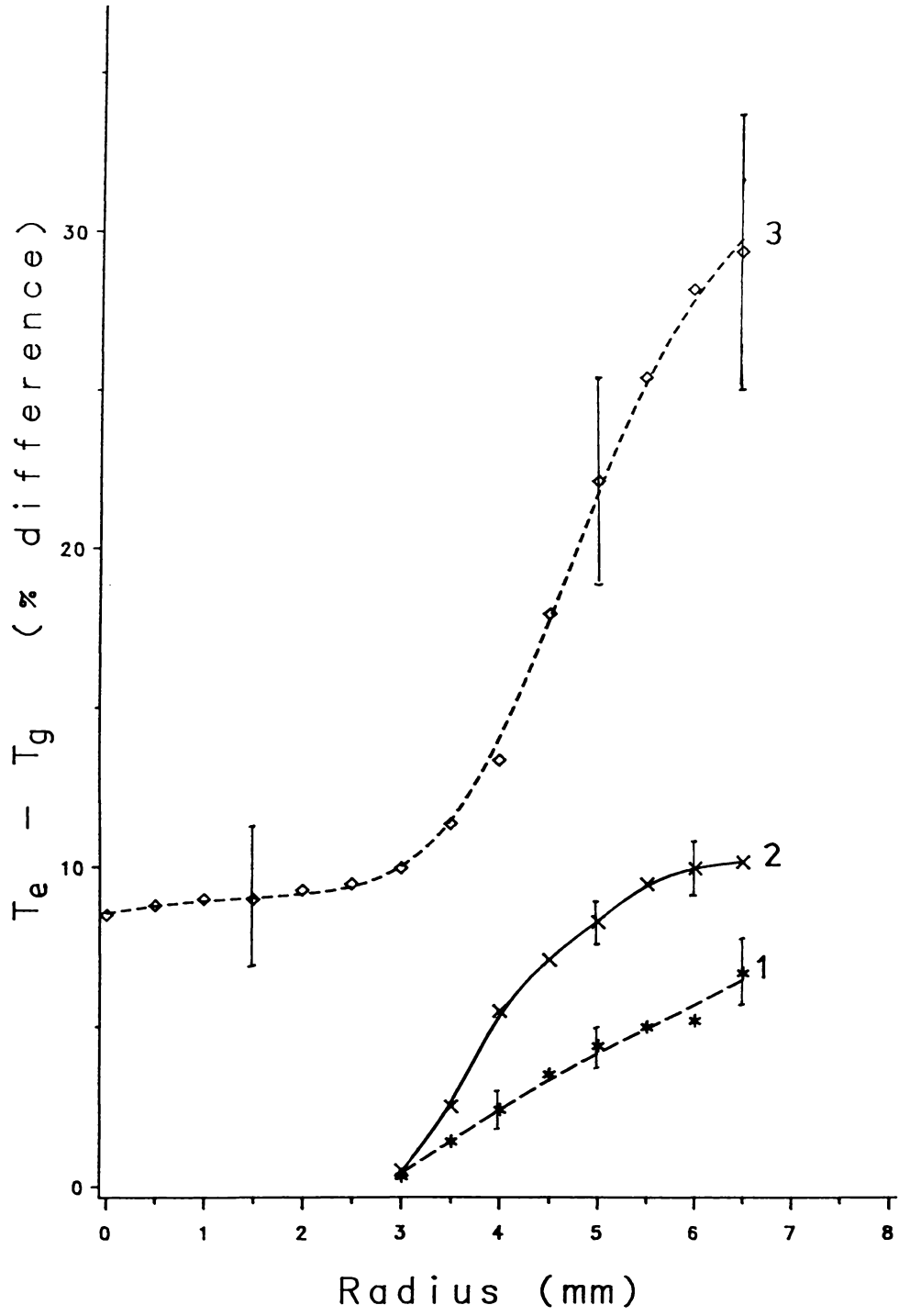

Figure 8.2: Distribution of the Temperature Difference $T_e - T_g$ in the ICPT; Coolant Flow Only.
Coolant flow-rate; 10l/min, Input power; 1.2kW.
Height; 1) 5mm above work-coil (radial).
2) 2.5mm above work-coil (radial).
3) 15mm below top of work coil (lateral).

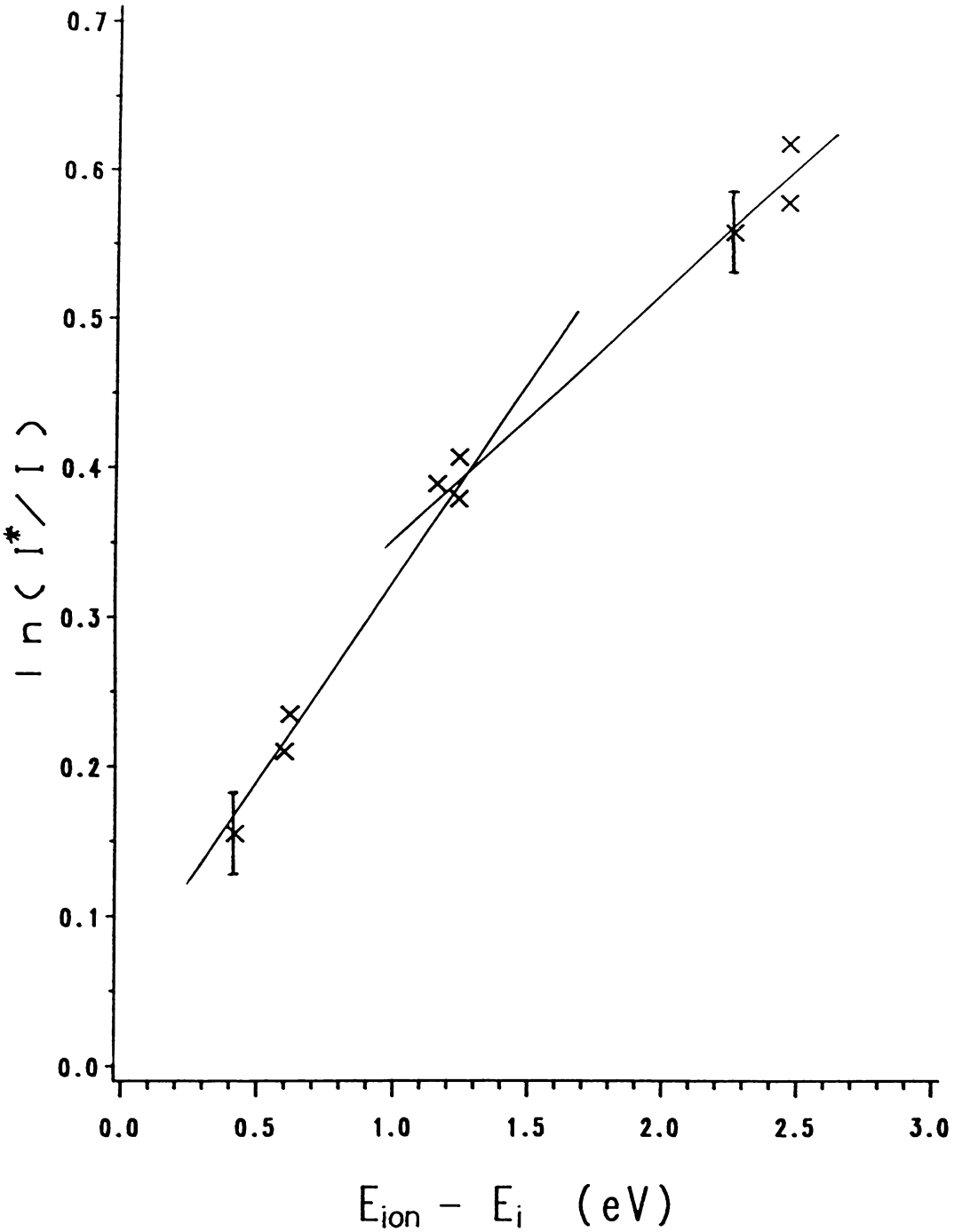

Figure 8.3: Deviation from a Boltzmann Distribution at the Edge of the Plasma.
Coolant flow-rate; 10l/min, Input power; 1.2kW.
Height; 5mm above work-coil.

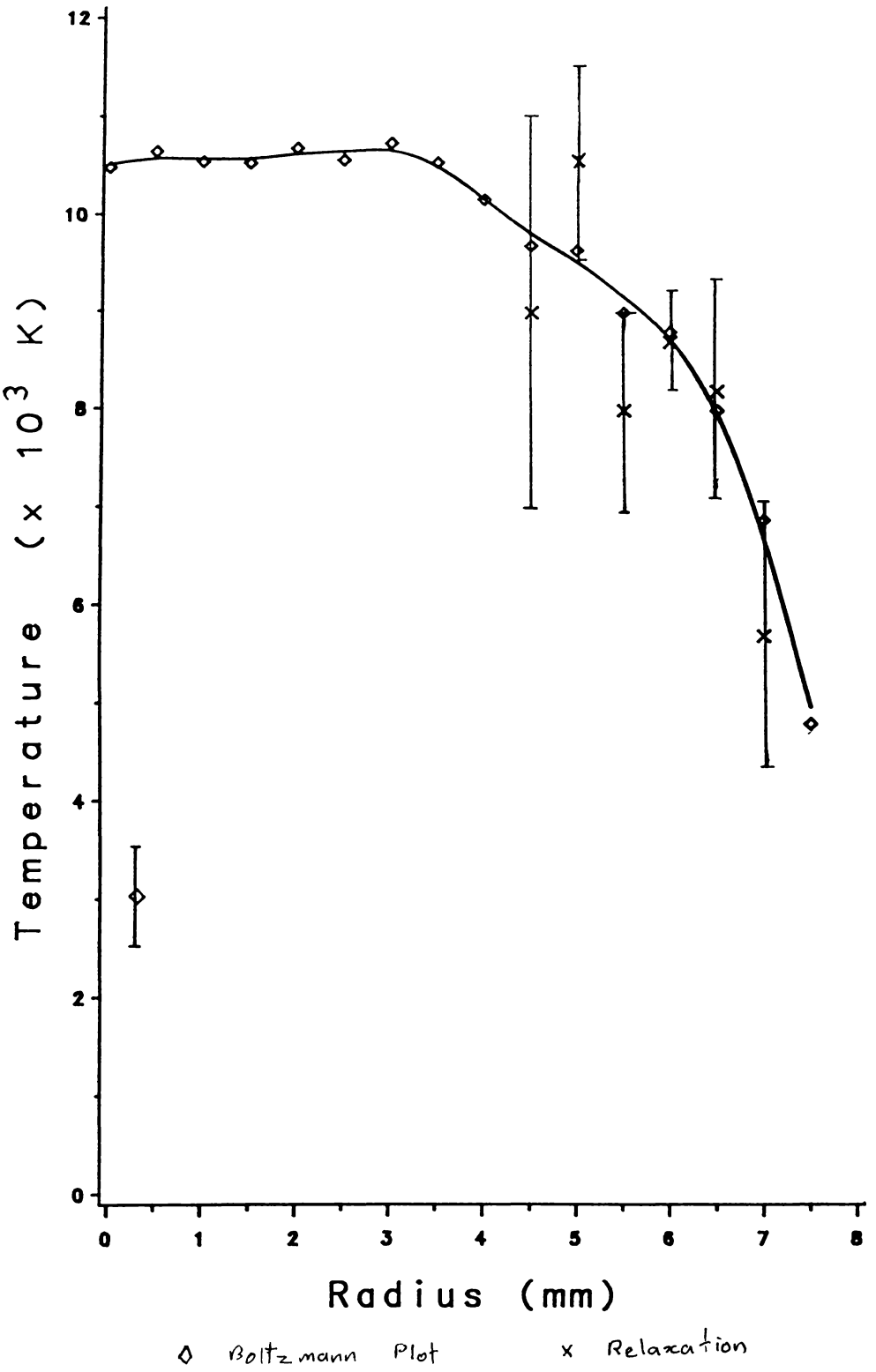

Figure 8.4: Temperature Distribution for the Coolant Only Plasma. Coolant flow-rate; 10l/min, Input power; 1.2kW. Height; 5mm above work-coil.

of observing qualitatively the effect that changing the operating parameters has on the radiative losses from the system as discussed in Chapter 3. The series of photographs (6.7 to 6.9) given previously, gave a comparison of the change in intensity when the RF field is removed between the 696.5nm and the 811.5nm argon I spectral lines at heights ranging from 15mm below the work-coil to 5mm above the work-coil and from the axis to the edge of the plasma (radius $\approx$ 7.5mm). The input power was 1200W, and the reflected power was maintained at less than 2W. These photographs indicated that the Argon 811.5nm spectral line is optically saturated up to height of approximately 5mm above the work-coil in the central region of the coolant-only plasma. While by comparison photograph 6.10 demonstrated that at the edges of the plasma (where the plasma is not in excitational equilibrium) the optical depth is insufficient and the spectral line is no longer saturated.

8.2.4. Blackbody Temperature

As was shown in Chapter 4, it is possible in principle to determine the blackbody temperature of the plasma from Planck's equation using the light intensity of a saturated spectral line. A measurement of the absolute intensity is required, necessitating the calibration of the optical system. The only available calibrated blackbody radiation source, a tungsten ribbon lamp, proved too feeble an emitter at the required wavelength, with the emitted intensity being less than a thousandth of the saturated spectral line intensity. This together with the reduced response of the photomultipler tube (R955) at wavelengths around 800 nanometres made an accurate intensity calibration impossible. Attempts to reduce the intensity emitted by the ICPT, by placing a beam-chopper in the optical path, were tried but proved unsatisfactory due to the extreme intensity differences. The degree of uncertainty arising from the use of an inadequate calibration source together with the possibility of errors arising from the measurement of radiation emitted from the boundary layers of the plasma made the determination of the blackbody temperature impractical. The availability of a suitable calibrated blackbody source such as a calibrated arc lamp together with end-on observations would overcome these problems.

8.2.5. Effects of the Variation of Input Power

Decreasing the power input to the plasma will decrease the local gradients of the various plasma parameters (for example temperature, density, conductivity) thereby increasing the diffusion time for any given particle, leading to a longer equilibration time. Therefore, it might be expected that lowering the input power would force the plasma closer to equilibrium.

With the RF generator operating in the continuous mode it was possible to maintain a plasma with an input power as low as 450 Watts. For pulsed operation, however, it was found that to repeatedly pulse the plasma over the time needed to complete a full lateral scan of the plasma required a minimum input power of 800 Watts. Below this power level the length of the off pulse could not be shortened sufficiently to prevent the plasma from occasionally failing to re-ignite. Over the power range used, 800 to 1200W, it was possible to maintain the plasma with a reflected power at less than 2W.

8.2.6. Variation of Temperature with Power

As in the previous section the temperature distribution was determined with the ICPT in the continuous mode from the Boltzmann plot of the excited argon spectral lines and the temperature difference using the relaxation method. The temperature decreased with decreasing power (Figure 8.5) from 10,500 K for an input power of 1200W, to $\approx$9000 K for input power of 800W in the central region of the plasma. And although the temperature difference $T_e - T_g$ was found to double from 6% to 12% of T_e at a radius of 6mm (Figures 8.6 and 8.7), this percentage difference between the plasma constituents is still relatively insignificant.

As the input power is decreased there is a reduction in the brightness of the plasma and a visible reduction in volume. However, the excited states still conform to a Boltzmann distribution and in the central region $\frac{I^*}{I}$ still approaches 1 although as the power was reduced this zone decreased in size. These changes and the slight increase in the temperature difference is probably due to the reduction in size of the plasma with the decrease in input power.

8.2.7. Radiative Losses

To investigate whether a decrease in input power affects the radiative losses from the plasma, the 811.5nm and 696.5nm spectral lines were monitored, at a height of 5mm above the work-coil as the input power was reduced from 1200W to 800W. While the intensity ratio of the 696.5nm line increased with decreasing power the spectral intensity of the 811.5nm line showed no evidence of an increase in intensity with the removal of the RF field until the power had been reduced to 900W (see photographs 8.1 to 8.4). Only at input powers below 900W is there a noticeable increase in the intensity of the 811.5nm line. With the reduction of input power there is an appreciable decrease in the size of the plasma. It is this size reduction that

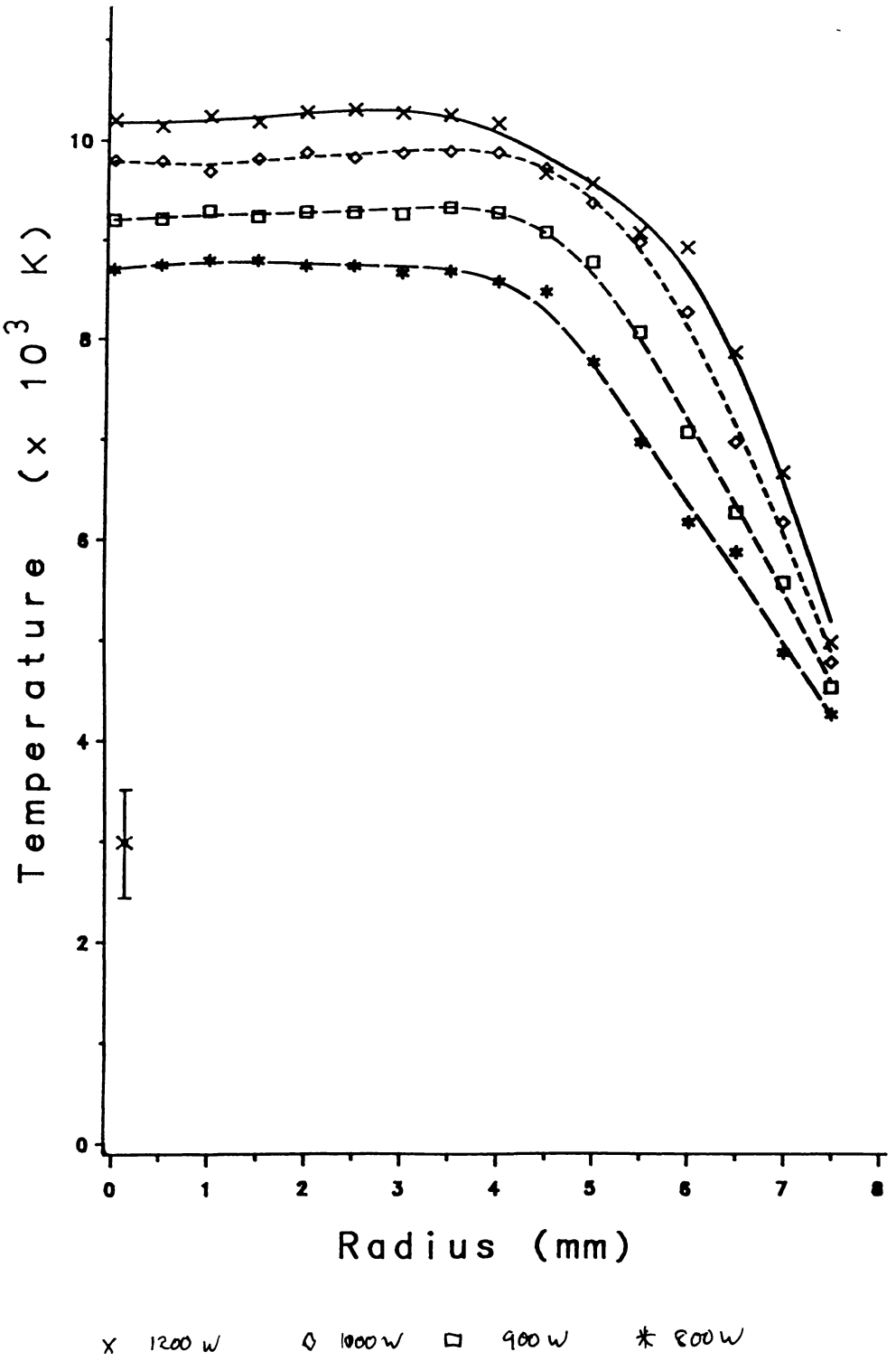

Figure 8.5: Variation of Temperature with Input Power.
Same parameters, other than input power, as Figure 8.4.

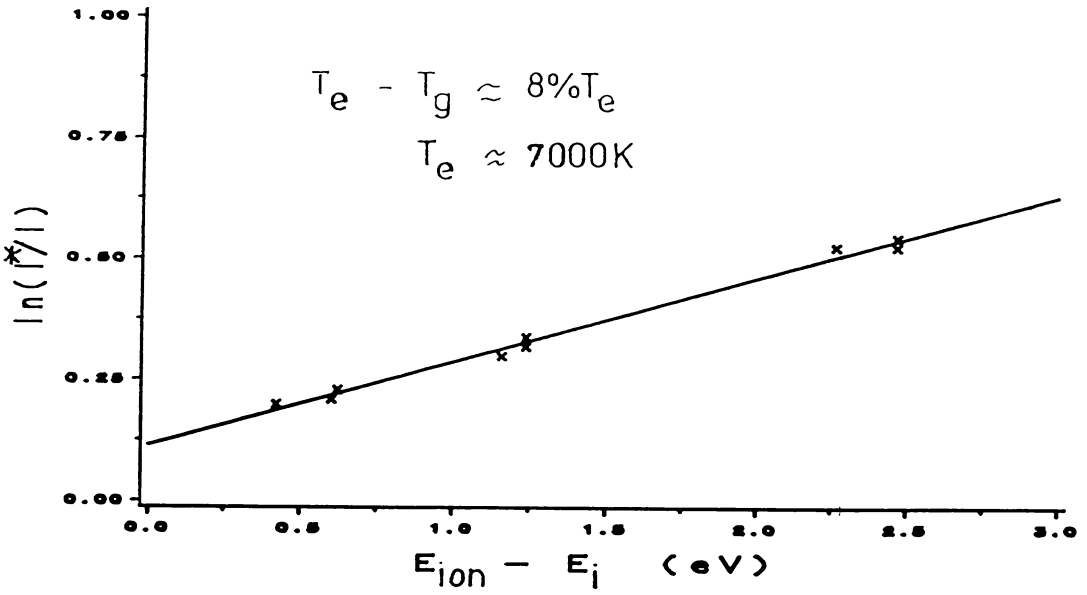

Figure 8.6: Temperature Difference $T_e - T_g$ at a Radius of 6mm; Input Power 1000 Watts.
Same parameters, other than input power, as Figure 8.1.

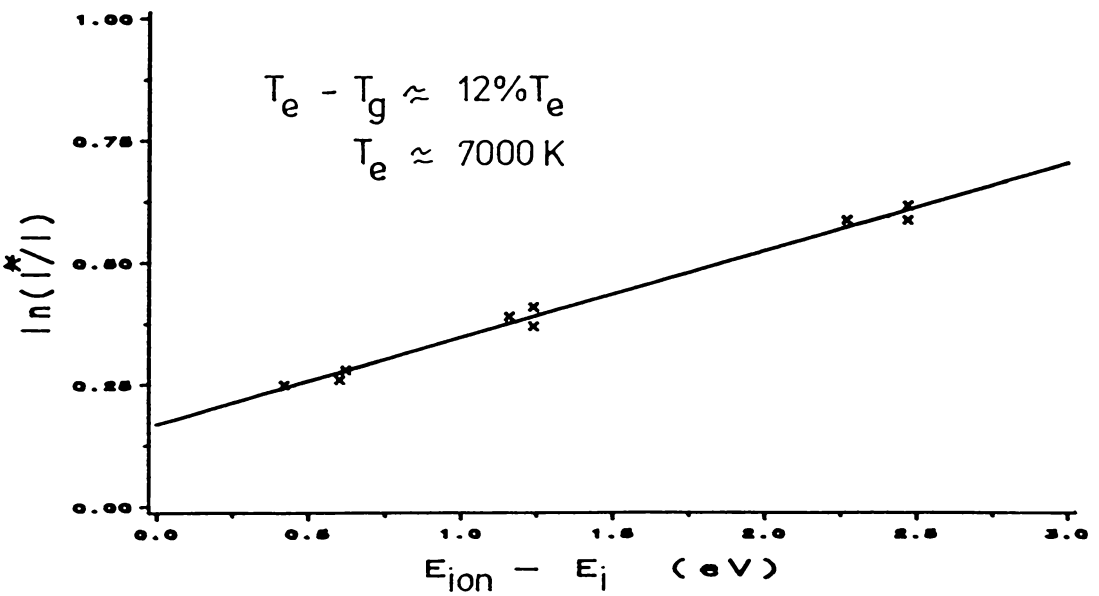

Figure 8.7: Temperature Difference $T_e - T_g$ at a Radius of 6mm; Input Power 800 Watts.
Same parameters, other than input power, as Figure 8.1.

reduces the optical depth of the plasma such that the 811.5nm line is no longer optically saturated below ≈ 900 Watts. These qualitative results indicate that decreasing the input power over the range of powers normally used in emission spectroscopy has a negligible effect on the radiative losses.

8.2.8. Conclusions

The results in this section demonstrates that the plasma produced in an ICPT with a single gas flow (coolant) is in at least pLTE in the central region ($r < 3mm$) and in excitational equilibrium out to a radius of $\approx$ 7mm, with a temperature difference $T_e - T_g$ ranging from $30\%T_e$ 15mm below the top of the work-coil to 6% 5mm above. A reduction in the input power, while decreasing the plasma temperature, does not effect the state of equilibrium prevailing in the plasma. The temperature difference $T_e - T_g$ was found to increase slightly but the excited argon states conformed to a Boltzmann distribution and the radiation of the 811.5nm spectral line is trapped in the region where the plasma is in excitational equilibrium. These results are in agreement with those obtained by Aspit (1971) for a 'physical' plasma.

8.3. Introduction of Aerosol Flow

8.3.1. Introduction

To utilise the ICPT as an emission source it is necessary to introduce a sample into the plasma. This is of course achieved by the introduction of an aerosol flow through the center of the plasma. This section investigates the effect of a flow of argon only (no sample) through the center of the plasma on the state of equilibrium. As mentioned previously a minimum flow-rate of 1 litre/minute is necessary to form a channel through the plasma however to ensure that a consistent supply of analyte, via the nebuliser, is introduced into the plasma a flow-rate of at least 2 litres/minute is required (Miller, 1978).

The introduction of the aerosol flow into the plasma resulted in a noticeable reduction in brightness of the plasma, with the aerosol channel being easily visible. Changes in the load characteristics required a minor re-adjustment to the tuning of the coupling circuit.

Using the same nine Argon I spectral lines as before the intensity ratios were obtained at a height of 5mm above the work-coil for a plasma having an input power of 1200W, with a coolant flow-rate of 10 litres/minute and aerosol flow-rates of one

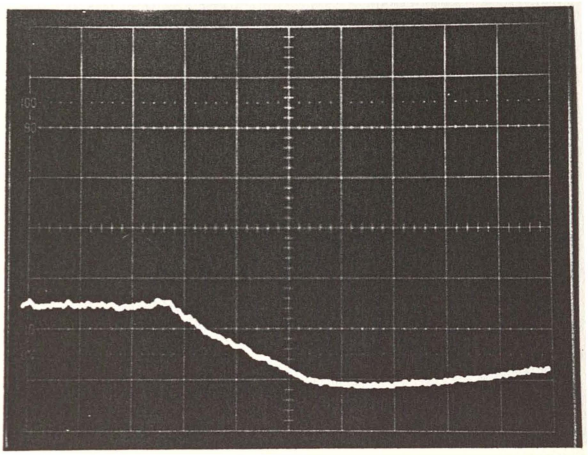

Photograph 8.1(a):Variation of Spectral Intensity with Input Power, Ar I 811.5nm Input Power 1100W.
Coolant flow-rate; 10l/min, Scale; 0.5V/div, 0.1ms/div.

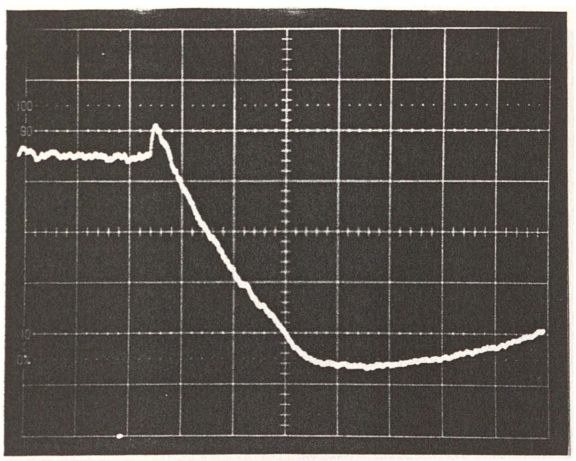

Photograph 8.1(b):Ar I 696.5nm Input Power 1100W.
Same parameters as Photo 8.1(a), Scale; 0.5V/div, 0.1ms/div.

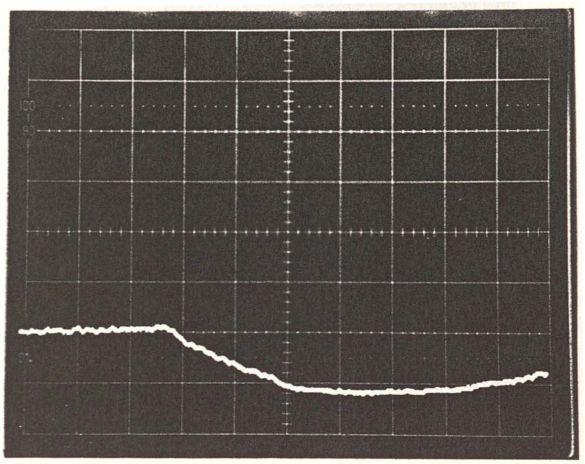

Photograph 8.2(a):Variation of Spectral Intensity with Input Power, Ar I 811.5nm Input Power 1000W.
Scale; 0.5V/div, 0.1ms/div.

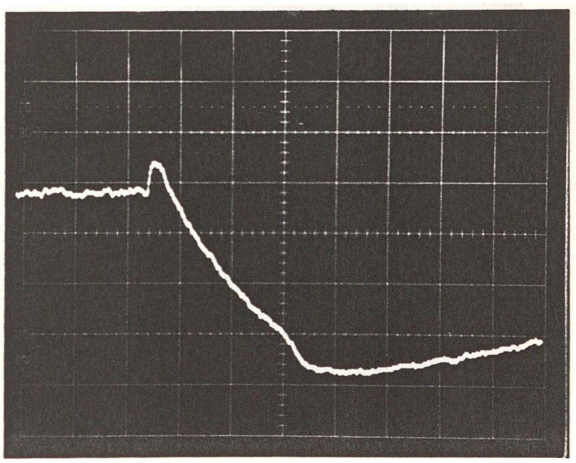

Photograph 8.2(b):Ar I 696.5nm Input Power 1000W.
Same parameters as Photograph 8.1 except Scale; 0.5V/div, 0.1ms/div.

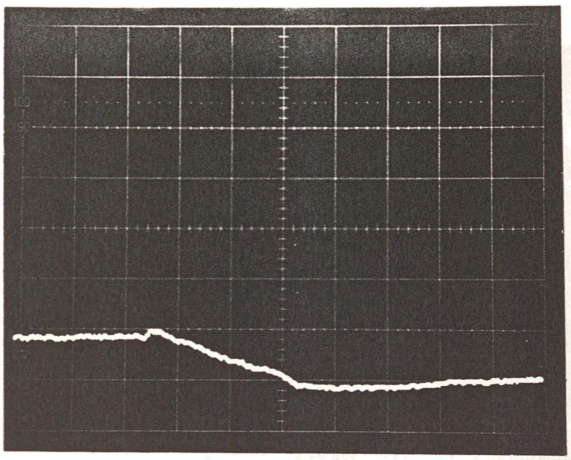

Photograph 8.3(a): Variation of Spectral Intensity with Input Power, Ar I 811.5nm Input Power 900W.
Scale; 0.5V/div, 0.1ms/div.

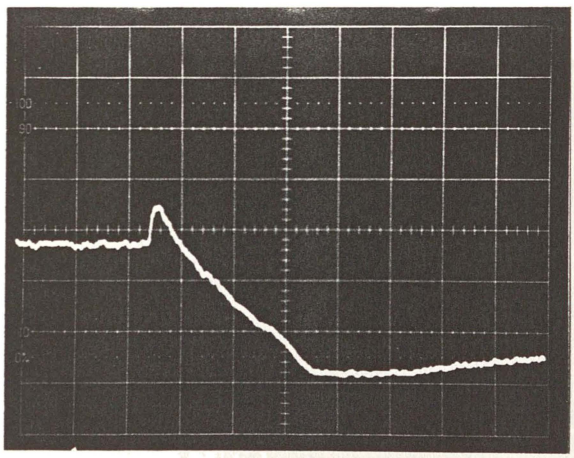

Photograph 8.3(b):Ar I 696.5nm Input Power 900W.
Same parameters as Photograph 8.1 except Scale; 0.5V/div, 0.1ms/div.

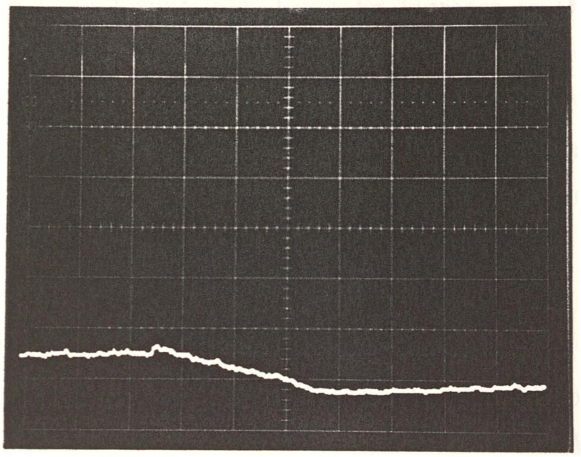

Photograph 8.4(a): Variation of Spectral Intensity with Input Power, Ar I 811.5nm Input Power 800W.
Scale; 0.5V/div, 0.1μs/div.

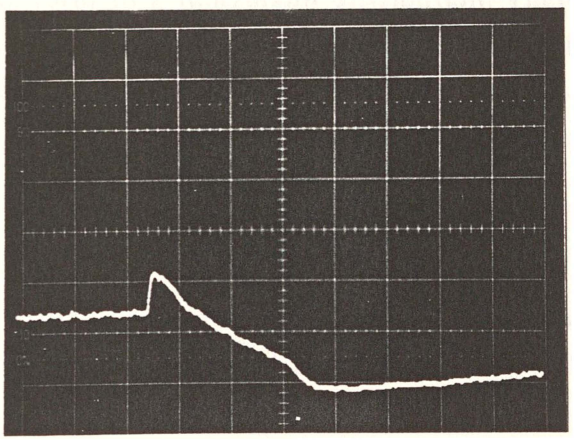

Photograph 8.4(b): Variation of Spectral Intensity with Input Power. Ar I 696.5nm. Input Power 800W.
Scale; 0.5V/div, 0.1ms/div.

and two litres/minute. As shown in section 7.3.3, with the decrease in intensity and corresponding increase in the margin of error made the acquisition of accurate results in the center of the plasma impossible. Even an increase in the lateral position data points to one hundred was insufficient with the present equipment to accurately resolve the very center of the plasma although this indicated that for a radius greater than 2mm the Abel's Transform yielded consistent results. Increasing the data points beyond this number was impractical under the present experimental arrangement.

8.3.2. Effects of the Introduction of an Aerosol Flow-rate

8.3.2.1. Aerosol Flow of One Litre per Minute

Repeating the experiments of section 8.2, with the addition of aerosol flow, the following results were obtained. With an input power of 1200W, a coolant flow of 10 litres/minute and at a height of 5mm above the work-coil, plots of $\ln(\frac{I^*}{I})$ versus $E_{ion} - E_c^*$ were performed which showed that at the edge of the plasma (7.0mm from axis) the behaviour of the excited states (Figure 8.8(a)) is similar to that obtained for the case of coolant flow only plasma (Figure 8.3) however, unlike this earlier case the excited argon states do not rapidly tend towards a Boltzmann distribution and then to $T_e = T_g$ as the center of the plasma is approached. These results are given in Figures 8.8(b) - 8.8(d) and show that the behaviour of the excited states is similar now to that prevailing at the edge of the plasma. Nowhere do the excited argon states conform to a Boltzmann distribution. There appears to be less of an increase for the lowest energy levels (4s - 4p transitions) than that required to yield a straight line. The results for the higher levels (4s - 5p and 4p -5d transitions) suggest that they are unaffected. To further study the effect of the aerosol flow the flow-rate was increased to that used for sample introduction.

8.3.2.2. Aerosol Flow of Two Litres per Minute

Maintaining the same experimental conditions as prevailing in the previous section the aerosol flow-rate was increased to 2 litres/minute. The results for this case are shown in Figures 8.9(a) to 8.9(f). At first inspection it appears that the linear relationship between $\ln(\frac{I^*}{I})$ and $(E_{ion} - E_c^*)$ has been re-established in certain regions of the plasma implying, at first glance, a Boltzmann distribution among the excited argon states with a temperature difference $T_e - T_g$ of approximately $10\%T_e$. However, a calculation of the electron temperature, from the slope of these graphs, yielded values exceeding 6×10^4 K, which is certainly not valid. Although the plasma is

obviously not in excitational equilibrium, as a comparison, it is useful to compare these temperature values with the radial temperature distribution as obtained from a Boltzmann plot of the relative intensities of the nine argon spectral lines measured in the continuous mode, all other operating conditions being identical, which are given in Figure 8.10. A comparison of the results shown in Figures 8.9 and 8.10 shows that only at large radii ($\approx$ 6mm) are the temperatures obtained consistent. Temperatures of the order of 6×10^4 and higher have not been previously reported for the ICPT (see Chapter 2). The increase in intensity of the spectral lines with the removal of the RF field is related to the difference in energy between the specific level and the ionisation energy. That different energy levels should increase to the same degree as shown in Figure 8.9(e) means that the respective excited states no longer conforms to a state of excitational equilibrium. These results suggest that the deviation has increased, affecting the the 5p levels in addition to the 4p already affected as shown in the previous section. The jump in intensity of the 4p - 5d levels has increased with respect to the 4s - 4p and the 4s - 5p transitions suggesting that the higher levels are still unaffected by the deviation from equilibrium and remain coupled to the continuum. As analytical operation of this particular ICPT required an aerosol flow of 2 litres/minute in the remaining experiments the aerosol flow was maintained at this level.

8.3.3. Variation of Input Power

The input power was reduced from 1200W in steps to 800W and the plasma which was cooled and maintained by a coolant flow of 10 litres/minute and an aerosol flow of 2 litres/minute was observed at a height of 5mm above the work-coil.

The following results were obtained.

The variation in the temperature distribution with the variation in input power was determined by the Boltzmann plot method under steady state conditions this is shown in Figure 8.11. This shows the typical annular shape of a ICPT plasma and the decrease in temperature and temperature gradients with decreasing power.

Radial intensities before and after pulsing off the RF field were obtained for input power levels of 1200 down to 800 Watts in 100 Watt steps. As for all other results in this thesis so far the reflected power was maintained at less than 2 Watts in each case. Using equation 4.21 cross-sections of the spectral intensity ratios at each power level were obtained.

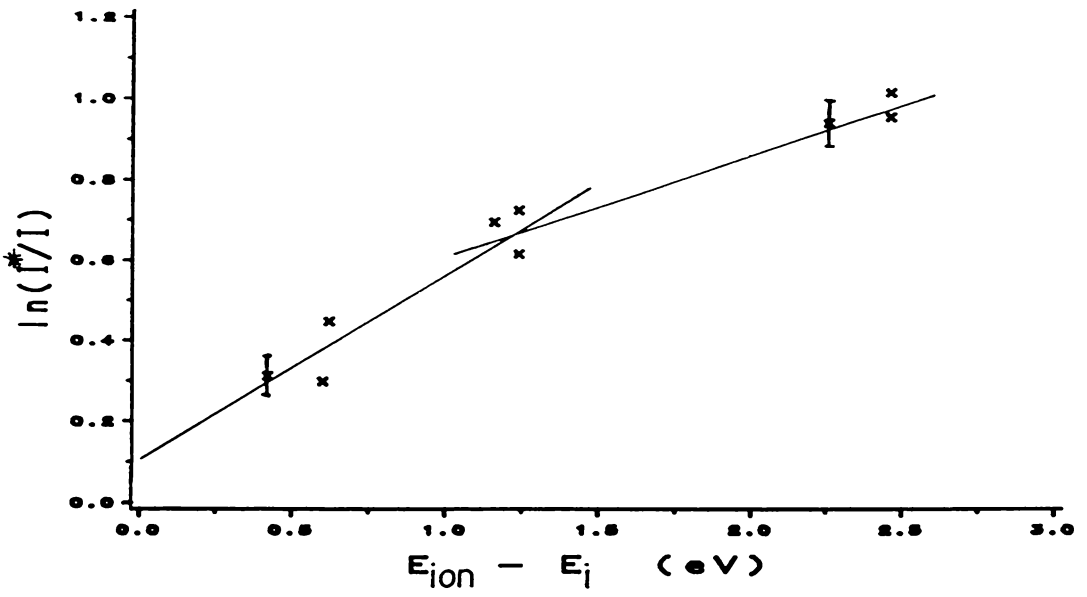

Figure 8.8(a): Intensity Ratio - Effect of Aerosol Flow; Edge of Plasma: Input Power; 1200W, Height; 5mm above coil, Coolant Flow; 10 l/min, Aerosol Flow; 1 l/min

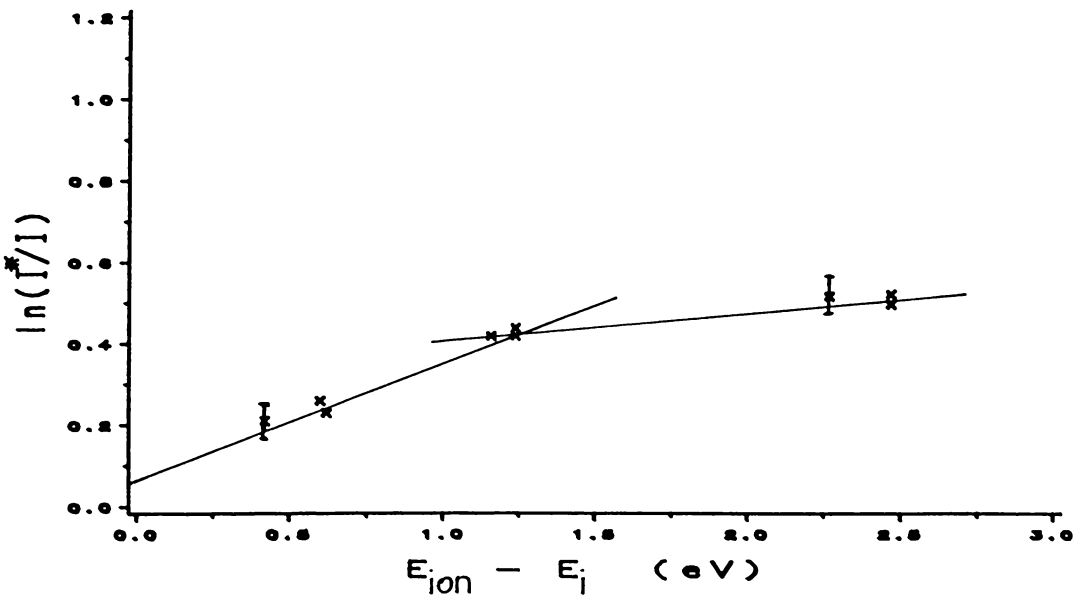

Figure 8.8(b): Intensity Ratio - Effect of Aerosol Flow; r = 6mm. Same parameters as Figure 8.8(a).

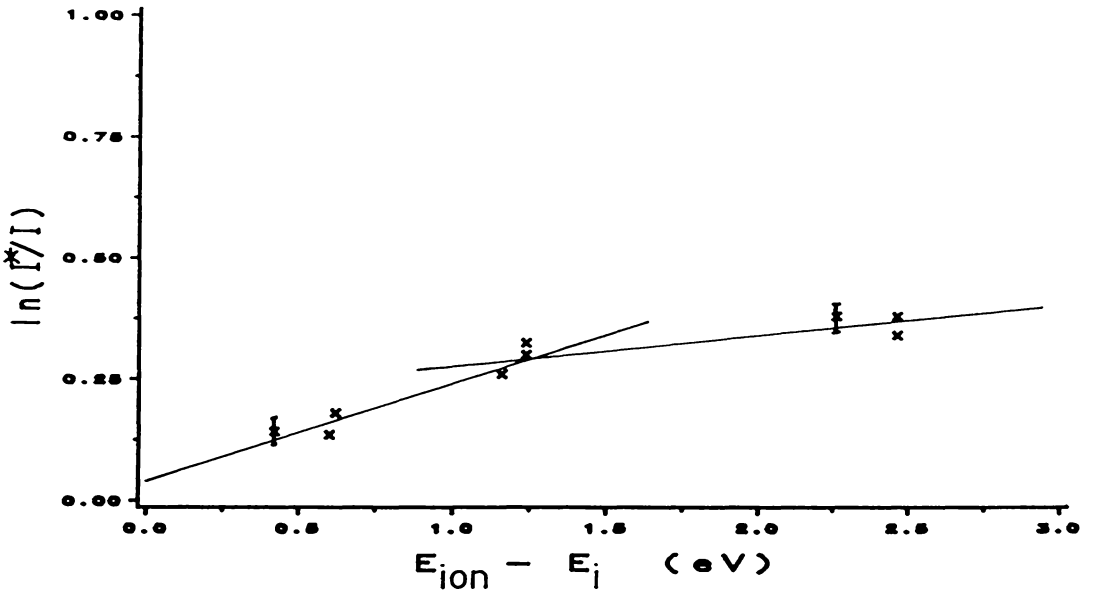

Figure 8.8(c): Intensity Ratio - Effect of Aerosol Flow; r = 5mm.
Same parameters as Figure 8.8(a).

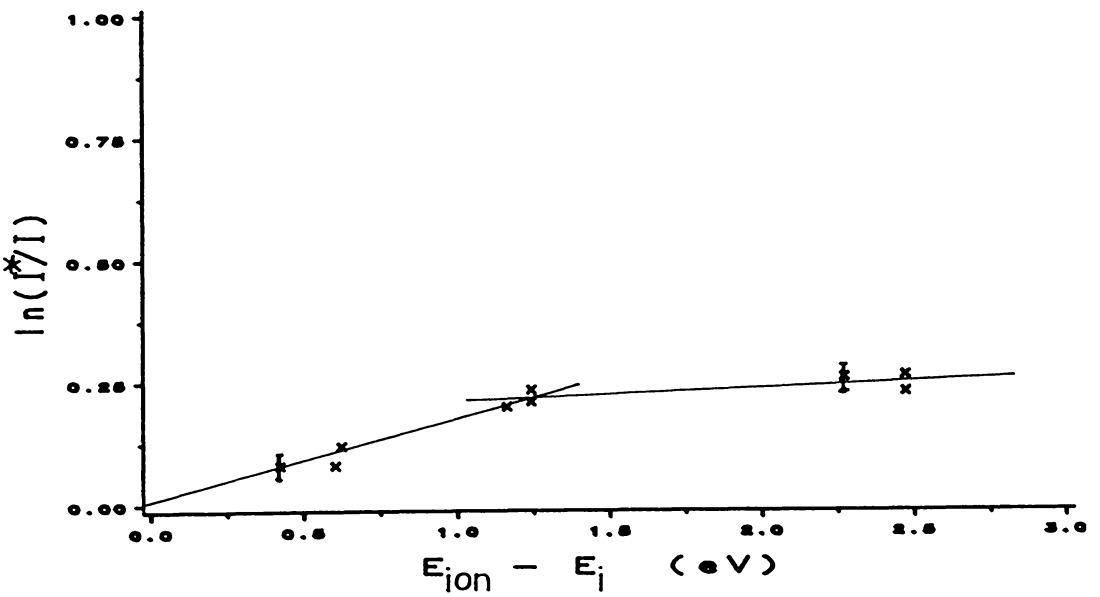

Figure 8.8(d): Intensity Ratio - Effect of Aerosol Flow; r = 4mm.
Same parameters as Figure 8.8(a).

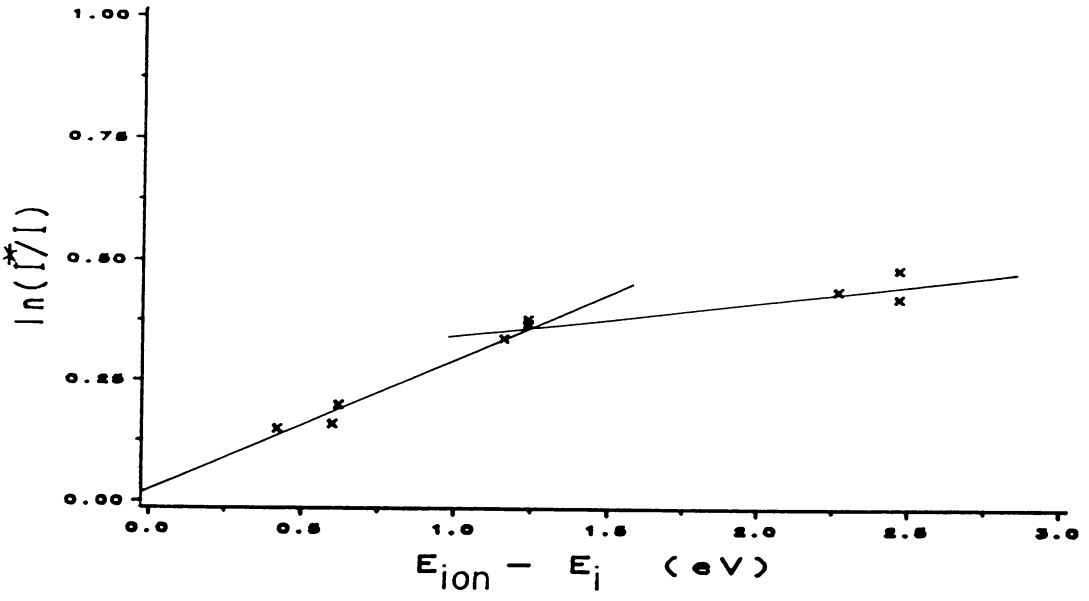

Figure 8.9(a): Intensity Ratio - Effect of Aerosol Flow 2 litres/minute; Edge of Plasma.
Same parameters as Figure 8.8(a).

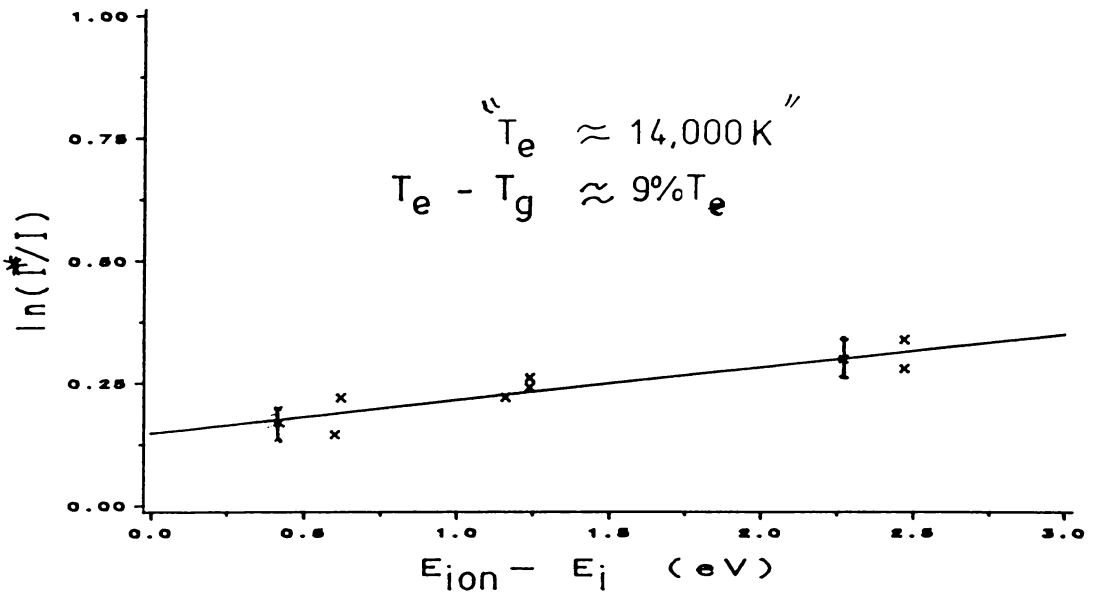

Figure 8.9(b): Intensity Ratio - Effect of Aerosol Flow 2 litres/minute; r = 6mm.
Same parameters as Figure 8.8(a).

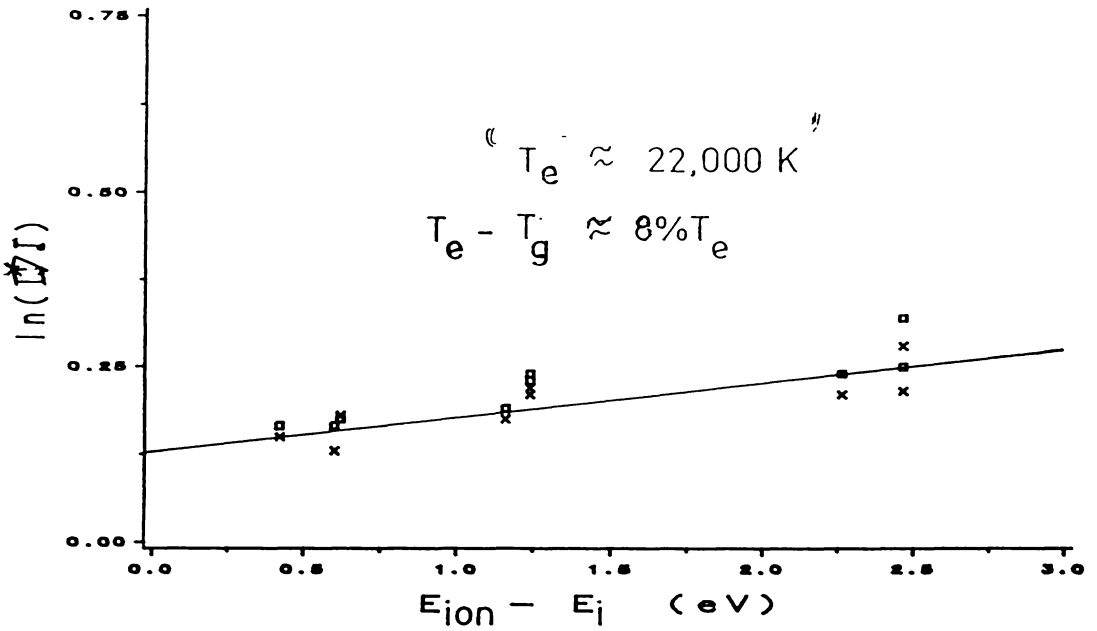

Figure 8.9(c): Intensity Ratio - Effect of Aerosol Flow 2 litres/minute; r = 5mm.
Same parameters as Figure 8.8(a).

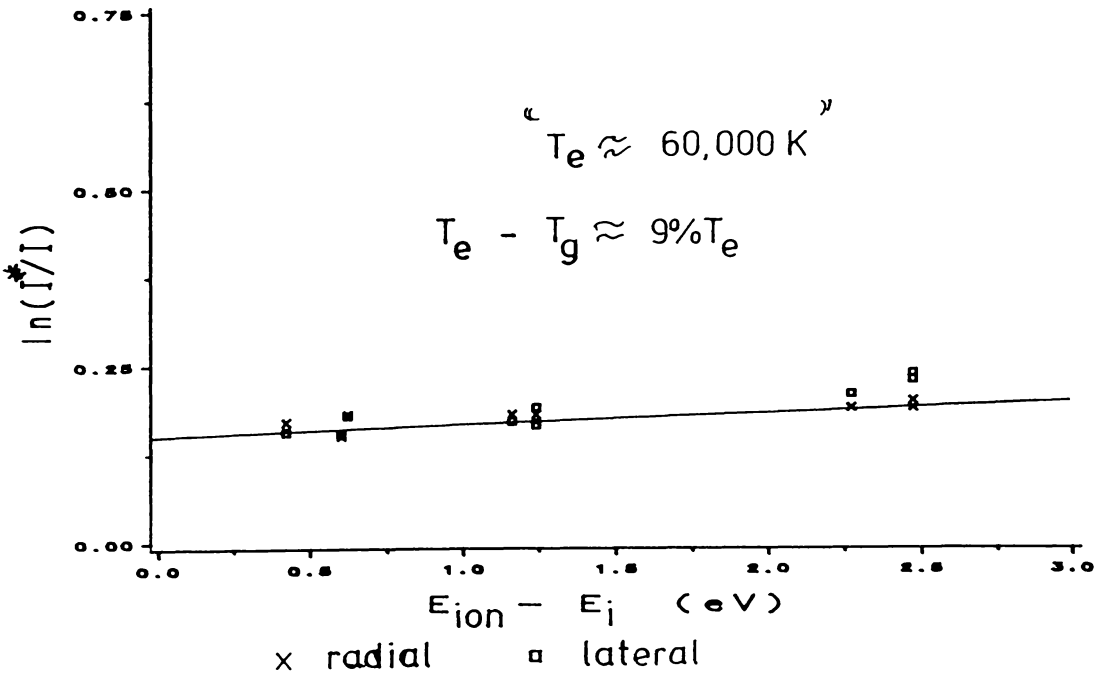

Figure 8.9(d): Intensity Ratio - Effect of Aerosol Flow 2 litres/minute; r = 4mm.
Same parameters as Figure 8.8(a).

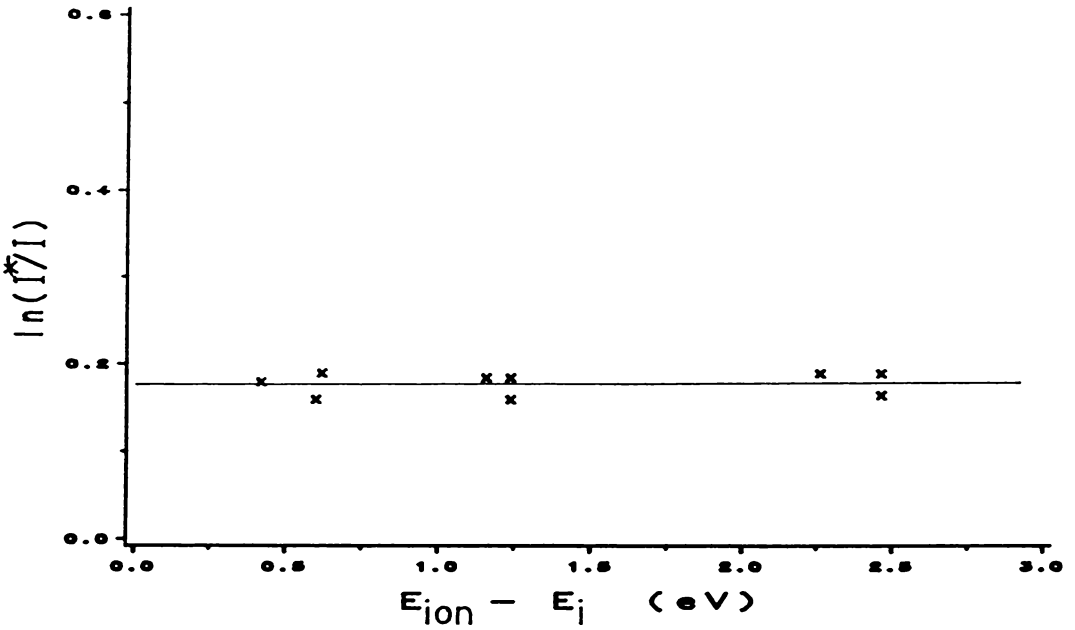

Figure 8.9(e): Intensity Ratio - Effect of Aerosol Flow 2 litres/minute; r = 3mm.
Same parameters as Figure 8.8(a).

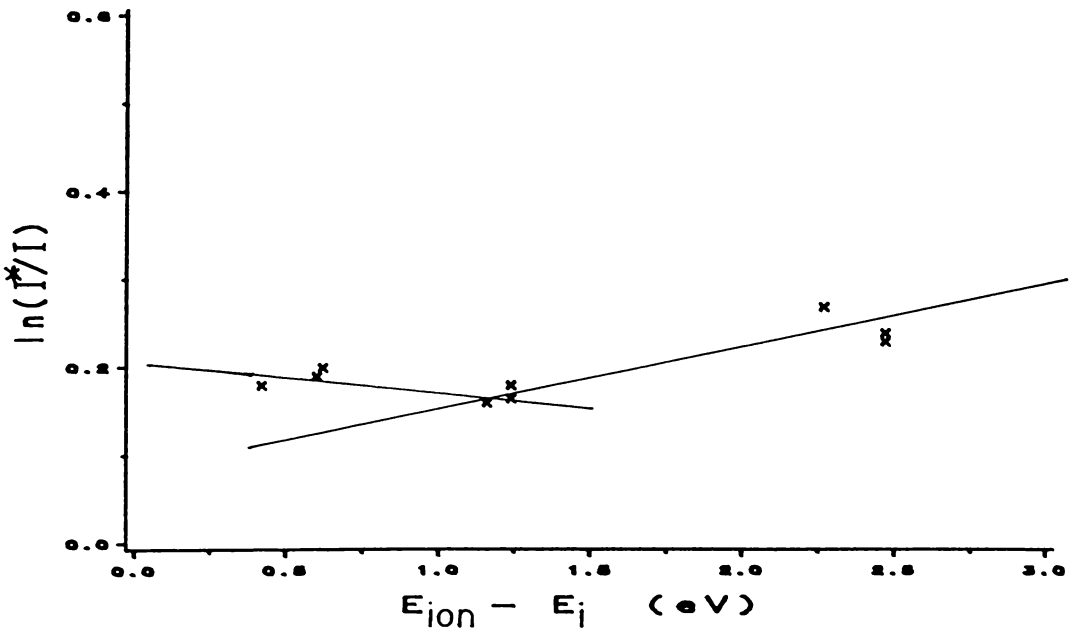

Figure 8.9(f): Intensity Ratio - Effect of Aerosol Flow 2 litres/minute; r = 2mm.
Same parameters as Figure 8.8(a).

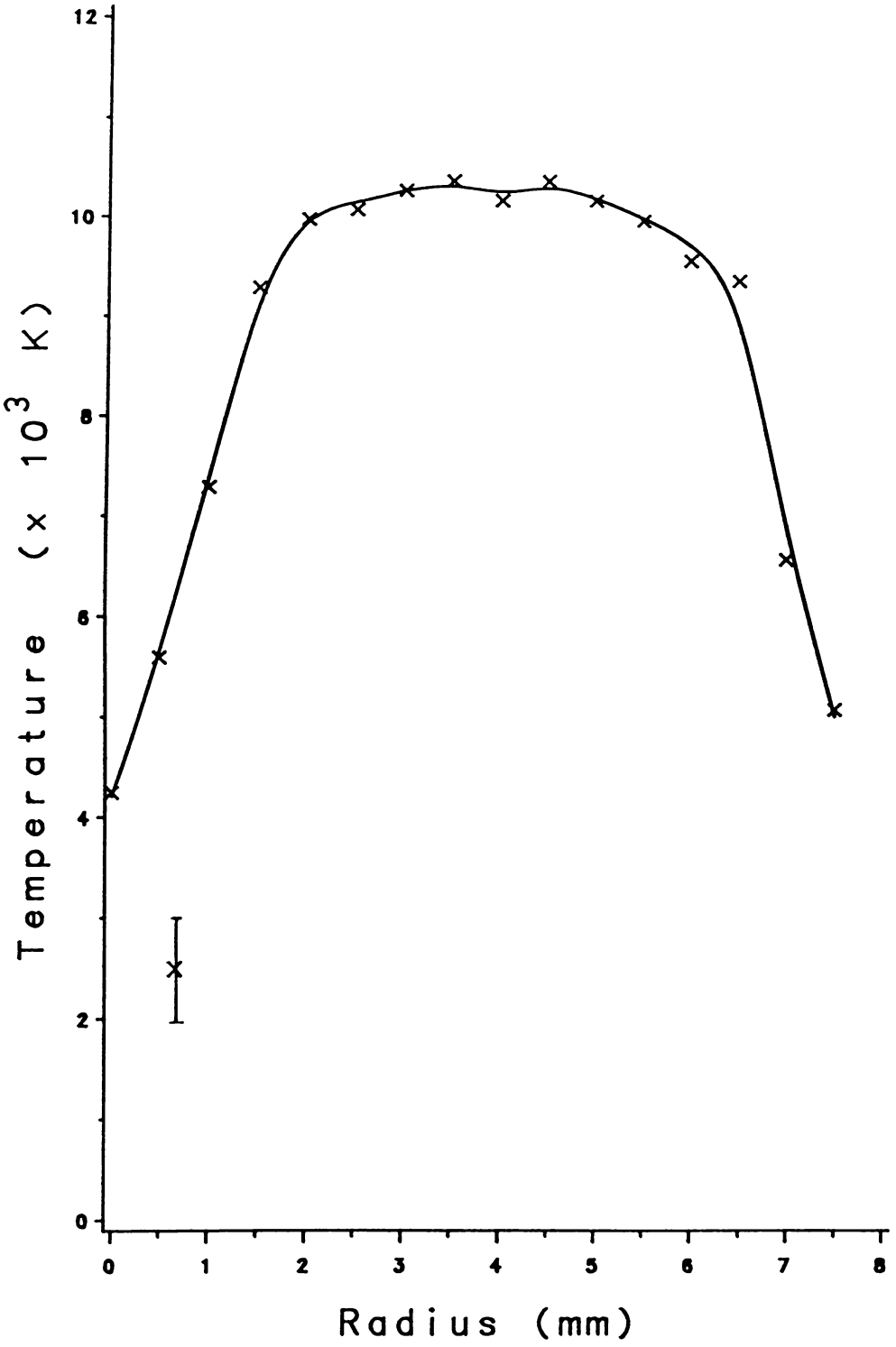

Figure 8.10: Radial Temperature Distribution with the Introduction of Aerosol Flow; 2 litres/minute.
Same parameters as Figure 8.8(a) except under steady state conditions.

The results for a input power of 1200 Watts is given in Figure 8.9(d) and assuming that the results are indicative of the presence of excitational equilibrium yielded a temperature difference $T_e - T_g$ of $\approx 10\%T_e$ but electron temperatures of greater than 6×10^4 K indicates that the Saha's equation is no longer valid under these circumstances.

In comparing the results for the temperature measurements for an input power of 1100 Watts with those obtained from the Boltzmann plot under steady state conditions, (Figure 8.11), it is evident that at this power level there is only one position where the ratio determined T_e derived from the linear plot of $\ln(\frac{I^*}{I})$ versus $E_{ion} - E_i$ is comparable. This is, at r = 6mm where the steady state temperature (T_{exc}) of 8900 K compares to the ratio method yielded an electron temperature of $\approx$ 9600 K, $T_e - T_g \approx 10\%T_e$. At smaller radii the values obtained for the temperature are as with the higher power input too high. At larger radii a linear plot is no longer possible.

With an input power of 1000 Watts, the area over which the electron temperatures derived from the ratio method that were consistent with those obtained from the steady state plasma increased. That is, the temperatures $T_e \approx 10{,}000\ K$, $T_e - T_g \approx 10\%T_e$, $T_{exc} \approx 8000\ K$ and $T_e \approx 7800\ K$, $T_e - T_g \approx 9\%T_e$, $T_{exc} \approx 8000\ K$ respectively at radii of 5mm and 6mm were in reasonable agreement.

Similar results were obtained at 900 Watts but with a slight increase in $T_e - T_g$ to $\approx 11\%T_e$.

At an input power level of 800 Watts (Figures 8.12(a) - 8.12(e)) a reasonable agreement between the two methods was obtained again only at radii of 5mm and 6mm. The results were ($T_e \approx 8100\ K$, $T_e - T_g \approx 12\%T_e$, $T_{exc} \approx 7800\ K$) and ($T_e \approx 6100\ K$, $T_e - T_g \approx 14\%T_e$, $T_{exc} \approx 6000\ K$). However the electron temperature determined for the radius of 4mm still does not agree satisfactorily ($T_e \approx 13{,}900\ K$, $T_e - T_g \approx 14\%T_e$, $T_{exc} \approx 8600\ K$).

The results given in this section show that decreasing the input power increases the temperature difference $T_e - T_g$ from approximately 9% to 14% of T_e but reduces the discrepancy over much of the cross-section of the plasma between the two different methods used to determine the value of the temperature.

8.3.4. The Effect on the Radiative Losses of the Introduction of an Aerosol Flow

The introduction of an aerosol flow through the center of the plasma was shown above to disturb the establishment of a Boltzmann distribution among the excited argon states. That the introduction of the aerosol flow through the center of the

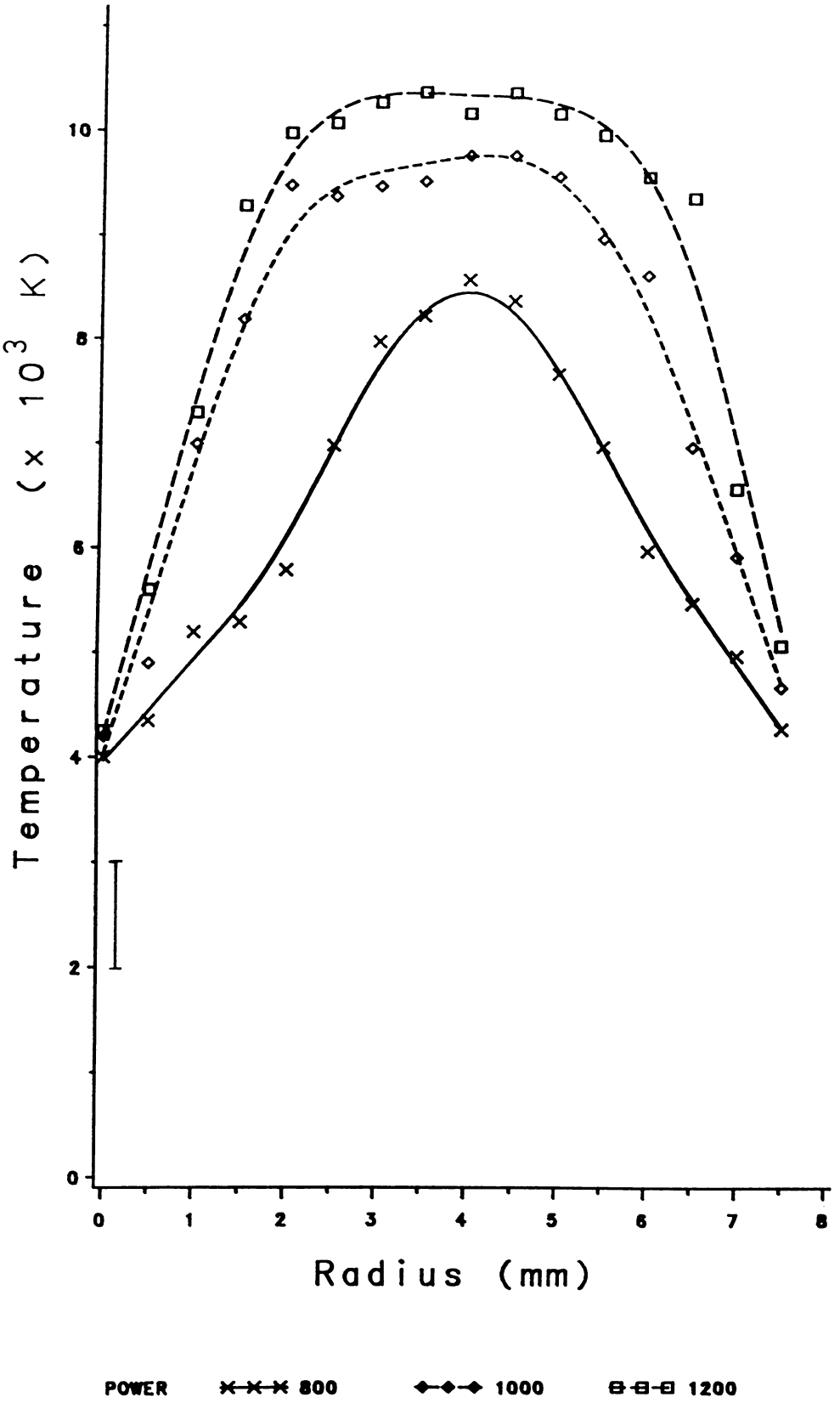

Figure 8.11: Variation in Radial Temperature Distribution due to Variation in Input Power, aerosol Flow-rate; 2 litres/minute.
Same parameters as Figure 8.8(a) except under steady state conditions.

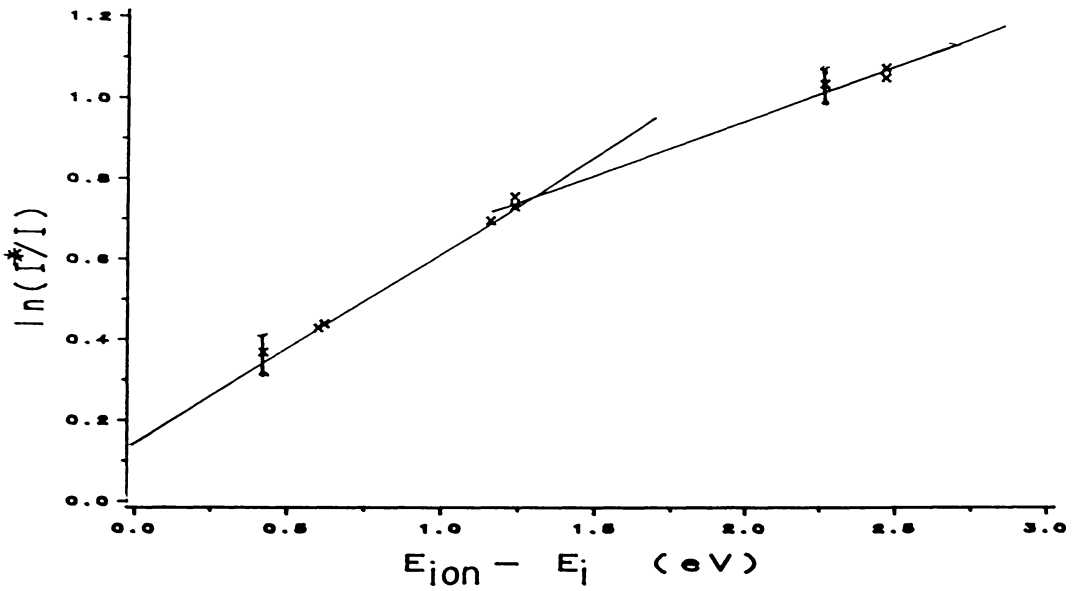

Figure 8.12(a): Intensity Ratio - Effect of Input Power on the State of Equilibrium; 800 Watts: Edge of Plasma.
Coolant Flow-rate; 10l/min, Aerosol Flow-rate; 2l/min, Height; 5mm above coil, Slit-width; 100μm.

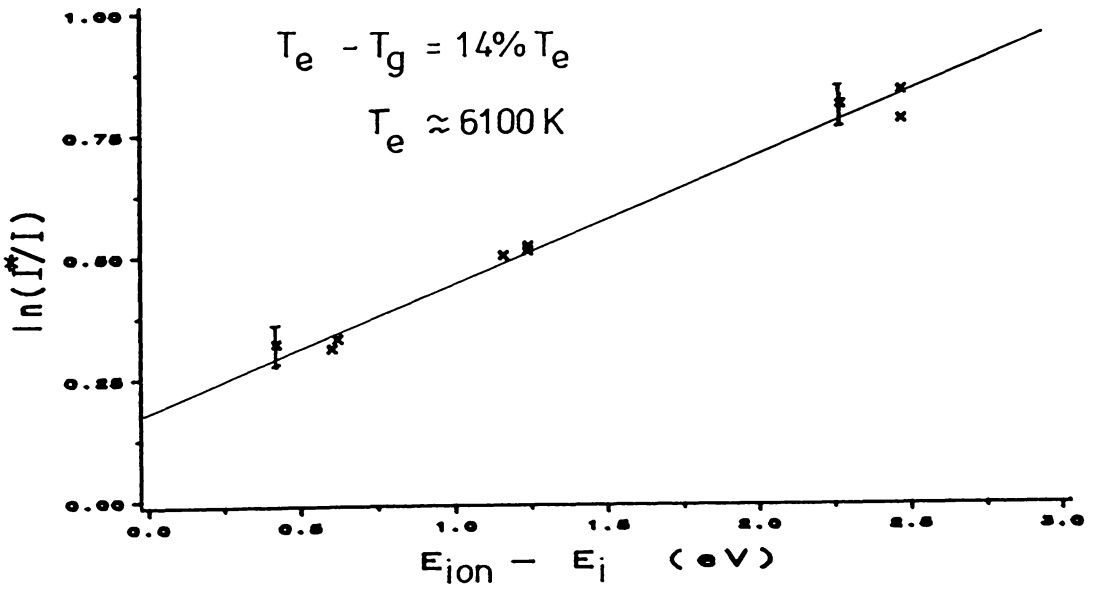

Figure 8.12(b): Intensity Ratio - 800 Watts, radius 6mm.
Same parameters as Figure 8.12(a).

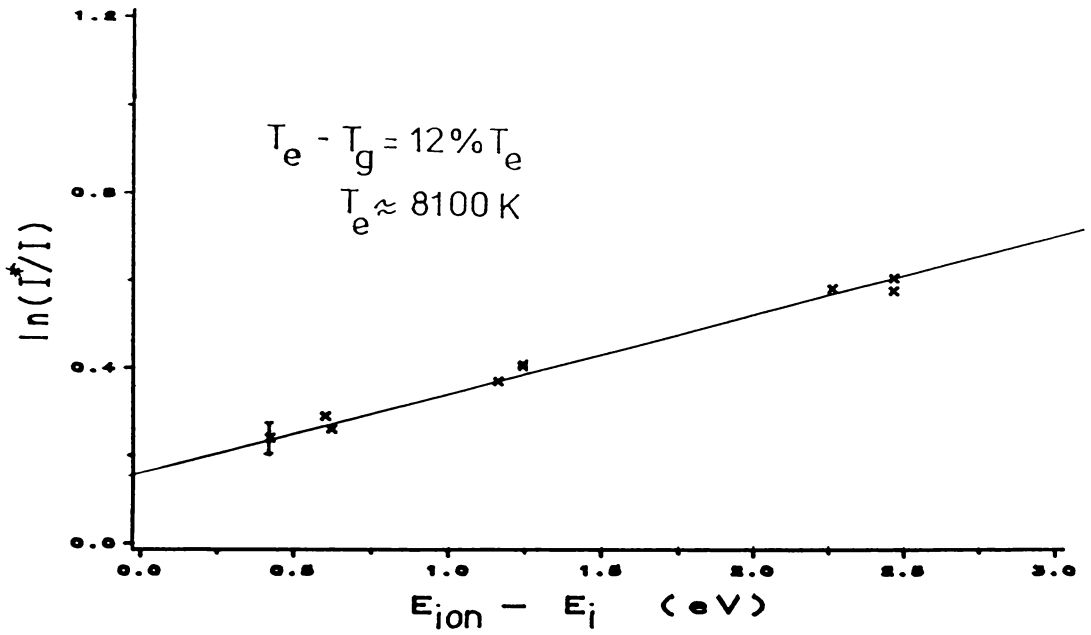

Figure 8.12(c): Intensity Ratio - 800 Watts radius 5mm.
Same parameters as Figure 8.12(a).

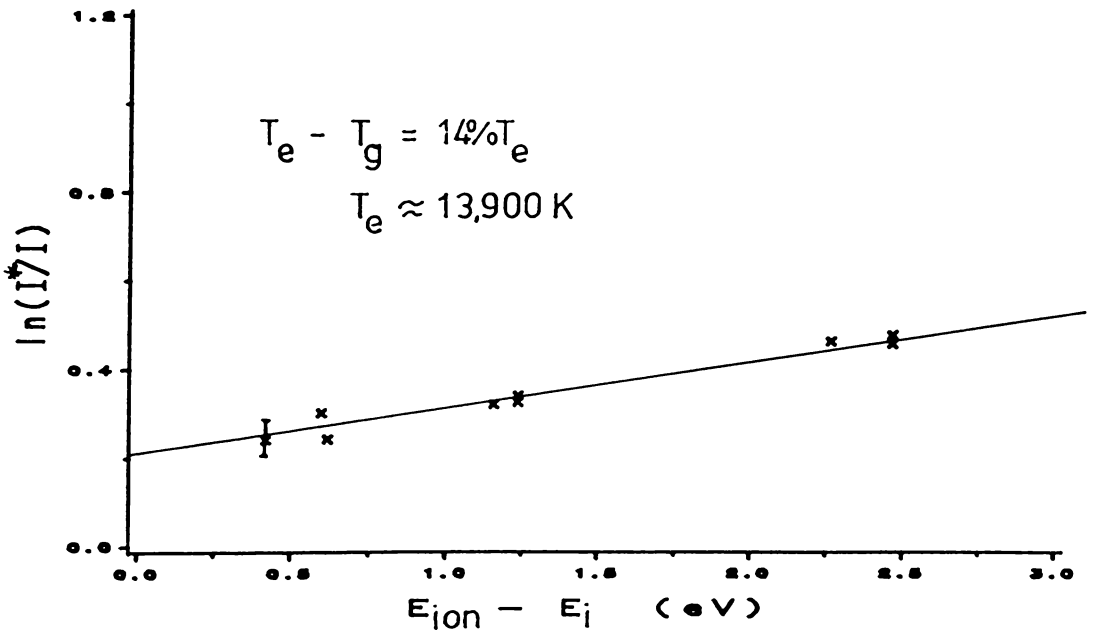

Figure 8.12(d): Intensity Ratio - 800 Watts radius 4mm.
Same parameters as Figure 8.12(a).

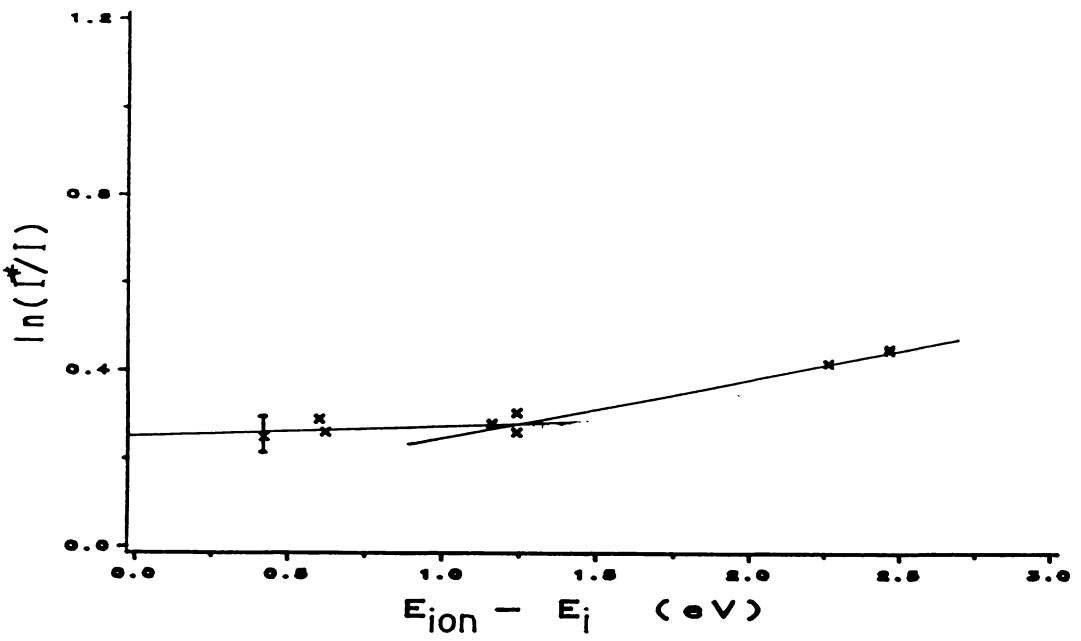

Figure 8.12(e): Intensity Ratio - 800 Watts radius 3mm.
Same parameters as Figure 8.12(a).

plasma is the major cause of the deviations from equilibrium present in the ICPT is further supported by the changes that occur in the behaviour of the 811.5nm argon I spectral line.

Photographs 8.5 to 8.9 illustrates the change in behaviour of the 811.5nm spectral line that occurs with the introduction of an aerosol flow through the center of the plasma as compared to a plasma formed from a coolant flow only (see photographs 6.7 - 6.9). Only in the middle of the work-coil does the spectral line appear to approach saturation. However, as Figure 8.13 shows, the 811.5 argon I spectral line can still not be considered to be optically thin in the region under study. By comparison however, with the results for the single flow (coolant) plasma where the 811.5nm line was shown to be saturated up to 5mm above the work-coil, these results indicate that the radiative losses have been increased with the introduction of the aerosol flow.

8.3.5. Conclusions

The results in this section indicate that the introduction of aerosol flow through the center of the plasma is a major cause of a deviation from excitational equilibrium in the ICPT. The smaller than expected increases in intensity of the 4s - 5p and 4s - 4p

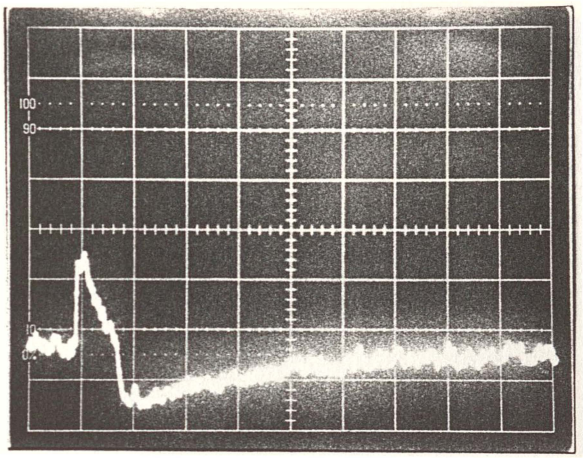

Photograph 8.5: Intensity Jump of the 811.5nm Ar Spectral line, Aerosol Flow 2 litres/minute, 15mm below coil.
Coolant flow-rate; 10l/min, Input power; 1200W, Scale; 0.2V/div, 0.2ms/div; PMT volts; 700V.

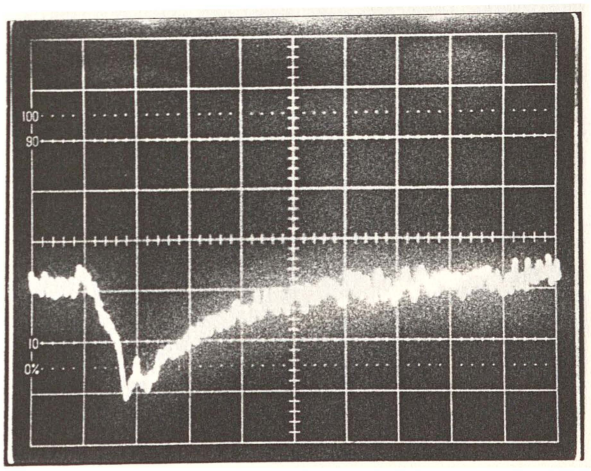

Photograph 8.6: Middle of Work-coil.
Same parameters as Photograph 8.5.

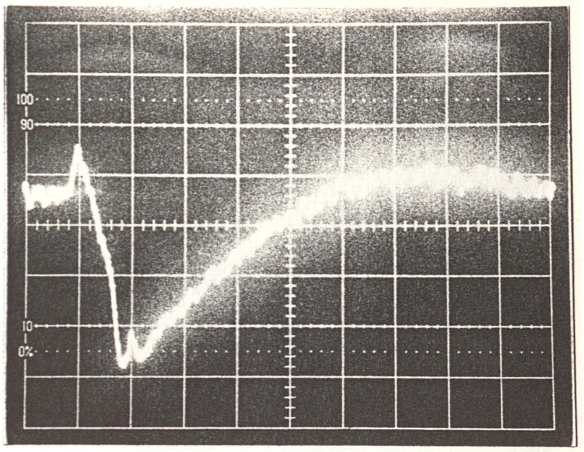

Photograph 8.7: 2.5mm above Work-coil.
Scale; 0.5V/div otherwise as Photograph 8.11.

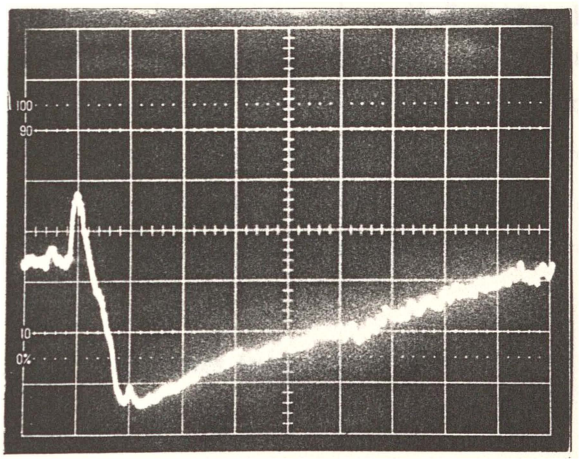

Photograph 8.8: 5mm above the Work-coil.
Same as Photograph 8.7.

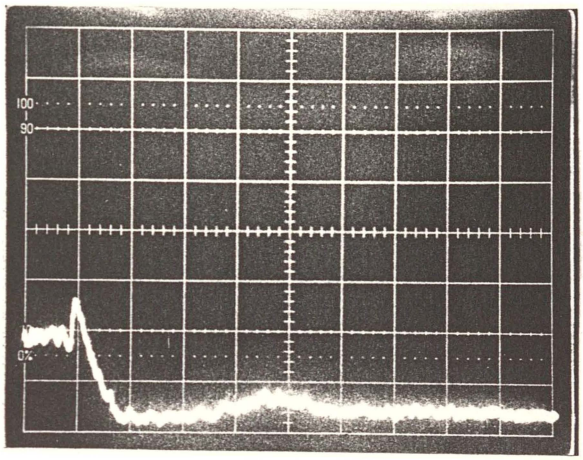

Photograph 8.9: 10mm above Work-coil.
Scale; 0.1V/div otherwise as Photograph 8.7.

transitions upon the removal of the RF field together with the increase in radiative loss of the near-infrared 4s - 4p being the result.

Temperatures obtained by means of a Boltzmann plot, under steady-state conditions, being less sensitive to deviations from excitational equilibrium than the intensity ratio method, yielded values typical of those obtained elsewhere (see Chapter 2). While these results provided a means of comparing the temperatures obtained by the two methods it also highlights the fact that temperature distributions for the ICPT obtained from Boltzmann plots of excited argon spectral lines must be regarded with suspicion.

8.4. The Introduction of Molecules into the Plasma

8.4.1. Introduction

For the ICPT to be used as a emission light source requires the introduction of molecular compounds in the form of gases or liquids carried by the aerosol flow. All of the experiments described up to now have involved plasma consisting of argon only. The introduction of molecular additives provides several possible additional

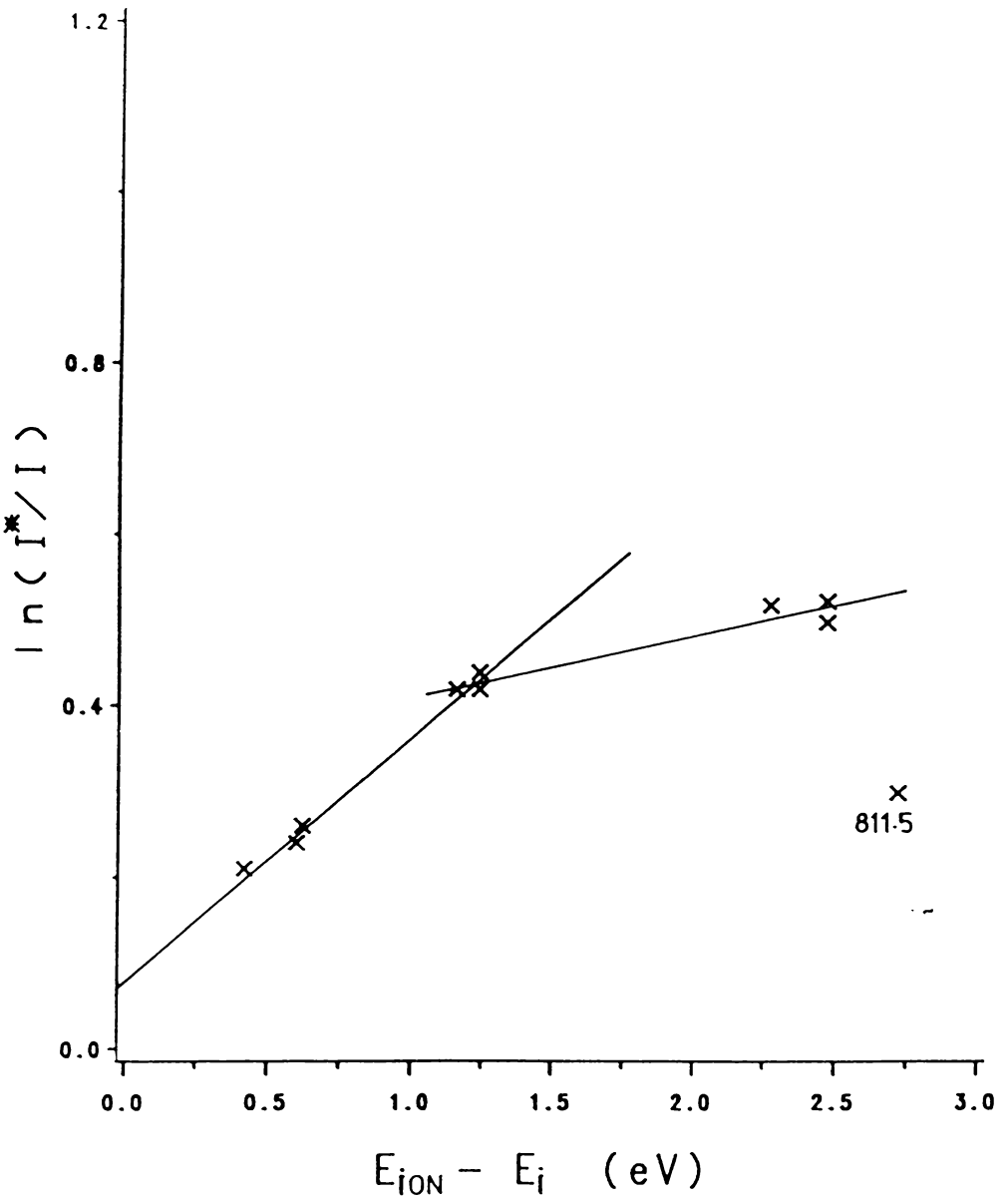

Figure 8.13: Comparison of the 811.5nm Argon Spectral Line with Optically Thin Argon I Spectral Lines.
Radius = 5mm.

means of energy exchange in the ICPT, from being solely by elastic collisions, to a system involving energy exchange via rotational and vibrational states, the exchange of excitation energies and the development of molecular ionisation and recombination. The presence of these alternative energy processes could be expected to facilitate the approach to equilibrium, and it is appropriate to study the effect of such substances on the plasma.

To investigate the effect of the introduction of molecules on the state of equilibrium four different molecules or combination of molecules were introduced; H_2, Air, H_2O and KCL in H_2O. The first two were studied by the introducing the molecules in the form of a mixture of argon and 4%H_2, or argon and 4% of air through the aerosol tube. The latter two solutions of water and water + 1%KCL were first passed through an argon operated spray nebuliser to convert the solution into a spray suitable for introduction into the plasma. The nebuliser used for this purpose (Varian Techtron standard variable type, efficiency $\approx 3\%$) required an argon flow-rate of at least 2 litres/minute to produce a consistent sample flow (Ong, 1977; Miller, 1978). This together with the loading factor caused by the introduction of molecular samples into the plasma led to all the results in this section being obtained under the following operating conditions, viz an input power of 1200W (reflected power < 2W), a coolant flow-rate 10 litres/minute, and an aerosol flow-rate 2 litres/minute. The measurements described below, as in previous sections, were made at a height of 5mm above the work-coil.

8.4.2. Introduction of Hydrogen

The introduction of hydrogen into the plasma is of special interest as it has often been used as a diagnostic tool to measure various properties of ICPT plasmas (e.g Visser *et al.*, 1976; Miller, 1978; Montaser, Fassel and Larsen, 1981; Uchida *et al.*, 1981). Generally, in these cases, it has been arbitrarily assumed that the addition of a small percentage of hydrogen had a negligible effect on the equilibrium state of the plasma. As the point of interest is in the state of equilibrium when the torch is used as an emission light source the addition of hydrogen was limited to the aerosol flow.

Ignition of the plasma was performed under normal operating conditions using argon (coolant only). Once the plasma was stablised and the aerosol of argon introduced, a mixture of argon + 4% hydrogen was gradually introduced into the aerosol flow slowly replacing the 2 litre/minute argon flow by a similar flow of the mixture. This gradual introduction caused a visible widening of the aerosol channel and an accompanying decrease in brightness accompanied by an increase in the

reflected power from less than 2 Watts to over 10 Watts. The matching unit was retuned to reduce the reflected power to less than 2 Watts. These changes in channel width and intensity can be seen by comparing Figures 7.15 and 8.14. These changes alone clearly cast doubt on the assumption that the addition of small amounts of hydrogen has a negligible effect on the equilibrium state of the ICPT plasma.

To investigate in detail the effect the addition of hydrogen on equilibrium in the plasma the experiments in section 8.3.2.2 were repeated with the 4% Hydrogen aerosol. Due to the decrease in intensity results could only be obtained out to a radius of 6.5mm with adequate accuracy. The pulsing off of the RF field still produced a sharp increase in the intensity of the excited argon states indicating that the temperatures were not equal. A scan of the plasma was made and using Equation 4.21 plots of $\ln\frac{I^*}{I}$ versus $E_{ion} - E_i$ were made. Some typical results are shown in Figure 8.15. The results of these experiments yielded results similar to those for the case of a pure argon aerosol in that, if excitational equilibrium was assumed because of the apparent linearity of the plots, the electron temperatures obtained ($2 - 3 \times 10^4 K$) were considerably higher than those obtained from a Boltzmann plot of spectral intensities obtained under steady state conditions ($6 - 9 \times 10^3 K$). Although an accurate measurement is no longer possible the difference between the electron and gas temperature appears to be reduced from 9-10% to 4-5% of T_e by the introduction of hydrogen into the aerosol.

8.4.3. Introduction of Air

The introduction of air into the plasma (Ar + 4%air) via the aerosol channel has a more drastic effect than a similar proportion of H_2 on the plasma with the aerosol channel widening appreciably more than for the case of hydrogen. The correction to the matching unit is more critical and care is required to avoid extinguishing the plasma. Once the Ar – 4%Air aerosol is introduced and the matching corrected the plasma is stable and is capable of being pulsed satisfactorily. The effect on channel width and intensity are shown by Figure 8.16 which gives the lateral and radial intensity of the Ar I 696.5nm spectral line.

The temperature measurements obtained using Equation 4.21 gives values nearer to credible values ($5.3 \times 10^3 K$ at r = 5.5mm, $1.8 \times 10^4 K$ at r = 4.5mm) than H_2 while there was a contradictory increase in the temperature difference between T_e and T_g ($10 - 14\% T_e$), a similar result as that obtained with the reduction of input power, and perhaps corresponds to the molecular aerosol providing a better means of energy

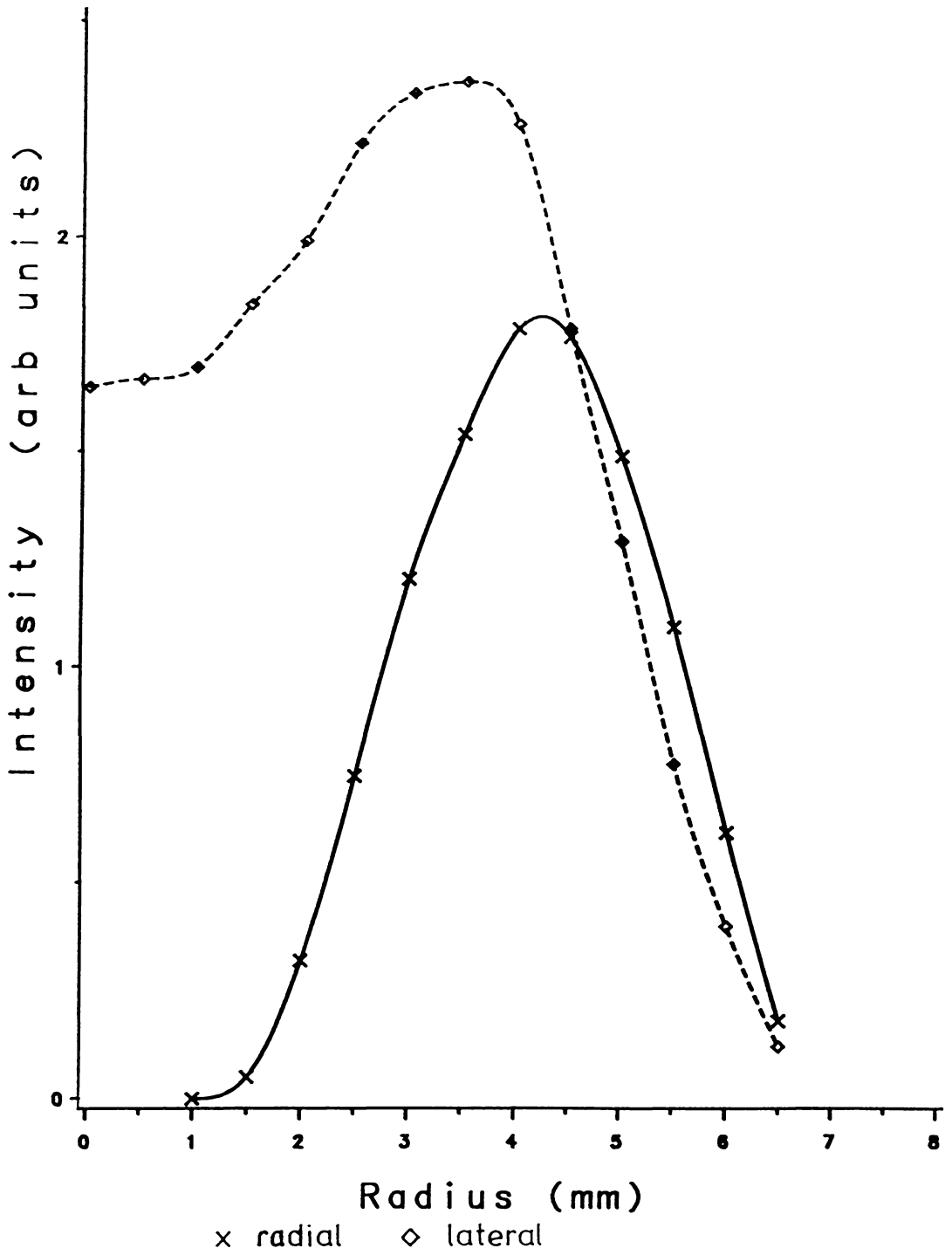

Figure 8.14: The Effect on Intensity and Aerosol Channel Width of the Introduction of 4% Hydrogen: Radial and Lateral intensities of 696.5nm Argon I Spectral Line.

Standard operating parameters with the exception of aerosol flow; Ar + 4% Hydrogen 2 litres/minute.

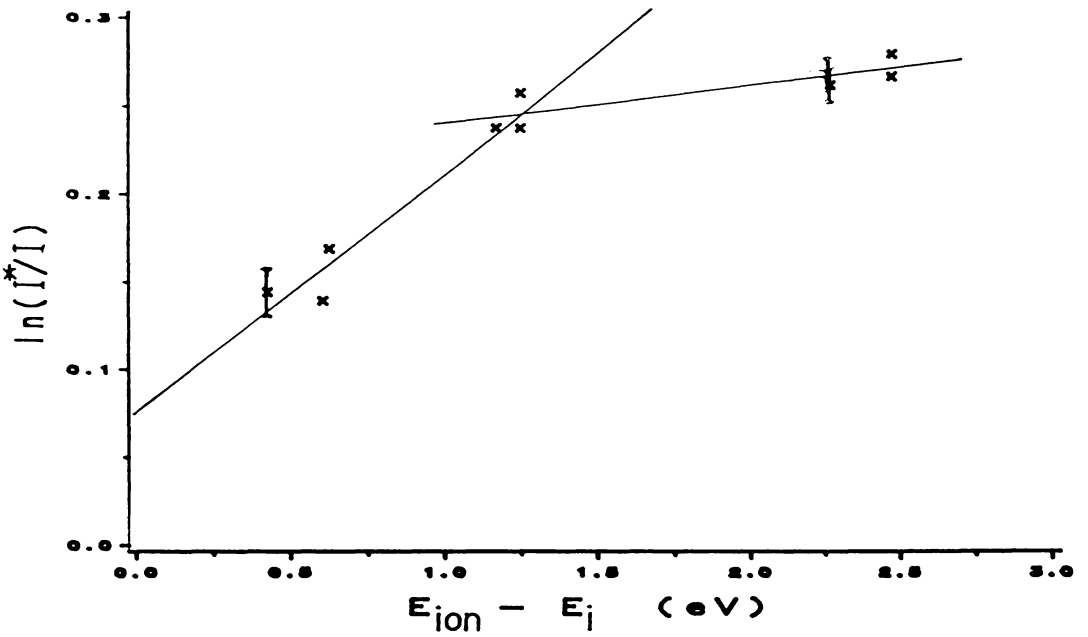

Figure 8.15(a): The Effect of the Introduction of 4% Hydrogen on the State of Equilibrium; Edge of plasma r = 6mm.
Standard operating parameters with exception of 4% Hydrogen aerosol.

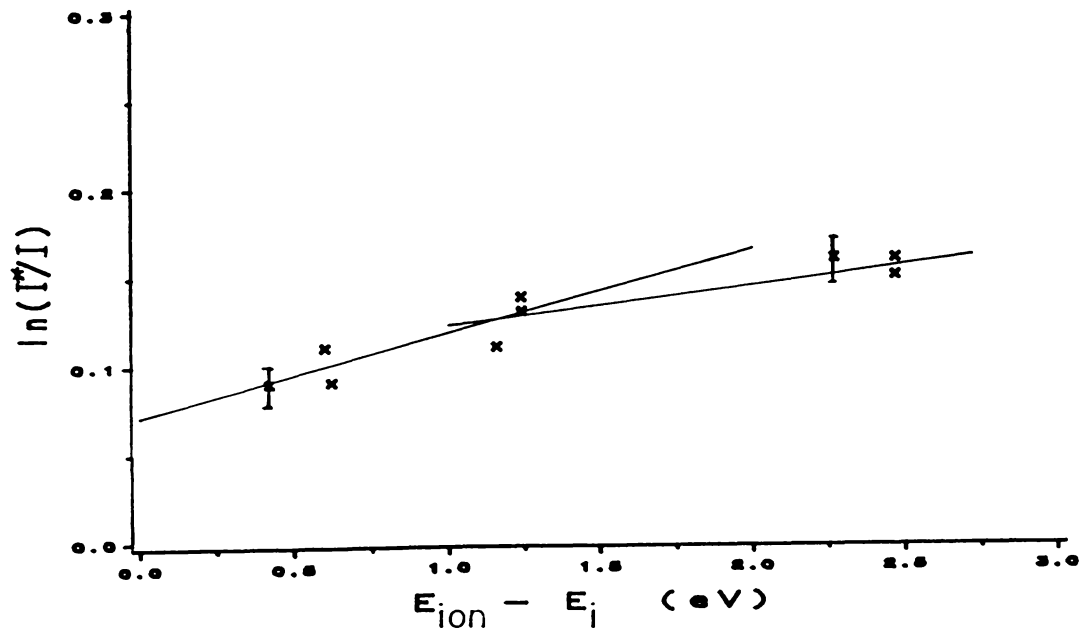

Figure 8.15(b): The Effect of the Introduction of 4% Hydrogen on the State of Equilibrium; r = 5mm.
Same parameters as Figure 8.15(a).

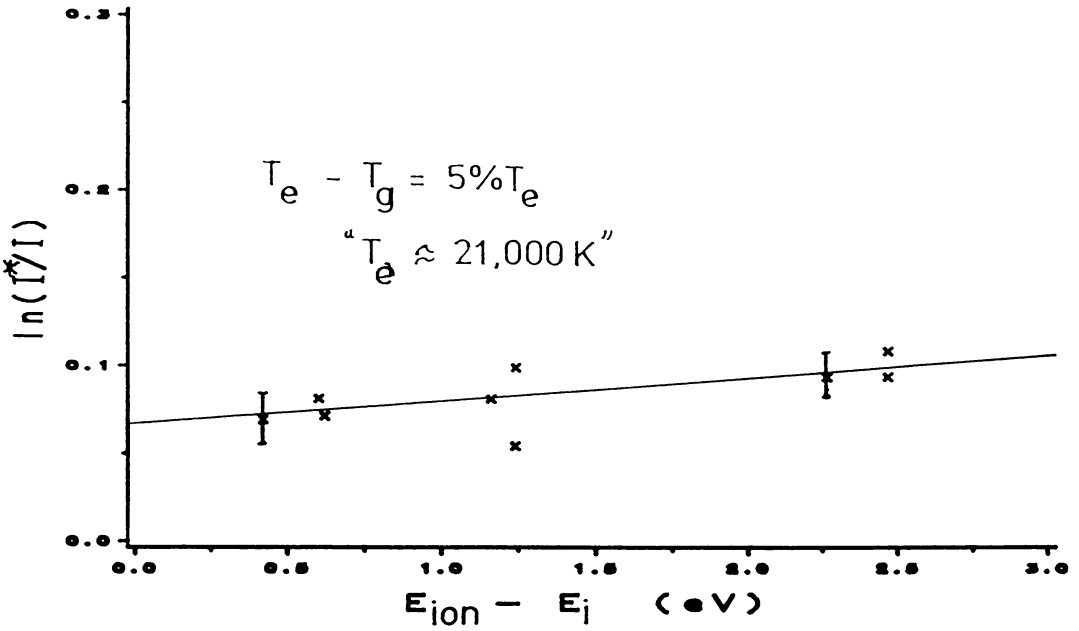

Figure 8.15(c): The Effect of the Introduction of 4% Hydrogen on the State of Equilibrium; r = 4mm.
Same parameters as Figure 8.15(a).

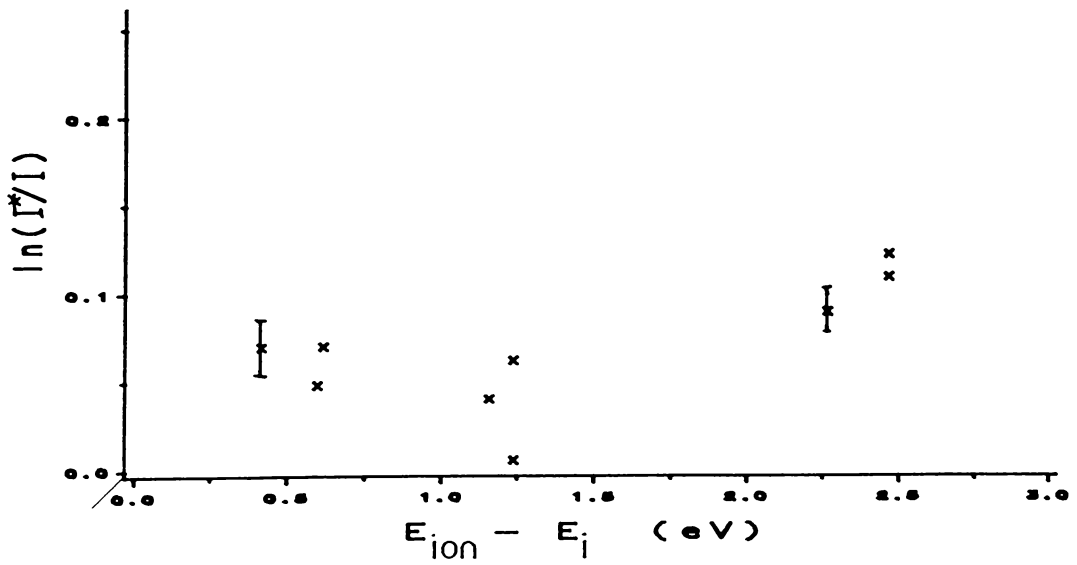

Figure 8.15(d): The Effect of the Introduction of 4% Hydrogen on the State of Equilibrium; r = 3.5mm.
Same parameters as Figure 8.15(a).

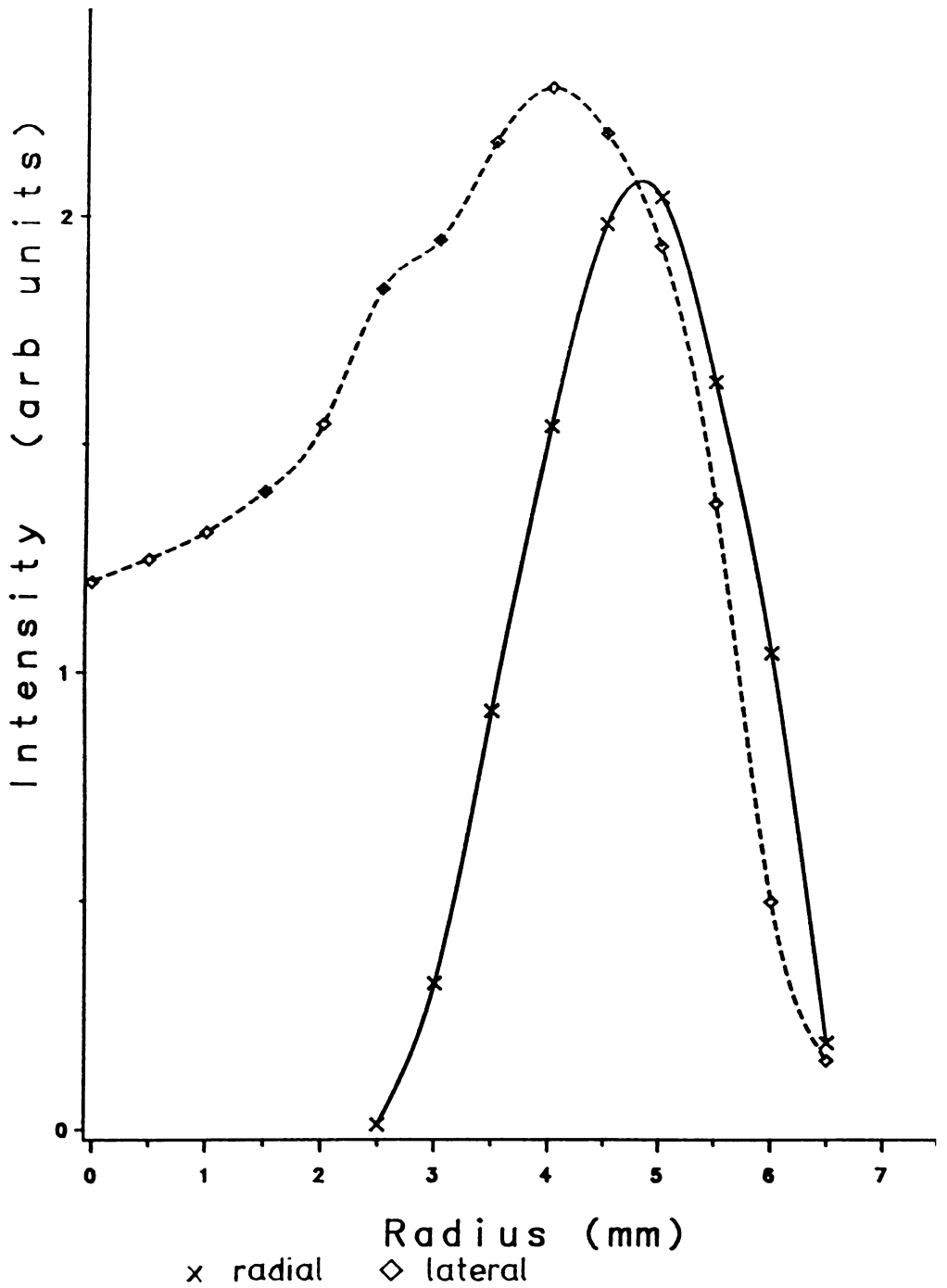

Figure 8.16: The Effect on Intensity and Aerosol Channel Width of the Introduction of 4% Air. Radial and Lateral intensities of 696.5nm Argon I Spectral Line.

Standard operating parameters with the exception of aerosol flow; Ar + 4% Air 2 litres/minute.

transfer within the plasma.

8.4.4. Introduction of Water

The effect of the introduction of water on the equilibrium state of the plasma is of interest since most samples are introduced into the plasma is in the form of solutions, most of which are water based.

A comparison of Figures 7.15 and 8.17 which show the radial intensity of the 696.5nm spectral line at a height of 5mm above the work-coil, demonstrates that the addition of water, via the nebuliser, into the aerosol flow has little effect on the shape of the plasma. Visually also little effect is noticed, and it is not necessary to re-tune the matching unit.

Results for the electron temperature and temperature difference (Figure 8.18) are also very similar to those obtained for a argon only aerosol flow, for example giving ($T_e \approx 4.5 \; x \; 10^4 \; K$ at r = 5mm; and $T_{exc} \approx 8600 \; K$, $T_e - T_g \approx 8\% T_e$).

8.4.5. The Addition of an Easily-Ionised Element

It is a well known property of the ICPT (Boumans and De Boer, 1975, 1977; Miller, 1978; Koirtyohann *et al.*, 1981; Blades and Horlick, 1981)that the addition of an easily-ionised element has relatively little effect on the analytical behaviour of the ICPT as an analytical light source. To see whether this continues over to its state of equilibrium a solution of 1%KCL was introduced, via the nebuliser, into the plasma. Results, both visual and those obtained using Equation 4.21 indicated that within error limits there is no change in the state of equilibrium of the plasma from that with the introduction of an aerosol of pure water.

8.4.6. The Effect of the Removal of the RF Field on the Introduced Elements

The presence of introduced impurities (H_2, N_2, O_2) in the central region of the plasma allows a glimpse into a region of the plasma where argon can not be used as a thermometric species. As a particular example, hydrogen which is another element which is strongly coupled to the continuum, and its behaviour was studied with the removal of the RF field.

Photograph 8.10 demonstrates the behaviour of the H_β 486.1nm spectral line at a height of 5mm above the work-coil with the introduction of Ar+4%H_2 at 2 litres/minute via the aerosol tube. It shows the familiar jump in intensity that is indicative of a deviation from LTE; however there are only a few strong hydrogen spectral lines, limiting the number of possible points for a plot corresponding to

Equation 4.21 and this, together with considerable scatter in the measurements precluded an accurate investigation of the state of equilibrium. Previous results using the two-line method applied to the H_β, H_γ, and H_δ spectral lines have yielded results which indicated a deviation from equilibrium (Visser *et al.*, 1976; Miller, 1978).

Attempts were made to investigate the opposite case by introducing an element (e.g. Cu, Hg) strongly coupled to the ground state, whose spectral line intensity would be expected to decrease sharply on removal of the RF field. Due to low emission intensity levels at suitable heights in the plasma this has been been unsuccessful.

8.5. Summary

The experiments described in this chapter have used the different relaxation times of the electrons and the neutral particles as a diagnostic tool to investigate the state of excitation and kinetic equilibrium present in the plasma under varying conditions of input power, gas flow-rate and the introduction of molecular compounds.

Initial experiments were performed on a plasma formed from a single flow of argon supplied as a coolant, similar to that investigated by Aspit (1971) with the exception of a central tube which constricted the gas flow. The plasma produced in these conditions was found to have a state of equilibrium at a height of 5mm above the work-coil where not only were the excited argon I states conforming to a Boltzmann distribution and in the central region of the plasma ($r \leq 3$mm) the electron and gas temperatures were found to be equal. Only at the edge of the plasma ($r \geq 7.5$mm) is there any evidence of a non-Boltzmann distribution. In between these zones the temperature difference does not exceed $\approx 6\% T_e$ which is insignificant for the majority of likely applications of the plasma, and is unlikely to affect the accuracy of the various diagnostic methods available in emission spectroscopy. The emission by the 811.5nm excited argon I state was saturated in the central regions of the plasma.

The introduction of an aerosol flow through the center of the plasma completely changes this picture. The decrease in intensity and increased scatter in the central region of the plasma ($r \leq 2$mm) meant that only the outer regions of the plasma could be accurately investigated. Plots of $\ln \frac{I^*}{I}$ versus $E_{ion} - E_i$ indicated that the plasma is not in excitational equilibrium over a large volume of the plasma. Where the results indicated that a linear plot could be fitted to the experimental data the electron temperatures obtained, using equation 4.21 and from a Boltzmann plot, which had agreed satisfactorily in the case of coolant only plasma now are in strong disagreement. Although an accurate measure of the temperature difference could no longer be made

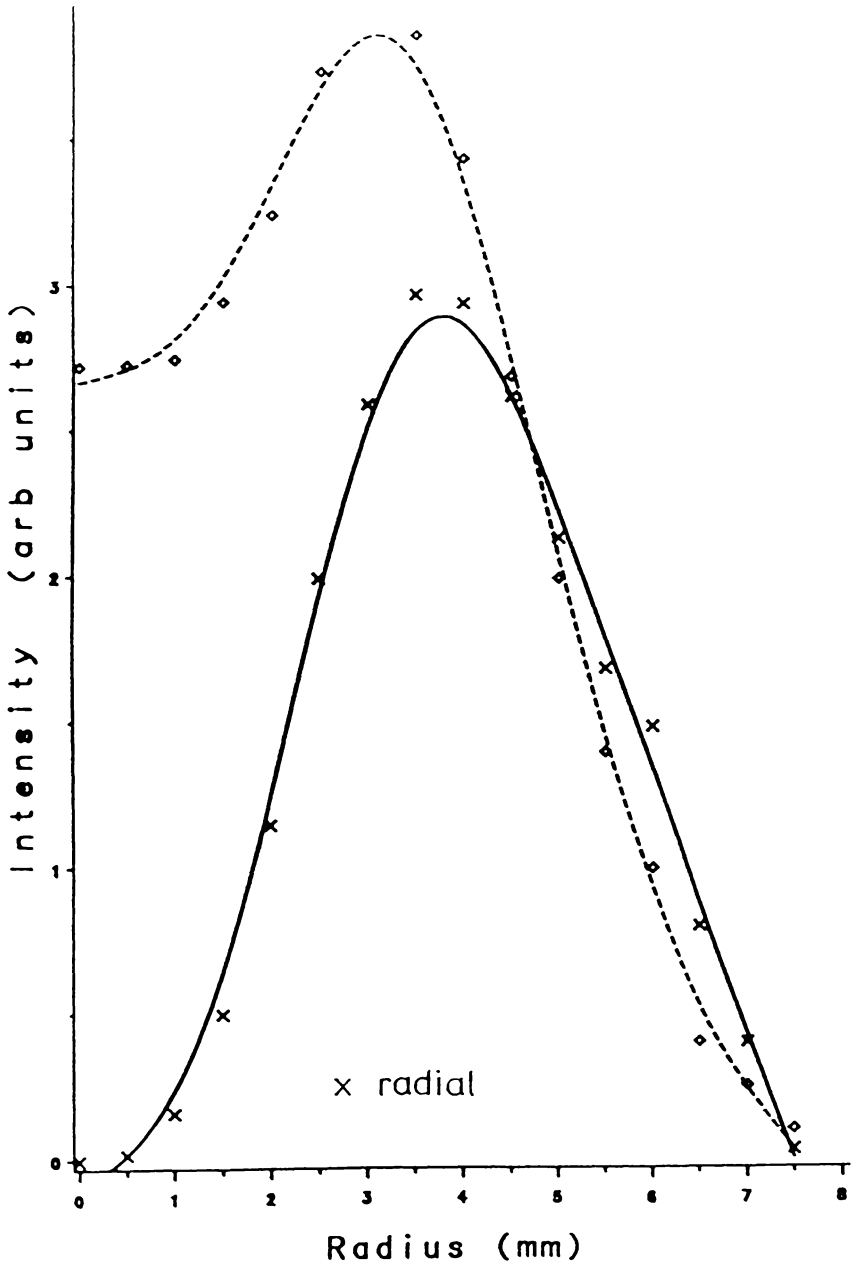

Figure 8.17: The Effect on Intensity and Aerosol Channel Width of the Introduction of Water. Radial and Lateral intensities of 696.5nm Argon I Spectral Line.

Standard operating parameters with the exception of aerosol flow; Ar + Water 2 litres/minute.

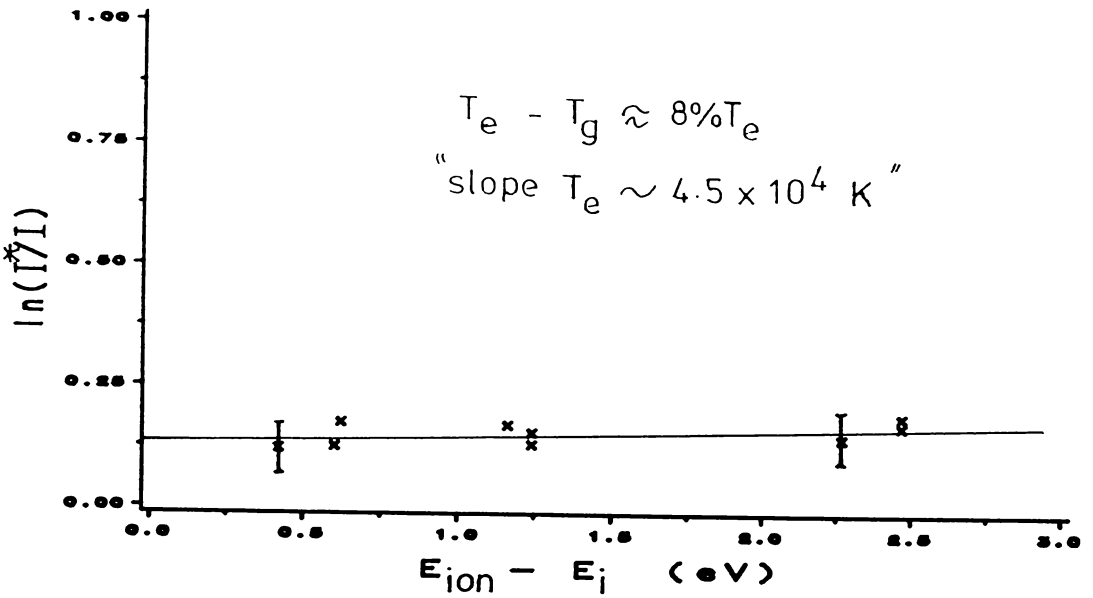

Figure 8.18(a): Intensity Ratios - The Effect of the Introduction of Water on the State of Equilibrium; r = 5mm.
Same parameters as Figure 8.17.

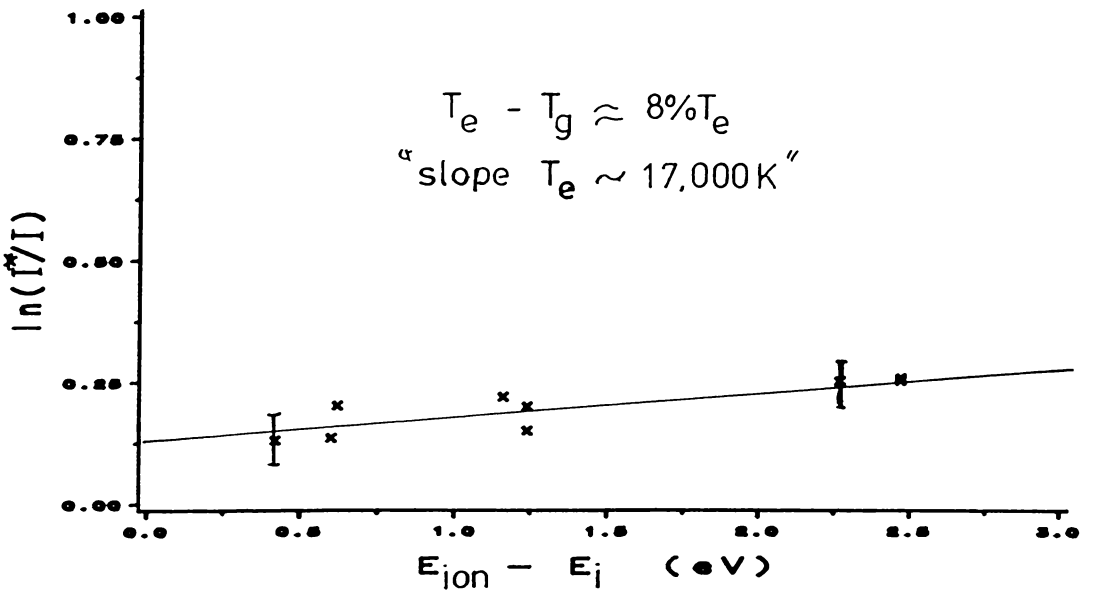

Figure 8.18(b): Intensity Ratios - The Effect of the Introduction of Water on the State of Equilibrium; r = 6mm. Same parameters as Figure 8.17.

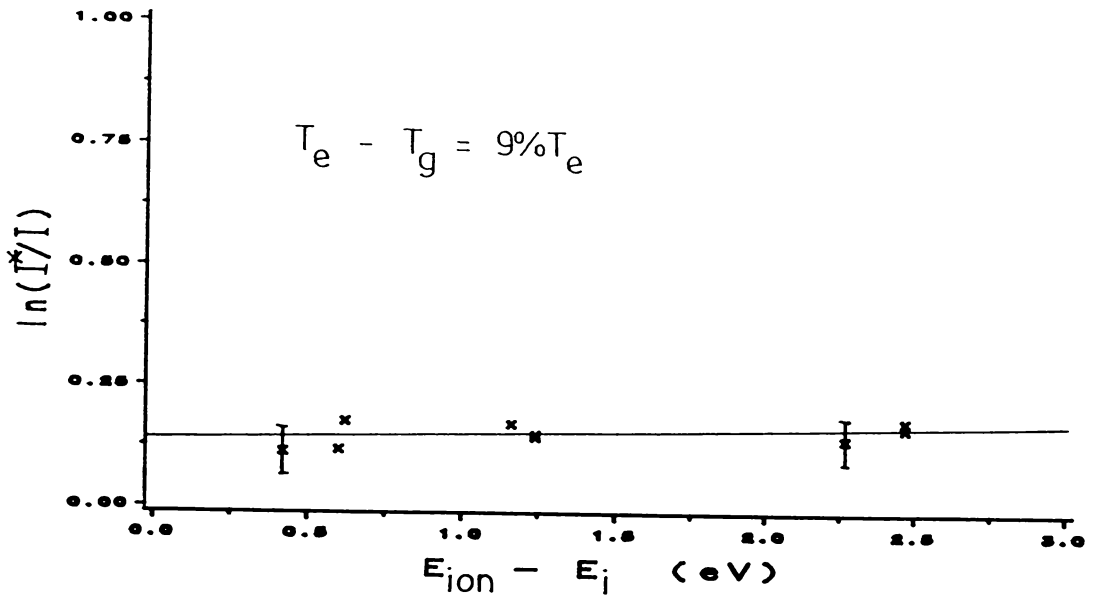

Figure 8.19(a): Intensity Ratios - The Effect of the Introduction of Easily-ionised Element (1%KCL) on the State of Equilibrium; r = 5mm.
Same operating parameters as Figure 8.18 with the exception of 1%KCL.

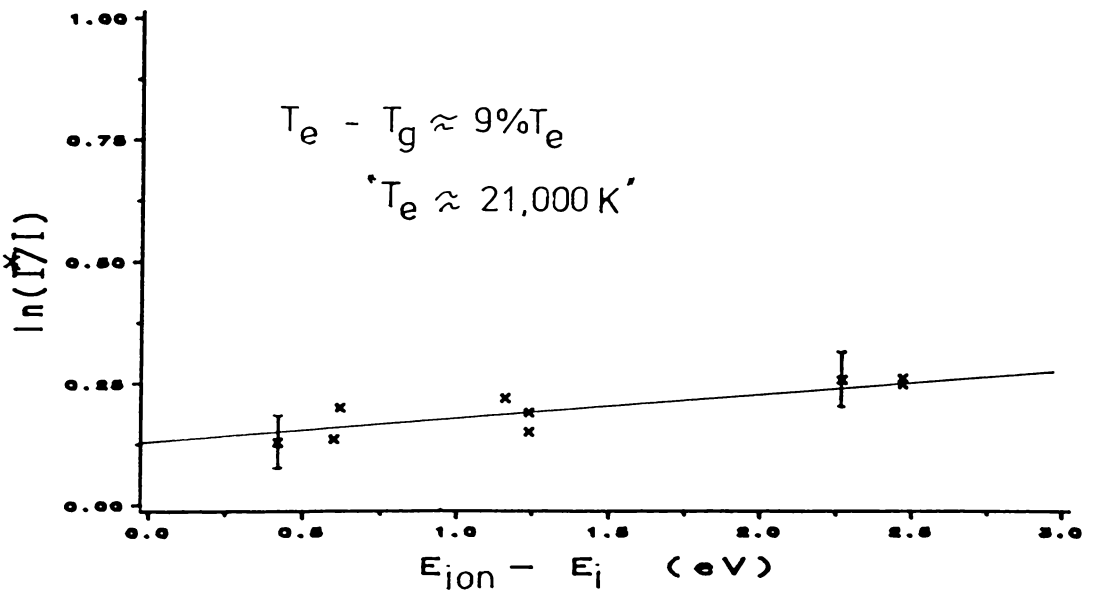

Figure 8.19(b): Intensity Ratios - The Effect of the Introduction of Easily-ionised Element (1%KCL) on the State of Equilibrium; r = 6mm.
Same parameters as Figure 8.19(a).

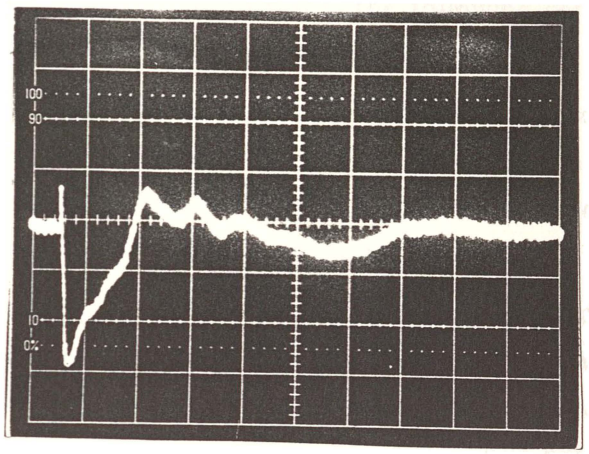

Photograph 8.10: Intensity Jump of the H_β Spectral Line.
Coolant flow-rate; 10 l/min, Aerosol flow-rate; 2 l/min Input power; 1200W.

the results obtained suggested that the difference between the electron and gas temperatures had increased only slightly ($\approx 10\% T_e$). This is still relatively small and in many experimental situations negligible. Those obtained by the Boltzmann plot ($\approx$ 10,000 K) are in agreement with similar results obtained elsewhere (see Chapter 2) whereas those obtained using equation 4.21 yielded electron temperatures apparently in excess of 60,000 K for a aerosol flow-rate of 2 litres/minute. Since the energy difference ($E_{ion} - E_i$) is small, the presence of scatter in the data will have a major effect on the calculated electron temperature. However, the degree of difference is both sufficiently large and highly consistent so that it can only arise from a deviation from equilibrium. The behaviour of 811.5nm spectral line supplied further evidence of the non-equilibrium by showing an increase in the radiative losses from the system with the introduction of an aerosol flow to the extent that it is no longer saturated in most regions of the plasma.

The effect of varying the operating conditions was shown to have a small effect on the state of equilibrium with respect to the introduction of the aerosol flow. Even the introduction of molecular additives, as in the case of a normal ICPT when used as an analytical tool, is shown to have a minor effect on the plasma, with the exception to

some extent of Hydrogen and air.

8.6. Conclusions

From the above experimental results, the following conclusions can be drawn as a result of measurements of the relaxation characteristics of the ICPT plasma.

i) the plasma in the central region of a single flow (coolant) argon ICPT is in a state of partial LTE. The difference between the excitation temperature and the gas temperature is negligible. The 811.5nm near-infrared spectral line of the 4s - 4p transition array is or is nearly optically saturated.

ii) The deviation of the excited state from a Boltzmann distribution at the edge of the plasma (coolant flow) and in the center, with the introduction of the aerosol flow, suggests that the plasma is not completely collision-dominated due to the loss of energy outside of the plasma. That is, while excitation and ionisation are produced by electron collisions, radiation competes with collisional processes in producing de-excitation and recombination. The increase in radiation losses as demonstrated by the change in the behaviour the 811.5nm spectral line indicates that radiative processes do play a role in establishing the state of equilibrium present in the plasma.

and

iii) The introduction of molecular compounds, especially aqueous solutions, into the plasma via the central channel has a very small effect on the state of equilibrium of the plasma with respect to the effect the introduction of the aerosol flow of argon alone has.

The lack of a Boltzmann distribution among the excited states at the edges of the plasma and the center of plasma with the introduction of the aerosol flow as well as the apparently high electron temperatures (60,000 K) obtained from Equation 4.21 is evidence of the breakdown in the assumption that the plasma is completely collision-dominated. In a plasma where the electron density has decreased due to convective losses to the extent that collisional processes no longer dominate down to the 4s level. Plus where the near-infrared 4s - 4p spectral lines are optically-thin (or at least no longer optically-saturated) implying that the absorption of the 4s - 4p line radiation no longer reduces the over-populated 4s level by the excitation of atoms in the 4s level to the 4p level. It then follows from the equilibrium relationships (Chapter 3) and the relaxation mechanism (Chapter 4) that the rapid removal of the supporting RF field would result in a smaller than expected jump in intensity for the optically-thin spectral

lines of the 4s - 4p transition array in comparison with the increase experienced by higher energy levels (4p - 5d etc) and intensity jumps would occur in the near-infrared spectral lines (e.g 811.5nm spectral line) which were previously saturated. These results are in agreement with those obtained experimentally when aerosol flow is introduced through the center of the plasma and thus implies that the 4s level in the ICPT is overpopulated with respect to the higher excited states under normal operating conditions.

To conclude, the excited states deviate from a Boltzmann distribution when the gas flow velocity is high, at the outer edges and the central region when an aerosol flow is introduced. The effect on the state of equilibrium of then varying the other operating conditions appears to be insignificant with respect to this. An explanation is offered that indicates that due to the loss of electrons from the plasma arising from the increased gas flow the plasma is no longer collision-dominated down to the 4s level thereby resulting in the over-population of the 4s level which is further increased by the additional loss of line radiation from the 4s - 4p transition array. Measurements of the electron density were obtained to evaluate the electron loss occurring upon the introduction of the aerosol flow. The results of which are given in Chapter 9.

Chapter 9

Electron Density

9.1. Introduction

Up to this point the experimental investigation has been focused on the state of equilibrium prevailing in the ICPT as revealed by the behaviour of the excited argon I spectral lines. It is evident from the results in the previous chapter that the deviation from a Boltzmann distribution among the excited states arises, in the central regions, from loss of energy from the system due to the flow of argon through the plasma especially with the introduction of the aerosol flow. In the previous chapter it was suggested that the reason the plasma was not in a state of excitational equilibrium was because of a decrease in the electron collision rate which implies a decrease in the electron density with the introduction of the aerosol flow. This necessitated knowledge of the electron density under the various operating conditions pertaining in the ICPT. As shown in Chapter 2, apart from values for the electron density calculated from the measured temperatures by using Saha's equation the experimental measurements of n_e have consistently been centered on electron density values of 10^{21} to 10^{22} m^{-3}.

Of the diagnostic methods available for determining the electron density in the ICPT none approach the sensitivity of the differential method used in the previous chapter. However, several methods exist for determining the electron density which are independent of the prevailing state of equilibrium and by comparing these results with those obtained from Saha's equation using temperatures obtained in Chapter 8, further insight into the causes of dis-equilibrium in certain regions of the ICPT plasma can be obtained.

The over-population of the electron density, with respect to the gas temperature, allows an estimation of the radiative-collisional recombination coefficient.

9.2. Electron Density

9.2.1. Experimental Methods of Determining the Electron Density Distribution

Four standard diagnostic techniques were considered to investigate the electron density distribution in the ICPT. These are the absolute intensity of the continuum intensity, electro-magnetic wave interferometry, Stark broadening of the H_β spectral line and from Saha's equation. These methods are described in the following subsections, and the results obtained are given in section 9.3.

9.2.2. Electron Density from the Continuum Intensity

Equation 2.5 (repeated here for convenience) shows that the electron density is readily derived from the intensity of the continuum with only a very weak dependence ($n_e \approx T_e^{\frac{1}{4}}$) on the assumed electron temperature

$$\epsilon_\lambda = C\,\xi(\lambda, T_e)\,\frac{n_e^2}{T_e^{\frac{1}{2}}}$$

where ϵ_λ is the absolute intensity of the continuum and ϵ contains the free-free and the free-bound Biberman factors and which depends only weakly on the temperature. Under the prevailing operating conditions other possible contributions to the continuum intensity, e.g negative-ion and molecular continua, are negligible.

The problems associated with this method were those common to measurements requiring the absolute intensity. It was necessary to accurately calibrate the detection system which together with the relatively low intensity of the continuum intensity introduces the main source of error. Another source of error is the presence of weak spectral lines. Each wavelength at which continuum intensity measurements were taken was checked for the presence of weak spectral lines by observing the change in intensity with slit-width. The absolute intensity calibration of the monochromator was made using a tungsten ribbon lamp. Numerous measurements of the continuum intensity were made between 420nm and 730nm where $\frac{\epsilon_\lambda}{\xi(\lambda, T)}$ is almost independent of the wavelength.

In this case where only one element and one ionisation stage is important, the electron density can be calculated with twice the accuracy of the combined experimental and theoretical accuracy of the absolute intensities (Griem, 1964). The error in the electron density measurements obtained using this method is of the order of 8%. The electron density results are given in section 9.3.

9.2.3. An Interferometric Method of Measuring the Electron Density

With an appropriate source of coherent electro-magnetic waves, it is possible to measure the refractive index of the plasma using a Michelson or similar sort of interferometer. One path of the interferometer is arranged to intercept the plasma, and the effective path-length or phase change caused by the plasma can be directly related to the plasma refractive index, and hence, as discussed below to the electron density of the ICPT plasma. There are also a number of possible sources of errors in measuring the free electron density, and these are also examined below.

The refractive index of a plasma is the linear combination of the phase refractivities of the various constituents (atoms, ions, electrons) if the measuring wavelength is small compared to the characteristic plasma lengths (Alpher and White, 1965). That is

$$(n - 1)_{plasma} = (n - 1)_{atom} + (n - 1)_{ion} + (n - 1)_e \tag{9.1}$$

where n is the refractive index.

The refractivity of species i (atoms or ions) in the plasma is a linear function of the associated plasma density n_i, given by

$$(n - 1)_i = 2\pi\bar{\alpha}_i(\lambda)n_i \tag{9.2}$$

where $\bar{\alpha}_i$ is the mean polarisabilities which is only weakly dependent on the measuring wavelength for atoms and ions.

As the ion polarisability is of the same order as the atoms and as the temperature is less than 13,000 degrees (the degree of ionisation is small) the effects introduced from the ions can safely be neglected.

The contribution arising from the electrons depends on the square of the measuring wavelength, and is given by

$$(n - 1)_e = -\frac{r_0}{2}\pi\lambda^2 n_e \tag{9.3}$$

where r_0 is the classical electron radius.

Therefore using Equation 9.1 together with Equations 9.2 and 9.3 the electron density can be determined by measuring the plasma refractive index. The refractivity of the plasma is dominated by the effect of the electrons and due to the scaling of the refractive index with electron density, and the cut-off wavelength given by

$$\lambda_c = 2\pi\left(\frac{m\epsilon_o}{n_e e^2}\right)^{\frac{1}{2}} \tag{9.4}$$

together with the expected value for the electron density, it is only feasible, in this case, to measure the refractive index in the IR region, e.g at wavelengths $>$ 1μm but $<<$ 1mm. This requirement meant that the only suitable wavelength source was an infrared laser and unless several different wavelength IR lasers were available, a measurement at only one wavelength could be made.

The only available IR laser was a CO_2 laser operating at a wavelength of 10.6μm. To establish the degree to which this reflected the electron density the effect of the other components constituenting the plasma has on the degree of refraction was estimated.

While the measuring wavelength of the CO_2 laser used is well away from spectral lines emitted by the plasma there is a possible contribution arising from the wings of remote spectral lines. In similar plasmas produced in arcs this has been shown to contribute less than 0.5% (Baessler and Kock, 1980) as most contributions cancel each other.

Another possible contribution to the measured plasma density arises from the excited electrons of atoms. When the measuring beam interacts with a highly excited atomic electron it behaves, to some extent, like a free electron and thus contributes to the measured density. In plasmas similar to the ICPT Griem (1964) estimated that this would increase the measured electron density by 1%. Baessler and Kock (1980) put an upper limit for the overestimation of the electron density by assuming all electrons bound in excited states were free. They showed that for a plasma at less than 13,000 degrees the contribution from all the excited states treated this way is less than 2.5% and implied that a refined calculation would yield a contribution more in line with Griem's estimate.

The remaining important source of error is provided by the refractive index of the atoms due to their polarisability. However the high electron densities obtained in the ICPT (10^{21} to 10^{22}) indicates that the ratio of atomic refractivity to the free electron refractivity is very small so that the electrons dominant the plasma refractivity. This ratio is given by

$$\eta_a : \frac{n_e}{n_a} \cdot \frac{\lambda^2}{\lambda_R^2} \eta_e \qquad (9.5)$$

where

η_a and η_e are the respective refractive indices

n_a and n_e the atomic and electron densities

and

λ_R the wavelength of the atomic resonance line (Argon $\lambda_R \approx 0.1 \mu m$)

Thus for a CO_2 laser and a plasma at atmospheric pressure with an expected electron density of approximately 10^{22} m^{-3}, the ratio of electron to atomic contribution to the results is approximately 100:1.

Combining these various systematic errors together yields a probable error in the electron density of approximately 2%.

A Michelson interferometer utilising a CO_2 laser was used to obtain the radial electron density distribution. The fringe shift N due to the presence of a plasma in one arm of a double-pass interferometer is given (Jahoda and Sawyer, 1971), to a good approximation, by

$$N = -\frac{e^2 \lambda_0}{4\pi^2 \epsilon_0 m c^2} \int_0^x n(x)_e dx \qquad (9.6)$$

where

e and m the electronic charge and mass

c the speed of light

ϵ_0 the permittivity of free space

$n(x)_e$ the electron density along the path

and

x the length of plasma the light passes through. Using a CO_2 laser having a wavelength of 10.6 microns, the number of fringes N is given by

$$N = 4.77\ x\ 10^{-21} \int_0^x n(x)_e dx \qquad (9.7)$$

The complete self-adjusting interferometer is described in Chapter 5; it uses feedback to a path shifting mirror mounted on a piezo-electric driver to ensure that the phase difference between the two paths of the interferometer is 90°. The output is taken from the voltage applied to the mirror to maintain this phase difference, this having been calibrated in terms of a half-wavelength shift (1 fringe) of the mirror. The amplifier response dV due to the differential phase change dN produced by the plasma's electrons gives with respect to the calibration voltage V_{pp}

$$\frac{dV}{dN} = V_{pp} \pi Sin\, \theta_0 \qquad (9.8)$$

where (see Figure 9.1)

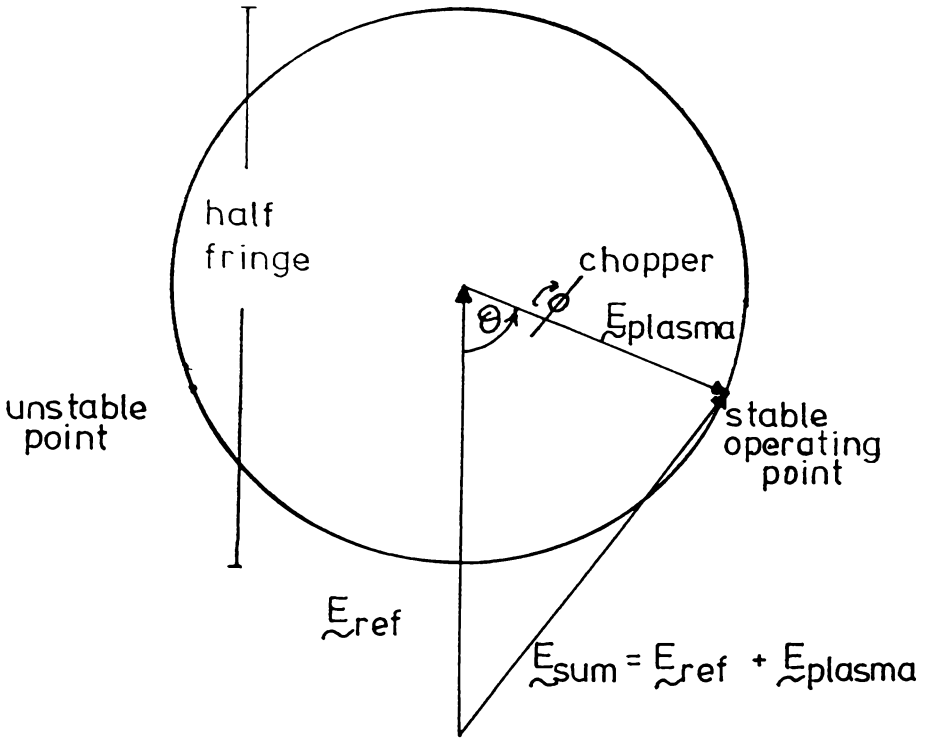

Figure 9.1: Vector Diagram of the Phase Stabilisation Method.

$$\theta_0 = Cos^{-1}\left(\frac{|E_{plasma}|}{2|E_{ref}|}\right) \tag{9.9}$$

Under the prevailing experimental conditions with a CO_2 laser, a plasma length of $\int dx = 4 \times 10^{-2}$ m and a value of $\theta_0 = 30^o$ then

$$dN = 3.5 \times 10^{21} \frac{dV}{V_{pp}} \text{ m}^{-3} \tag{9.10}$$

Thus by measuring the voltage necessary to maintain a phase difference of 90 degrees between the plasma and reference beams the electron density along that path is determined.

After a warm up interval period of approximately 30 minutes the interferometer remained stable for periods longer than 3 hours, that is, variations in the phase over this period were less than ± 3%. The interferometer was calibrated at the beginning of each scan of thirty steps across the plasma. The response time of the detector, being of the order of 45μs, prevented the study of the variation in electron density using the

interferometer when the RF field was pulsed off. Turbulence at the edges of the plasma and at heights over 10mm above the work-coil proved troublesome in the application of this method. This varied the electron density rapidly and therefore caused the translator to oscillate. To eliminate this required increasing the response time of the translator to such an extent that the time taken to complete a full scan approached the time period for which the laser could be stabilised. Therefore the accuracy of the measured electron density decreased with increasing height and increasing radius. Repeated scans of the plasma at a height of 5mm above the work-coil yielded a variation in the electron density measurements of ± 5%. The results are given in section 9.3

9.2.4. Electron Density Measurements from the Stark Broadening of H_β

The introduction of a small amount of hydrogen into the plasma allows the possibility of the measurement of the Stark broadening of the H_β spectral line. This would allow the electron density to be calculated, since the determination of the electron density from the half-width of the H_β spectral line is a standard technique in plasma spectroscopy (Griem, 1964; Huddlestone and Leonard, 1965; Dresvin *et al.* 1972; Lockte-Holtgreven, 1968). The electron density is given by

$$n_e = C(n_e, T)(\lambda_{\frac{1}{2}})^{\frac{3}{2}} \qquad (9.11)$$

where C depends weakly on n_e and T, values for which are given by Griem (1964). For a plasma with an electron density $n_e \approx 10^{22}\ m^{-3}$, the half-width $\lambda_{\frac{1}{2}} \approx 1nm$.

The effect of other line-broadening mechanisms and instrumental broadening was investigated for this case. It can be shown that for the temperature range present in the ICPT the Doppler broadened H_β line half-width amount to less than 0.05nm. This is negligible with respect to the total measured half-width using the standard deconvolution procedures. Broadening arising from other causes (resonance and van der Waals interactions) would also be smaller under these operating conditions than that arising from Doppler broadening (Griem, 1964). Instrument broadening is that broadening that arises due to imperfections in the measuring instrumentation. The profile of a spectral line obtained by a monochromator is not the true line profile. A spectral line of infinitesimal width is broadened by diffraction at the entrance and exit slits, imperfections in the lens and mirrors and any other optical parts. To confirm that instrument broadening was negligible in this case, a very narrow spectral line (HeNe laser) was scanned as Doppler and pressure broadening effects are negligible for such a line.

The electron density results obtained by this method are given in section 9.3.

9.2.5. Determination of Electron Density From Saha's Equation

Using the temperatures determined in Chapter 8 together with excitation temperatures determined by the two-line method using the relative intensities of the Fe 373.7nm and 374.94nm spectral lines from samples introduced through the center of the plasma, the electron density was calculated from Saha's equation. The results are given in the following section.

9.3. Electron Density Results

9.3.1. Introduction

The temperature measurements and profiles obtained in Chapter 8 indicated the degree of equilibrium prevailing under various operating conditions in various regions of the ICPT. How this relates to the electron density is shown by the results obtained by the four different methods used in this chapter and is the purpose of experiments detailed below.

9.3.2. Coolant Flow Only

The electron density was determined experimentally at a height of 5mm above the work-coil, under the same operating conditions as in Chapter 8, by the above three direct methods. By using the experimental values obtained for the temperature in Chapter 8 Saha's equation was used to calculate values for the electron density. As can be seen from Figure 9.2 not only is there a good agreement between the different direct experiment methods, but also the results obtained from the use of Saha's equation are in agreement (in the central region of the plasma) taking into account the degree of error inherent in the temperature measurements. This result supports the evidence obtained in Chapter 8 indicating that the central region of the plasma (coolant flow only) is in at least pLTE.

Results obtained at other heights above the work-coil indicated a similar agreement between the various methods, although the errors in these results increased with height above the coil. In the case of the interferometer the errors were due to increasing turbulence, and for the other experimental methods the errors arise from the decrease in emission intensity. Only Stark broadening was used at a height of 15mm above the work-coil. This is the normal observation height when the ICPT is used analytically and a measure of the electron density is important for use as a comparison. Due to the opaqueness present in the tube walls it was not possible to

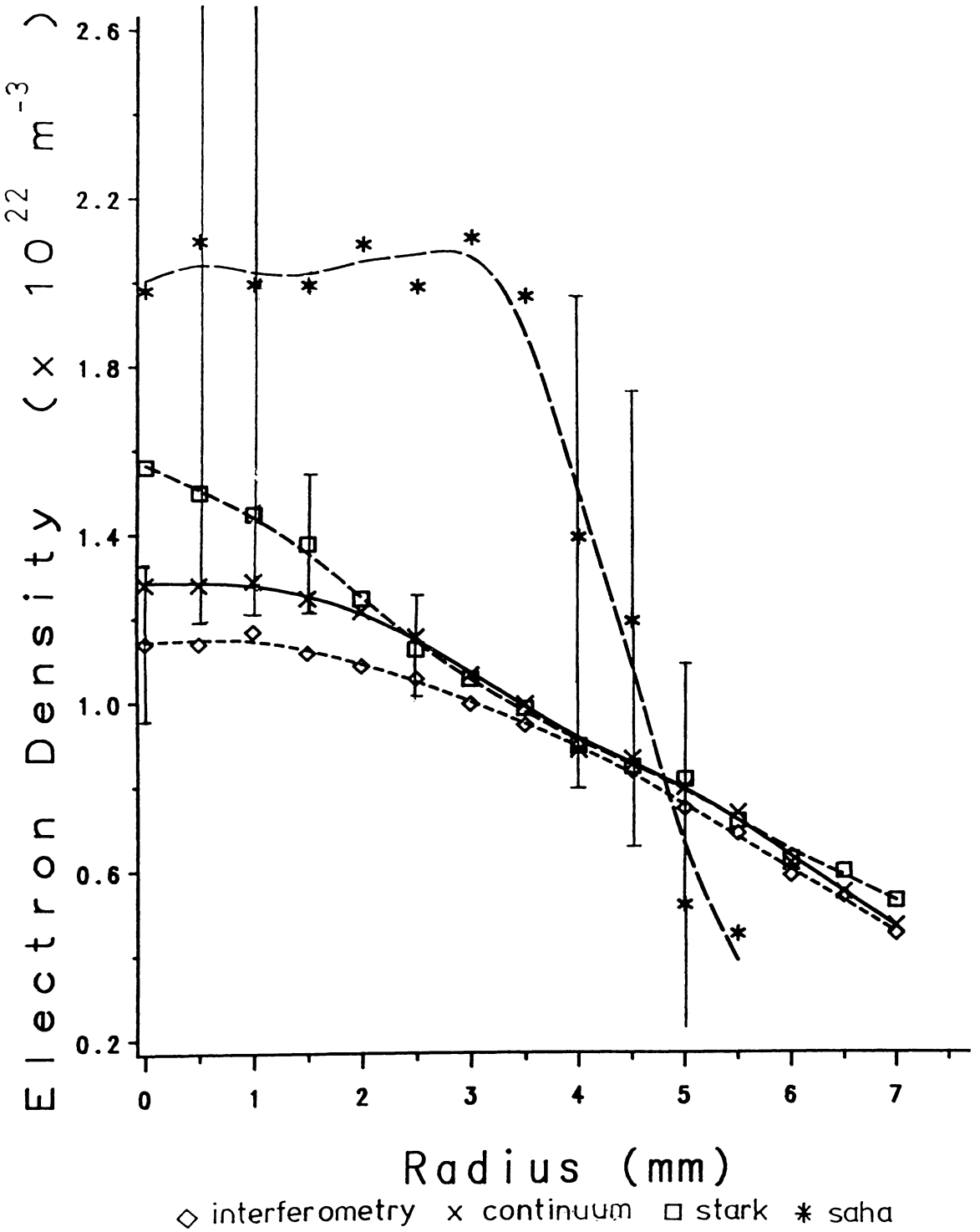

Figure 9.2: The Electron Density Distribution in the ICPT as determined by Four Different Diagnostic Methods; Coolant Flow Only.
Input Power; 1200W, Flow-rate; 10l/min, Height; 5mm above Work-coil.

obtain accurate electron densities below the top of the work-coil.

9.3.3. Introduction of the Aerosol Flow

Figure 9.3 shows the electron density with and without aerosol flow (2l/min) through the center of the plasma at a height of 5mm above the work-coil, as measured by the interferometer. This shows that while the electron density in the outer regions of the plasma remain unaffected the central density was decreased by approximately 33% by the introduction of the aerosol flow. Figure 9.4 gives the electron density distribution of the plasma with height above the plasma with an aerosol flow of 2 litres/minute.

Using the temperatures obtained in Chapter 8 together with Saha's equation the electron density distribution was calculated for the case of an aerosol flowing through the center of the plasma for which the results are displayed in Table 9.1. These results show that in the central region of the plasma the calculated values (i.e. based on temperature results) for the electron density are lower than those determined by direct measurement. This suggests that the Saha equation is not adequately applicable, especially to the central region, with aerosol flow. This corresponds to the presence of a significant deviation from equilibrium.

9.3.4. Introduction of Molecular Samples

As in Chapter 8 aerosol flows containing H_2 (4%), air (4%), and aerosols of H_2O and H_2O + 1%KCL, produces by a Varian nebuliser were introduced into the plasma. Figure 9.5 gives the electron density distribution for each case at a height of 5mm above the work-coil. These results demonstrate the insensitivity of the electron density to the addition of samples into the ICPT which is characteristic of this device.

As an additional means of comparing calculated values of the electron density using Saha's equation, in the central region of the plasma, with experimental results an aerosol containing $FeCl_3$ (concentration 2000 p.p.m) was introduced via the nebuliser. Using the two-line method the excitation temperature of the plasma was measured using the 373.71nm and 374.94nm iron spectral lines. Values of $\approx 7.5 \times 10^3$ K and 7.1×10^3 K were obtained at heights of 5 and 10mm respectively, using these values to calculate the electron densities from Saha's equation yielded values of $\approx 6.5 \times 10^{20}$ and 2.8×10^{20} m^{-3} while the corresponding direct experimental values indicated the electron density to be 7.8×10^{21} and 7×10^{21} m^{-3} at the respective heights. This difference between the values for the electron density obtained from Saha's equation and the directly measured values is further indication of a deviation

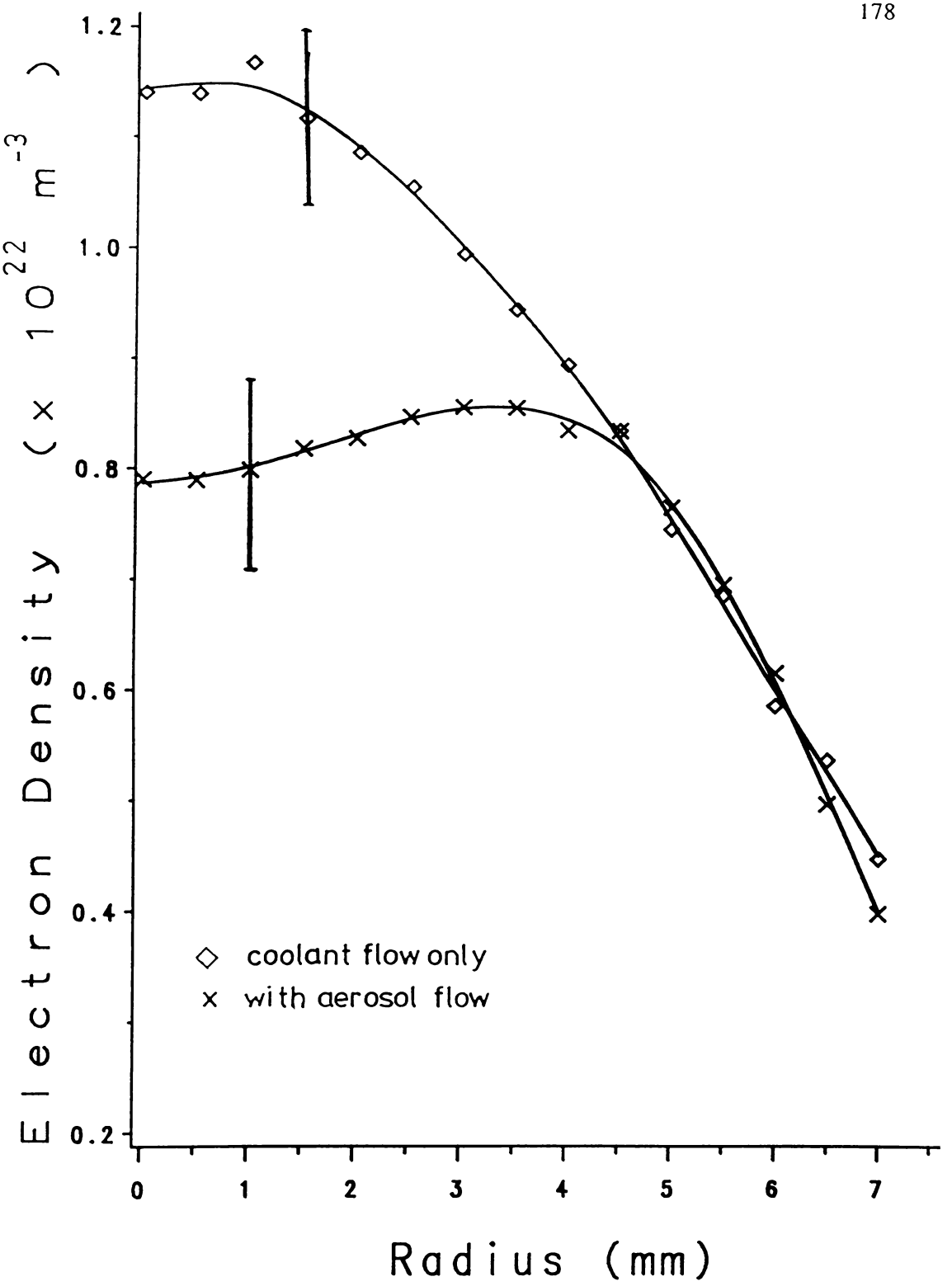

Figure 9.3: A Comparison of the Electron Density Distribution in the ICPT for a Plasma with and without Aerosol Flow.
Input Power; 1200W, Flow-rate; coolant 10l/min, aerosol 2l/min no sample Height; 5mm above Work-coil.

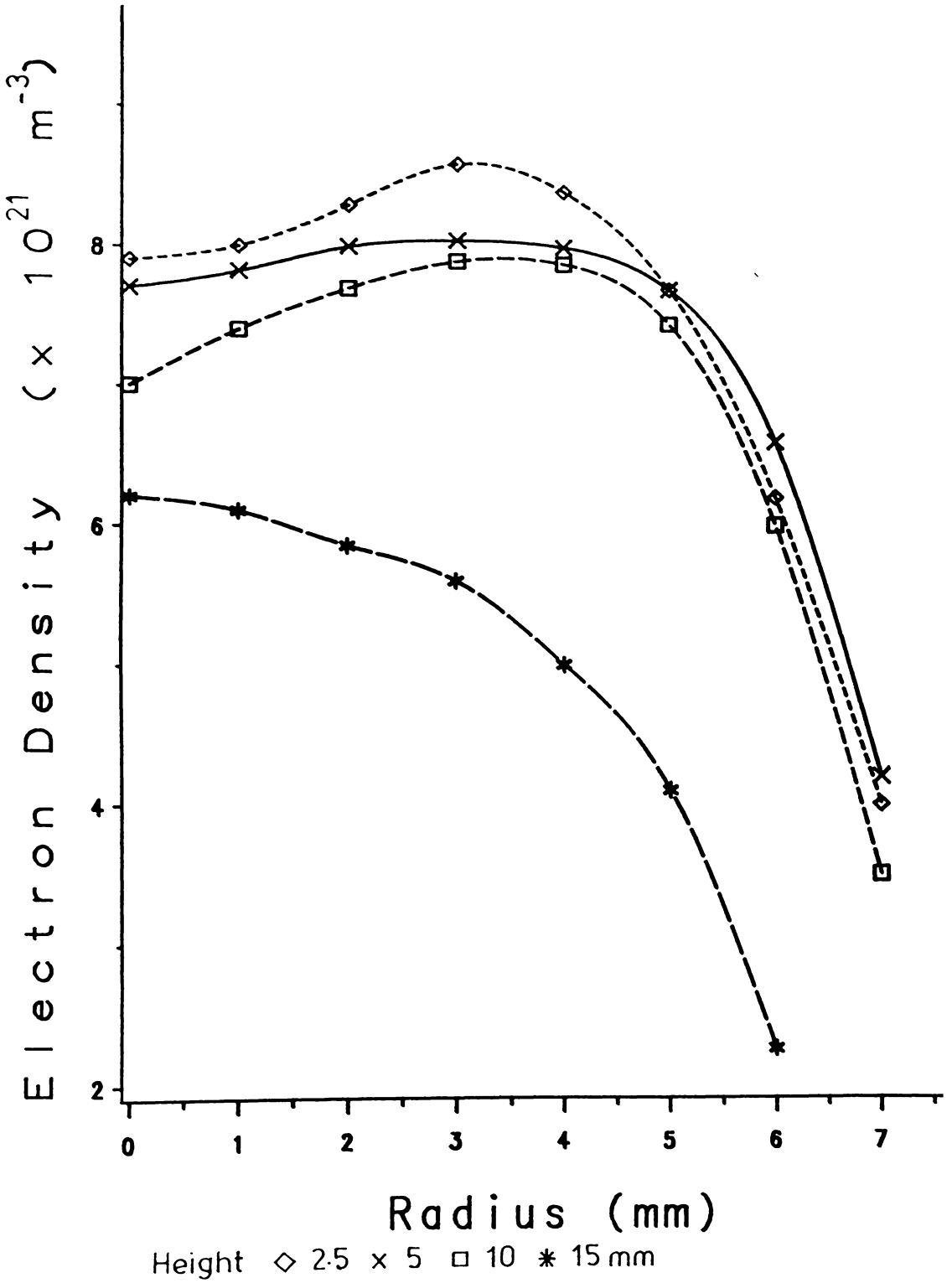

Figure 9.4: Variation in Electron Density with Height above the Work-coil.
Other than height, parameters same as Figure 9.3.

Radius (mm)	Measured n_e (m^{-3})	Calculated from Saha (m^{-3})
0.0	7.6×10^{21}	1.8×10^{16}
0.5	7.8×10^{21}	7.16×10^{18}
1.0	7.8×10^{21}	4.7×10^{20}
1.5	7.9×10^{21}	9.2×10^{21}
2.0	8.4×10^{21}	1.5×10^{22}

Table 9.1:
A Comparison of the Electron Density calculated from Saha's Equation with Experimental Determined Results for a Plasma with Aerosol Flow.

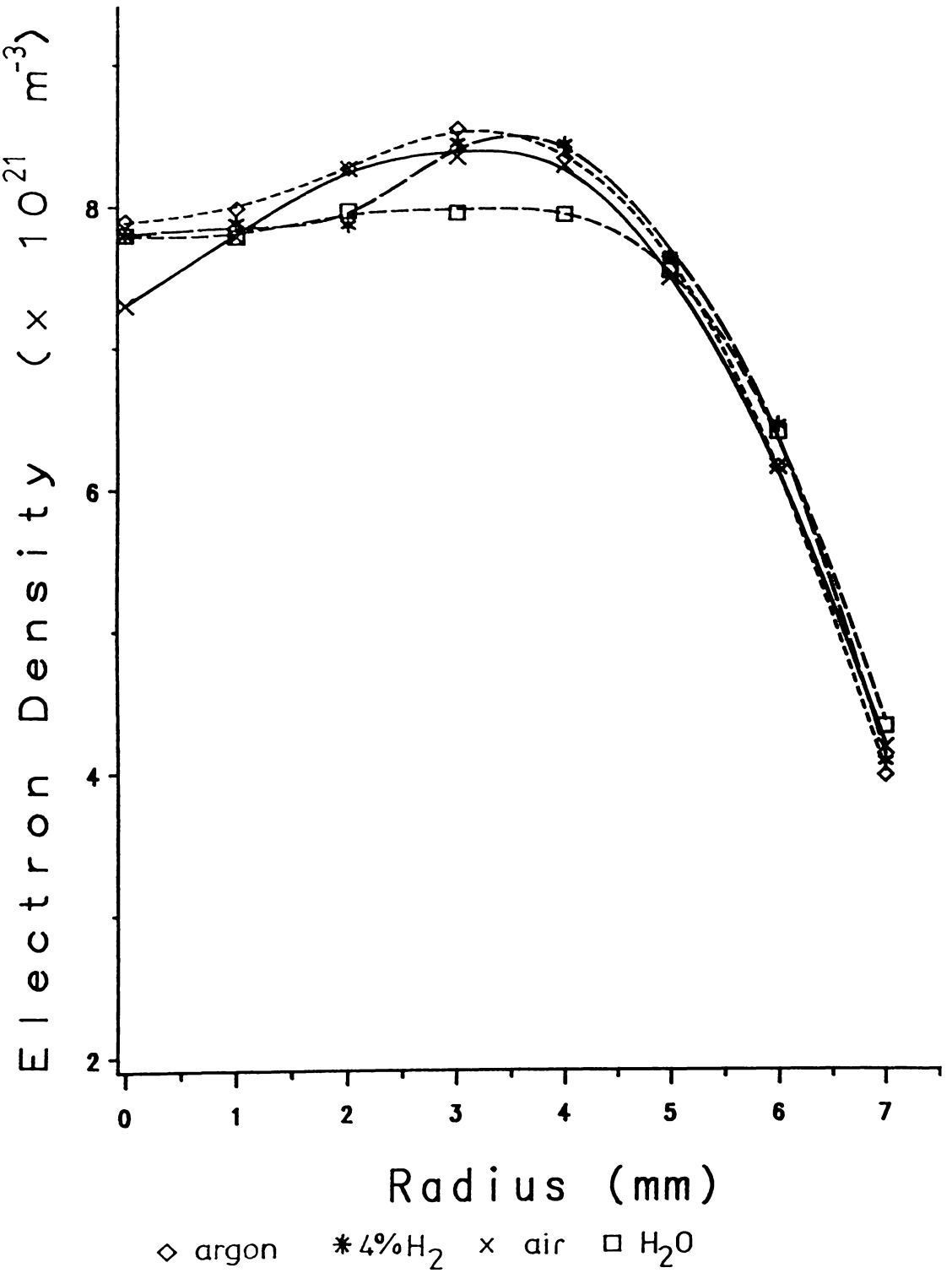

Figure 9.5: A Comparison of the Electron Density Distribution in the ICPT for a Plasma with the addition of molecular components into the Aerosol Flow.

Input Power; 1200W, Flow-rate; coolant 10l/min, aerosol 2l/min Height; 5mm above Work-coil.

from equilibrium arising from the introduction of the aerosol flow.

9.3.5. Discussion

In Chapter 3 equations relating the electron density for a plasma in LTE to the electron density of a plasma with a small deviation from equilibrium arising from the axial convective losses. In an attempt to demonstrate that this explains in part the deviation from equilibrium present in the ICPT the following calculations were performed.

First, using the results in Chapter 8 together with equation 3.29 it was possible to confirm, in agreement with the results of Stoke (1971), that atomic diffusion was negligible over the plasma volume of interest.

Secondly, since the central region of the plasma was shown, for coolant flow only, to be in at least pLTE. Comparing the electron density results obtained with this plasma with those results obtained from one formed with an aerosol flow passing through its center it is obvious that the aerosol has a major effect on the electron density (Figure 9.3). To establish whether convective losses are the dominant loss mechanism in the ICPT equation 3.25, repeated here for convenience

$$(n_e)_{equi} - n_e = \tau \nabla I$$

which in the case of convective losses being dominant reduces to

$$(n_e)_{equi} - n_e = \tau \left[u_z \frac{\partial n_e}{\partial z} \right]$$

was used to obtain an estimate of u_z. Assuming that the electron density results obtained for the central region of the coolant-only plasma are those of a plasma in equilibrium. And that the decrease in electron density with height, for the analytical plasma is due entirely to convective losses along the torch then this equation becomes

$$u_z = \frac{3.8 \times 10^{21} \times 2 \times 10^{-3}\ 0.2 \times 10^{21}}{2.5 \times 10^{-3}} \qquad (9.12)$$

giving a velocity of

$$u_z \approx 24 \text{ m/s} \qquad (9.13)$$

as compared to the ≈ 18 m/s expected, taking into account the aerosol flow-rate and aerosol tube diameter. It is also in excellent agreement with experimental results obtained elsewhere (Gouesbet *et al.* 1975, 1977; 15m/s and Barnes *et al.* 1981; 18 to 30m/s).

This result clearly demonstrates that convection is the dominant cause of the

deviation from excitational equilibrium in the central region of the plasma.

9.4. Recombination Rate

Following from Bates and Dalgarno (1962) in a plasma of moderate density, such as the ICPT

$$\frac{dn_e}{dt} = \Upsilon n_e^2 \tag{9.14}$$

where Υ, the collisional-radiative decay coefficient, is an effective two body rate coefficient defined by

$$\Upsilon = \alpha_{cr} - S\frac{n(1)}{n_{ion}} \tag{9.15}$$

where

α_{cr} is the collisional-radiative recombination coefficient

S is the collisional-radiative ionisation coefficient

$n(1)$ is the population density of the ground state

and

n_{ion} is the ion population density.

α_{cr} is an effective recombination coefficient and controls the plasma decay when the electron density is well above the equilibrium value. It follows that immediately after removal of the RF field the sharp increase in intensity of the excited argon spectral lines shows that the electrons have relaxed to the temperature of the heavy particles thus implying that the degree of ionisation in the plasma exceeds the equilibrium value. Therefore, provided recombination occurs within the volume, that is, the loss of recombining pairs from the plasma is small, the coefficient of recombination can be estimated from the decrease in intensity of the continuum. Results in Chapter 8 show that diffusion losses from the system are significant only when there is an aerosol flow. Thus (without aerosol flow) measuring the rate of decay in the electron density shortly after removal of the RF field and using the condition

$$\frac{dn_e}{dt} = -\alpha_{cr} n_e^2 \tag{9.16}$$

the collisional-radiative recombination coefficient α_{cr} can be determined.

The rate of decay in the electron density was measured at a height of 5mm above the work-coil for a plasma supplied with coolant gas of 10 litres/minute and input power of 1200 Watts. This yielded a value for α of $\approx 2-5 \times 10^{-17}$ m ^{3}s^{-1} which is of the same order of magnitude as that of the collisional-radiative recombination

coefficient for Hydrogen calculated by Bates, Kingston and McWhirter (1962), 1.7×10^{-17} m $^3s^{-1}$ at 8000 K.

9.5. Summary

The electron density present in the ICPT has been determined by several different methods and is consistent with values obtained elsewhere (see Chapter 2). The comparison of directly measured electron density and the value calculated from Saha's equation using experimentally determined temperatures allows a direct test of the validity of Saha's equation for the ICPT. In other words, this gives an independent measure of the degree of equilibrium in the plasma. The decrease in the electron density and the differences that arise between the values obtained using the Saha equation and the other three methods with the introduction of the aerosol flow confirms that the losses caused by this flow are the major reason for the deviation from equilibrium. This is further substantiated by the calculation of the diffusion velocity which yielded a result in good agreement with the available experimental data.

Chapter 10

Discussion and Conclusions

Much of the work presented in this thesis is fundamental in that the study of the transient behaviour of a ICPT plasma, in particular, and atmospheric pressure plasmas in general has seldom been reported in the literature. However, apart from the determination of the state of equilibrium and the excitation mechanism in an analytical plasma, this is a regime where quenching processes can be readily observed and with the increasing interest in plasma chemistry it is useful to establish the thermodynamic conditions prevailing under such circumstances.

The different relaxation times of the various components of the plasma have been used to provide a means of investigating the physical properties of the plasma. The resulting sharp increase of the (optically-thin) spectral line intensities upon the removal of the RF field is in itself an indication of the following properties prevailing in the plasma:

i) the electrons are at a higher temperature than the gas particles;

ii) the excited states above the resonance level are coupled by the free electrons to the continuum.

To determine the state of excitation equilibrium and the degree of deviation from kinetic equilibrium the variation in behaviour of the emission from the excited argon I states under different operating conditions was studied. For the evaluation of this data various requirements needed to be met and in the preliminary experimental work (Chapters 6 and 7) the (plasma) conditions required to enable the use of the relaxation method (Chapter 4) were examined, together with the necessary pre-requisites for spectroscopic measurements such as the existence of suitable optically-thin spectral lines. It was shown that valid measurements could be obtained using

argon spectral lines whose wavelengths were less than $\approx$ 760 nm. At wavelengths greater than this the spectral lines could no longer be considered optically thin, and indeed the 811.5nm argon I spectral line was found to be approaching optical saturation. This effect permitted the observation of changes in the radiative losses from the ICPT under different operating conditions.

One of the preliminary results which must be noted, since it has a bearing on all previous experimental studies where Abel's transform has been used to convert lateral results into radial ones, is the absence of axisymmetry. The standard method of establishing the presence of axisymmetry, a lateral scan of the spectral line intensity, was found to be insufficient. Scans of the plasma using the spectral line intensity ratio $\frac{I^*}{I}$ (where I and I^* are the intensities, of a particular spectral line, before and after the RF field is removed) revealed the presence of an asymmetry in situations where the standard method had indicated that the plasma was axisymmetrical. Nevertheless, scans of the intensity ratios show that the plasma was axisymmetrical at certain observation heights and under suitable operating conditions. However due to the vortex coolant flow pattern and the geometric shape of the work-coil, doubts remain as to whether the plasma in the ICPT can be considered completely axisymmetric anywhere. Although the measurement of flow patterns in the ICPT is very complex it will have to be in this area, together with further investigative work using the relaxation method, that this question can be answered.

As the plasma is close to equilibrium it was possible to use the equilibrium relations themselves as tools with which to investigate the degree of deviation from equilibrium and its cause. A series of experiments were performed to establish the cause of the deviation from equilibrium. With only a single gas flow (coolant), at the normal operating power of 1200W the relaxation method showed that the plasma formed could be considered to be in at least pLTE above the work-coil in the central region of the plasma, with the temperatures of the various different components being approximately equal. The plasma remained in excitational equilibrium out to radius of $\approx$7mm. The temperature difference $(T_e - T_g)$ in the region of RF heating (r $\approx$ 4-7mm) varied from approximately $6\%T_e$ at height of 5mm above the top of the work-coil to approximately $30\%T_e$ at a height 15mm below the top of the work-coil (i.e. 5mm below the bottom of the work coil). The argon excited states deviated noticeably from a Boltzmann distribution at radii greater than 7mm. Observations of the 811.5nm Ar I spectral line indicated that this line was optically trapped for the plasma in excitational equilibrium.

The next stage of the experimental investigation was to study the effect of operating the torch with its normal two gas flows by the introduction of an argon gas flow (aerosol) through the center of the plasma. This caused a significant deviation from pLTE over a large region of the plasma. At an aerosol flow of 1 litre/minute, the excited argon I states no longer conformed to a Boltzmann distribution. Although the results obtained with an aerosol flow-rate of 2 litres/minute appeared to indicate a return to excitation equilibrium, the values obtained for the electron temperature (> 60,000 K) clearly showed the system was inconsistent with predictions of the Saha equation. Observations of the 811.5nm spectral line showed that the near-infrared 4s - 4p transitions were no longer close to saturation. These results suggested that the introduction of the aerosol flow reduced the collision rate to such an extent that collision processes were no longer dominant down to the 4s level, implying that the 4s level is over-populated.

As the normal operating condition when the ICPT is employed for analytical work requires an aerosol flow of 2 litres/minute, further experiments were performed with constant gas flows of 10 and 2 litres/minute for coolant and aerosol respectively to investigate the effects of changing various other operating conditions. Lowering the input power to 800 Watts appeared bring the plasma closer to excitational equilibrium although the difference ($T_e - T_g$) between the temperatures increased.

The introduction of various samples into the plasma via the aerosol flow caused additional disturbance of the plasma equilibrium. Samples consisting of H_2 or air had the largest effect, although even this effect was small compared to that caused by the introduction of the aerosol flow. It may be noted that these results indicated that the commonly used assumption that the introduction of a small amount of hydrogen into a plasma for diagnostic purpose has a negligible effect on the plasma characteristics is an unrealistic simplification. The introduction of solution of pure water as a sample had very little effect, and similarly the introduction of an easily ionised element into the plasma also had little or no further effect on the plasma parameters.

The implication that a decrease in the collisional rate (as a result of the introduction of the aerosol flow) is the cause of the deviation from excitational equilibrium was investigated by undertaking measurements of the electron density. Measurements were obtained by four different experimental methods. Initial comparisons of results for the single flow plasma showed excellent agreement between all four methods in the central region of the plasma. However, for a plasma containing an aerosol flow (that is when the plasma deviated from excitational equilibrium) measurements of electron density using the method based on the use of Saha's

equation differed significantly from other three methods.

A comparison of the the electron densities before and after the introduction of the aerosol flow indicated that the dominant loss mechanism is consistent with being convection due to the forced flow of argon through the torch. An estimate of the the relevant velocity was obtained which was in good agreement with that obtained experimentally by Barnes and Genna (1981) and the expected value in the present experiments.

The results in this thesis demonstrate that it is the introduction of the aerosol flow through the center of the plasma that is the dominant cause of the deviation from equilibrium present in the central region of an ICPT. This decreases the electron density and it is this reduction together with the corresponding decrease in optical depth rather than temperature differences between the various plasma components which determines the plasma's characteristics. As a decrease in the electron density automatically implies a decrease in the collision rate (at constant temperature) and because electron collisional excitation is the dominant means of redressing the balance of a lower level being populated by radiative and collisional transitions from above, the de-population rate of this level is reduced. This effects the lower levels first (e.g. gives rise to an overpopulation of the 4s level), and as the deviation from excitational equilibrium increases, progressively affects the higher levels.

Initial experiments using the relaxation method indicated that the electron temperature remains higher than the gas temperature, due to the presence of RF heating, up to a height of 15mm above the work-coil; however, limitations imposed by the available diagnostic equipment restricted the majority of the investigative work to a height of 5mm above the work-coil. Thus while the plasma state at the normally used observation height of 15mm was not directly measured the evidence of a lack of axisymmetry together with the deviation from excitational equilibrium throws into doubt many of the results obtained elsewhere that have assumed the plasma is axisymmetric and/or that the Boltzmann distribution and the two-line method yielded accurate results, particularly for temperature measurements.

Other considerations were that with the absence of a suitable polychromator the experimental work was time consuming which led to the increased possibility of errors occurring unless there was considerable duplication of measurements. However these results provide a base from which to proceed. Modifications to decrease the switch-on time of the RF field, from $\approx 30\mu s$ down to $\approx 3\mu s$ (that is, the same as the switch-off time) would permit the study of the reverse processes to that studied here (e.g.

ionisation rate) and thus it would be possible to form a more complete picture of the thermodynamic state of a ICPT plasma.

To conclude, the results presented in this thesis in terms of the analytical properties of the ICPT indicated that the introduction of molecular samples into the plasma via the aerosol flow had very little effect on the properties of the plasma. The absence of excitational equilibrium in what is basically the energy source for A.E. spectroscopic analysis, implies that the sample being excited will also not be in excitational equilibrium. And while it was not possible to investigate whether the plasma has reached excitational equilibrium in the observation zone ($\approx$ 15mm above the work-coil) used for sample analysis, the presence of a temperature difference and the known analytical properties suggest that it has not.

As it is the gas flow through the torch (both coolant and aerosol) that is the cause of the deviation from equilibrium it is suggested that future development work should focus on low flow torchs along the lines of that developed by Angleys and Mermet (1984). In this development, the accent should be on the reduction on the aerosol gas flow necessary to introduce the sample into the plasma rather than concentrating solely on the coolant flow-rate.

In terms of the establishment of a theoretical model the results presented in this thesis suggest that further study along the lines of Aeschbach (1982), Huang and Liu (1986) would be useful in aiding the understanding the basic physical processes that shape the plasma. However, to understand the effect of the collisional and radiative processes which govern the population densities of the various energy states and thereby the emission characteristics of the ICPT, further work along the lines followed by Giannaris and Incropera (1973) is required.

Appendix A

Formation of the ICPT Plasma

A.1. Introduction

The relaxation method used to investigate the state of equilibrium prevailing in the steady-state ICPT required the repetitive pulsing of the RF field. Provided the off pulse was sufficiently short, enough electrons remained within the RF field to re-ignite the plasma. This allowed the study of repetitive pulses under identical operating conditions, without the somewhat laborious job of restarting the plasma, and also permitted the investigation of the formation of the plasma. As the circuitry used to reinstate the RF field during pulsing produced a relatively slow switch-on it was not possible to study in detail the re-ignition processes of the plasma (auto-ionisation, ionisation rate) and their effect on the development of the steady state. However as was noted in Chapter 6 the long term initial behaviour of the plasma ($\approx$ first 8 milliseconds) requires some explanation. Photographs 6.1 and 6.2 show the 696.5nm Ar I spectral line and the continuum intensity at 450.0nm over a period of 10 milliseconds from when the RF field is removed until the plasma has regained its original steady-state condition.

Initial measurements showed that the oscillatory behaviour occurs predominately above the work-coil (see Photographs A.1 to A.6) and increases with the length of time for which the RF field is removed (Photographs A.7 and A.8). This suggests that the variation in the emitted light intensity is due to the presence of bulk motion induced in the plasma by the heating of the argon upon the return of the RF field. This motion gradually decreases as the processes governing the behaviour of the plasma reached their steady-state levels.

To further investigate these intensity oscillations the variation in the intensity of

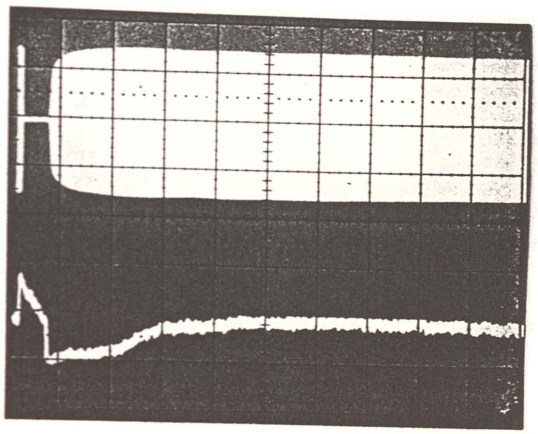

Photograph A.1: Intensity variation: 15mm below top of work-coil.
Spectral line; 696.5nm Ar I, Time-scale; 1 msec/div.

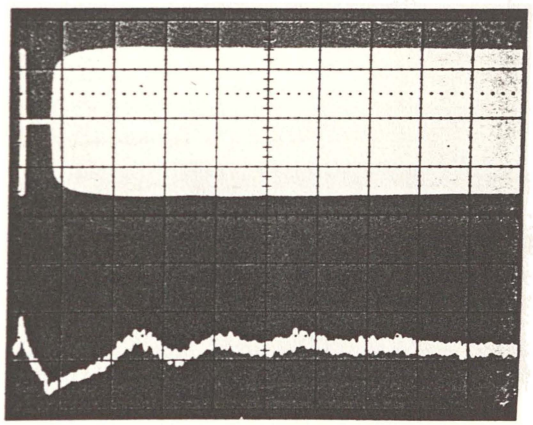

Photograph A.2: Intensity variation: middle of work-coil.
same parameters as Photograph A.1.

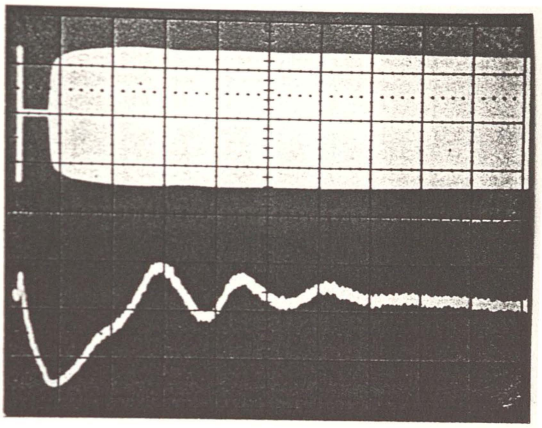

Photograph A.3: Intensity variation: 2.5mm above top of work-coil.
Same parameters as Photograph A.1.

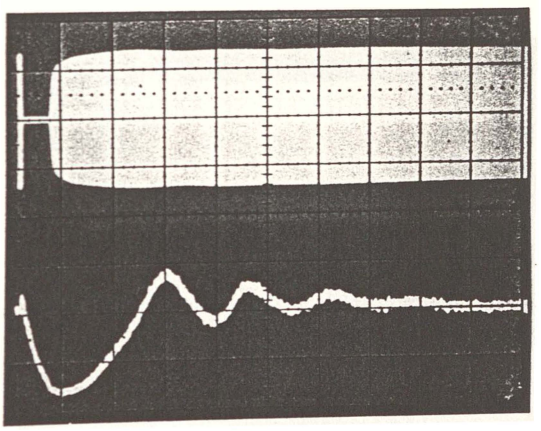

Photograph A.4: Intensity variation: 5mm above top of work-coil.
same parameters as Photograph A.1.

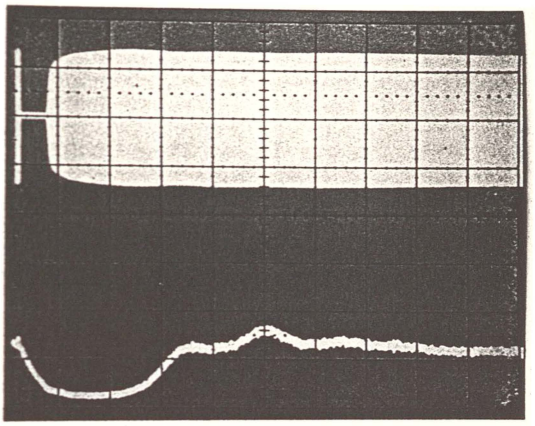

Photograph A.5: Intensity variation: 10mm above the top of work-coil.
Same parameters as Photograph A.1.

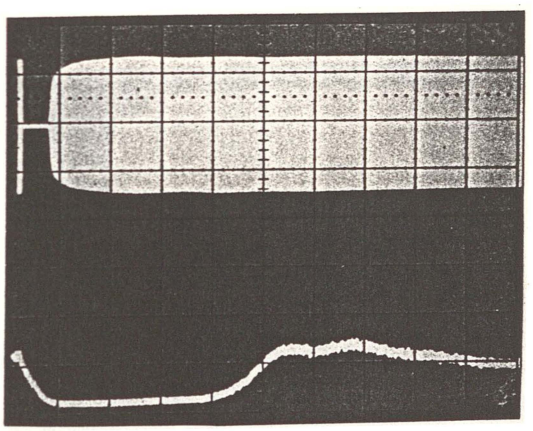

Photograph A.6: Intensity variation: 15mm above the top of work-coil.
same parameters as Photograph A.1.

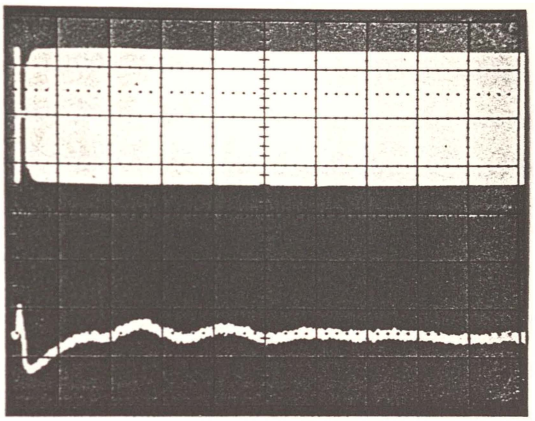

Photograph A.7: Dependence of Intensity variation on Pulse length. Pulse Length = $125\mu s$.
Same parameters as Photograph A.1.

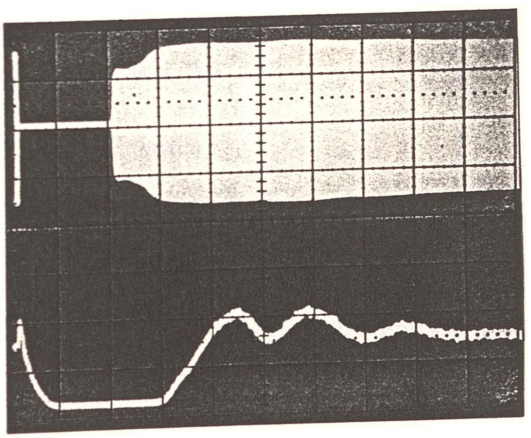

Photograph A.8: Dependence of Intensity variation on Pulse length. Pulse length = 1.8 ms.
same parameters as Photograph A.1.

the 696.5nm Ar I spectral line with respect to time were measured. Lateral scans of the the intensity for the first 10 milliseconds after the RF field was pulsed off were obtained. Using Abel's Transform these were converted to radial values and are given in Figure A.1. The plasma was formed under normal operating conditions, that is with an input power of 1200 Watts and a coolant only gas flow of 10 l/min. The observation height was 5mm above the top of the work-coil. The length of time the RF field remained off was set at 250μs and the time is taken from the instant the RF field is switched off. The radial variation in intensity with time suggests that the plasma is expanding and contracting.

Using the same nine argon spectral lines as were used previously in the body of the thesis an estimate of the excitation temperature was obtained from a Boltzmann plot over the same time interval as given in Figure A.1 (see Figure A.2). These results show that while the central region stabilises rapidly the outer regions of the plasma oscillates both in intensity and temperature around the final steady-state values.

From these results it is concluded that bulk motion of the plasma gives rise to the intensity oscillations. To confirm this conclusion it was noted that physical changes in the plasma volume are governed by the mean thermal velocity and it is possible to obtain an estimate of this velocity from the period of the plasma oscillations. That is, the diffusion velocity is given by

$$\bar{V} \approx \frac{s}{t} \tag{A1}$$

$$= \frac{(2 \times 10^{-2})}{(1.6 \times 10^{-3})} \tag{A2}$$

$$\approx 12.5\text{m/s} \tag{A3}$$

where s is the torch diameter and t is the period of oscillation. The diffusion velocity can also be calculated from the following.

Considering the motion of an argon atom as a random walk then the diffusion velocity in the horizontal direction is given by

$$\bar{V} = \frac{d}{T} \tag{A4}$$

where T is the time taken for N collisions and the distance d is defined by

$$d^2 = N\lambda^2 \tag{A5}$$

where λ is the mean free path. Thus it follows that since the collision frequency is given by

$$\upsilon = n\sigma\bar{v} \tag{A6}$$

where σ is the collision cross-section, n is the gas density and $\bar{v}$ is the mean thermal velocity then

$$\bar{V} = \frac{dn\sigma\bar{v}}{N} \tag{A7}$$

which reduces to

$$\bar{V} = \frac{\lambda}{d}\bar{v} \tag{A8}$$

since

$$N = \left(\frac{d}{\lambda}\right)^2 \tag{A9}$$

and

$$\lambda = \frac{1}{n\sigma}. \tag{A10}$$

Under the conditions prevailing in the ICPT ($n \approx 7 \times 10^{23}\ m^{-3}$, $\sigma \approx 10^{-20}\ m^2$) the mean free path would be $\approx 10^{-4}$ m. Substituting the value for the diffusion velocity given above yields a value for the mean thermal velocity of

$$\bar{v} = \frac{2 \times 10^{-2} \times 12.5}{10^{-4}}$$

$$= 2.5 \times 10^3\ m/s. \tag{A11}$$

Calculating the mean thermal velocity directly, using the temperature obtained in the main body of the thesis ($\approx$ 10,000 K), gives

$$\bar{v} = \left(\frac{8kT}{\pi m}\right)^{\frac{1}{2}}$$

$$= \left(\frac{8 \times 1.38 \times 10^{-23} \times 10^4}{40 \times 1.66 \times 10^{-27}}\right)^{\frac{1}{2}}$$

$$\approx 2.3 \times 10^3\ m/s \tag{A12}$$

The excellent agreement between these values thereby confirming that the oscillations in the emitted light intensity is due to bulk motion of the plasma.

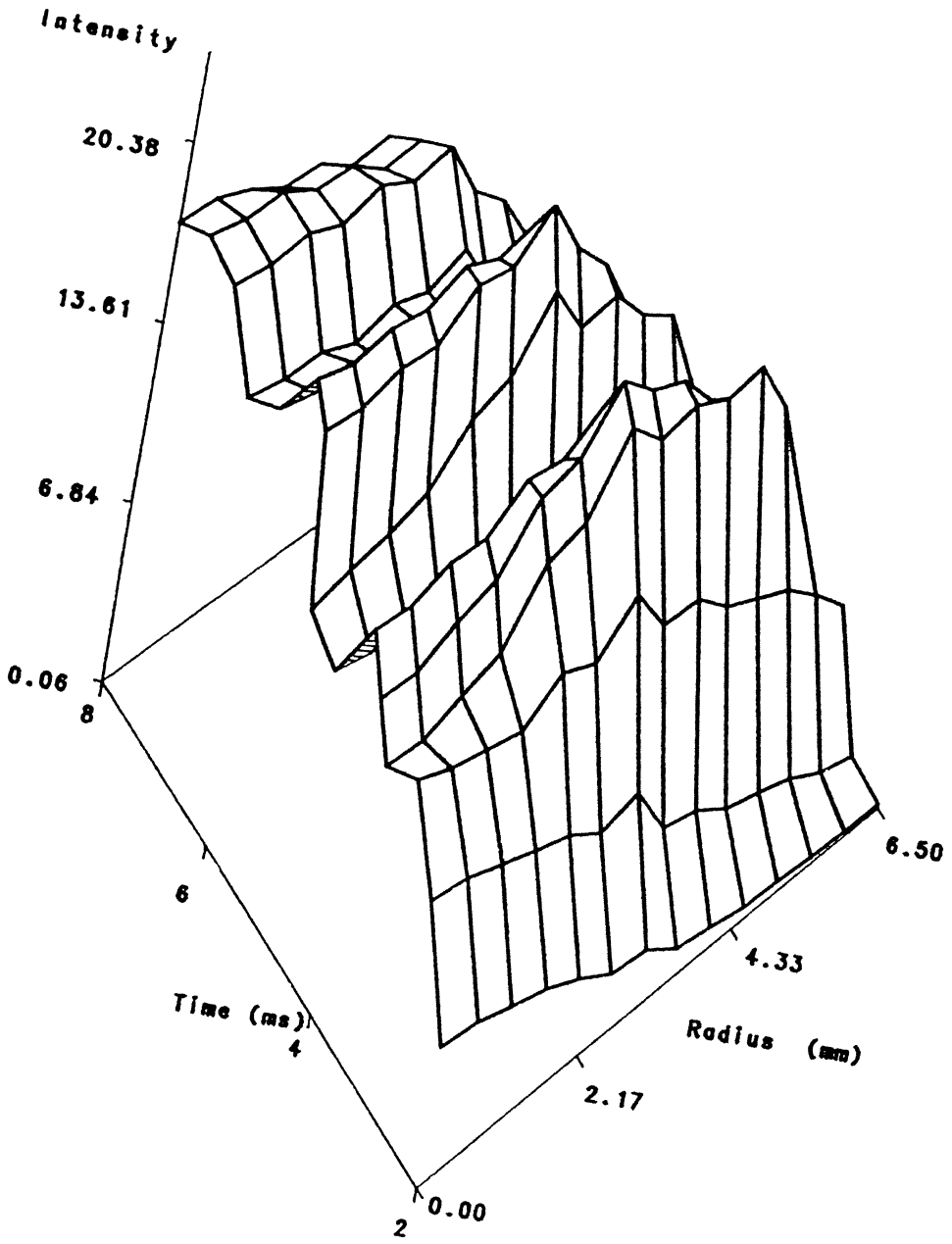

Figure A.1: Variation in the Radial Intensity of the 696.5nm Ar I Spectral Line with Time The time is taken from when the RF field is pulsed off. Off period = 250μs

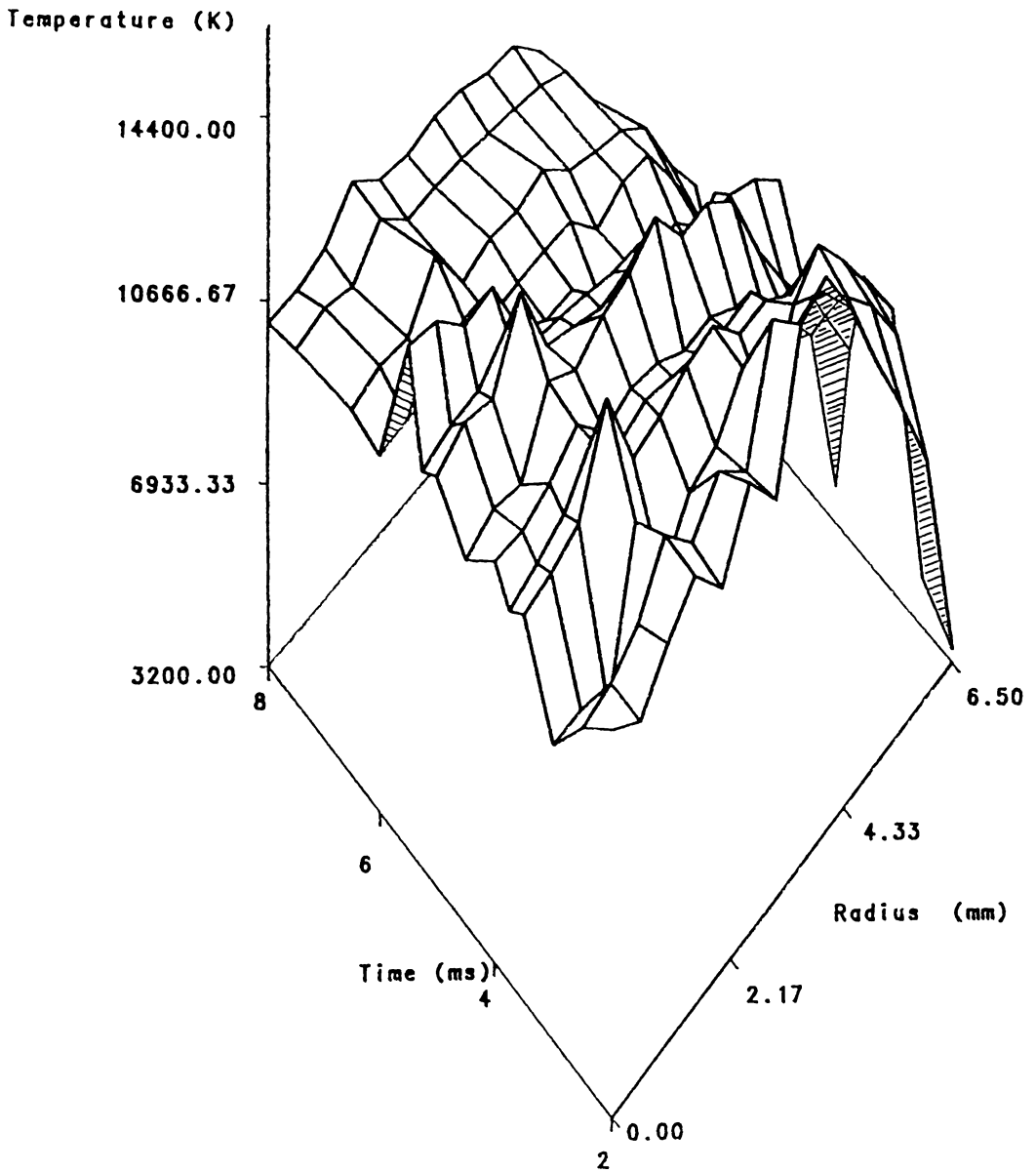

Figure A.2: Variation in the Excitation Temperature with Time.
Same parameters as Figure A.1

Appendix B

Plasma Torch Specifications

This Appendix details by means of schematic diagrams the Plasma Torch's design and specifications. The design is a modification of a torch used by Bouman and De Boer (1978). The modifications allow for the rapid replacement of any part of the torch assembly that arises from wear and tear or by accident. Re-alignment of the torch tubes is facilitated by the securing of each tube of the torch to a separate section of the torch base. The construction materials are aluminum for the base and quartz for the three tubes. Assembly is straight forward but it should be noted that for the successful operation of the torch the ends of the quartz tubes, especially the middle tube, should be flame polished.

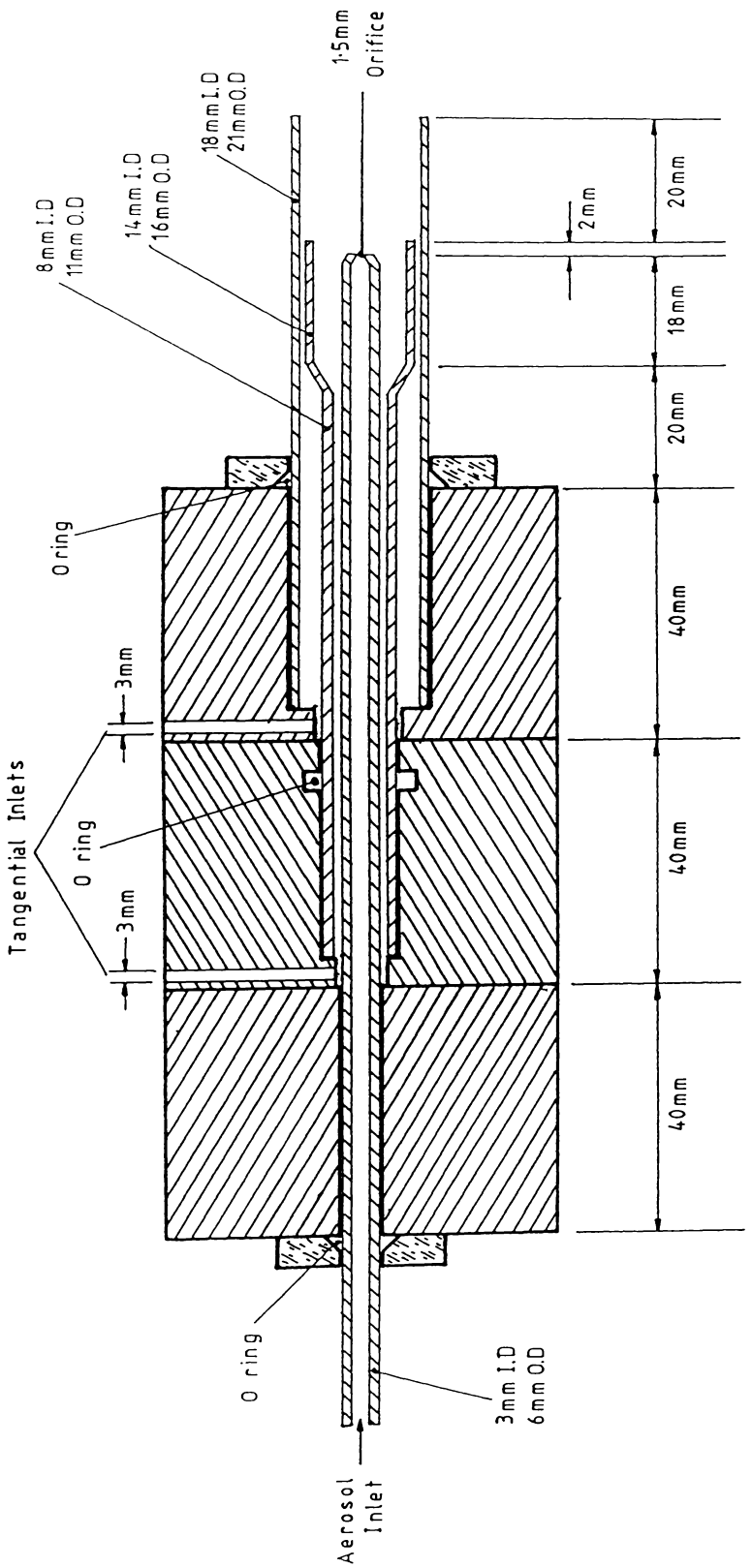

Figure B.1: Plasma Tube Configuration.

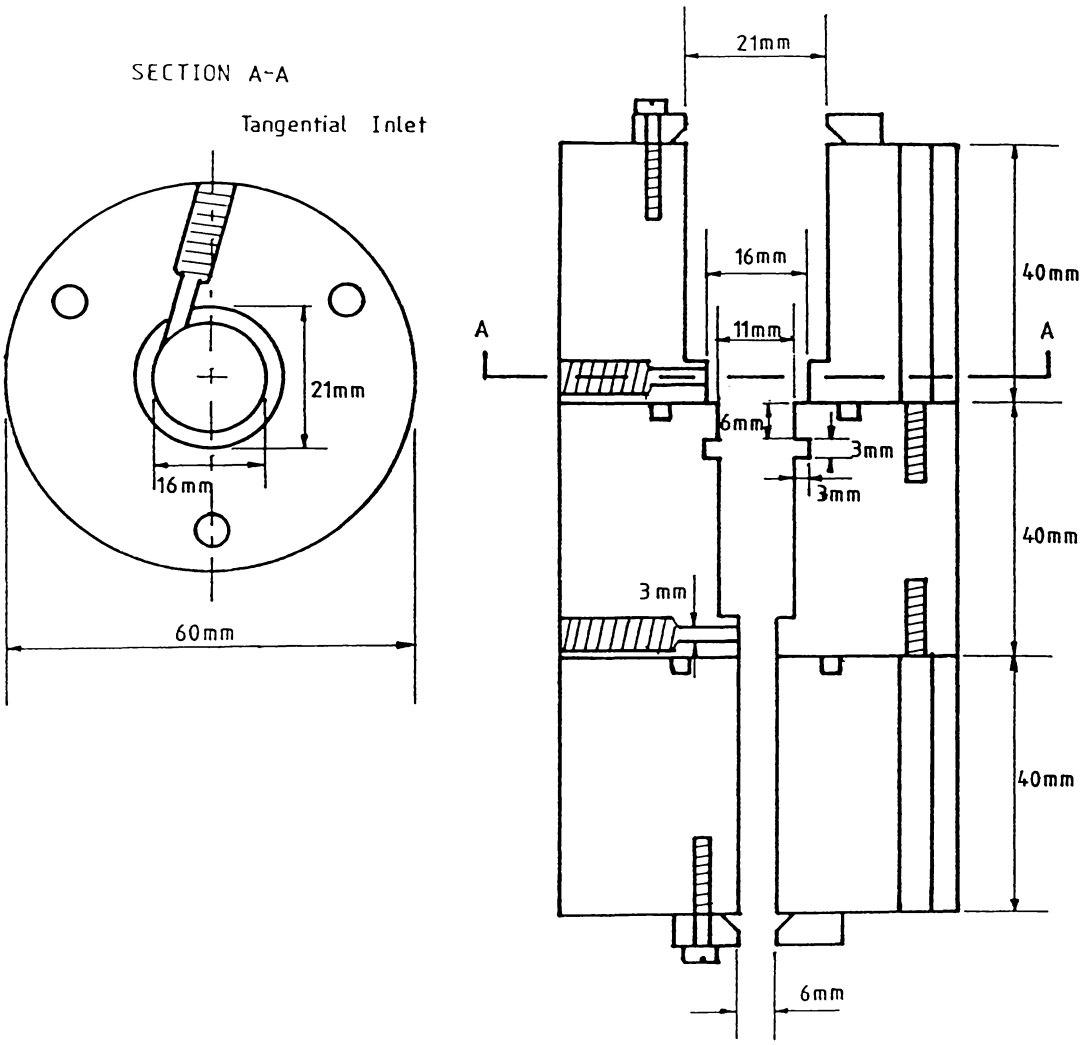

Figure B.2: Schematic of the Torch Base.

Appendix C

Circuit Diagrams of the Path-length Compensator

This appendix gives the circuit diagrams for the path-length compensator used in the interferometer described in Chapter 5 and that was used to obtain the electron density measurements given in Chapter 9. It contains the mirror drive, pyro-detector amplifier and chopper circuits.

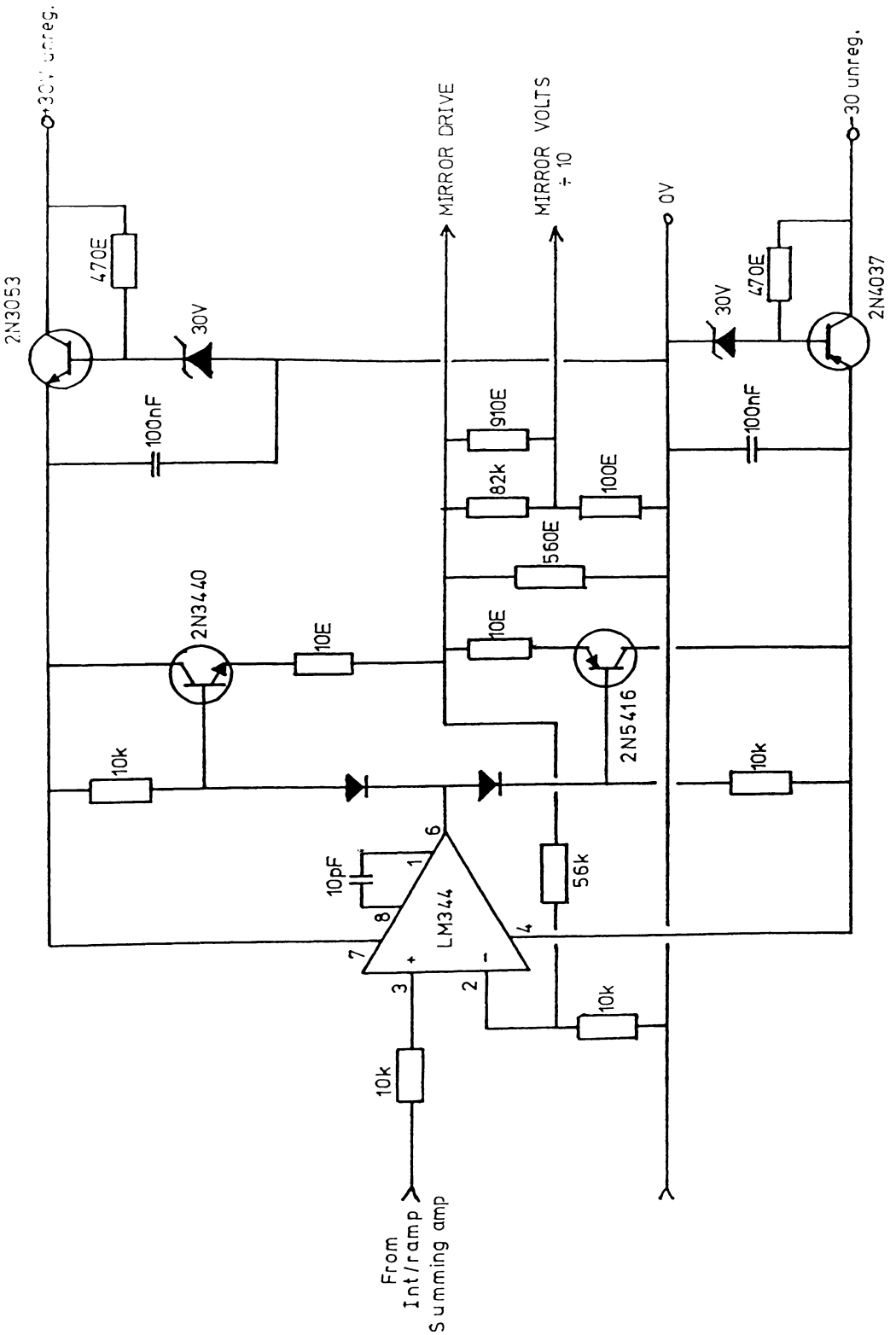

Figure C.1: Schematic of the Mirror Drive Circuit.

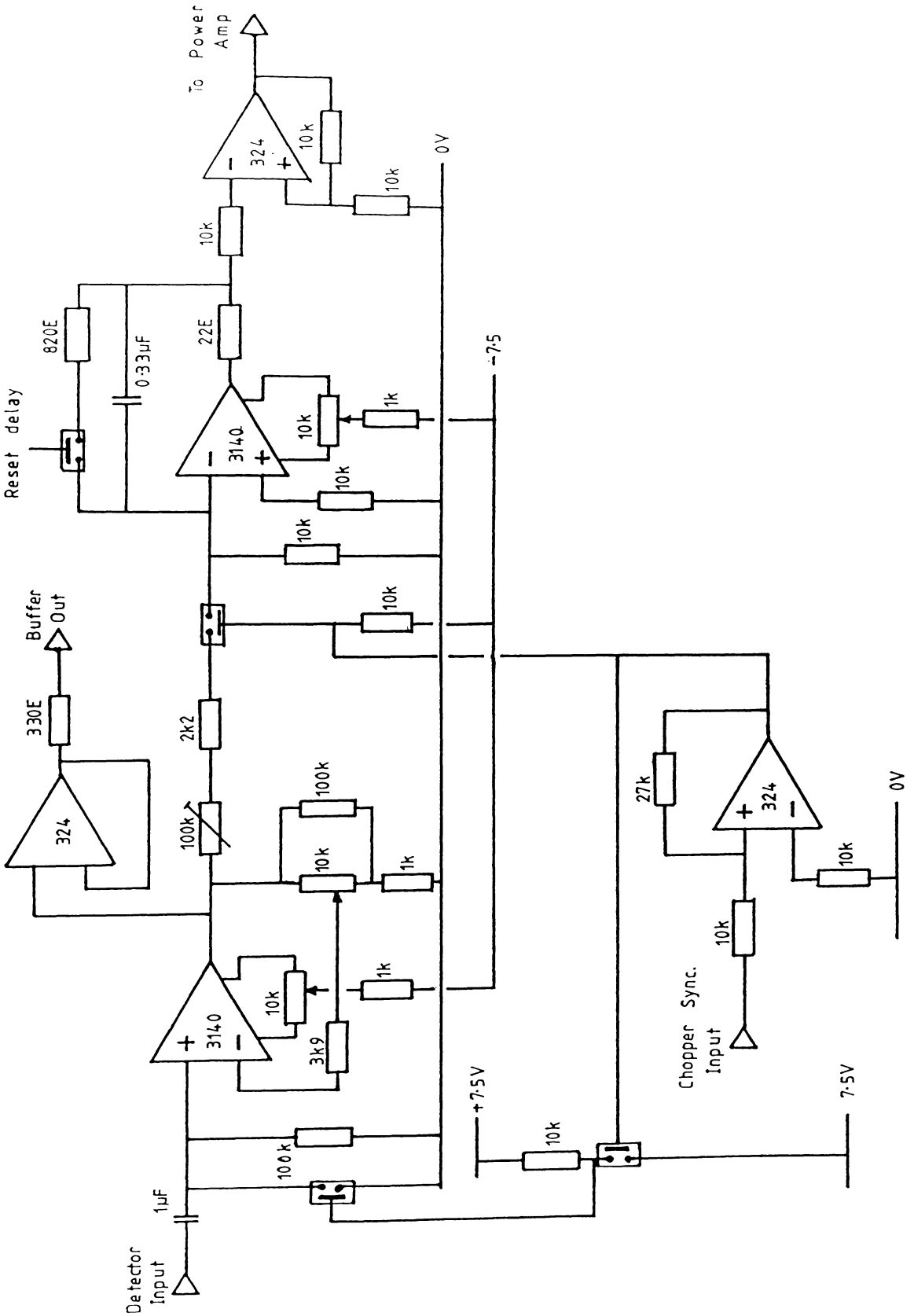

Figure C.2: Schematic of the Pyro-detector Amplifier Circuit.

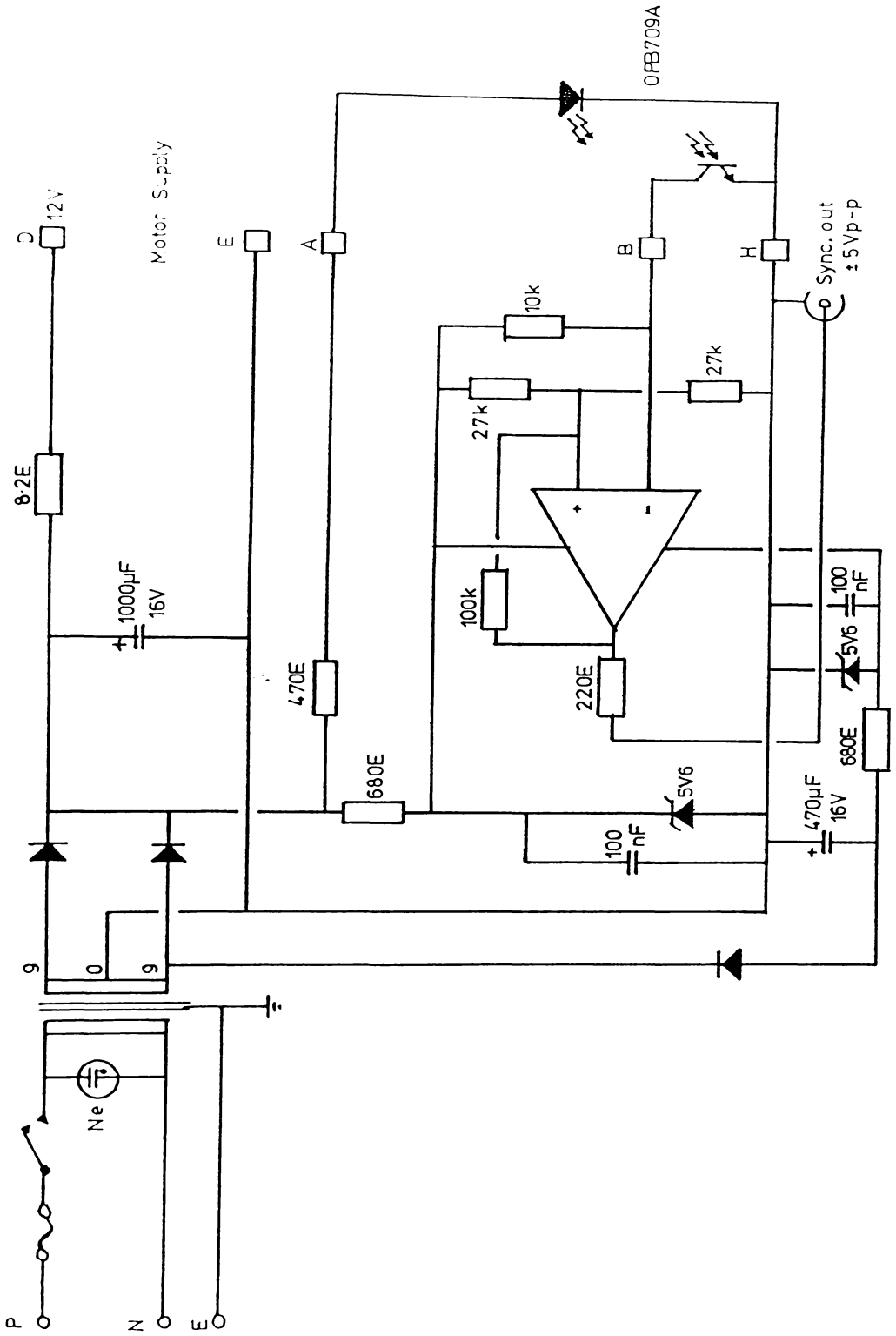

Figure C.3: Schematic of the Chopper Circuit.

Bibliography

Aeschbach, F. (1982). Evaluation eines Elektronendiffusionsmodelles zur Berechnung von nicht Gleichgewichts-Elektronenkonzentrationen im Induktivgekoppelten Argonplasma fur die spektrochemise Analyse. *Spectrochimica Acta* v37B(11), p987-998.

Adler, J.F., Bombelka, R.M. and Kirkbright, G.F. (1980). Electronic Excitation and Ionisation Temperature Measurements in a High-Frequency Inductively Coupled Argon Plasma Source and the Influence of Water-vapour on Plasma Parameters *Spectrochimica Acta* v35B, p163-175.

Alder, J.F. and Mermet, J.M. (1973). A spectroscopic study of some radio frequency mixed gas plasmas. *Spectrochimca Acta* v28B, p421-433.

Alexandrov, V.Ya., Gurevich, D.B. and Podmoshenskii, I.V. (1967). A Study of the Mechanism of Excitation and Ionisation in the Plasma of an Argon Arc. *Optical Spectroscopy* v23, p282-286.

Aleksandrov, V., Gruzdeva, N.S. and Podmoshenskii, I.V. (1974). Spectroscopic determination of ionisation equilibrium by modulation of discharge current. *Optical Spectroscopy*
v37(4), p369-371.

Aleksandrov, V., Gurevich, D., Podmoshenskii, I. and Khlopina, S. (1976). Recombination in a nitrogen arc. *Soviet Physics-Technical Physics* v21(3), p296-300.

Allemand, C.D. and Barnes, R.M. (1977). A Study of Inductively Coupled Plasma Torch Configurations. *Applied Spectroscopy* v31(5), p434-443.

Allemand, C.D. and Barnes, R.M. (1978). Design of a fixed-frequency impedance matching network and measurement of plasma impedance in an inductively coupled plasma for atomic emission spectroscopy. *Spectrochimica Acta* v33B, p513-534.

Apler, R.A. and White, D.R. in Plasma Diagnostic Techniques edited by Huddlestone, R.H. and Leonard, S.L. (1965). *Plasma Diagnostic Techniques*, Academic Press, New York.

Angleys, G. and Mermet, J.M. (1984). Theoretical Aspects and Design of a Low-Power, Low Flow-rate Torch in Inductively Coupled Plasma Atomic Emission Spectroscopy. *Applied Spectroscopy* v38(5), p647-653.

Apsit, A.R. (1971). Steady-state Inductive Discharge in Argon at Atmospheric Pressure. *Soviet Physics-Technical Physics* v15(7), p1180-1182.

Aref'ev, V.I., Grishin, S.D., Kuz'min, L.A., Leshkov, L.V. and Mikhalev, V.G. (1973). Aspects of a High-Frequency Induction Discharge in Argon. *Soviet Physics High Temperature* v11(2), p256-260.

Asinovskii, E.I., Vasilyak, L.M., Kirillin, A.V. and Markovets, V.V. (1975). Nanosecond Discharge in a Weakly Ionised Plasma. *Soviet Physics-High Temperature* v13(1), p40-44.

Bacri, J. and Lagreca, M. (1983). Departures from CLTE composition in a nitrogen arc at atmospheric pressure: II. Interpretation of departures from CLTE. *Journal of Physics D: Applied Physics* v16, p841-854.

Bacri, J., Gleizes, A., Gomes, A.M. et Vacquie, S. (1976). Mesure des densites locales d'atomes metastables dans un arc stabilise par parois. *Revue generale de L'electricite* v85, p705-709.

Baessler and Kock, (1980). An Interferometric and Spectroscopic Study on a High-Current Argon Arc. *Journal of Physics B* v13(7), p1351-1361.

Barber, C.R. (1946). Factors affecting the Reproducibility of Brightness of Tungsten Strip Lamps for Pyrometer Standardization. *Journal of Scientific Instruments* v23, p238-242.

Barnes, R.M. (1982). Recent advances in analytical atomic radiofrequency emission spectroscopy. *Philosophical Transactions of the Royal Society, London A* v305, p499-508.

Barnes, R.M. (1984). Progress in Inductively Coupled Plasma Analytical Spectroscopy. *Journal of Testing and Evaluation* v12, p194-202.

Barnes, R.M. (1985). Application of Inductively Coupled Plasma Spectroscopy for the Analysis of Ceramics and Glasses. *Materials Science Research* v19, p31-42.

Barnes, R.M. and Genna, J.L. (1981). Gas flow dynamics of an inductively coupled plasm discharge. *Spectrochimica Acta* v38B(4), p299-323.

Barnes, R.M. and Schleicher, R.G. (1981). Temperature and velocity distributions in an inductively coupled plasma. *Spectrochimica Acta* v36B, p81-101.

Barnett, W.B., Fassel, V.A. and Kniseley, R.N. (1970). An experimental study of internal standardization in analytical emission spectroscopy. *Spectrochimica Acta* v25B, p139-161.

Batal, A., Jarosz, J. and Mermet, J.M. (1981). A spectrometric study of a 40 MHz inductively coupled plasma-VI. Argon continuum in the visible region of the spectrum. *Spectrchimca Acta* v36B(10), p983-992.

Bates, D.R., Kingston, A.E. and McWhirter, R.W.P. (1962). Recombination between electrons and atomic ions I Optically thin plasmas. *Royal society of London. Proceedings. Section A.* v.A267, p297-312.

Bates, D.R. (1962). *Atomic and Molecular Processes.* Academic Press, New York.

Bates, D.R. and Dalgarno, G. (1962). Electronic Recombination Processes. *Atomic and Molecular Processes.* Academic Press, New York.

Berdyshev, A.V., Gol'farb, V.M., Dushin, A. and Zemlyankin, V.A. (1971). Experimental Determination of the Flow Parameters of Argon in the Channel of a High-Frequency Plasmatron. *Soviet Physics-High Temperature* v9(2), p329-334.

Berman, S.S. and McLaren, J.W. (1978). Establishment of Compromise Conditions for Multielement Analysis by Inductively Coupled Plasma Emission Spectroscopy: A Preliminary Report. *Applied Spectroscopy* v32(4). p372-377.

Biberman, L.M., Vorob'ev, V.S. and Yakubov, I.T. (1968). Nonequilibrium Low-Temperature Plasma I. Electron Concentration in Nonequilibrium Plasma. *Soviet Physics-High Temperature* v7(2), p193-202.

Biberman, L.M., Vorob'ev, V.S. and Yakubov, I.T. (1968). Nonequilibrium Low-Temperature Plasma II. Energy Distribution of the Free Electrons. *Soviet Physics-High Temperature* v6(3), p369-380.

Biberman, L.M., Vorob'ev, V.S. and Yakubov, I.T. (1970). Nonequilibrium Low-Temperature Plasma. IV. The Ionisation and Recombination Functions. *Soviet Physics-High Temperature* v7(4), p593-603.

Blades, M.W. (1982). Some considerations regarding temperature, electron density, and ionisation in the argon inductively coupled plasma. *Spectrochimca Acta* v37B(10),

p869-879.

Blades, M.W. and Caughlin, B.L. (1985). Excitation temperature and electron density in the inductively coupled plasma-aqueous vs organic solvent introduction. *Spectrochimica Acta* v40B(4), p579-591.

Blades, M.W. and Hieftje, G.M. (1982). On the significance of radiation trapping in the inductively coupled plasma. *Spectrochimca Acta* v37B, p191-197.

Blades, M.W. and Horlick, G. (1981). Interference from easily ionizable element matrices in inductively coupled plasma emission spectrometry-a spatial study. *Spectrochimica Acta* v36B(9), p881-900.

Blades, M.W. and Horlick, G. (1981). The vertical spatial characteristics of analyte emission in inductively coupled plasma. *Spectrochimica Acta* v36B(9), p861-880.

Bobrov, G. (1975). Anomalous skin effect in a plasma cylinder. *Soviet Physics-Technical Physics* v20(3), p305-312.

Bockasten, K. (1964). Transformation of Observed Radiances into Radial Distribution of the Emission of a Plasma. *Journal of the Optical Society of America* v51(9), p943-947.

Borst, W.L. (1974). Excitation of metastable argon and helium atoms by electron impact. *Physical Review A* v9(3), p1195-1200.

Boulos, M.I. (1985). The inductively coupled R.F. (radio frequency) plasma. *Pure and Applied Chemistry* v57(9), p1321-1352.

Boulos, M.I., Gagne, R. and Barnes, R.M. (1980). Effect of Swirl and Confinement on the Flow and Temperature Fields in an Inductively Coupled r.f. Plasma. *The Canadian Journal of Chemical Engineering* v58, p367-375.

Boumans, P.W.J.M, and de Boer, F.J., Dahmen, F.J., Hoelzel, H. and Meier, A. (1975) A comparative investigation of some analytical performance characteristics of an inductively-coupled radio frequency plasma and a capacitively-coupled microwave plasma for solution analysis by emission spectrometry. *Spectrochimca Acta* v30B, p449-469.

Boumans, P.W.J.M. and de Boer, F.J. (1972). Studies of flame and plasma torch emission for simultaneous multi-element analysis-I. Preliminary investigations. *Spectrochimica Acta* v27B, p391-414.

Boumans, P.W.J.M. and de Boer, F.J. (1975). Studies of an inductively-coupled argon plasma for optical emission spectroscopy-III. Interference effects under compromise conditions for simultaneous multi-element analysis. *Spectrochimica Acta* v31B, p355-375.

Boumans, P.W.J.M. and de Boer, F.J. (1975). Studies of an inductively-coupled high-frequency argon plasma for optical emission spectroscopy-II. Compromise conditions for simultaneous multi-element analysis. *Spectrochimica Acta* v30B, p309-334.

Bourasseau, D., Cabannes, F. and Chapelle, J. (1970). Etude de l'equilibre thermodynamique local dans des jets de plasma d'argon. *Astronomy and Astrophysics* v9, p339-349.

Britske, M.E., Ignatko, V.P. and Sukach, Yu.S. (1972). Investigation of a Low-power, High-Frequency Discharge in Argon at Atmospheric Pressure. *Soviet Physics-High Temperature* v10(2), p265-272.

Burmistrov, A.V. and Manoshkin, Yu.V. (1976). Gas breakdown in an rf H discharge. *Soviet Physics-Technical Physics* v21(12), p1488-1491.

Burmistrov, A.V. and Manoshkin, Yu.V. (1977). Gas Breakdown in an RF H discharge. *Soviet Physics-Technical Physics* v21(12), p1488-1491.

Buzykin, O.G. and Burmistrov, A.V. (1983). Breakdown of air in an rf induction discharge. *Soviet Physics-Technical Physics* v28(1), p52-53.

Caughlin, B.L. and Blades, M.W. (1984). An evaluation of the ion-atom emission intensity ratios and local thermodynamic equilibrium in an inductively coupled plasma. *Spectrochimica Acta* v39B(12), p1583-1602.

Chase, J. (1969). *Journal of Applied Physics* v40, p318.

Cheng, T.K. and Casperson, L.W. (1975). Plasma diagnosis by laser beam scanning. *Journal of Applied Physics* v46(5), 1961-1965.

Condon, E.U. and Shortley, G.H. (1935). *The Theory of Atomic Spectra* (1963 ed). Cambridge University Press, London.

Cremers, C.J. and Birkebak, R.C. (1966). Application of the Abel Integral Equation to Spectrographic Data. *Applied Optics* v5(6), p1057-1063.

Czernichowski, A., Chapelle, J. and Cabannes, F. (1970). Etude de jets laminaires de

plasma d'argon et de neon hors d'equilibre. *Academie des sciences. sB. Sciences Physiques* v270(1), p54-57.

Dahlquist, R.L. and Knoll, J.W. (1978). Inductively Coupled Plasma-Atomic Emission Spectrometry: Analysis of Biological Materials and Soils for Major, Trace, and Ultra-trace Elements. *Applied Spectroscopy* v32(1), p1-28.

Desai, S.V., Daniel, E.S. and Corcoran, W.H. (1968). *Review of Scientific Instruments* v39, p612.

Desai, S.V. and Corcoran, W.H. (1968, 1969). *Journal of Quantitative Spectroscopy and Radiative Transfer.* v8, p1721; v9, p1371.

Deutsch, M and Beniaminy, I (1982). Derivative-free inversion of Abel's integral equation. *Applied Physics Letters* v41(1), p27-28.

Deutsch, M and Beniaminy, I (1983). Abel inversion with a simple analytic representation for experimental data. *Applied Physics Letters* v42(3), p237-239.

Deutsch, M and Beniaminy, I (1983). Inversion of Abel's integral equation for experimental data. *Journal of Applied Physics* v54(1), p137-143.

Devine, D.J., Brown, R.M. and Fry, R.C. (1981). A Method for Extending or Repairing Inductively Coupled Plasma (ICP) Torches. *Applied Spectroscopy* v35(3), p332-334.

Dickinson, G.W. (1969). Emission Spectrometric Detection of the Elements at Nanogram per Milliliter Level using Induction-Coupled Plasma Excitation. *Analytical Chemistry* v41(8), p1021-1024.

Donskoi, A.V., Klubnikin, V.S. and Salangin, A.A. (1983). Effect of gas motion on the properties of a two-temperature argon arc plasma in a channel. *Soviet Physics-Technical Physics* v28(4), p424-428.

Drawin, H.D. (1979). Plasma properties and atomic processes at medium and high pressures. *Journal de Physique* v40, pC7-149-170

Dresvin, S.V. (1977). *Physics and Technology of Low Temperature Plasmas.* english edition edited by Echert, H.V., The Iowa State University Press / AMES.

Dresvin, S.V. and El'-Mikati, Kh. (1978). Measurement and calculation of gasdynamic parameters of a high-frequency induced discharge. *Soviet Physics-High Temperature*

v15(6), p1158-1164.

Dresvin, S.V. and Klubnikin, V.S. (1971). Disequilibrium in an Argon Plasma Jet from a High-Frequency Induction Discharge at Atmospheric Pressure. *Soviet Physics-High Temperature* v9(3), p475-482.

Dresvin, S.V., Donskoi, A.V. and Gol'dfarb, V.M. (1966). Determination of the Conductivity of a High-frequency Induction Discharge in Argon by Calorimetric and Spectral Means. *Soviet Physics-Technical Physics* v10(9), p1270-1274.

Dymshits, B.M. and Koretskii, Ya.P. (1969). Evaluation of the effect of electromagnetic forces on the channel of a constricted induction discharge. *Soviet Physics-Technical Physics* v14(6), p779-782.

Ebdon, S. (1986). The Versatile Inductively-Coupled Plasma. *Chemistry in Britain* v22(2), p123.

Edmonds, T.E. and Horlick, G. (1977). Spatial Profiles of Emission from an Inductively Coupled Plasma Source Using a Self-scanning Photodiode Array. *Applied Spectroscopy* v31(6), p536-541.

Ellis, E. and Twiddy, N.D. (1969). Time-resolved optical absorption measurements of excited-atom concentrations in the argon afterglow. *Journal of Physics B:* v2, p1366-1377.

Engelhardt, W. (1973). Establishment of partial local thermal equilibrium in transient and inhomogeneous plasmas. *The Physics of Fluids* v16(2), p217-220.

Fassel, V.A. (1979). Simultaneous or Sequential Determination of the Elements at all Concentration Levels-Renaissance of an Old Approach. *Analytical Chemistry* v51, 1290A-1308A.

Faires, L.M., Bieniewski, T.M., Apel, C.T. and Niemczyk, T.M. (1985). "Top-Down" Verus "Side-On" Viewing of the Inductively Coupled Plasma. *Applied Spectroscopy* v39(1), p5-9.

Faires, L.M., Palmer, B.A. and Brault, J.W. (1985). Line width and line shape analysis in the inductively coupled plasma by high resolution Fourier transform spectrometry. *Spectrochimca Acta* v40B(1-2), p135-143.

Ferreira, C.M. and Loureiro, J. (1984). Characteristics of high-frequency and direct-current argon discharges at low pressures: a comparative analysis. *Journal of Physics D:*

Applied Physics v17, p1175-1188.

Fisun, O.I. (1973). Model of "Ionisation and Recombination Channels" in the Kinetics of Ionisation Relaxation. *Soviet Physics-High Temperature* v10(6), p1062-1067.

Fortin, M. et Meubus, P. (1979). Manifestations et mesures de concentration de metastables dans les jets de plasma d'argon ou d;helium a pression atmospherique dans regions de basses temperatures. *Canadian Journal of Physics* v57, p1594-1603.

Fujimoto, T. (1980). Kinetics of Ionisation-Recombination of a Plasma and Population Density of Excited Ions. I. Equilibrium Plasma. *Journal of the Physical Society of Japan* v47(1), p265-272.

Fujimoto, T. (1980). Kinetics of Ionisation-Recombination of a Plasma and Population Density of Excited Ions. II. Ionising Plasma. *Journal of the Physical Society of Japan* v47(1), p273-281.

Fujimoto, T. (1980). Kinetics of Ionisation-Recombination of a Plasma and Population Density of Excited Ions. III. Recombinig Plasma-High Temperature Case. *Journal of the Physical Society of Japan* v49(4), p1561-1568.

Fujimoto, T. (1980). Kinetics of Ionisation-Recombination of a Plasma and Population Density of Excited Ions. III. Recombinig Plasma-High Temperature Case. *Journal of the Physical Society of Japan* v49(4), p1569-1576.

Furuta, N. and Horlick, G. (1982). Spatial characterization of analyte and excitation temperature in an inductively coupled plasma. *Spectrochimca Acta* v37B(1), p53-64.

Furuta, N., Nojiri, Y. and Fuwa, K. (1985). Spatial profile measurement of electron number densities and analyte line intensities in an inductively coupled plasma. *Spectrochimca Acta* v40B(3), p423-434.

Galan, de L. (1984). Some considerations on the excitation mechanism in the inductively coupled argon plasma. *Spectrochimca Acta* v39B, 537-550.

Galan de, L. and Samaey, G.F. (1970). Measurement of degrees of atomization in premixed, laminar flames. *Spectrochimica Acta* v25B, p245-259.

Gaucherel, P., Rowe, B., Queffelec, J.L., Jemaa, N.B. and Gomet, J.C. (1979). Observation de L'emission de L'exciplexe Ar H dans des Jets de Plasma D'argon-hyrogene Rarefies. *Journal de Physique* v40, pC7 91-92.

Gettel, L.E. and Curzon, F.L. (1982). Energy transport in DC and AC vortex stablised arcs. *Journal of Physics D: Applied Physics* v15, p845-865.

Giannaris, R.J. and Incropera, F.P. (1973). Radiative and collisional effects in a Cylindrically confined plasma-I. Optically thin considerations. *Journal of Quantitative Spectroscopy and Radiative Transfer* v13, p167-181.

Gippius, E.F., Lljukhin, B.I. and Kolesnikov, V.N. (1979). Some Remarks on the Non-Equilibrium Plasma Diagnostics. *Journal de Physique* v40(7), pC7 871-872.

Glasser, J., Chapelle, J. and Boettner, J.C. (1978). Abel inversion applied to plasma spectroscopy: a new interactive method. *Applied Optics* v17(23), p3750-3754.

Gleizes, A., Kafrouni, H. and Vacquie, S. (1979). Mechanisms of the Electron Disappearance in a Decaying Plasma Arc. *Journal de Physique* v40, pC7 235-236.

Gol'dfarb, V.M. (1973). Arc Plasma Diagnostic Techniques. *Soviet Pkysics-High Temperature* v11(1), p180-191.

Gol'farb, V.M., Donskoi, A.V., Dresvin, S.V. and Rezvov, V.A. (1980). Properties of a Low-Frequency Discharge in a Transformer Plasmatron. *Soviet Physics-High Temperature* v17(4), p698-702.

Gold, D. (1977). Plasmascope - New Opto-electronic Method for Velocity-Measurements in Thermal Plasmas *Journal of Physics E* v10(4), p395-399.

Golubkov, G.V., Kuznetsov, N.M. and Yegorov V.V. (1979). The role of single-step ionisation by thermal electron-atom collisions. *Journal De Physique Colloque C7* v40, p89-90.

Gomes, A.M. (1983). Criteria for partial LTE in an argon thermal discharge at atmospheric pressure; validity of the spectroscopically measured electronic temperature. *Journal of Physics D: Applied Physics* v16, p357-378.

Gottscho, R.A., Burton, R.H., Flamm, D.L., Donnelly, V.M. and Davis, G.P. (1984). Ion dynamics of rf plasmas and plasma sheaths: A time-resolved spectroscopic study. *Journal of Applied Physics* v55(7), p2707-2714.

Gottscho, R.A. and Miller, T.A. (1984). Optical Techniques in Plasma Diagnostics. *Pure and Applied Chemistry* v56(2), p189-208.

Gouesbet, G. (1975), Laser-Doppler Anemometry with a 5 MW Laser in Argon

Plasma-Flow. *Academie des sciences. sB. Sciences Physiques* v280, p597.

Gouesbet, G. and Trinite, M. (1977). Interferential Laser Doppler Velocimetry in a High-Frequency Plasma Jet. *Letters in heat and Mass Transfer* v4, p141.

Greenfield, S., Jones, I.L. and Berry, C.T. (1964). High-pressure Plasmas as Spectroscopic Emission Sources. *Analyst* v89, p713-720.

Greenfield, S., McGeachin, H.McD. and Smith, P.B. (1975). Plasma Emission Sources in Analytical Spectroscopy-I. *Talanta* v22, p1-15.

Greenfield, S., McGeachin, H.McD. and Smith, P.B. (1976). Plasma Emission Sources in Analytical Spectroscopy-III. *Talanta* v23, p1-14.

Griem, H.R. (1964). *Plasma Spectroscopy*, McGraw-Hill, New York.

Griem, H.R. (1974). *Spectral Line Broadening by Plasmas*. Academic Press, New York.

Grinchenko, B.I. and Chinnov, V.F. (1980). Relaxation of Dense Plasma of Heavy Inert Gases. *Soviet Physics-High Temperature* v18(2), p251-255.

Grossl, M., Helm, H., Langenwalter, M. and Mark, T.D. (1979). Stationary afterglow study of the singly charged atomic ions in pure Ar and Kr. *Journal De Physique Colloque C7* v40, p51-52.

Gruzdeva, N.S., Nikolaevskii, L.S. and Podmoshenskii, I.V. (1974). Spectroscopic study of non-equilibrium in highly ionised helium. *Optical Spectroscopy* v37(6), p591-594.

Gurevich, D.B. and Podmoshenskii, I.V. (1963). The Relationship between the Excitation Temperature and the gas Temperature in the Positive Column of an Arc Discharge. *Optical Spectroscopy* v15, p319-322.

Haddad, G.N. and Farmer, A.J.D. (1984). Temperature determinations in a free-burning arc: I. Experimental techniques and results in argon. *Journal of Physics D: Applied Physics* v17, p1189-1196.

Hasegawa, T., Fuwa, K. and Haraguchi, H. (1984). A Steady State Approximation of Population Density Distributions of Argon Atoms in an Inductively Coupled Plasma as an Excitation Source for Atomic Spectrometry. *Chemistry Letters* p2027-2030.

Haydon, S.C. and Plumb, I.C. (1978). Time-resolved studies of the electrical breakdown of a gas at radio frequencies. *Journal of Physics D: Applied Physics* v11,

p1721-1730.

Heine, D.R., Babis, J.S. and Denton, M.B. (1980). Qualitative Aspects of an Inductively Coupled Plasma in the Spectral Region between 120 and 185nm. *Applied Spectroscopy* v34(5), p595-598.

Helbig, V. and Nick, K.P. (1981). Investigation of the Stark broadening of Balmer beta. *Journal of Physics B: Atomic and Molecular Physics* v14, p3573-3583.

Herzberg, G. (1950). *Spectra of Diatomic Molecules* 2nd Edition. Van Nostrand, Princeton.

Hirsh, M.W. and Oskam, H.J. (1978). *Gaseous Electronics, v1 Electrical Discharge.* Academic Press, New York.

Holstein, T. (1947). Imprisonment of Resonance Radiation in Gases. I. *Physical Review* v72(12), p1212-1233.

Holstein, T. (1951). Imprisonment of Resonance Radiation in Gases. II. *Physical Review* v83, p1159-1168.

Houk, R.S., Fassel, V.A. and LaFreniere, B.R. (1986). Direct Detection of Vacuum Ultraviolet Radiation through an Optical Sampling Orifice: Spatially Resolved Emission Studies of Argon Resonance Lines from an Inductively Coupled Plasma. *Applied Spectroscopy* v40(1), p94-100. Houk, R.S., Svec, H.J. and Fassel, V.A. (1981). Mass Spectrometric Evidence for Suprathermal Ionisation in an Inductively Coupled Argon Plasma. *Applied Spectroscopy* v35(4), p380-384.

Huang, M. and Liu K. (1986). Decay of an Inductively Coupled Argon Plasma Above the Load Coil. *Journal of Analytical Atomic Spectrometry* v.1, p153-156.

Huddlestone, R.H. and Leonard, S.L. (1965). *Plasma Diagnostic Techniques.* Academic Press, New York.

Human, H.G.C. and Scott, R.H. (1976). The shapes of spectral lines emitted by an inductively coupled plasma. *Spectrochimica Acta* v31B, p459-473.

Ivanov, V.A., Kagan, Yu.M. and Mozorov, A.O. (1976). Determination of the concentration of molecular ions in a discharge in inert gases. *Optical Spectroscopy* v41(5), p436-439.

Ivanov, Yu.A., Lebedev, Yu.A. and Trofimov, V.N. (1980). Thermocouple

Diagnostics in a Nonequilibrium Plasma. *Soviet Physics-High Temperature* v17(4), p828-834.

Johnson, P.D. (1966). *Physics Letters* v20, p499.

Jarosz, J., Mermet, J.M. and Robin, P.J. (1978). Spectrometric Study of a 40 MHz Inductively Coupled Plasma III. Temperature and Electron Density. *Spectrochimica Acta* v33B, p55.

Kachanov, A.V., Trekhov, E.S. and Fetisov, E.P. (1970). Electrodynamic Model of a High-frequency Plasma Torch. *Soviet Physics-Technical Physics* v15(2), p248-251.

Kalinin, S.V. and Minaev, P.V. (1981). Experimental Study of the Optical Properties of a Low-temperature Neon Plasma Diagnostics and Analysis of the State of a Nonequilibrium Plasma. *Soviet Physics-High Temperature* v18(3), p453-460.

Kalnicky, D.J., Kniseley, R.N. and Fassel, V.A. (1975). Inductively coupled plasma-optical emission spectrocopy. *Spectrochimca Acta* v30B, p511-525.

Kannappan, D. and Bose, T.K. (1977). Transport properties of a two-temperature argon plasma. *The Physics of Fluids* v20(10), p1668-1673.

Kasakov, A.I. and Gol'dfarb, V.M. (1980). Effect of Molecular Gas Impurities on Steady-state and Decaying Argon-arc Plasmas. *Soviet Physics High Temperature* v17(5), p928-935.

Kato, K., Fukushima, H. and Nakajima, T. (1984). Observation of spectral line profiles emitted by an inductively coupled plasma-I. On the wavelength shift of spectral lines. *Spectrochimica Acta* v39B(8), p979-991.

Katsonis, K. and Drawin, H.W. (1980). Transition Probabilities for Argon(I). *Journal of Quantative Spectroscopy and Radiative Transfer* v23, p1-55.

Kawaguchi, H., Ito, T. and Mizuike, A. (1981). Axial profiles of excitation and gas temperatures in an inductively coupled plasma. *Spectrochimca Acta* v36B(7), p615-623.

Kawaguchi, H., Oshio, Y. and Mizuike, A. (1982). Interferometric measurements of spectral line widths emitted by an inductively coupled plasma. *Spectrochimca Acta* v37B(9), p809-816.

Khait, V.D. (1981). Stability of an hf Induction Discharge in a Dense Plasma. *Soviet Physics-High Temperature* v18(4), p695-702.

Kleinmann, I and Svoboda, V. (1969). *Analytical Chemistry* v41, p1029.

Klimontovich, Yu.L. (1979). Kinetic theory of spectral line broadening in a nonequilibrium plasma. *Journal de Physique* v40, pC7-113.

Klubnikin, V.S. (1975). Thermal and Gasdynamic Characteristics of an Argon Induction Discharge. *Soviet Physics-High Temperature* v.13, p439-446.

Kniseley, R.N., Amenson, H., Butler, C.C. and Fassel, V.A. (1974). An Improved Pneumatic Nebulizer for Use at Low Nebulizing Gas Flows. *Applied Spectroscopy* v28(3), p285-286.

Koirtyohann, S.R., Jones, J.S., Jester, C.P. and Yates, D.A. (1981). Use of spatial emission profiles and a nomenclature system as aids in interpreting matrix effects in the low-power argon inductively coupled plasma. *Spectrochimca Acta* v36B, p49-59.

Kornblum, G.R. and de Galan, L. (1974). Arrangement for Measuring Spatial Distributions in an Argon Induction coupled RF plasma. *Spectrochimica Acta* v29B, p249.

Kornblum, G.R. and de Galan, L. (1977). Spatial distribution of temperature and the number densities of electrons and atomic and ionic species in an inductively coupled RF argon plasma. *Spectrochimica Acta* v32B, p71-96.

Kudryavtsev, A.A. and Skrebov, V.N. (1982). Conditions for Equilibrium Distribution of Atoms over Excited States in a Low-Temperature Plasma. *Soviet Physics-High Temperature* v19(6), p1127-1134.

Kudryavtsev, A.A. and Skrebov, V.N. (1983). Ionisation relaxation in a plasma produced by a pulsed inert-gas discharge. *Soviet Physics-Technical Physics* v28(1), p30-35.

Labat, J.M., Vukicevic, J., Labat, O. and Djenize, S. (1979). Line radiation of argon plasma in early afterglow. *Journal De Physique Colloque C7* v40, p9-10.

Larson, G.F. and Fassel, V.A. (1979). Line Broadening and Radiative Recombination Background Interferences in Inductively Coupled Plasma-Atomic Emission Spectroscopy. *Applied Spectroscopy* v33(6), p592-599.

Lee, H.E. (1983). Solutions of plasma arc equations by the orthogonal collocation method. *Journal of Physics D: Applied Physics* v16, 2191-2204.

Leonard, S.L. (1972). Evidence for Departures from Equilibrium in an RF Induction Plasma in Atmospheric-pressure Argon. *Journal of Quantitative Spectroscopy and Radiative Transfer* v12, p619-626.

Lesinski, J., Gagne, R. and Boulos, M.I. (1981). Laser Doppler Anemometry Measurements in Gas-Solid Flows. *5th International Symposium on Plasma Chemistry* v2, p527.

Lochte-Holtgreven, W. Editor (1968). *Plasma Diagnostics* Amsterdam - New Holland Publishing Company.

Lovett, R.J. (1982). A rate model of inductively coupled argon plasma analyte spectra. *Spectrochimca Acta* v37B(11), p969-985.

Majumdar, N.K. (1983). Gas Temperature in a Laboratory Plasma. Exploration of its Use as a Basic Parameter. *Il Nuovo Cimento* v77B(2), p162-180.

Marr, G.V. (1969). *Plasma Spectroscopy*. Elsevier Publishing Company, New York.

McLaren, J.W. and Mermet, J.M. (1984). Influence of the dispersive system in inductively coupled plasma atomic emission spectrometry. *Spectrochimica Acta* v39B(9-11), p1307-1322.

Mermet, J. and Robin, J. (1975). Etude des Interferences dans un Plasma Induit par Haute Frequence. *Analytica Chimica Acta* v70, p271-279.

Mermet, J.M. (1975). Comparaison des temperatures et des densites electroniques mesurees sur le gaz plasmagene et sur des elements excites dans un plasma h.f. *Spectrochimica Acta* v30B, p383-396.

Mermet, J.M. (1975). Spectroscopie Atomique. *Journal De Physique Colloque C7* v281, p273-275.

Mermet, J.M. and Trassy, C. (1981). A spectrometric study of a 40 MHz inductively coupled plasma-V. Discussion of spectral interferences and line intensities. *Spectrochimca Acta* v36B(4), p269-292.

Meubus, P. (1982). Transient conditions in inductively heated plasmas: Thermodynamic equilibrium and temperature measurements. *The Canadian Journal of Chemical Engineering* v60, p886-892.

Mihalas, D. (1978). *Stellar Atmospheres 2nd Ed.* W.H. Freeman & Co. San Francisco.

Miller, E.J. and Sandler, S.I (1973). Transport properties of two-temperature partially ionised argon. *The Physics of Fluids* v16(4), p491-494.

Miller, G.P. (1978). Further Experiment on Inductively-Coupled RF Plasma Torches. *MSc Thesis* University of Waikato.

Mills, J.W. and Hieftje, G.M. (1984). A detailed consideration of resonance radiation trapping in the argon inductively coupled plasma. Spectrchimica Acta v39B(7), p859-866.

Mitchell, A.C.G. and Zemansky, M.W. (1971). *Resonance Radiation and Excited Atoms.* Cambridge University Press, London.

Mitin, R.V., Zvyagintsev, A.V. and Gonchar, N.I. (1981). Threshold conditions of an induction discharge. *Soviet Physics-High Temperature* v18(3), p497-500.

Monaser, A. and Fassel, V.A. (1982). Atomic Emission Spectroscopy with a Skimmed Inductively Coupled AR Plasma. *Applied Spectroscopy* v36(4), p454-459.

Montaser, A. and Fassel, V.A. (1982). Electron Number Density Measurements in Ar and Ar-N_2 Inductively Coupled Plasmas. *Applied Spectroscopy* v36(6), p613-617.

Montaser, A., Fassel, V.A. and Larsen, G. (1981). Electron Number Densities in Analytical Inductively Coupled Plasmas as Determined via Series Limit Line Merging. *Applied Spectroscopy* v35(4), p385-389.

Montaser, A., Fassel, V.A. and Zalewski, J. (1981). A Critical Comparison of Ar and Ar-N_2 Inductively Coupled Plasmas as Excitation Sources for Atomic Emission Spectrometry. *Applied Spectroscopy* v35(3), p292-302.

Montford van, P.F.E. and Agterdenbos, J. (1981). Some Fundamental Considerations on Analytical High-Frequency Plasmas. *Talanta* v28, p629-635.

Mullen, van der J., Sijde van der, B. and Schram, D.C. (1980). Experimental evidence for the complete saturation phase in the argon neutral system. *Physics Letters* v79A(1), p51-54.

Nestor, O.H. (1960). Numerical Methods for Reducing Line and surface Probe Data. *SIAM Review* v2(3), p200-207.

Nick, K., Richter, J. and Helbig, V. (1984). Non-LTE Diagnostic of an Argon Arc Plasma. *Journal of Quantative Spectroscopy and Radiative Transfer* v32(1), p1-8.

Numano, M. and Onishi, H. (1979). Excitation temperature of a rapidly varying plasma. *Journal De Physique Colloque C7* v40, p49-50.

Olsen, H.N. (1959). Thermal and Electrical Properties of an Argon Plasma. *The Physics of Fluids* v2(6), p614-623.

Ong, C.B. (1977). Experiments on Inductively-Coupled RF Plasma Torches. *MSc Thesis* University of Waikato.

Osipov, A.I. (1972). Dynamics of a Nonequilibrium gas. *Soviet Physics-High Temperature* v9(6), p1277-1288.

Polak, L.S. and Slovetskii, D.I. (1975). Effect of Traces of Molecular Gases on Deviations from Thermodynamic equilibrium in Low-Current Electric Arcs in Argon. Experimental Study of Arc Parameters and Level Populations. *Soviet Physics-High Temperature* v12(5), p921-930.

Polak, L.S. and Slovetskii, D.I. (1975). Effect of small inpurities in molecular gases on deviation from thermodynamic equilibrium in low-current electric arcs. The dissociation of nitrogen. *Soviet Physics-High Temperature* v13(1), p7-16.

Raaijmakers, I., Boumans, P.W., Van der Sijde, B. and Schram, D.C. (1983). A theoretical study and experimental investigation of non-LTE phenomena in an inductively-coupled argon plasma-I. Characterization of the discharge. *Spectrochimca Acta* v38B(5/6), p697-706.

Raizer, Yu.P. (1980). Channel Arc Model. *Soviet Physics-High Temperature* v17(5), p1096-1098.

Ranson, P. and Chapelle, J. (1979). Calculation of the Free-Bound Continuum of Rare Gases. *Journal de Physique* v40, pC7-93.

Ranson, P. et Chapelle, J. (1971). Mesure de Densite des Atomes Metastables dans un Jet Laminaire de Plasma D'argon. *Journal De Physique Colloque C7* v32, pC5b-39.

Reed, T.B. (1961). *Journal of Applied Physics* v32, p2534-2535; v32, p2534-2535.

Reeves, R.D., Nikdel, S. and Winefordner, J.D. (1980). Molecular Emission Spectra in the Radio-frequency-excited Inductively Coupled Argon Plasma. *Applied Spectroscopy* v34(4), p477-483.

Ripson, P.A.M., Jansen, L.B.M. and de Galan, L. (1984). Inductively Coupled Argon

Atomic Emission Spectroscopy with an Externally Cooled Torch. *Analytical Chemistry* v56, p2329-2335.

Plas, van der P.S. and de Galan, L. (1984). A radiatively cooled torch for ICP-AES using 1 l/min of argon. *Spectrochimca Acta* v39B(9-11), p1161-1169.

Robinson, I.G. (1971). Adaptive Gaussian Integration. *The Australian Computor Journal* v3(3), p126-129.

Rogoff, G.L. (1972). Gas Heating Effects in the Constriction of a High-Pressure Glow Discharge Column. *The Physics of Fluids* v15(11), p1931-1940.

Rosado, R.J., Schram, D.C. and Leclair, J. (1979). Continuous emission, Lowering of the ionisation potential and total excitation cross-sections of an atmospheric thermal plasma. *Journal De Physique Colloque C7* v40, p285-286.

Rovenskii, R.E., Belousova, L.E. and Gruzdev, N.S. (1966). *Soviet Physics-High Temperature* 4, p328.

Rovinskii, R.E. and Sobolev, A.P. (1976). High-Pressure induction discharge. I. Predominate radial heat transfer. *Soviet Physics-Technical Physics* v20(8), p1060-1063.

Rovinskii, R.E. and Sobolev, A.P. (1976). High-Pressure induction discharge. II. Induction discharge as a source of visible light. *Soviet Physics-Technical Physics* v20(8), p1064-1068.

Rozovskii, M.O. (1975). Variational Approach to the Calculation of a High-Frequency Induction Discharge. *Journal of Applied Mechanics and Technical Physics* v2, p42-47.

Rykalin, N.N., Kulagin, I.D., Sorokin, L.M. and Gugnyak, A.B. (1976). RF plasmatron with external electrodes and a longitudinal forced gas flow. *Soviet Physics-Technical Physics* v21(4), p424-427.

Sandus, O. The Isointensity Method for Gas Temperature Measurements. *U.S. Army Technical Report 4515* 1973.

Schleicher, R.G. and Barnes, R.M. (1975). Remote Coupling Unit for Radiofrequency Inductively Coupled Plasma Discharges in Spectrochemical Analysis. *Analytical Chemistry* v47(4), p724-728.

Schneider, J. and Robertson, S. (1979). Feedback-stabilized fractional fringe laser interferometer for plasma density measurements. *Review of Scientific Instruments*

v50(7), p856-858.

Scholz, P.D. and Anderson, T.P. (1968). Local Thermodynamic Equilibrium in an RF Argon Plasma. *Journal of Quantitative Spectroscopy and Radiative Transfer* v8. p1411-1418.

Schrack, R.A. (1953). Radio-Frequency Power Measurements. *National Bureau of Standards Circular 536.*

Schram, D., Raaymakers, I., van der Sijde, B., Schenkelaars, H. and Boumans, P. (1983). Approaches for Clarifying Excitation Mechanisms in the Spectrochemical Excitation Sources. *Spectrochimica Acta* v38B(11-12), p1545-1557.

Scott, R.H., Fassel, V.A., Kniseley, R.N. and Nixon, D.E. (1974). Inductively Coupled Plasma-Optical Emission Analytical Spectrometry. *Analytical Chemistry* v46(1), p75-80.

Sebastain, J.L., Colomer, V., Rodrigueuz-Vidal, M. and Peon, J. (1979). A study of two microwave interferometers for the determination of the plasma electron density. *Journal of Physics D: Applied Physics* v12, p417-423.

Shamin, A and Wooding, E.R. *Physics Letters* v34A, p719.

Shaw, J.F., Mitchner, M. and Kruger, C.H. (1970). Effects of Nonelastic Collisions in Partially Ionised Gases I. Analytical Solutions and Results. *The Physics of Fluids* v13(2), p325-338.

Shaw, J.F., Mitchner, M. and Kruger, C.H. (1970). Effects of Nonelastic Collisions in Partially Ionised Gases II. Numerical Solution and Results. *The Physics of Fluids* v13(2), p339-345.

Sijde, van der V., Pots, B.F. and Schram, D.C. (1979). A Collisional Radiative Model of the Argon Ion System Tested for a Large Range of Electron Densities. *Journal de Physique* v40, pC7 23-24.

Skrebov, V.N. and Eikhvald, A.I. (1976). Investigation of the inhomogeneous plasma of a pulsed discharge in argon by laser diagnostic methods. *Optical Spectroscopy* v41(1), p7-11.

Soshnikov, V.N. and Trekhov, E.S. (1966). The Theory of High-Frequency Vortex Discharges at High Pressure. I. *Soviet Physics-High Temperature* v4(2), p166-172.

Stokes, A.D. (1971). Thermal equilibrium in argon induction discharges. *Journal of*

Physics D: Applied Physics v4, p916.

Stokes, A.D. (1971). Transition probabilities in the neutral argon spectrum. *Journal of Physics D: Applied Physics* v4, p930-937.

Stubley, E.A. and Horlick, G. (1984). Some Near-IR Spectral Emission Characteristics of the Inductively Coupled Plasma. *Applied Spectroscopy* v38(2), p162-168.

Talayrach, B., Besombes-Vailhe, I. and Triche, H. *Analysis* v1, p135.

Taylor, C.E. and Floyd, T.L. (1980). Evaluation of a Multichannel Inductively Coupled Plasma-Optical Emission Spectrometer Modified to Minimize and Correct Scattered Light Effects. *Applied Spectroscopy* v34(4), p472-477.

Thomason, W.H. and Elbers, D.C. (1975). An inexpensive method to stabilize the frequency of a CO_2 laser. *Review of Scientific Instruments* v46(4), p409-412.

Thompson, M. (1985). The Capabilities of Inductively Coupled Plasma Atomic-emission Spectrometry-Some Conjectures and Refutations. *Analyst* v110, p443-449.

Thorne, A.P. (1974). *Spectrophysics.* Chapman and Hall and Science Paperbacks, London.

Trekhov, E.S., Fomenko, A.F. and Khoshev, Yu. M. (1969). Parameters of Stationary Inductive Discharges at Atmospheric Pressure. *Soviet Physics-High Temperature* v7(5), p860-865.

Tsendin, L.D. (1978). Electron energy distribution in an rf electric field. *Soviet Physics-Technical Physics* v22(8), p925-928.

Turk, G.C. and Watters, Jr, R.L. (1985). Resonant Laser-Induced Ionisation of Atoms in an Inductively Coupled Plasma. *Analytical Chemistry* v57, p1979-1983.

Uchida, H., Kosinski, M.A., Omenetto, N. and Winefordner, J.D. (1984). Studies on lifetime measurements and collisional processes in an inductively coupled argon plasma using laser induced fluorescence. *Spectrochimca Acta* v39B(1), p63-68.

Uchida, H., Tanabe, K., Nojiri, Y., Haraaguchi, H. and Fuwa, K. (1981). Spatial distributions of metastable argon, temperature and electron number density in an inductively coupled argon plasma. *Spectrochimica Acta* v36B(7), p711-718.

Uchida, H., Tanabe, K., Nojiri, Y., Haraguchi, H. and Fuwa, K. (1980). Mesurement of metestable argon in an inductively coupled argon plasma by atomic absorption

spectroscopy. *Spectrochimica Acta* v35B, p881-883.

Vacquie, S., Kafrouni, H et Dinguirard, J. (1975). Etude de la Coupure d'un Arc Stabilise par Parois. *Journal of Physics D: Applied Physics* v8, p191-200.

Vanmarcke, M. and Wieme, W. (1979). Theory of Resonance Radiation Imprisonment. *Journal de Physique* v40(7), pC7 39-40.

Vanmarcke, M. and Wieme, W. (1979). Visible Afterglow Emission of a Pulsed Xenon Discharge. *Journal De Physique Colloque C7* v40, p35-36.

Vashukov, S.I. and Marusin, V.V. (1976). Electron Velocity Distribution in a Weakly Ionised hf Plasma. *Soviet Physics-High Temperature* v14(6), p1045-1053.

Veillon, C. and Margoshes, M. (1968). An evaluation of the induction-coupled, radio-frequency plasma torch for atomic emission and atomic absorption spectrometry. *Spectrochimica Acta* v23B, p503-512.

Venugopalan, M. (1971). *Reactions under Plasma Conditions v1 and v2*. Wiley-Interscience, New York.

Visser, K. Hamm, F.M. and Zeeman, P.B. (1976). Temperature Determination in an Inductively Coupled rf Plasma. *Applied Spectroscopy* v30(1), p34-38.

Voropaev, A.A. and Dresvin, S.V. (1973). Two-temperature Model of a Laminar Arc Under Conditions of Forced Blowing of Gas through a Plasmatron. *Soviet Physics-High Temperature* v11(2), p333-341.

Walters, P.E., Chester, T.L. and Winefordner, J.D. (1977). Measurement of Excitation, Ionisation, and Electron Temperatures and Positive Ion Concentrations in a 144 MHz Inductively Coupled Radiofrequency Plasma. *Applied Spectroscopy* v31(1), p1-8.

Ward, A.F. (1978). Inductively coupled argon plasma spectroscopy. *American Laboratory* v10(11), p79-87.

Wiese, W.L., Kelleher, D.E. and Paquette, D.R. (1972). Detailed Study of the Stark Broadening of Balmer Lines in a High-Density Plasma. *Physical Review A* v6(3), p1132-1153.

Wilhelm, J. and Winkler, R. (1979). Progress in the kinetic description of non-stationary behaviour of the electron ensemble in the non-isothermal plasma. *Journal de*

Physique v40(7), pC7-251-267.

Windsor, D.L. and Denton, M.B. (1978). Evaluation of Inductively Coupled Plasma Optical Emission Spectroscopy as a method for the Elemental Analysis of Organic Compounds. *Applied Spectroscopy* v32(4), p366-371.

Winge, R.K., Fassel, V.A., Kniseley, R.N., DeKalb, E. and Haas Jr., W.J. (1977). Determination of trace elements in soft, hard and saline waters by the inductively coupled plasma, multi-element atomic emission spectroscopic (ICP-MAES) technique. *Spectrochimica Acta* v32B, p327-345.

Wolcott, J.F. and Sobel, C.B. (1978). A Simple Nebulizer for an Inductively Coupled Plasma System. *Applied Spectroscopy* v32(6), p591-593.

Zeeman, P.B., Terblanche, S.P., Visser, K. and Hamm, F.H. (1978). Temperature Determination on a 9.2 MHz Inductively Coupled Plasma Source Using N_2^+ Bands as Monitor. *Applied Spectroscopy* v32(6), p572-576.

Zheleznyak, M.B. (1973). Temperature Dependence of the Coefficient of Dissociative Recombination in Inert Gases. *Soviet Physics-High Temperature* v11(1), p194-195.